# Involvement of the lysosomal protein NPC1 in the pathogenesis of Huntington's disease

Emily Clark

Cardiff University

School of Biosciences

PhD

2017

**DECLARATION**

This work has not been submitted in substance for any other degree or award at this or any other university or place of learning, nor is being submitted concurrently in candidature for any degree or other award.

Signed …………………………………………………… (candidate)   Date…………….…………

**STATEMENT 1**

This thesis is being submitted in partial fulfillment of the requirements for the degree of PhD

Signed …………………………………………………… (candidate)   Date…………….…………

**STATEMENT 2**

This thesis is the result of my own independent work/investigation, except where otherwise stated, and the thesis has not been edited by a third party beyond what is permitted by Cardiff University's Policy on the Use of Third Party Editors by Research Degree Students. Other sources are acknowledged by explicit references.  The views expressed are my own.

Signed …………………………………………………… (candidate)   Date…………….…………

**STATEMENT 3**

I hereby give consent for my thesis, if accepted, to be available online in the University's Open Access repository and for inter-library loan, and for the title and summary to be made available to outside organisations.

Signed …………………………………………………… (candidate)   Date…………….…………

**STATEMENT 4: PREVIOUSLY APPROVED BAR ON ACCESS**

I hereby give consent for my thesis, if accepted, to be available online in the University's Open Access repository and for inter-library loans **after expiry of a bar on access previously approved by the Academic Standards & Quality Committee.**

Signed …………………………………………………… (candidate)   Date…………….…………

## Abstract

Huntington's disease is an autosomal dominant inherited neurodegenerative disease, with cognitive, motor and psychiatric defects and no known therapy. Altered lipid metabolism and lysosomal dysfunction have been seen in Huntington's disease (HD), including lysosomal expansion, a key feature of a type of disease known as lysosomal storage disorders (LSDs). HD shares similarities with one LSD in particular, Niemann-Pick type C (NPC), suggesting common mechanisms.

We have identified NPC-like phenotypes in HD models, including lipid storage, trafficking defects, and lysosomal $Ca^{2+}$ dysfunction, and the NPC protein NPC1 directly interacts with both normal and mutant huntingtin. We therefore tested the approved NPC therapy miglustat in HD models, and found beneficial effects. Lipid trafficking, $Ca^{2+}$ signalling and lysosomal storage phenotypes in HD iPSC-derived neuronal cells were improved after miglustat treatment, and climbing ability in *Drosophila melanogaster* HD models was partially improved.

Nucleic acid vectors are an essential tool in HD research and therapy. Lipid- and polymer-based vectors enter the cell via the endocytic system, and may cause altered function. Use of these vectors alone induced lysosomal expansion, phospholipid storage, and altered expression of endocytic proteins, potentially producing artefacts or interfering with delivery of therapies.

We have found evidence that HD has lysosomal storage defects which may be due to disruption of NPC1, a previously unidentified component of HD pathology. Our observations also support the theory that huntingtin may be associated with the lysosome under normal as well as pathogenic conditions. The presence of related mechanisms in these two diseases suggests that knowledge from NPC and the LSD field may be useful in HD, and we have demonstrated that the NPC1 therapy miglustat is beneficial in HD models, a finding which will be developed to therapeutic tests in HD patients.

## Acknowledgements

**Table of Contents**

## Table of Figures

## Abbreviations

**7DHC** 7 dehydrocholesterol

**ABCA1** ATP-binding cassette transporter 1

**AP1-4** adaptor proteins 1-4

**ApoE** apolipoprotein E

**ASM** acid sphingomyelinase

**ATP** adenosine triphosphate

**BCA** bicinchoninic acid

**BDNF** bone derived neurotrophic factor

**BSA** bovine serum albumin

**CAD** cationic amphiphilic drug

**CESD** cholesterol ester storage disease

**CLEAR** co-ordinated lysosomal expression and regulation

**Co-IP** coimmunoprecipitation

**DHCR7** 7-dehydrocholesterol reductase

**DMEM** Dulbecco's modified Eagle's medium

**DMSO** dimethylsulphoxide

**ECL** enhanced chemiluminescence reagent

**EEA1** early endosome antigen 1

**ER** endoplasmic reticulum

**ESCRT** endosomal sorting complexes required for transport

**FBS** fetal bovine serum

**FITC** fluoroscein isothiocyanate

**FITC-CtxB** FITC-tagged cholera toxin B subunit

**GAG** glycosaminoglycan

**GAPDH** glyceraldehyde 3-phosphate dehydrogenase

**GBA** glucocerebrosidase

**GCS** glucosylceramide synthase

**GLUT** glucose transporter

**GPN** Gly-Phe β-napthylamide

**GSL** glycosphingolipid

**GWA** genome-wide association

**HBSS** Hank's balanced salt solution

**HD** Huntington's disease

**HDAC** histone deacetylase

**HDL** high-density lipoprotein

**HPβCD** hydroxypropyl-β-cyclodextrin

**HRP** horseradish peroxidase

**HSP** heat shock protein

**Htt** huntingtin

**ICC** immunocytochemistry

**IP$_3$** inositol trisphosphate

**iPSC** induced pluripotent stem cells

**LAL** lysosomal acid lipase

**LAMP** lysosomal-associated membrane protein

**LBPA** lyso-bisphosphatidic acid

**LDL** low-density lipoprotein

**LSD** lysosomal storage disease

**LXR** liver X receptor

**MJD** Machado-Jacob disease

**MPS** mucopolysaccharidosis

**mRNA** messenger RNA

**mTORC** mammalian target of rapamycin complex

**NMDA** N-methyl D-aspartate receptor

**NPA** Niemann-Pick type A

**NPB** Niemann-Pick type B

**NPC** Niemann-Pick type C disease

**NSC** neuronal precursor cell

**nt** nucleotide

**PBS** phosphate buffered saline

**PEI** phosphatidylethyleneimine

**PFA** paraformaldehyde

**PKC** protein kinase C

**PM**      plasma membrane

**PolyQ**   polyglutamine

**PVDF**    polyvinylidene fluoride

**REST**    repressor element 1 silencing transcription factor

**RFP**     red fluorescent protein

**RNA**     ribonucleic acid

**RNAi**    RNA interference

**SCA**     spinocerebellar ataxia

**SDS**     sodium dodecyl sulphate

**SERCA**   sarco/endoplasmic reticulum $Ca^{2+}$ ATPase

**siRNA**   small interfering RNA

**SLOS**    Smith-Lemli-Opitz syndrome

**SREBP**   sterol response element binding protein

**SSD**     sterol sensing domain

**TBS**     Tris buffered saline

**TF**      transcription factor

**TFEB**    transcription factor EB

**TLC**     thin layer chromatography

**UAS**     upstream activating sequence

**VSGP**    vertical supranuclear gaze palsy

# CHAPTER 1 INTRODUCTION

In this introduction I will first cover some relevant general background, with an overview of the endocytic and lysosomal system and of lipid metabolism. Lysosomal function and dysfunction is the main focus of this thesis, both for the work on Huntington's disease and the chapter on nucleic acid delivery vectors. Lipid metabolism is relevant as both Niemann-Pick type C (NPC) and Huntington's disease (HD) have defects in lipid trafficking and recycling, and changes to synthesis, so background information on cholesterol and glycosphingolipids is useful.

Secondly, I will briefly discuss lysosomal involvement in disease, both in lysosomal storage disorders and in neurodegeneration. Both of these are relevant to our HD study, as similar mechanisms are present in many neurodegenerative diseases, and we have also identified lysosomal storage phenotypes in this disease. Then, I will give more detail on NPC, as we have identified NPC-like phenotypes and involvement of the NPC1 protein in HD. I will also give some background on HD, including a review of the existing literature on changes to lysosomal function and lipid metabolism.

More detail and more explanation of why and how we have chosen to investigate specific areas will be covered in individual chapter introductions.

## 1.1 Lysosomes and the endocytic system

### 1.1.1 The endocytic system

The endocytic system and related vesicle trafficking pathways form a complex, dynamic network, which is highly organised and tightly interconnected (Figure 1.1). Vesicles mature and fuse and are sorted into different pathways and compartments to different destinations. The lysosome is a central component of this system.

Endocytosis takes up plasma membrane (PM) and external fluid phase into vesicles within the cell, which are then sorted and trafficked through early endosomes to recycling endosomes or maturing multi-vesicular bodies/late endosomes, and ultimately to the lysosome. Autophagic and phagocytic vesicles are also trafficked to and fuse with the lysosome. Materials such as lipids are removed during maturation or once they have been degraded in the lysosome, and are trafficked out into the cell to be reused, including along delivery pathways to the Golgi and ER. Proteins produced in the Golgi or ER are often transported to their destinations, including the late

endosome and lysosome, via vesicular pathways, or are exocytosed, and recycling endosomes, multi-vesicular bodies and lysosomes can also be exocytosed, for a range of different purposes.

Vesicles mature by changes in protein composition, by removal or degradation of materials - for example, formation of lysolipids - and by changes to pH and calcium content. These are controlled by signals such as changing composition and position within the cell.
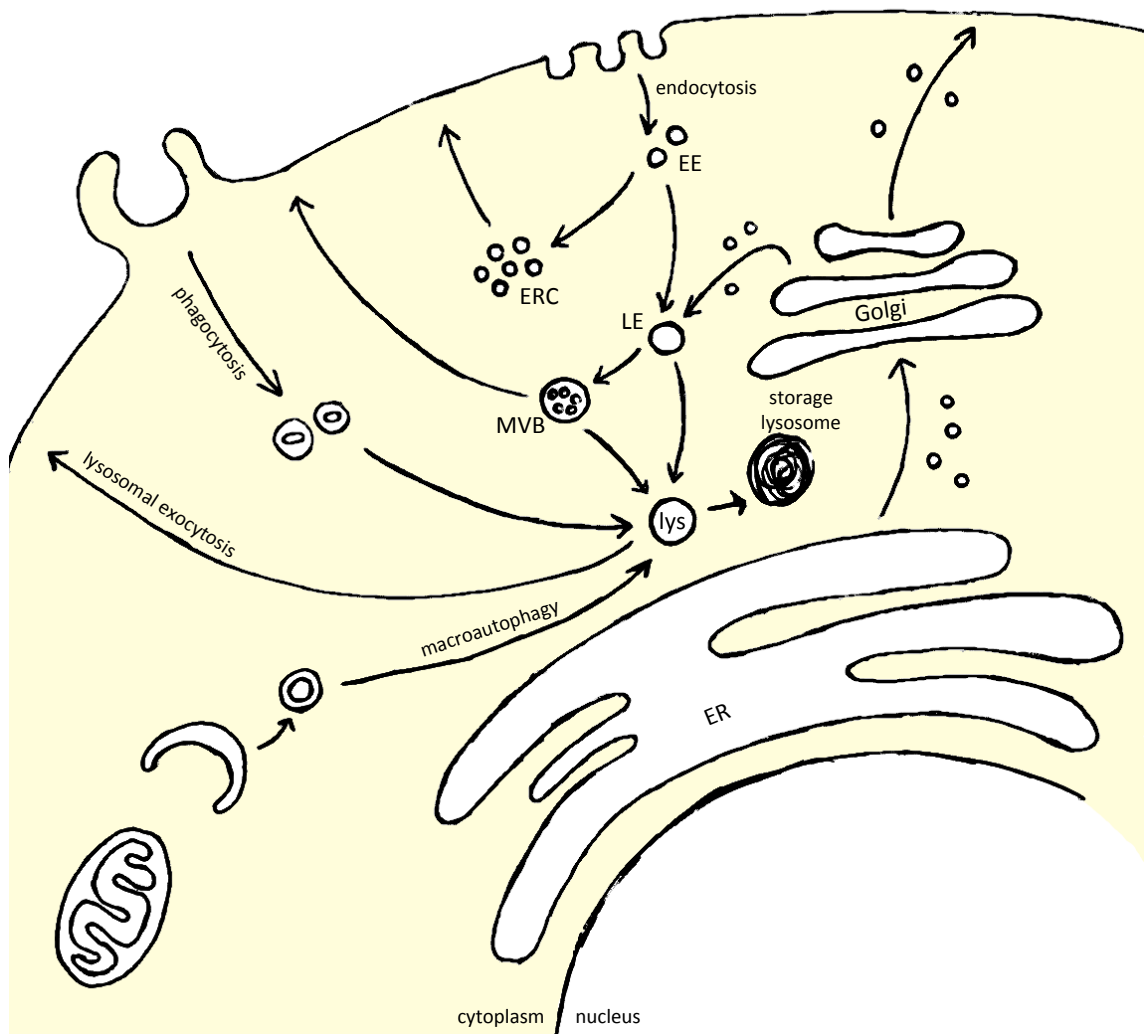
**Figure 1.1 The endocytic system**
Outline of the endocytic system and vesicular trafficking, including endocytic, phagocytic and autophagic pathways which carry material to the lysosome, and exocytic and secretory pathways from the ER, Golgi and endocytic system. Abbreviations: ER = endoplasmic reticulum, lys = lysosome, EE = early endosome, LE = late endosome, ERC = endocytic recycling compartment, MVB = multivesicular body.

### 1.1.2 Entry into the endocytic system

Endocytosis allows the cell to take up molecules that are unable to cross the plasma membrane, as well as internalising plasma membrane proteins, receptors and lipids. The best described pathway is clathrin mediated endocytosis, which uses clathrin proteins to sort membrane proteins and domains and promote the formation of vesicles (Grant & Donaldson, 2009). There are also a number of other pathways often grouped together as clathrin independent endocytosis, which differ in the proteins and cargoes involved. Some of these use other coat proteins, such as caveolin, whereas others are independent of both dynamin and the known coat proteins and act via other membrane proteins, lipid accumulation or other unknown methods to trigger invagination and budding of vesicles (Mayor, Parton & Donaldson, 2014; Howes, Mayor & Parton, 2010).

Autophagy is a set of processes, including macroautophagy and chaperone mediated autophagy, which select materials from within the cell to be degraded (García-Arencibia *et al.*, 2010). These cargoes can range from individual proteins which are not dealt with by the ubiquitin proteasome system, to whole organelles, in particular defective mitochondria, which are removed if they function poorly in order to protect the cell from oxidative damage. Targets for autophagy are selected by protein chaperones (Kaushik & Cuervo, 2012) or by the formation of membrane structures called autophagosomes (Rubinsztein, Shpilka & Elazar, 2012), and then trafficked to the lysosome for degradation. Defects in autophagy, including issues with cargo selection, vesicle formation, or trafficking, lead to failure to clear toxic materials and are common in neurodegenerative disease (Nixon, 2013; Menzies, Fleming & Rubinsztein, 2015).

### 1.1.3 Targets of the endocytic system

Some materials which enter the endocytic system are quickly recycled and returned to the plasma membrane from the early and recycling endosome compartments. This particularly includes plasma membrane lipids and proteins which are sorted and returned, because they are needed at the cell surface or are part of the early trafficking machinery. This kind of trafficking is also used as a mode of regulation for some cell surface receptors and channels, such as glucose uptake (GLUT) channels, the low-density lipoprotein (LDL) receptor or the receptor for brain-derived neurotrophic

factor (BDNF). Endocytosed material can also be transported to the Golgi from many stages of the endocytic system (Grant & Donaldson, 2009), or processed all the way to the lysosome to be degraded and removed (Luzio *et al.*, 2009).

Vesicles from many stages are also exocytosed, for several purposes. Early endosomes or recycling vesicles can be returned to the plasma membrane in order to recycle contents quickly, as mentioned above. Multi-vesicular bodies are also exocytosed, producing exosomes, which carry proteins and RNAs and may have roles in cell-cell signalling, interaction and immunity (Théry, Zitvogel & Amigorena, 2002; Raposo & Stoorvogel, 2013). Exocytosis of lysosomes can act as a secretory system (Blott & Griffiths, 2002) or a mechanism for cells to repair plasma membrane damage (Reddy, Caler & Andrews, 2001; Medina *et al.*, 2015).

### 1.1.4 Vesicular trafficking

Trafficking and sorting in the endocytic and vesicular pathways involves a complex network of proteins and other factors. Movement of vesicles requires transport along the cytoskeleton by motors such as dynein. Sorting in the endocytic system is controlled by multiple signals and factors, including protein motifs recognised by machinery like clathrin and the adaptor proteins, and by ESCRT (endosomal sorting complexes required for transport) (Schmidt & Teis, 2012). Fusion requires complexes of proteins called SNAREs, membrane-anchored proteins with α-helical domains, which are delivered to target membranes or recruited into vesicles during vesicle formation (Hong, 2005). Tethering factors help direct vesicles to their targets, and then vesicular SNAREs interact with their partners on target membranes and form bundles, bringing membranes into close proximity and contributing to driving membrane fusion (Cai, Reinisch & Ferro-Novick, 2007). Small GTPases including Rabs and Rhos, specific to different compartments, trigger or mediate several steps in this process and are another important contributor to organisation and sorting within this system.

### 1.1.5 Lysosomes

The lysosome is an essential cellular compartment involved in endocytic trafficking and in degradation and recycling of molecules, and is fundamental to the normal functioning of a cell. Lysosomes are small membrane-bound organelles with an internal pH of pH 4-5, and contain a broad range of hydrolytic and degradative enzymes with acidic pH optima (Platt, Boland & van der Spoel, 2012; Cox & Cachón-

González, 2012). The low pH is maintained by the vacuolar ATPase, a protein complex which uses ATP to pump $H^+$ ions into the lysosome (Finbow & Harrison, 1997; Maxson & Grinstein, 2014). The inner surface of the lysosomal limiting membrane is a layer of highly glycosylated proteins called a glycocalyx, which protects the lysosome itself from degradation by the active enzymes inside. The lysosome is the main site where molecules, membranes and old organelles are broken up into components which can be reused. Both autophagy, a mechanism for clearing waste or problems within the cell, and phagocytosis (Criscitiello *et al.*, 2013; Vural & Kehrl, 2014), either of pathogens or dead cells, target their cargoes to the lysosome to be destroyed.

The lysosome is a dynamic compartment, closely linked to the late endosome and other organelles such as the Golgi which receive the products of degradation. Lipids can be processed and removed from the late endosome, and proteins such as the mannose-6-phosphate receptor (M6PR) or NPC1 shuttle back and forward along endocytic and vesicle trafficking pathways (Zhang *et al.*, 2001; Ko *et al.*, 2001), demonstrating that the identity of individual endocytic compartments is somewhat complex. Degradation may instead happen in a hybrid compartment formed when the late endosome and lysosome interact (Luzio *et al.*, 2014); in this model, lysosomes are more like storage sites for degradative enzymes, which fuse with late endosomes when required then reform once materials have been processed and removed (Luzio *et al.*, 2014). There are also subpopulations of lysosomes, which can differ in localisation within the cell (perinuclear versus close to the surface), pH (Johnson *et al.*, 2016), degree of motility, protein composition, and function. One example is secretory lysosomes, which can potentially be exocytosed if necessary (Blott & Griffiths, 2002), and storage bodies in lysosomal storage disorders could also be described as a separate subpopulation.

The lysosome also has a role in intracellular $Ca^{2+}$ signalling. While the endoplasmic reticulum (ER) and mitochondria are the classical $Ca^{2+}$ stores in the cell, lysosomes have more recently been shown to act as $Ca^{2+}$ stores, although the proteins involved in lysosomal $Ca^{2+}$ signalling, particularly in filling the store, are not fully characterised (Lloyd-Evans & Platt, 2011; Patel & Cai, 2015). Release of $Ca^{2+}$ from lysosomal stores is required for endocytic trafficking and fusion events, (Lloyd-Evans *et al.*, 2010; Li, Garrity & Xu, 2013; Patel & Cai, 2015), and can also act as a trigger for and a modulator

of global $Ca^{2+}$ signalling (López Sanjurjo *et al.*, 2013; López Sanjurjo, Tovey & Taylor, 2014; Penny *et al.*, 2015). Defects in lysosomal $Ca^{2+}$ are seen in a number of diseases, including Alzheimer's disease and lysosomal storage diseases, indicating the importance of the lysosome in $Ca^{2+}$ signalling and localisation (Lloyd-Evans *et al.*, 2008; Ruas *et al.*, 2010; Lloyd-Evans & Platt, 2011).

Lysosomes are formed by budding of vesicles from the Golgi and fusion with or maturation of endocytic vesicles. Signalling from a number of areas, including cellular nutrient sensors and autophagic trafficking, converges on mTORC (mammalian target of rapamycin, a central regulator of cell metabolism and energy balance) and TFEB (transcription factor EB) and a gene network known as CLEAR (coordinated lysosomal expression and regulation) (Settembre & Medina, 2015; Napolitano & Ballabio, 2016), and regulates formation of lysosomes and production of lysosomal proteins.

Soluble proteins are trafficked to the lysosome via the mannose-6-phosphate pathway, and membrane proteins via vesicle trafficking pathways involving specific motifs and adaptor proteins (Saftig & Klumperman, 2009; Luzio *et al.*, 2014). Proteins can also reach the lysosome via exocytosis and re-internalisation through the endocytic pathway, which is useful when other pathways are defective and is the mechanism which allows cross correction and correction of lysosomal defects by exogenously added proteins.

## 1.2 Mammalian lipid metabolism

### 1.2.1 Overview

Mammalian lipids have diverse roles, including nutrition, cell structure, and signalling. The major classes are glycerolipids, sphingolipids, and sterols (Figure 1.2), but within these classes there are hundreds of lipids with different structures and properties. Metabolism and distribution of lipids are controlled by both cell signalling and lipid biophysical properties, and this produces complex and highly organised systems. Membrane lipid composition differs between organelles and contributes to function via changes to properties such as fluidity and curvature, by providing targets for signalling and trafficking, and by regulating membrane proteins (van Meer & de Kroon, 2010). Interlocking metabolic pathways and co- and cross-regulation of different types of lipids produces coordinated changes in membrane properties, allowing the cell to

respond to conditions, for example nutrient availability (Gaspar *et al.*, 2011) or pathogen invasion (Mazzon & Mercer, 2014), and regulate activity such as vesicle formation (Johansen, Ramanathan & Beh, 2012).
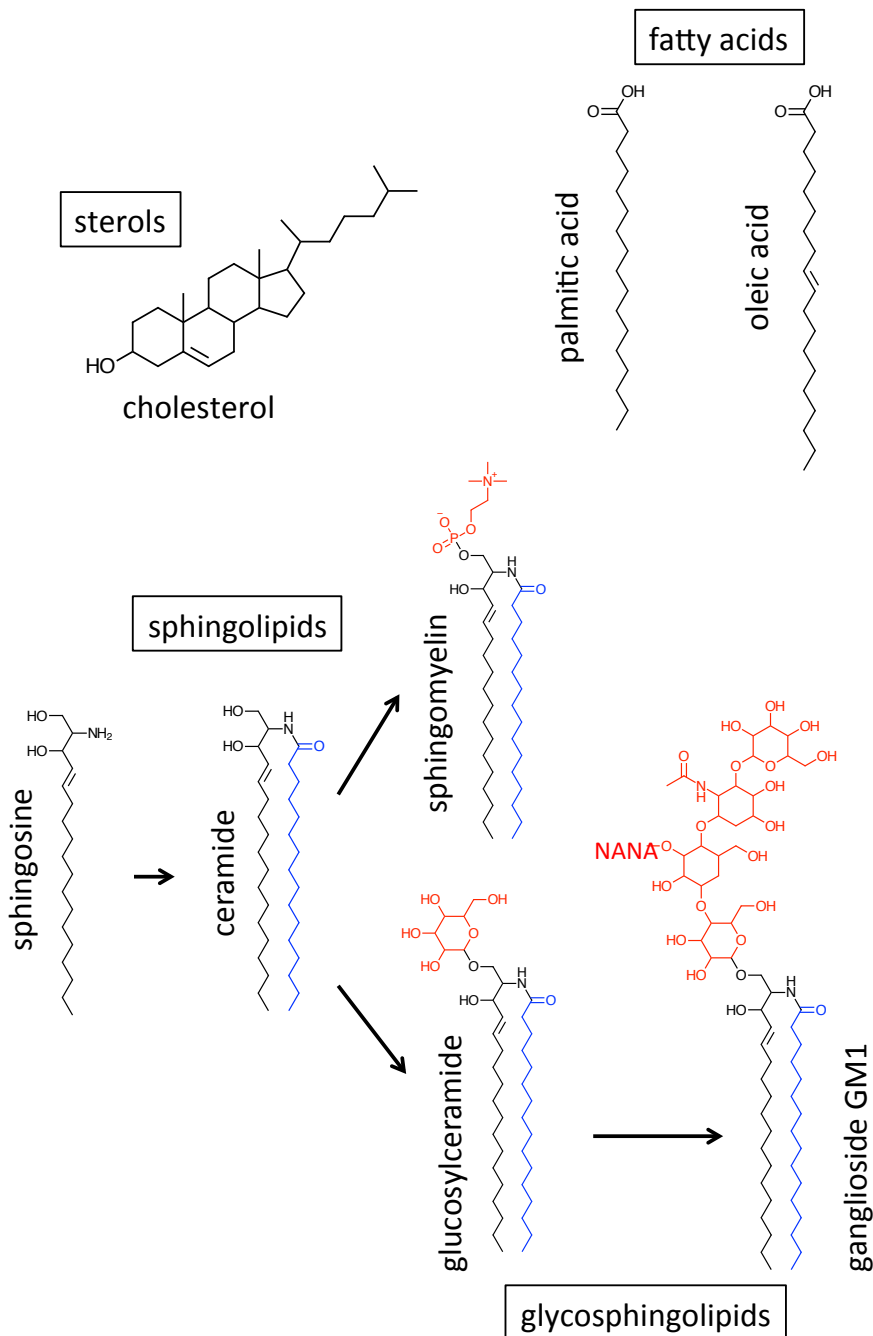


**Figure 1.2 Mammalian lipids**
Structures of some major species of mammalian lipids. Cholesterol is the primary sterol in mammalian cells. Mammalian fatty acids most commonly have 16 or 18 carbon chains, with 0-2 unsaturated double bonds, and are used to produce sphingolipids, triacylglycerides and phospholipids. The simplest sphingolipids, ceramides, are derived from a sphingoid base such as sphingosine with a fatty acid moiety, and can be modified to produce glycosphingolipids by addition of sugar head groups. NANA = n-acetylneuraminic acid, a sialic acid.

**1.2.2 Sterols**

In mammals, sterols - primarily cholesterol - are obtained from both dietary intake and *de novo* synthesis (Ikonen, 2008). Uptake and recycling of sterols requires trafficking through the endocytic and lysosomal system, and sterol distribution and metabolism are under tight control. Cholesterol is important for modulation of membrane fluidity and curvature, and sterols are used in synthesis of bile acids and steroid hormones. The brain contains approximately a quarter of the body's cholesterol in cell membranes and myelin, which does not come from the diet as it cannot cross the blood-brain barrier and is largely synthesised by glia (Petrov, Kasimov & Zefirov, 2016). Cholesterol is synthesised from HMG-CoA (3-hydroxy-3-methylglutaryl-coenzyme A). The initial and rate-limiting step is reduction by HMG-CoA reductase to produce mevalonic acid, which leads via multiple steps to the first sterol precursor, lanosterol. Two possible pathways lead from lanosterol to cholesterol, known as the Bloch (Olson, Lindberg & Bloch, 1957; Gautschi & Bloch, 1958) and Kandutsch-Russell (Kandutsch & Russell, 1960) pathways (Figure 1.3), which have the same steps and enzymes but the double bond in the side chain is removed at different stages (Mitsche *et al.*, 2015). The balance between these two pathways, and so the levels of the differing intermediates, varies between tissues, with the brain primarily using the Kandutsch-Russell pathway (or a modified version) (Mitsche *et al.*, 2015). Cholesterol can be further modified by the addition of hydroxyl groups, producing oxysterols which have signalling roles and also allow the molecule to leave the cell and be trafficked to the liver for clearance (Ikonen, 2008).

Uptake of extracellular cholesterol derived from the diet or from synthesis by other cells is also an important source. Cholesterol is packaged into lipoproteins, released, and picked up by low-density lipoprotein (LDL) receptors on other cells. Receptors with LDL bound are internalised to endocytic sorting compartments, where the receptors are returned to the cell surface and the released lipoproteins are trafficked to the lysosome and processed by acid lipase to produce free cholesterol (Ikonen, 2008). Cholesterol from recycled cell membranes is also processed in the late endosome and lysosome.

HMG-CoA
(3-hydroxy-3-methyglutaryl-CoA)

↓ HMG-CoA reductase

mevalonic acid

↓
↓
↓

lanosterol ⟶ dihydrolanosterol
24-DHC reductase

Bloch                                    Kandutsch-Russell

lathosterol

↓

7DHC
7-dehydrocholesterol

↓ 7-DHC reductase

desmosterol ⟶ cholesterol
24-DHC reductase
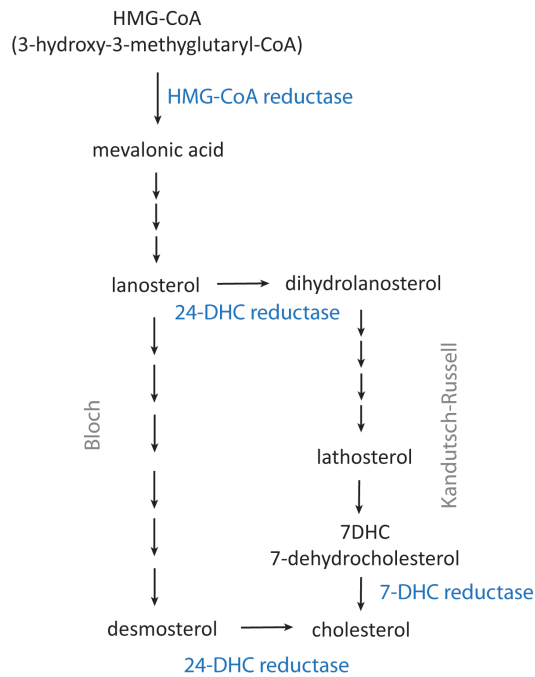
**Figure 1.3 Cholesterol metabolism**
Outline of *de novo* cholesterol synthesis.  HMG-CoA reductase catalyses synthesis of mevalonic acid, the rate limiting step, which is converted to lathosterol.  24-dehydrocholesterol reductase can act on either lathosterol, desmosterol or the intermediate sterols.  Multiple arrows indicate steps not shown, key sterol intermediates are named, and key enzymes are given in blue.

From the late endosome and lysosome, cholesterol returns to other cellular compartments by a number of routes (Ikonen, 2008; Miller & Bose, 2011). The lysosomal membrane proteins LIMP2 (Neculai *et al.*, 2013), LAMP1 and LAMP2 (Li & Pfeffer, 2016) are potentially able to transport cholesterol, and as cholesterol exit from the lysosome is affected by loss of the NPC proteins NPC1 and NPC2 (Ikonen, 2008) it has been suggested that these proteins are also involved in cholesterol transport (Sturley *et al.*, 2004), though there is no direct evidence of this. From the lysosome, cholesterol is trafficked to the Golgi and endocytic recycling compartments via Rab-mediated pathways (Hölttä Vuori *et al.*, 2002), and to some extent to the cell surface, whereas newly-synthesised cholesterol from the ER is transported mainly to the plasma membrane (Ikonen, 2008). Cholesterol is also transported from the late endosome and lysosome to the mitochondria, a route involving a late-endosomal sterol-binding protein called MLN64 (Zhang *et al.*, 2002; Charman *et al.*, 2010). Cholesterol is trafficked via vesicle transport routes, via membrane contact points (Chu *et al.*, 2015), and via cytoplasmic lipid binding proteins.

The major sensors of cellular cholesterol are SREBPs (sterol regulatory element binding proteins) in the ER. Reduced sterol levels lead to transport of SREBP from the ER to the Golgi, followed by cleavage and entry into the nucleus, where it upregulates genes for sterol synthesis and uptake including HMG-CoA reductase and the LDL receptor. In high sterol conditions the ER proteins SCAP (SREBP cleavage-activating protein) and INSIG (insulin induced gene 1) bind cholesterol and oxysterols (Radhakrishnan *et al.*, 2007) and block export of SREBP, preventing gene activation (Ikonen, 2008). High levels of oxysterols also activate liver X receptors (LXRs), nuclear receptors which suppress cholesterol synthesis and uptake and upregulate trafficking and secretion proteins such as ABCA1 (ATP-binding cassette transporter A1) and apolipoprotein E to reduce cellular cholesterol (Zhao & Dahlman-Wright, 2010). Other regulatory pathways are less well characterised. High lysosomal cholesterol activates mTORC1 via the lysosomal membrane protein SLC38A9 (a member of the solute carrier family), a signal which is blocked in low cholesterol conditions by the NPC protein NPC1 (Castellano *et al.*, 2017). Cholesterol metabolism also interacts with or is regulated by other lipids (Ridgway *et al.*, 1999), including sphingosine-1-phosphate (Vienken *et al.*, 2017), interactions which contribute to the adaptability of cellular lipid membrane properties.

**1.2.3 Glycerolipids**

Glycerolipids are composed of fatty acids attached to a glycerol backbone, sometimes with additional headgroups. The major classes are triacylglycerides (three acyl chains per glycerol molecule) which are primarily storage lipids, and phospholipids (two acyl chains and a phosphate group) which are the main component of cell membranes. The term phospholipid here (and usually) refers to these phosphoglycerolipids, although sphingolipids with a phosphate head group are also phospholipids. They modify membrane curvature (Farge, 1995) and stability, and the integration and function of membrane proteins, and thereby affect membrane trafficking and function. One class of phospholipids, the phosphatidylinositols, are important signalling lipids in the cell (Irvine *et al.*, 1988; Hughes & Putney, 1990; Abel, Anderson & Shears, 2001). They are the substrates for production of the inositol phosphate second messengers, particularly $IP_3$ which has roles in $Ca^{2+}$ signalling.

Fatty acids are long carbon chains with a carboxylic acid head. Biosynthesis involves the enzyme complex fatty acid synthase, which controls repeated addition of acetyl-

CoA to form a chain, which can then be attached to glycerol to create glycerolipids. These lipids can also be absorbed from the diet. Degradation of fatty acids occurs by oxidation in the mitochondria. Fatty acid synthesis in mammalian cells generally produces chain lengths of 16 (palmitic) or 18 (oleic) carbons, with 0-2 unsaturated bonds (Figure 1.2). Some tissues produce shorter or much longer fatty acids for different roles, and this chain length also varies between organisms.

### 1.2.4 Sphingolipids

Sphingolipids are formed from sphingoid bases, lipids composed of a long carbon chain with an amine head group rather than a carboxylic acid. Addition of fatty acids and head groups produces a number of important lipids. Sphingosine is the main sphingoid base in mammals, usually with an 18 carbon chain, and phosphorylation of sphingosine produces sphingosine-1-phosphate, a highly-active and wide-ranging signalling molecule which is dysregulated in many diseases, including cancer and neurodegeneration (Spiegel & Milstien, 2003; Maceyka *et al.*, 2012; Liu, Zhang & Yi, 2012). Sphingosine bound to a fatty acid produces ceramide, which is involved in apoptotic signalling, and addition of a phosphate group to ceramide produces sphingomyelin, a major structural lipid particularly important in myelin.

Sphingolipid synthesis and recycling (Figure 1.4) are closely linked, as sphingosine can only be produced from degradation of existing sphingolipids. The salvage pathway is a core part of biosynthesis of these lipids. Ceramide can be synthesised in the ER and converted to sphingomyelin or glycosphingolipids in the Golgi, and sphingolipids can be taken up or recycled from cell membranes into the endocytic system. In the lysosome, sphingolipids are broken down to sphingosine, which exits the lysosome by an unknown route, potentially involving NPC1 (Lloyd-Evans *et al.*, 2008), for use in the cell (Kitatani, Idkowiak-Baldys & Hannun, 2008; Huwiler *et al.*, 2000).

### 1.2.5 Glycosphingolipids

Addition of sugar head groups to ceramide produces glycosphingolipids (GSLs), which are important molecules with roles in signalling and cell interaction. The first step in synthesis is addition of a single sugar to produce glucosylceramide (Figure 1.4), from which the rest of the GSLs - dozens of species in mammalian cells - are produced. They are important for developmental signalling (Pontier & Schweisguth, 2011) and in the nervous system, with mutations causing loss of GSL synthesis often leading to defects

in neuronal development or maintenance (Yu *et al.*, 2011). They are also involved in membrane microdomains and cellular trafficking (Mayor, Parton & Donaldson, 2014; Pontier & Schweisguth, 2011), and are targets for invasion by infectious disease such as cholera.
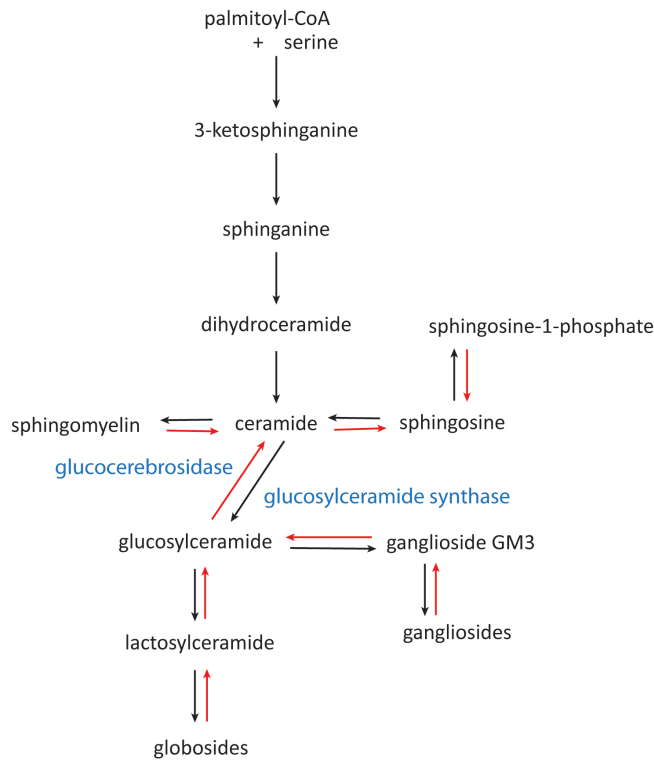


**Figure 1.4 Sphingolipid metabolism**
Outline of relevant pathways in sphingolipid metabolism, including *de novo* synthesis of ceramide, production of sphingosine by ceramide degradation, and addition of sugar head groups to ceramide to produce glycosphingolipids (GSLs) including the gangliosides. Glucosyl-ceramide synthase, which catalyses addition of the first sugar group to ceramide, is the target of miglustat.

## 1.3 Lysosomes in disease

Lysosomal dysfunction and changes to related mechanisms such as autophagy and protein homeostasis contributes to a broad range of diseases. Loss of lysosomal function leads to lysosomal storage disorders (LSDs) but partial defects can also contribute to disease, particularly in neurodegeneration (Maxfield, 2014; Nixon, 2016; Zhang, Sheng & Qin, 2009) but also in cardiovascular disease (Terman *et al.*, 2008; Maxfield, 2014) and cancer (Kirkegaard & Jäättelä, 2009). Defects in lysosomal acidification have been observed in Alzheimer's disease (Colacurcio & Nixon, 2016),

and autophagy is reduced in several neurodegenerative diseases and boosting it can be beneficial, as it enables clearance of aggregated proteins or defective organelles (Nixon, 2013; García-Arencibia *et al.*, 2010; Menzies, Fleming & Rubinsztein, 2015). Lysosomal function can decrease or alter with age, and so is a contributing factor in healthy aging and risk of age-related disease (Carmona-Gutierrez *et al.*, 2016; Colacurcio & Nixon, 2016; Nixon, 2016).

LSDs are a group of at least 60 inherited disorders caused by genetic defects in lysosomal enzymes or, more rarely, in proteins involved in lysosomal structure and function, or cellular trafficking (Cox & Cachón-González, 2012; Platt, Boland & van der Spoel, 2012). Loss of protein function causes accumulation of materials in the lysosome and late endocytic system, leading to cellular damage and disease. These disorders are heterogeneous in severity, primary and secondary storage materials, cellular phenotypes and clinical symptoms. Storage materials can include a broad range of carbohydrates, proteins or lipids; or several different classes of compounds can be stored in a single disease. While individually rare, the combined incidence of these diseases has been estimated as 12.5 - 13.3 per 100,000 (Meikle *et al.*, 1999; Poupetová *et al.*, 2010). Many of them are neurological, including many childhood neurodegenerative diseases (Vellodi, 2005; Platt, Boland & van der Spoel, 2012). For the majority of these diseases, pathogenesis is only partially understood (Cox & Cachón-González, 2012), and there is little in the way of treatment.

Their heterogeneity can make these diseases difficult to classify usefully. One approach is to group them based on the primary storage material (Vellodi, 2005), which can be useful when common phenotypes are due to common mechanisms, but less useful if not. Alternatively, these diseases can be divided into categories based on whether the affected protein is a specific degradative enzyme or a lysosomal membrane protein (Platt, Boland & van der Spoel, 2012), though some LSDs do not fit these two categories or are not well enough understood. Loss of a specific enzyme leads to primary accumulation of a single substrate, for example accumulation of glucosylceramide due to loss of glucocerebrosidase (GBA) in Gaucher disease. The disorders in the second group can be clear, for example if a specific solute channel is lost (Kalatzis *et al.*, 2001), or can be more complicated, with involvement of proteins of unknown function or storage of multiple materials, as in NPC.

Research into lysosomal storage disorders has not only helped patients but has helped understand the lysosome itself, and has provided insight into pathogenic mechanisms present in other diseases (Cox & Cachón-González, 2012). The field has also made major contributions towards the development of technologies and treatments such as enzyme replacement (Desnick, Thorpe & Fiddler, 1976; Neufeld, 2006) and gene therapies (Sands & Davidson, 2006; Biffi, 2016). Better understanding of lysosomal function and pathways such as protein homeostasis and autophagy (García-Arencibia *et al.*, 2010) has informed research into healthy aging and risk factors for many diseases (Carmona-Gutierrez *et al.*, 2016; Nixon, 2016; Zhang, Sheng & Qin, 2009).

## 1.4 Niemann-Pick type C disease

### 1.4.1 Outline

Niemann-Pick type C (NPC) is an inherited recessive lysosomal storage disease with predominantly neurodegenerative symptoms (Vanier, 2010). Classical NPC disease develops in infancy or early childhood and patients generally do not survive past early adulthood. However, adult-onset forms have also been identified, especially as sequencing has improved (Sévin *et al.*, 2007). Classical NPC cases are very rare, with an estimated clinical incidence of 0.8 - 1.1 per 100,000 (Wassif *et al.*, 2015; Vanier, 2010). NPC2 mutations, which cause 2 - 5% of cases, are even rarer, with an estimated incidence of 1 in 2,900,000 (Wassif *et al.*, 2015). However, the incidence of adult onset NPC (caused by variant NPC1 mutations) may be as high as 2.8 - 5.3 per 100,000, based on recent analysis of datasets from large human sequencing projects (Wassif *et al.*, 2015). While NPC1 mutation is recessive, there is evidence that heterozygote carriers also have altered cellular function and risk of other neurodegenerative diseases (Yu *et al.*, 2005; Kluenemann *et al.*, 2013). The pathological course of the disease is complex, involving storage of multiple lipids in lysosomes, and the mechanisms are not yet understood (Vanier, 2010).

### 1.4.2 Clinical symptoms

NPC patients have both neurological and visceral symptoms, though the neurological symptoms are the main component. Disease course is variable, but if visceral symptoms are present they appear before neurological defects, are less severe, and can sometimes stabilise or reduce, whereas the neurological defects are progressive

(Vanier, 2010). The visceral (or systemic) features of the disease consist of enlargement of the liver and spleen (hepatosplenomegaly), and occasionally lung problems, due to accumulation of lipids in these organs. Neurological symptoms mainly include ataxia due to degeneration of cerebellar purkinje neurons, dystonia (muscle contractions affecting posture) and bradykinesia (slow execution of movement) motor defects in speech (dysarthria) and swallowing (dysphagia), progressive dementia, and vertical supranuclear gaze palsy (VSGP; a defect in eye movement and tracking) (Salsano *et al.*, 2012), and sometimes muscle weakness and seizures.

### 1.4.3 Genetic basis

NPC is an inherited disorder, caused by mutations in one of two genes. In approximately 95% of cases the *NPC1* gene is affected, with the remaining cases caused by mutations in a second gene, *NPC2* (Vanier, 2010), which produces a disease that is clinically identical and pathologically extremely similar. Neither NPC1 or NPC2 (Figure 1.5) are degradative enzymes and the function of NPC1 is still poorly understood.
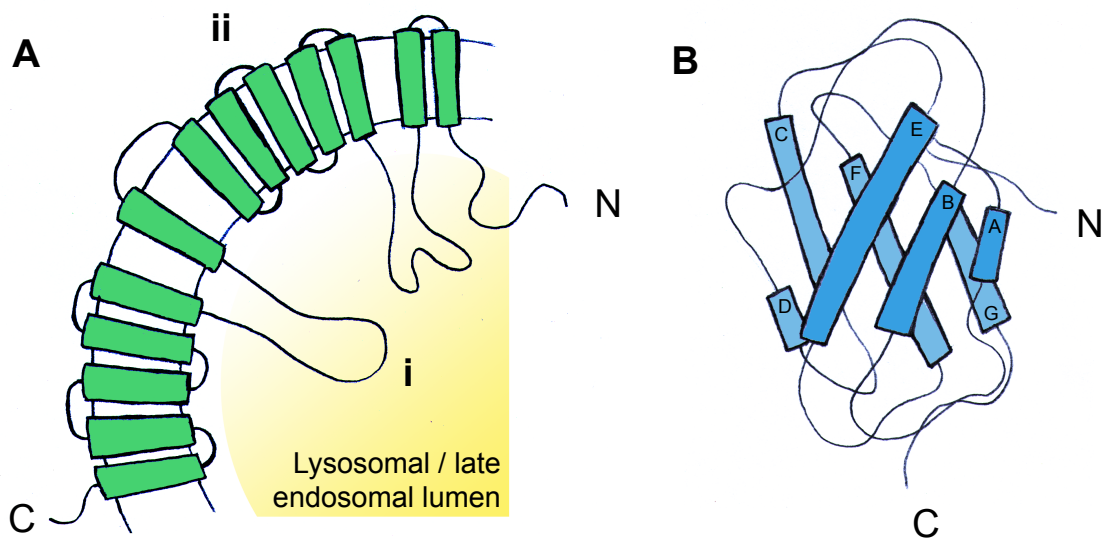


**Figure 1.5 Structure of NPC proteins**
**A** Predicted topology of NPC1, a 1278 amino acid protein predicted to have 13 transmembrane domains (green), a cysteine-rich loop region (**i**) and a region with homology to sterol sensing domains (**ii**). **B** Structure of NPC2, a soluble lysosomal protein of 130 amino acids. The two β sheet regions are coloured blue. Cholesterol binds in a pocket between the two β sheets, towards the C terminal end of the protein.

NPC2 is a small soluble lysosomal protein, which is also secreted by the liver (Klein *et al.*, 2006), epididymus (Naureckiene, 2000) and astrocytes (Mutka *et al.*, 2004). It binds cholesterol (Friedland *et al.*, 2003; Xu *et al.*, 2007) and is suggested to be involved in cholesterol transport, possibly from inner lysosomal membranes (membranes within the lysosome that are being degraded) to the lysosomal outer membrane from where it can be trafficked and recycled (Rosenbaum & Maxfield, 2011). Its role as a secreted protein is not yet clear, though it could be involved in cholesterol transport or binding in bile and plasma (Klein *et al.*, 2006). Interestingly, NPC2 homologues in ants are involved in chemosensing (Ishida *et al.*, 2014), and the family of homologues in *Drosophila melanogaster* may be immune signalling proteins (Shi, Zhong & Yu, 2012), with both these roles involving lipid binding.

NPC1 is a large 13 transmembrane domain protein present in the late endosome/lysosome outer membrane. Crystal and cryo-EM structures of NPC1 were published in 2016 (Gong *et al.*, 2016; Li *et al.*, 2016; Zhao *et al.*, 2016), including one bound to a protein of the ebola virus which uses NPC1 as a receptor for cell entry (Carette *et al.*, 2011). One major theory is that NPC1 may be a transporter of some kind. Involvement in cholesterol transport has been suggested (Sturley *et al.*, 2004; Rosenbaum & Maxfield, 2011), but there is no direct evidence for this, and there are other potential routes for lysosomal cholesterol trafficking including the LIMP2 protein (Neculai *et al.*, 2013). Cholesterol can also leave the NPC lysosome via increased traffic to the mitochondria (Charman *et al.*, 2010), via upregulation of Rab9 (Walter, Davies & Ioannou, 2003) or ABCA1 (Boadu, Nelson & Francis, 2012), or via modulation of $Ca^{2+}$ signalling (Chen, Li & Ioannou, 2010; Lloyd-Evans *et al.*, 2008). NPC1 could also transport other substrates, as it belongs to a family of bacterial proteins called the RND permeases, a class of multi-substrate transporters, and can transport known RND permease substrates acriflavine and oleic acid (but not cholesterol) when expressed in *E. coli* (Davies, 2000). Ncr1, the yeast orthologue of NPC1, has a role in sphingolipid trafficking and can rescue loss of NPC1 function in mammalian cells (Malathi *et al.*, 2004).

There is strong evidence that NPC1 may have signalling functions. A region corresponding to predicted transmembrane domains 2-6 has around 30% sequence similarity to sterol sensing domains (SSDs) in proteins such as the sterol regulatory

element binding protein (SREBP) and Patched (Carstea *et al.*, 1997), both proteins which signal based on cholesterol binding, although overall similarity of NPC1 to other SSD proteins is lower than to the RND permease family. It has also recently been shown that NPC1 is part of a signalling complex via which mTORC1 responds to levels of lysosomal cholesterol: in low cholesterol, NPC1 binds to SLC38A9 and inhibits its activation of mTORC1 (Castellano *et al.*, 2017). While the authors state this requires cholesterol transport by NPC1, there does not seem to be any evidence that transport rather than sterol sensing is required.

Despite defects in NPC1 and NPC2 leading to very similar diseases - almost identical in cellular phenotypes – it is not yet clear whether the two proteins interact or how they are related. An NPC1 and NPC2 double knock-out mouse model did not have any worsening in disease phenotypes, suggesting that the two proteins act in the same pathway (Sleat *et al.*, 2004). Additionally, levels (Blom, 2003; Chen, Gordon & Ioannou, 2005), glycosylation (Chen, Gordon & Ioannou, 2005) and localisation (Chen, Gordon & Ioannou, 2005; Blom, 2003) of NPC2 are reported to be abnormal when NPC1 defects are present, so the similarity in phenotype could be due to presence of NPC2 defects in both cases. The two proteins may also directly interact. Potential interaction regions have been identified (Wang *et al.*, 2010; Zhao *et al.*, 2016), and one study has observed an interaction via affinity chromatography (Deffieu & Pfeffer, 2011). NPC2 potentially delivers cholesterol to NPC1 (Infante *et al.*, 2008; Gong *et al.*, 2016) or removes it. It has been suggested that this is a component of transport of cholesterol out of the lysosome or to the lysosomal outer membrane (Sturley *et al.*, 2004; Wang *et al.*, 2010), although there is no direct evidence that NPC1 transports cholesterol and the proposed NPC2 binding site within NPC1 is in the lumenal N-terminal domain which would be separated from the membrane by distance and the glycocalyx (Gong *et al.*, 2016). Another possibility is that this interaction has a signalling role, as cholesterol binding to NPC1 is likely to be a signalling event (see above), an interesting possibility considering the signalling roles of NPC2 proteins in insects (Ishida *et al.*, 2014; Shi, Zhong & Yu, 2012).

**1.4.4 Pathology**

Defects in NPC1 or NPC2 lead to storage of multiple lipids in lysosomes, including cholesterol, sphingomyelin, sphingosine, glycosphingolipids and the lysosomal and late

endosomal lipid lyso-bisphosphatidic acid (LBPA). Alongside lipid storage, the other key cellular phenotypes of the disease are a severe defect in lysosomal $Ca^{2+}$ signalling and a profound block in endocytic trafficking.

Identification of the initial defect and the mechanisms that cause each component, and therefore the pathogenic cascade, has been very difficult. The relative importance of the different storage materials in NPC is debated (Lloyd-Evans & Platt, 2010), further confounding attempts to understand pathogenesis and the normal functions of NPC1 and NPC2. While cholesterol has classically been considered the most important component, strong evidence also exists for the importance of glycosphingolipids (Vruchte, 2004) and sphingosine (Lloyd-Evans *et al.*, 2008). Not all tissues or cell types have increases in total lipid, but the blocks in trafficking are present and these cell types show lysosomal storage when provided with excess lipid in culture (Sokol *et al.*, 1988).

Cholesterol is the primary storage material by mass in peripheral tissues. While total cholesterol in the brain is unchanged, neurons have mislocalised cholesterol (Karten *et al.*, 2002) and can be made to store higher levels of cholesterol if grown in lipid- or serum-containing medium, indicating that the same defect in trafficking is present and the lower levels may be due to the different cholesterol use and trafficking in the brain. However, the exact involvement of NPC1 and NPC2 in cholesterol trafficking is not clear (see above), and it has been shown both that cholesterol-lowering therapies are not beneficial against neurological symptoms (Erickson *et al.*, 2000) and that effective NPC therapies do not have to lower cholesterol to improve function (Vruchte, 2004).

Sphingosine is highly elevated in NPC patients compared to normal levels, with a very high fold increase in the brain (Sturley *et al.*, 2004; Lloyd-Evans *et al.*, 2008). While total levels of sphingosine are low (in both normal conditions and NPC) the impact of changes to this lipid may be considerable, as exit of sphingosine from the lysosome is required for the production of sphingosine-1-phosphate (Tettamanti *et al.*, 2003), a potent signaling lipid involved in $Ca^{2+}$ signalling, cell survival and other intra- and extracellular pathways (Maceyka *et al.*, 2005). Sphingosine accumulation is an early event in pathogenesis, occurring before increases in cholesterol, and increased lysosomal sphingosine causes decreased lysosomal $Ca^{2+}$ signalling (Lloyd-Evans *et al.*,

2008). It has been proposed that NPC1 defects initially cause sphingosine accumulation, which disrupts $Ca^{2+}$ and cellular signalling (Hannun & Bell, 1989) and leads to trafficking defects and secondary storage of multiple lipids (Lloyd-Evans et al., 2008).

The cellular defects present in NPC patients primarily cause degeneration of the cerebellar Purkinje neurons, but the mechanisms behind this specific sensitivity are not yet known. Other regions are also affected, particularly later in the disease course, including other motor regions - striatal neurons derived from the NPC mouse model have defects in cholesterol processing and response to BDNF (Henderson et al., 2000).

### 1.4.5 Potential therapies

NPC remains a poorly understood disease, and available treatments mainly consist of symptom management. Miglustat is currently the only disease modifying therapy, approved in Europe but not the USA, although progress is also being made in developing cyclodextrin as another potential therapy.

| Therapy | Status | Mechanism |
|---|---|---|
| HPβCD | Experimental; in Phase 2 trial | Unknown (Pontikis et al., 2013) |
| Miglustat | Approved therapy other than in the US, where patient numbers are too low for FDA approval | Inhibition of sphingolipid biosynthesis (Lachmann et al., 2004) |
| Curcumin | Not approved as a therapy but taken as a dietary supplement | Calcium modulator (Lloyd-Evans et al., 2008) |
| Anti-inflammatory drugs | Experimental or not approved (failed to show benefit) | Suppression of neuroinflammation (Smith et al., 2009a) |
| Phytic acid | Experimental; to be tested in animal models | $Zn^{2+}$ chelation (E. Maguire, E. Clark et al, unpublished data) |
| HDAC (histone deacetylase) inhibitors | Experimental; moving towards Phase 1 trials | Presumed chaperoning of NPC1 (Helquist et al., 2013), although some evidence of effect in NPC1-null cells so other mechanisms may be involved |
| HSP70 | Experimental; in Phase 2 trial | Stabilisation of lysosomes and acid-sphingomyelinase activity (Kirkegaard et al., 2010) |

**Table 1.1** Some potential therapies for Niemann-Pick type C disease

The iminosugar miglustat is an inhibitor of glucosylceramide synthase and therefore of glycosphingolipid (GSL) synthesis. Originally a potential anti-retroviral drug, it was developed as a substrate reduction therapy for the glycosphingolipidoses, primary lysosomal storage diseases where enzymatic GSL degradation in lysosomes is defective and GSLs are stored (Platt et al., 2001). GSLs are also prominent storage lipids in NPC,

and some trafficking defects and other phenotypes are similar in both diseases, so miglustat was developed for NPC (Lachmann *et al.*, 2004; Patterson *et al.*, 2007). It improves trafficking in cells, is beneficial in the NPC1 mouse model and was found to reduce lysosomal storage in an initial off-label trial (Lachmann *et al.*, 2004) and to stabilise neurological disease in full clinical trials (Patterson *et al.*, 2007; Wraith *et al.*, 2010; Fecarotta *et al.*, 2015).

Cyclodextrins are cyclic oligosaccharides used as chaperones or solubilising agents in drug delivery. They are able to solubilise lipids and remove them from membranes, and have been used as a tool to manipulate and investigate membrane cholesterol (Christian *et al.*, 1997). Treatment with hydroxypropyl-β-cyclodextrin (HPβCD) greatly reduces lipid storage in NPC cells and produces dramatic improvement in the mouse model of the disease (Davidson *et al.*, 2009), and clinical trials begun in 2013 in the USA and shortly after in Europe. The mechanism by which HPβCD treatment improves NPC is not yet known, particularly as as HPβCD improves neurological symptoms without crossing the blood brain barrier (Pontikis *et al.*, 2013), but it may involve direct binding and removal of cholesterol (Rosenbaum & Maxfield, 2011) or modulation of trafficking and $Ca^{2+}$ signalling (Chen, Li & Ioannou, 2010).

## 1.5 Huntington's disease

### 1.5.1 Outline

Huntington's disease (HD) is an inherited autosomal dominant neurodegenerative disorder with an incidence of 5 - 10 per 100,000 in European and American populations (Pringsheim *et al.*, 2012; Evans *et al.*, 2013). It is caused by a dominant mutation in huntingtin, which leads to protein aggregation, cellular toxicity, and neuronal death, particularly in the striatum. Onset of disease is around 40 years of age, and patients undergo psychiatric, motor and cognitive decline, and die after 15-20 years (Roos, 2010). Juvenile forms also exist, related to more extreme mutations and with an age of onset below 20 years, with an incidence of about 5-10% of all HD cases (Quarrell *et al.*, 2012).

### 1.5.2 Clinical symptoms

Huntington's disease is characterised by a triad of motor, cognitive and psychiatric symptoms, alongside other features such as defects in metabolism and sleep (Roos,

2010; Novak & Tabrizi, 2010). The onset of disease is defined by the appearance of motor defects, but cognitive and psychiatric symptoms are often present much earlier, in the 'premanifest' period, although the earliest symptoms and those that are first noticed vary between patients (Novak & Tabrizi, 2010).

The classical symptom of Huntington's disease is chorea, which consists of quick, irregular, involuntary movements. Other motor defects include dystonia (muscle contractions leading to twisting or abnormal posture), bradykinesia (slow execution of movement), rigidity and dysphagia (difficulty swallowing). The balance of these symptoms can vary between patients, and more extreme mutations or early onset can correlate with a more dystonic rather than choreic form of the disease (Louis *et al.*, 2000).

Psychiatric disturbance includes a high incidence of depression, which is to some extent a direct component of the disease rather than a response to diagnosis (Novak & Tabrizi, 2010; Paulsen *et al.*, 2005). Suicide rates can be significantly higher in Huntington's patients than in the general population (Sørensen & Fenger, 1992). Anxiety, irritability, obsessive-compulsive behaviour and sometimes psychosis are also observed. Cognitive symptoms centre around disorganisation and loss of executive function, impulsivity, and deterioration of memory (Roos, 2010; Novak & Tabrizi, 2010).

### 1.5.3 Genetic basis

Huntington's disease is associated with a single gene, *huntingtin (HTT)*, which was localised to chromosome 4 by Gusella *et al* in 1983 (Gusella *et al.*, 1983) and identified ten years later by a collaborative research group with access to multiple Huntington's disease families (Group, 1993). The gene codes for a large (3144 amino acid) widely expressed protein called huntingtin (HTT), the function of which is not yet fully understood.

Huntingtin (Figure 1.6) is a large protein (3144 amino acids, 348kDa), the full structure of which is not known. The N-terminal region contains, very near the start of the protein, the polyglutamine (polyQ) stretch followed by a proline-rich region. There are a number of functional motifs present in the protein which include multiple protein interaction domains called HEAT repeats, 40-amino-acid motifs named after the four proteins in which they were first identified: <u>h</u>untingtin, <u>e</u>longation factor 3, regulatory

<u>A</u> subunit of protein phosphatase 2A, and <u>t</u>arget of rapamycin 1 (Andrade & Bork, 1995). Huntingtin also has sites for protease cleavage (Cattaneo, Zuccato & Tartari, 2005); targets for addition of the small protein tags SUMO (Steffan *et al.*, 2004) and ubiquitin (Kalchman *et al.*, 1996) which are involved in cellular signalling, trafficking, and protein degradation;  targets for palmitoylation (Huang *et al.*, 2004) and myristoylation (Martin *et al.*, 2014), addition of fatty acid groups which modulate signalling and act as membrane anchors; and residues which are targets for phosphorylation (Humbert *et al.*, 2002; Luo *et al.*, 2005), suggesting huntingtin is regulated by many systems. Alternative splicing (Hughes *et al.*, 2014), proteolysis, and modification of huntingtin produce multiple forms of the protein.
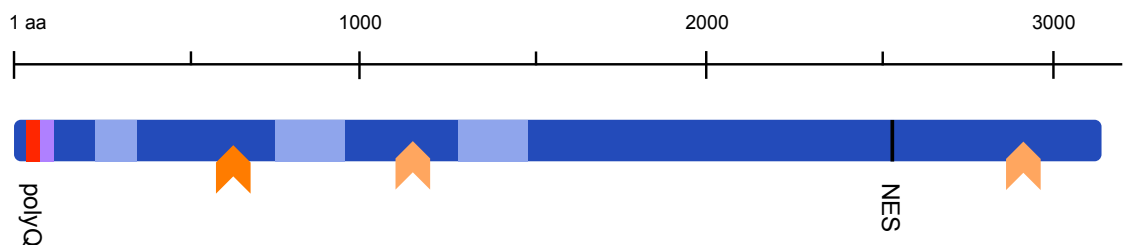


**Figure 1.6 Key features of huntingtin**
Diagram of huntingtin, with some known motifs. Indicated are the polyglutamine repeat section (polyQ, red bar), the proline-rich domain (purple bar), the HEAT repeat clusters (pale blue), the nuclear export sequence (NES, black line), and areas with protease sites (orange arrows). Scale is amino acid (aa) number.

The first exon of the gene contains a repeat of the CAG trinucleotide, which is translated to glutamine (Q), producing a polyglutamine stretch in the protein. In humans this normally contains up to 30 CAG repeats, and expansion of the CAG repeat above 40 units leads to Huntington's disease with complete penetrance.  The effects of intermediate CAG lengths are uncertain: 36 – 40 CAG repeats are associated with partial penetrance (some but not all gene carriers end up with disease) or very late onset of disease. The CAG trinucleotide repeat is unstable during replication and is prone to expansion through generations, particularly if the CAG repeat is in the 30 – 35 range and particularly in the male line (Trottier, Biancalana & Mandel, 1994). CAG repeat length correlates with age of onset, with juvenile Huntington's disease commonly associated with repeats of over 60 trinucleotide units, which are due to expansion in an allele from an affected parent (Roos, 2010). Rarely, patients can carry

two expanded *HTT* alleles, and homozygosity is associated with a normal age of onset but more severe clinical course once disease appears (Squitieri *et al.*, 2003).

The connection between this protein defect and pathogenesis of the disease is not understood. Expansion of the polyglutamine repeat causes the protein to become prone to aggregation, and most evidence suggests that the pathogenic effects stem from both this gain of function and, to some extent, from loss of normal huntingtin functions.

### 1.5.4 Pathology

The key step in the pathology of Huntington's disease, as in all neurodegenerative diseases, is the death of neurons. In HD, cell death is greatest among the medium spiny neurons of the striatum, as well as the rest of the basal ganglia (the caudate and putamen). Later in the disease course, or in more severe HD cases, cell loss becomes more extensive, particularly following the affected motor circuits which extend to and from the basal ganglia into the cortex and cerebellum. Intracellular aggregates of mutant huntingtin are also found in both the nucleus and cytoplasm of neurons throughout these same affected brain regions in post-mortem brains and in animal models (DiFiglia *et al.*, 1997; Arrasate & Finkbeiner, 2012). Defects in synaptic structure and function are also observed in HD, particularly reduced production and trafficking of the survival factor BDNF and altered receptor expression, which leads to excitotoxicity (Sepers & Raymond, 2014).

## 1.6 Cellular Pathology of Huntington's disease

### 1.6.1 Outline

The network of HD pathogenesis is not yet clear, but many components of cellular dysfunction have been identified (Landles & Bates, 2004; Ross & Tabrizi, 2011). These include changes to lipid metabolism and lysosomal function which are of particular interest to us, as they suggest possible links to the lysosomal diseases we study.

### 1.6.2 Mutant huntingtin

The expansion of the polyglutamine repeat in huntingtin (Figure 1.6) leads to protein aggregation, abnormal splicing and post-translational modifications, and abberant interactions with other proteins. Splicing of mutant huntingtin mRNA is altered (Sathasivam *et al.*, 2013; Mort *et al.*, 2015), as is cleavage of the protein by proteases

(Lunkes *et al.*, 2002; Warby *et al.*, 2008; Kim *et al.*, 2001), and protein phosphorylation (Warby *et al.*, 2005; Luo *et al.*, 2005), producing multiple modified proteins, some of which may only be present in the mutant and not the normal state. It is unclear what the toxic species of huntingtin is, and whether the aggregates or inclusions are themselves harmful or can be protective in some cases, by removing mutant protein from circulation. Aggregation and abnormal interactions can also sequester other proteins and thereby disrupt cellular function (Yang & Hu, 2016).

**1.6.3 Defects in cellular trafficking**

HD cells have defects in many aspects of cellular transport and trafficking, a central defect which contributes to other pathogenic events. In fact, a number of huntingtin binding partners are endocytic proteins (Tourette *et al.*, 2014; Pal *et al.*, 2006). While the initial stages of clathrin-mediated endocytosis are not altered (Li *et al.*, 2009; Trushina *et al.*, 2006), both clathrin (Yu *et al.*, 2014a) and caveolin (Trushina *et al.*, 2006) are disrupted by mutant huntingtin, and caveolin-dependent endocytosis is affected (Trushina *et al.*, 2006). Formation and exit of vesicles from the recycling endosome is impaired (Li *et al.*, 2009; Akbergenova & Littleton, 2017) and trafficking of key proteins to and from the cell surface is disrupted, including BDNF receptors (Liot *et al.*, 2013), the glutamate transporter EAAC1 (Li *et al.*, 2010), and the iron binding and uptake protein transferrin (Li *et al.*, 2009). Mutant huntingtin disrupts trafficking and vesicular secretion of BDNF in neurons (Del Toro *et al.*, 2006) and insulin in β cells (Smith *et al.*, 2009b), and trafficking of secreted proteins between the Golgi and lysosome (Del Toro *et al.*, 2009). Axonal trafficking is impaired (Weiss & Littleton, 2016) due to sequestration of essential proteins in huntingtin aggregates (Trushina *et al.*, 2004). Transport of mitochondria through the cell, a vital process particularly in neurons for energy balance and survival, is also impaired in HD (Li, Orr & Li, 2010).

**1.6.4 Transcriptional dysregulation**

Transcriptional dysregulation is present in HD, altering many pathways and thereby affecting cellular function (Giacomello *et al.*, 2013; Marchina *et al.*, 2014; Friedrich *et al.*, 2012; The HD iPSC Consortium, 2012). Some of this dysregulation may be an indirect result of cellular dysfunction, but huntingtin itself may also directly affect gene expression in cells. Huntingtin is present in the nucleus as well as the cytoplasm: protease-cleaved N-terminal fragments of huntingtin localise to the nucleus, and both

production of these fragments and their nuclear localisation are increased in mutant huntingtin (Wheeler *et al.*, 2000; Tao & Tartakoff, 2001). Mutant huntingtin binds to the transcription factor (TF) REST (Zuccato *et al.*, 2003; Conforti *et al.*, 2013) (repressor element 1 silencing transcription factor), which controls BDNF expression. Mutant huntingtin may alter transcription by affecting TF function, or by altering trafficking between the nucleus and cytoplasm.

## 1.6.5 Ca$^{2+}$ dyshomeostasis

Defects in cellular Ca$^{2+}$ homeostasis are present in HD and are comparatively well characterised. The presence of mutant huntingtin predisposes cells to elevated cytosolic Ca$^{2+}$ by affecting three major components of cellular Ca$^{2+}$ signalling, leaving HD cells more sensitive to excitotoxic cell death (Bano *et al.*, 2011). Entry of Ca$^{2+}$ into the cell is increased (Giacomello *et al.*, 2013), via increases in store-operated Ca$^{2+}$ entry (Giacomello *et al.*, 2013) and activity of the glutamate NMDA (N-methyl-D-aspartate) receptors (Bezprozvanny & Hayden, 2004; Del Toro *et al.*, 2010). Dysregulation of transcription and defects in cellular trafficking in HD may both contribute to increased levels of NMDARs at the cell surface. Secondly, release of Ca$^{2+}$ from the ER is increased due to sensitisation of the inositol triphosphate receptor InsP$_3$R1 (Bezprozvanny & Hayden, 2004), and levels and responses of the ER uptake pump SERCA (sarco/endoplasmic reticulum Ca$^{2+}$ ATPase) are altered - SERCA2 is decreased, SERCA3 is increased (Cesca *et al.*, 2014), and Ca$^{2+}$ release in response to SERCA inhibition (by cyclopiazonic acid) is increased (Costa *et al.*, 2010; Giacomello *et al.*, 2013). Finally, mitochondrial ability to buffer Ca$^{2+}$ is decreased (Panov *et al.*, 2002; Lim *et al.*, 2008), with several reports showing that the mitochondrial permeability transition, and so the switch to apoptotic signalling, occurs at lower Ca$^{2+}$ concentrations in HD models than in controls (Giacomello, Hudec & Lopreiato, 2011; Bezprozvanny & Hayden, 2004). There is no existing information on changes to lysosomal Ca$^{2+}$ in HD, but this is altered in several LSDs (Lloyd-Evans & Platt, 2011) and other neurodegenerative diseases (Lloyd-Evans *et al.*, 2010) and would be interesting to examine in HD.

## 1.6.6 Mitochondrial dysfunction

Mutant huntingtin causes severe disruption to mitochondria via a number of mechanisms including defective trafficking (Reddy & Shirendeb, 2012) and, potentially, disrupted autophagy. Evidence from knockout models indicates that normal huntingtin

is required for normal mitochondria (Ismailoglu *et al.*, 2014). The effects of mutant huntingtin include increased mitochondrial fission (Reddy & Shirendeb, 2012) and inhibition of the import of proteins into the mitochondria (Yano *et al.*, 2014).

### 1.6.7 Lysosomal dysfunction

Lysosomal defects have been observed in HD models. In HD model cells expressing full length or truncated huntingtin, or constructs matching fragments produced by caspase cleavage, huntingtin associates with the autophagic and endosomal-lysosomal systems, increases autophagic activation, and promotes the formation of enlarged lysosomal structures (Kegel *et al.*, 2000; Martin *et al.*, 2014). Huntingtin is also secreted via lysosomes, and both secretion and localisation to the lysosome are increased when mutant huntingtin is present (Trajkovic, Jeong & Krainc, 2017). Accumulation of lysosomes in the perinuclear region, with associated defects in lysosome dynamics and autophagic trafficking has been reported in a striatal cell line from a HD mouse model (ST*Hdh*) and HD patient fibroblasts (Erie *et al.*, 2015).

Recently, lysosomal expansion, identified by increased Lysotracker staining (a marker of lysosomal storage diseases (Lachmann *et al.*, 2004; Vruchte *et al.*, 2014)), was observed in induced pluripotent stem cell (iPSC) lines derived from mouse models and HD patient cells (Camnasio *et al.*, 2012; Castiglioni *et al.*, 2012). The lysosomal membrane protein LAMP-2A is also increased in HD models (Koga & Cuervo, 2011). Lysosomal changes may be related to association of huntingtin with lipid membranes and trafficking pathways, and huntingtin has been shown to be involved in cellular organisation and transport of endosomes and lysosomes (Caviston *et al.*, 2011).

### 1.6.8 Defects in autophagy

Autophagy is disrupted in HD. The presence of mutant huntingtin increases activation of autophagy (Ravikumar *et al.*, 2004; Kegel *et al.*, 2000), but the system is not effective at clearing toxic cargo (Martin *et al.*, 2015; Martinez-Vicente *et al.*, 2010). Mutant huntingtin interferes with recognition and clearance of appropriate cargo (Martinez-Vicente *et al.*, 2010), and also disrupts trafficking of autophagosome structures from sites of formation in the cell to the lysosome for clearance (Wong & Holzbaur, 2014). This leads to the presence of empty autophagic vacuoles, and accumulation of toxic materials which should have been cleared.

As well as macroautophagy, chaperone mediated autophagy, a pathway which targets specific proteins for lysosomal degradation, is increased in HD models (Koga & Cuervo, 2011), potentially as an attempt by the cell to compensate for failure to clear cargoes. Although debated, mutant huntingtin may also damage the activity of the ubiquitin proteasome system, another route for proteolytic degradation of some proteins (Imarisio *et al.*, 2008). Defects in clearance pathways exacerbate other HD defects, particularly the presence of huntingtin aggregates and defective mitochondria, increasing cell toxicity.

## 1.6.9 Lipid dyshomeostasis

### 1.6.9.1 Cholesterol

Cholesterol metabolism is altered in HD. Expression of the cholesterol biosynthetic genes HMG-CoA reductase, lanosterol 14α-demethylase (*Cyp51*), and 7-dehydrocholesterol reductase (*DHCR7*) is reduced in both rodent models (Valenza *et al.*, 2005; 2007b) and patients (Valenza *et al.*, 2005). Activity of HMG-CoA reductase (the major rate-limiting step in cholesterol biosynthesis) is reduced in some models (Valenza *et al.*, 2005; 2010), and the cholesterol precursors lanosterol and lathosterol are also decreased in mice (Valenza *et al.*, 2010) and patients (Leoni *et al.*, 2011).

There are reports of both increased and decreased cholesterol levels (Valenza *et al.*, 2010; 2005; 2007b) in HD cells (Del Toro *et al.*, 2010; Luthi-Carter *et al.*, 2010), mouse brain (Trushina *et al.*, 2006), and brains of patients (Del Toro *et al.*, 2010). For example, cholesterol was found to be increased in the striatum of the YAC72 HD mouse model by filipin staining and thin layer chromatography (Trushina *et al.*, 2006), whereas a second group using mass spectrometry identified a decrease in cholesterol in the same model (Valenza *et al.*, 2010). Importantly however, in the small number of papers that present images of cellular cholesterol staining, most show a change in localisation of cholesterol from normal labelling throughout the cell to bright punctate structures very similar to lipid storage bodies in NPC (Trushina *et al.*, 2006; Del Toro *et al.*, 2010; Marullo *et al.*, 2012).

Several different methods and multiple models have been used in these studies, so interpretation and comparison of these results is difficult (Valenza & Cattaneo, 2011) and this may contribute to the variability seen. Comparison of two versions of the cholesterol enzymatic assay in HD cells showed an increase in cholesterol by one

protocol but not a second (Marullo *et al.*, 2012), and this group also point out that the enzymatic assay can detect sterols other than cholesterol, a limitation we have also seen. This assay will therefore detect total rather than specific sterol changes, and multiple sterols are altered in HD. This study also demonstrated that extraction methods and growth conditions can confound measurements of cholesterol (Marullo *et al.*, 2012). The different models used may also account for some of the variability, possibly representing different 'disease' stages or aspects. The balance of sterol and lipid metabolism may also differ between the species studied (Quinn, Georgiou & Payne, 1985; Bergen & Mersmann, 2005; Yin *et al.*, 2012).

The mechanisms behind these changes, and the relationships between reduced biosynthesis and altered levels of cholesterol in HD are not yet clear. Altered cholesterol levels in HD may affect regulation of cholesterol metabolism via SREBP, or mutant huntingtin may interfere with regulation via ER proteins upstream of SREBP (Yang *et al.*, 2010). Valenza *et al.* (2005) report that SRE (sterol response element) activation is reduced in the presence of mutant huntingtin despite normal levels of SREBP, and that SREBP nuclear localisation is reduced (Valenza *et al.*, 2005). Interestingly however, Luthi-Carter *et al*. report that inhibition of SREBP signalling via modulation of SIRT2 is beneficial to Huntington's cell models (Luthi-Carter *et al.*, 2010), demonstrating that the interactions between cholesterol levels, cholesterol synthesis and cellular pathology in Huntington's disease are not straightforward. Alterations to sterol precursors may also modulate sterol synthesis: in Smith-Lemli-Opitz syndrome (SLOS), mutations in *DHCR7,* which encodes the final enzyme in cholesterol biosynthesis, lead to increased sterol precursors (DeBarber *et al.*, 2011) and accumulation of LDL-derived cholesterol (Wassif *et al.*, 2002), and *DHC7R* expression is reduced in HD (Valenza *et al.*, 2005).

Altered lipid trafficking may also contribute. Mutant huntingtin interacts aberrantly with caveolin-1, an endocytic protein involved in cholesterol trafficking, and this contributes to cholesterol storage (Trushina *et al.*, 2006; 2013). In NPC, cholesterol trafficking defects are present without increases in total cholesterol in some tissues (Lloyd-Evans & Platt, 2010), such as the brain, due to low cholesterol uptake and turnover. Mislocalisation of cholesterol to different compartments could interfere with cellular detection of, and response to, sterol levels, and the difference in cellular

handling of sterol synthesis versus uptake of extracellular cholesterol could produce complex results.

### 1.6.9.2 Gangliosides

A small number of studies have identified changes in gangliosides and in ganglioside metabolism in HD, particularly in GM1 (Del Toro *et al.*, 2010; Maglione *et al.*, 2010). Two groups have reported reduced expression of several ganglioside synthetic enzymes in mouse models (R6/1 and YAC128) and in samples from human brain (Desplats *et al.*, 2007; Maglione *et al.*, 2010; Denny *et al.*, 2010). The consistently reduced enzymes were glucosylceramide synthase (the first step in ganglioside synthesis), in both mouse models but not in human samples (Maglione *et al.*, 2010; Denny *et al.*, 2010), and *B4galnt1* (GM2 synthase), *St3gal5* (GM3 synthase) and the sialtransferase *St8sia3* in at least one mouse model and human samples (Desplats *et al.*, 2007; Maglione *et al.*, 2010).

Levels of gangliosides are also altered in HD, although the changes vary between reports. Both increased (Del Toro *et al.*, 2010) and decreased (Maglione *et al.*, 2010) GM1 have been seen in HD cell models. Significant decreases in GM1 have been seen in two HD mouse models, YAC128 (Maglione *et al.*, 2010) and R6/2 (Di Pardo *et al.*, 2013), and decreases in both GM1 (Desplats *et al.*, 2007) and total ganglioside (Denny *et al.*, 2010) have been reported in R6/1 mice. In human samples, there was a significant decrease in gangliosides in HD patient caudate samples compared to controls (Desplats *et al.*, 2007), but an increase in most gangliosides in the cerebellum of patients (a significant increase in the case of GM1) (Denny *et al.*, 2010).

Interesting effects have been obtained by manipulating GM1 in Huntington's models. Treatment with GM1 is reported to be beneficial in Huntington's cells (Maglione *et al.*, 2010) and mice (Di Pardo *et al.*, 2012). Treatment with fingolimod, a sphingosine-1-phosphate receptor agonist, reduces movement defects and Huntington's pathology in R6/2 mice, and was shown to restore reduced GM1 in these models and increase GM1 synthase and GM1 levels in cells (Di Pardo *et al.*, 2013). On the other hand, Del Toro *et al.* report that cell surface levels of GM1 are higher in Huntington's cells than controls, and that this leads to changes in overall membrane fluidity and distribution of membrane domains. This contributes to redistribution of proteins such as NMDA receptor components and therefore to increased susceptibility to excitotoxicity in

Huntington's (Del Toro *et al.*, 2010). It is possible that lipid distribution is disrupted in Huntington's disease and addition of GM1 alters membrane lipid content and has a general protective effect, as systemic GM1 addition has also been reported to be protective against excitotoxic insult such as the drugs that are sometimes used to model striatal damage in Huntington's disease (Lombardi, Zanoni & Moroni, 1989).

## 1.7 Huntingtin function

The normal function of huntingtin is not currently known, but there are many theories. A recent excellent review by Saudou and Humbert covers this topic in detail (Saudou & Humbert, 2016). While some genetic diseases provide insight into the identity or function of that gene, it is difficult to infer huntingtin function from Huntington's disease. The disease is complex, and the CAG expansion may be a gain of function, a loss of function, or some combination of the two. Mutant huntingtin is sufficient to rescue loss of some normal huntingtin functions in null models, for example neurogenesis (White *et al.*, 1997), but conditional knockouts of huntingtin in adult mouse brain show some phenotypic similarity – motor defects and striatal degeneration – to Huntington's disease (Dragatsis, Levine & Zeitlin, 2000), suggesting that some of the huntingtin function required in adult brain may be lost in the mutant. Null models, which are useful for identifying protein function, are rare for huntingtin as research largely focuses on the CAG expansion and the disease state. Homozygous knockout of the huntingtin gene is embryonic-lethal in mice, at around day E7.5 – E8.5 (Duyao *et al.*, 1995; Nasir *et al.*, 1995), and huntingtin is required for normal neurogenesis in both zebrafish (Henshall *et al.*, 2009) and mice (White *et al.*, 1997). Interestingly, given the changes to lipid metabolism in HD, huntingtin-null mouse neural stem cells have increased cholesterol content (Ritch *et al.*, 2012).

Huntingtin homologues are present across mammals, other vertebrates, insects and sea urchins (Tartari *et al.*, 2008). While some segments of the protein are generally conserved, including the protein-interaction HEAT domains (Tartari *et al.*, 2008), exon 1 is less well conserved, and the polyglutamine region important in HD is not present in all species. The polyglutamine repeat is present in vertebrates but not in insects, and the proline-rich region is largely present only in mammals (Tartari *et al.*, 2008; Saudou & Humbert, 2016). Therefore, *Drosophila* and sea urchins have no polyglutamine

region, fish and other vertebrates have 4Q, and mammals show a gradual increase, with humans having a polymorphic stretch of 15-30Q, and mice having 7, shorter than most mammals (Tartari *et al.*, 2008).

Huntingtin is ubiquitously expressed (Marques Sousa & Humbert, 2013), though it is highest in the brain and testes. Within cells, huntingtin is present in both the nucleus and cytoplasm, associated with cytoskeleton and cellular transport pathways, and in the endo-lysosomal system (Kegel *et al.*, 2000; Trajkovic, Jeong & Krainc, 2017), though localisation may differ between cell types (De Rooij *et al.*, 1996; Hughes & Jones, 2011). It is also secreted, and may be able to influence cells externally (Pecho-Vrieseling *et al.*, 2014; Trajkovic, Jeong & Krainc, 2017). Studies of huntingtin localisation have some limitations, as the antibodies available for huntingtin are not entirely specific (Hughes & Jones, 2011), and target different motifs. Tagged huntingtin is also commonly used, and if only certain fragments are labelled with the antibody or tag then an incomplete picture of huntingtin localisation will be obtained. It is also difficult to say whether small fragments match the behaviour of endogenous protein isoforms, although the extensive proteolytic cleavage and the agreement between studies performed using diverse methods suggests that these results are also relevant.

Many proteins which interact with huntingtin have been identified, via individual studies or techniques such as yeast two-hybrid screens (Harjes & Wanker, 2003; Kaltenbach *et al.*, 2007; Tourette *et al.*, 2014; Saudou & Humbert, 2016). These include a number of proteins involved in endocytosis and vesicle trafficking, such as adaptor protein AP-2A, components of the clathrin vesicle coat complex and the dynein transport complex (Kaltenbach *et al.*, 2007; Tourette *et al.*, 2014), and huntingtin-associated protein 1 (HAP-1), an endocytic regulator (Mackenzie *et al.*, 2017). These interactors also include many cell signalling proteins, transcription factors and regulators of gene expression (Kaltenbach *et al.*, 2007; Tourette *et al.*, 2014), including the Repressor element-1 silencing transcription factor (REST), an important neuronal repressor (Zuccato *et al.*, 2003). These give us an indication of the networks which huntingtin may be involved in or influence.

There are many possible roles of huntingtin based on the observed effects and characteristics of the protein. Huntingtin is suggested to be involved in endocytosis (Velier *et al.*, 1998), membrane trafficking, axonal transport, mitochondrial function

(Ismailoglu *et al.*, 2014), gene regulation, and possibly nuclear trafficking and anti-apoptotic effects (Saudou & Humbert, 2016).

## 1.8 Models of Huntington's disease

### 1.8.1 Modelling HD

In order to investigate pathogenic mechanisms and develop therapies for HD, we require models of the disease. In the case of HD, the genetic basis of disease is known, which is helpful in making models (unlike diseases such as Alzheimer's or Parkinson's without clear causes). Even so, these models are not necessarily useful for all purposes, and the degree to which each model translates or recapitulates human disease must be assessed. A broad range of model systems exist (and continue to be developed) including cells, rodents and large organisms, which are used to study disease mechanisms, potential therapies, and normal huntingtin function.

Most HD models have been produced via genetic modification to introduce a mutant form of huntingtin into the system. This however encompasses a great deal of variation in genotype and other factors, including different CAG repeat lengths, whether full length or partial protein was used, whether endogenous protein was altered or mutant protein added, and what species the huntingtin is from. Some of the possible genetic variables are listed in Table 1.2.

It is also possible to derive very useful HD models from patients who have the disease. Thanks to the generosity and willingness of patients to be involved in research, clinical and genetic information from individuals and families is available, as well as tissue such as blood, skin cells and postmortem brain, and permission to develop cell lines and induced pluripotent stem cells (iPSCs) for use in research. These give insight into real disease cases to compare to and validate generated models, and iPSCs can be differentiated into cell types of interest (particularly medium spiny neurons) and provide human neurons to use in research.

Formerly, drugs have been used to produce partial models of HD. The mitochondrial poisons malonate and 3-nitropropionic acid (Brouillet, 2014) and excitotoxic compounds kainic acid and quinolinic acid (Lombardi, Zanoni & Moroni, 1989) produce neuronal loss which mimics the specific neurodegeneration seen in HD, and were commonly used to produce rodent models of striatal neurodegeneration. These are

now rarely used to model disease or test treatments for HD, but they are useful for producing lesions for cell replacement experiments (Dunnett & Rosser, 2007), and are interesting as they demonstrate the specific sensitivity of the striatum to these types of insult, which may be a component of HD pathogenesis.

| Factor | Potential alterations |
|---|---|
| Length of CAG repeat | Disease models exist using anything from 30-350 CAG repeats<br>Instability of CAG repeat length is seen in certain tissues (De Rooij *et al.*, 1995) |
| Species of gene | Modification of endogenous gene<br>Expression of human gene in other systems<br>Partially humanised gene (for example knock-in of human exon 1 into mouse *huntingtin*) |
| Allele number | Heterozygous or homozygous for mutant huntingtin<br>Additional copy of mHtt with endogenous alleles also present |
| Expression | Endogenous expression<br>Over-expression of wtHtt or mHtt<br>Expression of mHtt in addition to endogenous levels of wtHtt<br>Inducible expression of mHtt<br>Transient or stable expression systems |
| Protein | Full length modified endogenous protein<br>Full length protein expressed separately<br>Partial Htt protein: using just the first exon or the N-terminal region is fairly common, as is expression of specific small fragments to investigate specific functions or pathogenic effects, for example suspected proteolytic cleavage products (Martin *et al.*, 2014), membrane binding regions (Burke *et al.*, 2013) or autophagic modifiers (Martin *et al.*, 2014) |
| Modifications | Fluorescent labelling and other tags.<br>Deletion of regions of interest, for example the suspected NES (Xia *et al.*, 2003) or kinase target sites (Humbert *et al.*, 2002) |

**Table 1.2** Some variables in genetic models of Huntington's disease

### 1.8.2 Cell models

Cell models for HD can be derived from patients or from animal models, or generated in cultured cell lines. We have used a number of different cell lines in this project, which are listed in the Methods chapter and discussed further where appropriate. For us, and more generally, the different cell models available are useful for different applications and research questions, and may be more or less relevant to the situation present in human disease.

Of particular interest is the development of iPSCs for HD (Brooks, Jones & Dunnett, 2012; The HD iPSC Consortium, 2012; Castiglioni *et al.*, 2012), and the differentiated cell types which can be derived from them. This provides a valuable approach which gives us many more cell models, most importantly the ability to work on human patient neurons.

### 1.8.3 Animal models

Whole organism models of HD fall into three broad groups: small organism models of huntingtin function, rodent models of pathogenesis and disease, and more rarely, large animal models of disease. In this project, we have used Drosophila and tissues from mouse models, and these will be discussed further in appropriate chapters.

Invertebrate models including *Drosophila melanogaster* (Ravikumar *et al.*, 2004; Green & Giorgini, 2012; Lewis & Smith, 2016) and *Caenorhabditis elegans* (Gidalevitz *et al.*, 2013) have been used in studies of huntingtin protein function and basic effects of the presence of mutant protein. For example, *C. elegans* has been used to identify genes which modify toxicity (Lejeune *et al.*, 2012) and aggregation (Teuling *et al.*, 2011) of mutant huntingtin, and *Drosophila* have been used to screen for drugs (Newman *et al.*, 2011; Calamini, Lo & Kaltenbach, 2013) and modifier genes (Lewis & Smith, 2016). Both huntingtin knock-out (Diekmann *et al.*, 2009; Henshall *et al.*, 2009) and mutant huntingtin (Williams *et al.*, 2008) zebrafish have been used for studies of huntingtin function and HD pathogenesis.

There are many mouse models of HD, as well as transgenic rat models. These are widely used in disease research and therapeutic testing, and their use is well established. While they are extremely useful, there are problems with mouse models of HD, as is the case for mouse models of many neurodegenerative diseases. Though the disease-causing mutation is known, reproducing this mutation in mice is not sufficient to fully recapitulate human disease.

Large animal models include transgenic pig (Baxa *et al.*, 2013), sheep (Jacobsen *et al.*, 2010; Handley *et al.*, 2016) and primate (Chan *et al.*, 2015) models. These models have only been developed recently, and work so far has focused on producing and characterising them, and presumably on developing assays to explore functional and behavioural defects in these animals, as has been necessary for other disease models in animals such as sheep (Perentos *et al.*, 2015; McBride, Perentos & Morton, 2016).

## 1.9 Potential therapies for Huntington's disease

While treatments to manage symptoms are available, there is currently no therapy that modifies disease progression in HD, and finding one is a primary target of current research. The major approaches are small molecule therapies against a broad range of

potential targets (Imarisio *et al.*, 2008), cell transplantation to repair degeneration (Dunnett & Rosser, 2007), and gene therapy to correct the initial defect in huntingtin.

Small molecule targets in HD pathogenesis include enhancing autophagic clearance of mutant and aggregated huntingtin (Ravikumar *et al.*, 2004); upregulating or supplying chaperones to handle mutant protein (Sittler *et al.*, 2001); inhibiting huntingtin fragmentation by proteases (Sánchez *et al.*, 1999; Bonelli *et al.*, 2004); correcting mitochondrial function (Varma *et al.*, 2007); and suppressing excitotoxicity (Del Toro *et al.*, 2010; Schiefer *et al.*, 2002).

HD is potentially a good target for genetic therapies, as it is caused by a known mutation in a single gene and, in most cases, can be identified well ahead of disease onset by genetic testing in affected families. This will involve either suppressing expression of huntingtin (Alterman *et al.*, 2015; Grondin *et al.*, 2015), using *HTT*-targeted siRNAs (Godinho *et al.*, 2013) or oligonucleotides (Wyant, Ridder & Dayalu, 2017) against huntingtin generally or the mutant form specifically, or development of methods to remove the CAG repeat expansion from the gene entirely, using gene editing technologies such as CRISPR or viral systems (Casaca-Carreira *et al.*, 2015; 2016; Kolli *et al.*, 2017). While gene editing is in early stages, a trial of antisense oligonucleotides was begun in 2016 by Ionis Pharmaceuticals.

## 1.10 Aims

Our aim is to investigate the possible LSD phenotypes in HD which are indicated by the existing Huntington's disease literature. We aim to characterise these changes and investigate the mechanism behind them, and to see whether this allows us to develop therapies or useful knowledge from the LSD field or from NPC specifically to help understand or treat HD.

# CHAPTER 2 MATERIALS AND METHODS

## 2.1 Materials

Reagents were purchased from Sigma Aldrich unless otherwise stated.

## 2.2 Cell culture

### 2.2.1 Cell lines

Multiple cell lines were used for different experiments over the course of this project. Details are given in Table 2.1. Neural precursor cells differentiated from HD patient iPSCs were a generous gift from Prof. Nick Allen, Cardiff University.

### 2.2.2 Culture conditions

Cells were grown in tissue-culture coated flasks (Nunc, ThermoFisher) in a humidified incubator with 5% $CO_2$. Detailed cell culture conditions for different cell lines are given in Table 2.1. Serum - both fetal bovine serum (FBS) and horse serum - was heat-inactivated at 60°C for 30 min before use. Adherent cells were passaged once they reached 70-100% confluency, using 1% trypsin in Dulbecco's phosphate buffered saline (DPBS). Cell stocks were initially frozen at -80°C using a ThermoFisher "Mr. Frosty" cell freezing container (to provide a rate of freezing of approximately 1°C per minute, optimal for cell survival), and subsequently stored in a liquid $N_2$ cell bank, using a freezing medium consisting of FBS with 10% HybriMax DMSO.

### 2.2.3 NPC2 supplementation

To produce conditioned medium (Chapter 4), control and NPC2 HF cells were seeded in T25 culture flasks and grown to confluency. 24 hours before beginning the experiment, culture medium was removed from confluent cells in T25 flasks. Cells were washed twice with DPBS, and 5 mL fresh culture medium was added. After 24 hours, this conditioned medium was collected, filtered using a 0.22 μm syringe filter to remove cells, and used to treat experimental cells.

To treat experimental cells, cells were grown on coverslips to approximately 70% confluency. Culture medium was removed, cells were washed twice with DPBS, and fresh conditioned medium was added. Cells were incubated in conditioned medium for 24 hours before fixation, staining and imaging as described below.

| Cell lines | Code | Description | Species | Origin | Temp. | Incubator | Adherent | Medium | Treatments |
|---|---|---|---|---|---|---|---|---|---|
| STHdh | ST*Hdh* control | Embryonic striatal line from control mouse homozygous for huntingtin with humanised exon 1 and Q7/Q7, immortalised using large T antigen | mouse | Coriell CH00097, generated by MacDonald *et al.* (Trettel *et al.*, 2000) | 33°C | humidified & 5% CO$_2$ | Adherent | DMEM with 10% FBS (Biosera) and 2 mM L-glutamine | Selection by addition of 0.4 mg/mL Geneticin (G418, Enzo Life Sciences) |
| | ST*Hdh* HD | Embryonic striatal line from HD mouse model homozygous for huntingtin with humanised exon 1 and Q111/Q111, immortalised using large T antigen | mouse | Coriell CH00095, generated by MacDonald *et al.* (Trettel *et al.*, 2000) | | | | | |
| ST14A | ST14A control | Rat embryonic striatal cell line expressing human exon 1 (1-548) fragment with Q15 | rat | Coriell CH00066, generated by Cattaneo *et al.* (Cattaneo & Conti, 1998) | 33°C | humidified & 5% CO$_2$ | Adherent | DMEM with 10% FBS (Biosera) and 2 mM L-glutamine | N/A |
| | ST14A HD | Rat embryonic striatal cell line expressing high levels of human exon 1 (1-548) fragment with Q120 | rat | Coriell CH00067, generated by Cattaneo *et al.* (Cattaneo & Conti, 1998) | | | | | |
| PC12 | PC12 A9 | Originally derived from rat pheochromocytoma of adrenal gland, containing no huntingtin construct | rat | Gift from Prof. Buchman, Cardiff University | 37°C | humidified & 5% CO$_2$ | Non-adherent | DMEM:F12 with 15% horse serum, 2.5% FBS and 2 mM L-glutamine | Selection by addition of 0.2 mg/ml Geneticin (G418, Enzo Life Sciences) and 0.2 mg/ml Zeocin (ThermoFisher), induction of expression by 48 hr treatment with 40 µM Ponasterone A (ThermoFisher) |
| | PC12 wtHtt | PC12 cells containing an inducible full-length human huntingtin with Q23 and a C-terminal RFP tag | rat | Coriell CH00285 | | | | | |
| | PC12 mHtt | PC12 cells containing an inducible full-length human huntingtin with Q73 and a C-terminal RFP tag | rat | Coriell CH00287 | | | | | |

| Cell lines | Code | Description | Species | Origin | Temp. | Incubator | Adherent | Medium | Treatments |
|---|---|---|---|---|---|---|---|---|---|
| Human fibroblast (HF) | HF control | Fibroblast cells from a clinically normal 1 yr old male | human | Coriell GM05399 | 37°C | humidified & 5% $CO_2$ | Adherent | DMEM with 10% FBS (Biosera) and 2 mM L-glutamine | N/A |
| | HF control 54yr | Fibroblast cells from a clinically normal 54 yr old female | human | Coriell GM04787 | | | | | |
| | HF HD Q60 | Fibroblast cells from a 29 yr old female HD patient with 18 and 60 CAG repeats in Htt (age of onset 18 years) | human | Coriell GM03621 | | | | | |
| | HF HD Q180 | Fibroblast cells from a 6 yr old male HD patient with an extreme CAG repeat (approximately 180) in Htt | human | Coriell GM09197 (Sathasivam *et al.*, 1997) | | | | | |
| | HF SCA1 | Fibroblast cells from a 29 yr old male SCA1 patient with 29 and 52 CAG repeats in ATXN-1 | human | Coriell GM06927 | | | | | |
| | HF MJD | Fibroblast cells from a 44 yr old male SCA3/MJD patient with 23 and 71 CAG repeats in ATXN-3 | human | Coriell GM06153 | | | | | |
| | HF NPC2 | Fibroblast cells from a male compound heterozygote NPC2 patient | human | Coriell GM18455 (Park *et al.*, 2003) | | | | | |
| SH-SY5Y | SH-SY5Y | Originally derived from biopsy of a human neuroblastoma patient | human | Gift from Prof. Buchman, Cardiff University | 37°C | humidified & 5% $CO_2$ | Adherent | DMEM with 10% FBS (Biosera) and 2 mM L-glutamine | N/A |
| CHO-H1 | CHO-H1 | Epithelial cell line derived from Chinese hamster ovary | hamster | Lab stock | 37°C | humidified & 5% $CO_2$ | Adherent | DMEM:F12 with 10% FBS (Biosera) and 2 mM L-glutamine | N/A |
| S2R+ | S2R+ | Cell line originally derived from *Drosophila melanogaster* (Schneider, 1972; Yanagawa, Lee & Ishimoto, 1998). | fly | Gift from Dr. Lopez de Quinto, Cardiff University | RT (20-25°C) | ambient conditions | Partially adherent | Schneider insect medium (Gibco) with 10% FBS (Biosera), 2 mM L-glutamine and penicillin-streptomyin | N/A |

| Cell lines | Code | Description | Species | Origin | Temp. | Incubator | Adherent | Medium | Treatments |
|---|---|---|---|---|---|---|---|---|---|
| iPSC-derived cells | control | Neural precursor cells derived from iPSCs from a clinically normal donor with one huntingtin allele containing 33 CAG repeats | human | Gift from Prof. Allen, Cardiff University (Trettel *et al.*, 2000; The HD iPSC Consortium, 2012) | 37°C | humidified & 5% $CO_2$ | Adherent | Advanced DMEM:F12 (Life Technologies) with 1% L-glutamine, 1% penicillin / streptomycin, MACS NeuroBrew-21 without RA (Miltenyi) and 50 nM basic fibroblast growth factor (FGF; Peprotech) | N/A |
| | Q60 | Neural precursor cells derived from iPSCs from an HD patient with one huntingtin alleles containing 18 and 60 CAG repeats (same patient as Coriell GM03621 fibroblasts) | | | | | | | |
| | Q109 | Neural precursor cells derived from iPSCs from an HD patient with one huntingtin allele containing 109 CAG repeats and one normal allele | | | | | | | |

**Table 2.1 Cell lines and conditions**

### 2.2.4 Nucleic acid vector treatments

Nucleic acid vectors (Table 2.2) were used according to their manufacturer's suggested protocols for RNAi or transfection experiments, but addition of genetic material was omitted. All of these protocols state that the concentrations and proportions of vector should be optimised for the particular cell line and experiment, but all of the protocols also give a suggested starting range. We selected the upper value of this range throughout, and scaled it to the 96 well plate format if necessary. Volumes and preparation procedures are given in Table 2.2.

For Lysotracker plate assays, cells were grown and treated in 96 well plates (Corning CellBIND), at 50,000 cells per well for 24 hr treatments or 5,000 cells per well for 72 hr treatments. For live imaging and fixed staining, cells were grown in 96 well plates with a growth surface suitable for microscopy (μ-Plate, ibidi), and were seeded at 20,000 cells per well for 24 hr treatments or 2,000 cells per well for 72 hr treatments. Cells were left to adhere and grow for 24 hr before treatments were added. After staining, cells were imaged in 100 μL DPBS. We chose 24 and 72 hours as they are commonly used times for drug and siRNA treatments and therefore a reasonable estimate of the time that cells will be exposed to these vectors in practical use.

| Vector | Supplier | Volume per well (μL) | | Preparation | Incubation before addition (min) |
|---|---|---|---|---|---|
| | | Vector | FBS-free medium | | |
| **Lipofectamine** | Invitrogen | 0.5 | 10 | - | 5 |
| **Lipofectamine 3000** | Invitrogen | 0.3 | 10 | Vortex 5 s | 10 |
| **INTERFERin** | Polyplus | 1.5 | 50 | Vortex 10 s | 10 |
| **JetPEI** | Polyplus | 0.4 | 20 (*NaCl buffer*) | Vortex 15 s | 20 |
| **FuGENE HD** | Promega | 0.6 | 10 | - | 10 |
| **ViaFect** | Promega | 0.3 | 10 | - | 10 |
| **TurboFect** | Thermo | 0.3 | 10 | - | 10 |

**Table 2.2 Nucleic acid vector treatments**

## 2.3 Fixed cell staining and immunocytochemistry

### 2.3.1 Fixation

Unless otherwise stated, cells grown on acid-washed glass coverslips or in plates for microscopy were washed once with DPBS, fixed in 4% paraformaldehyde (PFA; Taab) in DPBS at room temperature for 10 minutes, then washed three times in DPBS and either used or stored in DPBS at 4°C. PFA fixation rather than solvent or alcohol based methods were used as we were mostly imaging cellular lipids, which are altered or removed by methanol and some other fixatives. Where necessary, particularly for staining lysosomal proteins such as LAMPs, cells were permeabilised using either a 30 second incubation in ice cold methanol or, if lipids needed to be preserved, a 30 minute incubation in 0.2% saponin in DPBS.

| Target | Supplier | Host species | Target species | Dilution |
|--------|----------|--------------|----------------|----------|
| Primary antibodies: | | | | |
| huntingtin | Merck Millipore (MAB2166) | mouse | human | 1:200 |
| LAMP1 (human) | Developmental Studies Hybridoma Bank (H4A3) | mouse | human only | 1:100 |
| LAMP1 (mouse) | Developmental Studies Hybridoma Bank (1D4B) | rat | mouse only | 1:50 |
| LAMP2 (mouse) | Developmental Studies Hybridoma Bank (ABL-93) | rat | mouse only | 1:50 |
| NPC1 | Novus Biologicals (NB400-148) | rabbit | human, mouse, rat, hamster | 1:250 |
| NPC1 | Merck Millipore (MABS739) | rabbit | human, mouse, rat | 1:250 |
| NPC2 | Sigma Aldrich (HPA000835) | rabbit | human, mouse, rat | 1:250 |
| Secondary antibodies: | | | | |
| DyLight 488 anti-rabbit IgG | Vector Laboratories (DI-1488) | goat | rabbit | 1:250 |
| DyLight 488 anti-mouse IgG | Vector Laboratories (DI-2488) | horse | mouse | 1:250 |
| DyLight 594 anti-rabbit IgG | Vector Laboratories (DI-1594) | goat | rabbit | 1:250 |
| DyLight 594 anti-mouse IgG | Vector Laboratories (DI-2594) | horse | mouse | 1:250 |

**Table 2.3 Antibodies used for immunocytochemistry**

**2.3.2 Immunocytochemistry**

For immunocytochemistry (ICC), fixed cells were incubated in blocking buffer (DPBS with 1% BSA and 0.1% saponin) with appropriate antibody dilutions at 4°C overnight, washed, and incubated in DPBS with appropriate secondary antibodies for 30 min at room temperature. Antibodies used are listed in Table 2.3. DyLight 488 antibodies were imaged using 485 nm excitation / 520 nm emission and DyLight 595 using 565 nm excitation / 620 nm emission.

Two different NPC1 antibodies were used as the Novus antibody NB400-148 changed partway through the project and new batches no longer specifically bound NPC1. Several alternative antibodies were tested, some of which were potentially useful for western blot, but the Millipore MABS739 was the best of those tested for ICC.

**2.3.3 Cellular lipid staining**

*2.3.3.1 Cholesterol*

Cellular cholesterol was visualised using filipin, a naturally ultraviolet fluorescent polyene antibiotic that specifically stains cholesterol (Cattaneo & Conti, 1998; Bergy & Eble, 1968; Robinson & Karnovsky, 1980; Vruchte, 2004). PFA-fixed cells were incubated in complete DMEM with 187.5 μg/mL filipin (filipin complex from *Streptomyces filipinensis*) for 30 minutes at room temperature, then washed in DPBS. Filipin was imaged at 380 nm excitation / 480 nm emission.

*2.3.3.2 Ganglioside GM1*

The glycosphingolipid ganglioside GM1 was visualised using fluorescein isothiocyanate-labelled cholera toxin B subunit (FITC-CtxB), which specifically binds to GM1 (Hansson, Holmgren & Svennerholm, 1977) (and which includes only the targeting component of the toxin and not the active subunit). PFA-fixed cells were incubated in blocking buffer (DPBS with 1% BSA and 0.1% saponin) with 1 μg/ml FITC-CtxB at 4°C, then washed in DPBS. FITC-CtxB was imaged at 485 nm excitation / 520 nm emission.

*2.3.3.3 Lyso-bisphosphatidic acid*

Lyso-bisphosphatidic acid (LBPA), a late endosomal lipid, also referred to as bis-monoacylglycerophosphate, was visualised using a commercially available antibody (Kobayashi *et al.*, 1999). PFA-fixed cells were incubated in blocking buffer (DPBS with 1% BSA and 0.1% saponin) with 1 μg/ml anti-LBPA antibody (Echelon) at 4°C overnight,

washed in DPBS, then incubated with fluorescent secondary antibody at room temperature for 30 minutes and washed again in DPBS.

### 2.3.3.4 Sphingomyelin

Sphingomyelin was labelled using lysenin, a toxin from the earthworm *Eisenia foetida* which specifically binds sphingomyelin (Yamaji *et al.*, 1998). Lysenin toxin was not consistently available over the course of the project: initially, lysenin toxin and the anti-lysenin antibody were both obtained from Peptides International, but the supply of lysenin was disrupted and we switched to using lysenin which was purified from *Eisenia foetida* (of European origin) in the lab, with the same anti-lysenin antibody.

To label sphingomyelin, PFA-fixed cells were incubated in blocking buffer (DPBS with 1% BSA and 0.1% saponin) for 30 minutes at room temperature, then in blocking buffer with 0.5 µg/ml lysenin (or appropriate dilutions of purified lysenin) at 4°C overnight. Cells were washed in DPBS (3 x 5 min), then incubated in blocking buffer with anti-lysenin antibody (1:1000) for 1 hour at room temperature, washed again (3 x 5 min in DPBS), and finally incubated in blocking buffer with fluorescent-tagged anti-rabbit secondary antibody (1:200) and washed once more (3 x 5 min in DPBS).

### 2.3.4 Nuclear counterstains

To counterstain nuclei for imaging in the DAPI fluorescent channel, live or fixed cells were incubated in DPBS with 4 µg/ml Hoechst (Invitrogen) for 10 minutes at room temperature in the dark, then washed in DPBS and imaged. Hoechst was imaged at 380 nm excitation / 480 nm emission.

### 2.3.5 Mountants

Two mountants were used - initially 0.4 g/mL Mowiol 4-88 in DPBS, with DABCO added for slides which needed to be preserved, and later Fluoroshield (Sigma). Both are aqueous mounting media, which were used to mount coverslips on glass slides, and were left to dry overnight before slides were imaged.

## 2.4 Live cell imaging

### 2.4.1 Lysotracker Green for lysosomal visualisation

Lysotracker Green (Molecular Probes, ThermoFisher) was used to measure or image lysosomes, following the same protocol for both plate assays and microscopy. For plate assays, cells were grown until they reached a confluent monolayer, whereas for

microscopy, cells were grown to be suitable for imaging. Live cells were washed once with DPBS, incubated in DPBS with 200 nM Lysotracker Green for 10 minutes at 37°C, then washed again and read or imaged in DPBS with excitation/emission wavelengths of 485 nm and 520 nm respectively.

### 2.4.2 Lysosensor Green for lysosomal visualisation

Live cells were washed once with DPBS, incubated in DPBS with 1 µM Lysosensor Green (ThermoFisher) for 15 minutes at 37°C, then washed again and imaged in DPBS with excitation/emission wavelengths of 485 nm and 520 nm respectively.

### 2.4.3 LipidTOX Red Phospholipidosis reagent

Cellular phospholipid accumulation was imaged using LipidTOX Red Phospholipidosis detection reagent (Molecular Probes, ThermoFisher). Live cells were washed once with complete medium, incubated in complete medium with 1X LipidTOX Red reagent for 4 hours at 37°C, then washed in DPBS and imaged in DPBS with excitation/emission wavelengths of 565 nm and 615 nm respectively.

## 2.5 Live cell functional assays

### 2.5.1 Ganglioside GM1 trafficking assay

FITC-CtxB was used to assay internalisation and trafficking of ganglioside GM1 (Sugimoto *et al.*, 2001). Surface GM1 was labelled with FITC-CtxB by incubating live cells in cold complete medium with 1 µg/mL FITC-CtxB for 30 minutes below 16°C (to suppress endocytosis (Tomoda, Kishimoto & Lee, 1989; Punnonen, Ryhänen & Marjomäki, 1998)). Cells were washed with pre-warmed medium then returned to normal culture conditions for the trafficking 'chase' period. The length of this chase is dependent on cell type, but here we used a 1 hr 30 min incubation for both the ST14A cells and the iPSC-derived neural precursor cells. After trafficking, three back-exchange washes were performed using cold complete medium with 1% BSA and 0.1 mg/mL heparin, and cells were imaged either live or after fixation at excitation/emission wavelengths of 485 nm and 520 nm.

### 2.5.2 Annexin V apoptosis assay

Phosphatidylserine is a phospholipid normally present on the inner leaflet of the plasma membrane, which only flips to the outer leaflet when the cell commits to apoptosis (Segawa & Nagata, 2015). Annexin V can bind phosphatidylserine in the

presence of Ca$^{2+}$, so extracellular addition of tagged Annexin V to live cells, under conditions which prevent internalisation, can be used as an apoptotic marker (Walton *et al.*, 1997).

Cells grown in chamberslides (µ-Slide 8 well, ibidi) or 96 well plates (µ-Plate, ibidi) were washed in cold DPBS and incubated in Ca$^{2+}$-containing Hank's balanced salt solution (HBSS) with Alexa Fluor 488 Annexin V (Molecular Probes) and Hoechst below 16°C for half an hour. Cells were then washed once, gently, and imaged in Ca$^{2+}$-containing HBSS at 485 nm excitation / 520 nm emission.

### 2.5.3 Horseradish peroxidase endocytic uptake assay

Uptake of horseradish peroxidase (HRP) from culture medium can be used as a measure of fluid phase endocytosis (Gu *et al.*, 1997; Lloyd-Evans *et al.*, 2008).

Confluent cells were washed twice with DPBS, then incubated in complete medium with 3 mg/mL HRP and 2 mg/mL BSA for 2 hours at normal culture conditions. They were then washed extensively (6 x 10 min) in cold DPBS with 3 mg/mL dextran, on ice, then cells were lysed by one freeze-thaw cycle and incubation in DPBS with 0.1% Triton X-100 for 1 hour. Protein content was then measured by BCA assay, and HRP was detected using a TMB (3,3',5,5'-tetramethylbenzidine) assay.

For the TMB assay (Thermo TMB Substrate Kit, 34021), diluted samples were added to a 96 well plate in 100 µL per well. Reaction solution containing TMB and H$_2$O$_2$ was added (100 µL per well), and the assay was incubated at room temperature until blue colour develops. The assay was stopped by addition of 100 µL 1 M sulphuric acid per well, and absorbance was measured at 450 nm.

## 2.6 Live cell Ca$^{2+}$ imaging

Cellular Ca$^{2+}$ signalling was measured via live cell Ca$^{2+}$ imaging, using the ratiometric cytoplasmic Ca$^{2+}$ probe Fura-2 (Grynkiewicz, Poenie & Tsien, 1985). Excitation of Fura-2 at 340 nm leads to a Ca$^{2+}$-responsive emission at 510 nm, whereas excitation at 380 nm is not Ca$^{2+}$-responsive. Using a ratio of these two values reduces the effect of factors such as photo-bleaching or differences in fluorophore loading, and allows accurate Ca$^{2+}$ measurements (Grynkiewicz, Poenie & Tsien, 1985). Fura-2 is provided to cells in a membrane permeant form (Fura-2,AM), with an AM ester attached which allows it to cross the cell membrane and is then cleaved by cellular esterases.

Cells for $Ca^{2+}$ imaging were grown in 8 well chamberslides (μ-Slide, ibidi). Medium was removed and cells were washed twice in cold complete medium with 1% BSA, then incubated in cold complete medium with 1% BSA, 0.05% pluronic acid and 5 μM Fura-2,AM (ThermoFisher) for 1 hr below 16°C. Cells were then washed three times in HBSS (with 1 mM $CaCl_2$, 1 mM $MgCl_2$ and 10 mM HEPES, pH 7.4) and imaged in minimal (50 μM) $Ca^{2+}$ HBSS. Drugs were added to wells as 2X or 3X solutions in minimal $Ca^{2+}$ HBSS. Reduction of $Ca^{2+}$ in the extracellular medium prevents store-operated $Ca^{2+}$ entry in response to intracellular $Ca^{2+}$ signalling, which would further elevate cytosolic $Ca^{2+}$ and prevent measurement of signalling events, but a minimal $Ca^{2+}$ concentration is required to prevent damage to cells.

To measure the $Ca^{2+}$ content of lysosomes, the other major $Ca^{2+}$ stores of the cell must be clamped first. If these stores are not activated first, the elevation of cytosolic $Ca^{2+}$ caused by lysosomal $Ca^{2+}$ release leads to $Ca^{2+}$ mediated release from the ER and store-operated $Ca^{2+}$ entry: this makes it impossible to isolate and measure the lysosomal $Ca^{2+}$ release as ER $Ca^{2+}$ release causes large changes in cytosolic $Ca^{2+}$ which mask the small, localised lysosomal signalling events (Grienberger & Konnerth, 2012; Morgan, Davis & Galione, 2015).

Ionomycin (Merck Millipore) is a $Ca^{2+}$ ionophore (Liu & Hermann, 1978) which allows $Ca^{2+}$ to cross most cellular membranes other than the lysosome, where the glycocalyx and lipid composition prevent it from acting. Ionomycin can be used to block other $Ca^{2+}$ stores, and lysosomal $Ca^{2+}$ release can then be triggered using GPN (Gly-Phe β-napthylamide; Alfa Aesar), which is cleaved by cathepsin C in lysosomes and causes osmotic swelling and rupture of lysosomes (Berg *et al.*, 1994).

Thapsigargin is an inhibitor of the ER $Ca^{2+}$ uptake pump SERCA (sarco/endoplasmic reticulum $Ca^{2+}$ ATPase). Treatment with thapsigargin inhibits uptake of $Ca^{2+}$ to the ER and so reveals elevation of cytoplasmic $Ca^{2+}$ by ER $Ca^{2+}$ leak channels, ultimately leading to $Ca^{2+}$ mediated ER $Ca^{2+}$ release (Lytton, Westlin & Hanley, 1991).

## 2.7 *Drosophila melanogaster*

### 2.7.1 Maintenance

*Drosophila melanogaster* were maintained on a maize-dextrose-yeast diet, at 25°C for experimental flies and at room temperature (20-22°C) for stocks. Flies were

anaesthetised using $CO_2$ for handling and sorting. Equipment and plasticware was cleaned and frozen between uses.

**2.7.2 Fly stocks**

The fly stocks used are listed in Table 2.4. Experimental flies were produced using crosses between elav-GAL4 male flies and either UAS-GFP, UAS-wtHtt (58360) or UAS-mHtt (56774) virgin females.

*Drosophila melanogaster* has four pairs of chromosomes (one XY pair and three autosomal pairs), though the fourth pair is very small. To write a fly genotype (including modifications), a semicolon (;) is used to separate each pair of chromosomes, and a slash (/) is used to separate chromosomes within a heterozygous pair. Wildtype, unaltered chromosomes are not included, and only one chromosome of a homozygous pair is given. Genes are often named for the phenotype of the null fly, and alleles are given in superscript. The GAL4-UAS system (Duffy, 2002) which we use here is described briefly in Chapter 5.1.

| Name | Genotype | Source |
|------|----------|--------|
| WT | wildtype | Gift from Prof. White-Cooper, Cardiff University |
| elav-GAL4 | $elav^{c155}$ | Gift from Prof. van der Goes van Naters, Cardiff University |
| GMR-GAL4 | *If/CyO ; GMR-GAL4* | Gift from Prof. van der Goes van Naters, Cardiff University |
| UAS-GFP | *w ; UAS-GFP/CyO ; UAS-GFP* | Gift from Prof. van der Goes van Naters, Cardiff University |
| UAS-wtHtt-B | *w\* ; P{w$^+$, UAS-exon1Htt-Q25-Cerulean}2* | Bloomington 58360 (Leonie Quinn, University of Melbourne) |
| UAS-mHtt-G | *w\* ; P{w$^+$, UAS-exon1Htt-Q96-Emerald}3/TM6B* | Bloomington 56774 (Leonie Quinn, University of Melbourne) |
| UAS-wtHtt | *w$^{1118}$; P{UAS-HTT.FL.16Q}2/CyO* | Bloomington 33810 (Vitruvian, LLC) |
| UAS-mHtt | *w$^{1118}$; P{UAS-HTT.FL.128Q}3* | Bloomington 33808 (Vitruvian, LLC) |

**Table 2.4 Fly stocks used**

**2.7.3 Treatment**

To add miglustat (Toronto Research Chemicals) to fly food, we first diluted miglustat to appropriate concentrations in DPBS, using 1 mL of DPBS per 100 mL of food. Fly food which was liquid but partially cooled was measured in a beaker, miglustat solutions were added and thoroughly stirred in, and food was poured into vials and left to set

and dry. Cotton wool bungs were added to food vials the next day, and trays were stored at room temperature wrapped in autoclave bags. For all experiments except initial miglustat toxicity tests, treatments were begun when crosses were performed so that experimental flies were on treatments during development, as defects were apparent early in adulthood in HD model flies (within the first 4 days).

### 2.7.4 Lifespan

For lifespan assays, crosses were performed on food containing appropriate concentrations of miglustat. Flies were collected once a day as they emerged, and maintained in tubes with males present for the first two days, so that all flies were mated. Flies were then anaesthetised using $CO_2$, experimental flies were selected, counted, and sorted into tubes. After initial setup, use of $CO_2$ was kept to a minimum to avoid interference with lifespan or climbing assays (Bartholomew *et al.*, 2015).

Flies were maintained at 25°C in tubes containing 20-30 flies, and were changed to fresh food every 2-3 days. Vials were checked regularly and flies were counted when they died or were censored (removed from the experiment for some reason other than death; usually flies which escaped from vials). Kaplan-Meier analysis (Kaplan & Meier, 1958; Rich *et al.*, 2010) was performed in Prism.

### 2.7.5 Climbing

Climbing assays (negative geotaxis) were performed on the same cohort of flies as the lifespan experiments. Flies were transferred to clean vials marked with lines at heights of 5 cm and 10 cm from the base, and allowed to acclimatise briefly. Flies were tapped sharply down to the base of the vial, then filmed using the camera on a Fairphone FP1U smart phone as they climbed. The assay was repeated 3-5 times, 1 minute apart. Climbing was analysed based on either the number of flies which had passed a marked threshold, or on the average height climbed after the selected time. Vials were washed in warm water and detergent, rinsed with ethanol, and frozen between uses. No difference in climbing was seen between fresh vials and those which had been cleaned using this method (not shown).

### 2.7.6 Tissues

Tissue were collected for biochemical analysis in several experiments. Adult flies were anaesthetised, sorted into tubes, then frozen at -80°C. Whole flies were used, or heads were separated and collected using fine forceps and a needle. Tissue was weighed,

then flies were crushed. For lipid analysis, extractions were performed on crushed flies without further homogenisation, and for protein extraction flies were homogenised in lysis buffer (10 mM Tris-HCl pH 7.5, 150 mM NaCl, 0.5 mM EDTA, 0.5% IGEPAL).

To collect larvae, food containing larvae was collected into 25% sucrose in DPBS and shaken to mix thoroughly. Larvae floated to the surface and were transferred to fresh tubes, leaving fly food behind. They were washed thoroughly in DPBS, then all liquid was removed and tissue was weighed. Larvae were then frozen at -80°C. They were crushed using a Dounce homogeniser until all cuticles were broken, then lysis buffer was added and tissue was passed through a 21G needle 5-10 times.

## 2.8 Protein biochemistry

### 2.8.1 BCA assay

Protein content of cell or tissue samples was determined using the bicinchoninic acid (BCA) assay. Homogenised samples were centrifuged to pellet membranes and the protein-containing supernatant was diluted in MilliQ water and added to 96 well plates (Greiner) in triplicate, with standard solutions of bovine serum albumin (BSA) in MilliQ water. The assay solution of BCA and copper sulphate was added and incubated at 37°C with shaking until the assay developed (green to purple), absorbance was measured at 570 nm, and protein concentrations were calculated using BSA standards.

### 2.8.2 Co-immunoprecipitation

To analyse interactions between huntingtin and NPC1, co-immunoprecipitation experiments were performed (Berggård, Linse & James, 2007). PC12 cells with inducible expression of control (Q23) or mutant (Q73) huntingtin with RFP tags were used, and anti-RFP magnetic beads (Chromotek) were used to immunoprecipitate tagged huntingtin before testing for the presence of NPC1 in the resulting samples.

To prepare cell samples, PC12 cells with inducible huntingtin constructs were grown and treated with 40 µM Ponasterone A (ThermoFisher) for 48 hr, washed in ice-cold DPBS, and lysed using ice-cold lysis buffer (10 mM Tris-HCl pH 7.5, 150 mM NaCl, 0.5 mM EDTA, 0.5% IGEPAL CA-630) with protease inhibitors (Mammalian Protease Inhibitor Complex III, ThermoFisher). Homogenates were centrifuged at 20,000 g for 10 min at 4°C, BCA assays were performed, and samples were diluted to 4 mg/ml cellular

protein using dilution buffer (10 mM Tris-HCl pH 7.5, 150 mM NaCl, 0.5 mM EDTA) with protease inhibitors.

Anti-RFP magnetic agarose beads (RFP-Trap, Chromotek) were washed 3 times in ice cold dilution buffer. Cell homogenate was added to beads (25 µL of beads to 1 mg of protein sample), and incubated at 4°C overnight with constant agitation to allow proteins to bind to RFP-Trap beads.

After incubation, beads were magnetically separated from samples using a QuadroMACS separator (Miltenyi Biotec) and washed 3 times in dilution buffer with protease inhibitors. Protein was eluted from the beads by incubation in 2X western blot sample buffer (see below) for 10 minutes at 95°C, and samples were magnetically separated (as above) to remove beads before loading on polyacrylamide gels for western blot analysis.

### 2.8.3 Western blot

*2.8.3.1 Sample preparation*

Unless otherwise described, cell samples were homogenised by freeze-thawing three times in MilliQ water, then passing the solution 5-10 times through a 21G needle. Protein concentration was measured via BCA assay, and unless otherwise stated 10 µg of sample protein was prepared in sample buffer (β-mercaptoethanol with sodium dodecyl sulphate (SDS) and glycerol) and denatured by incubation for an hour at 60°C.

*2.8.3.2 Separation*

Protein samples were resolved on polyacrylamide gels, using a Tris-glycine running buffer. 10% gels (with a 4% stacking gel) were used for most experiments except for co-immunoprecipitation experiments, where a 6% gel with no stacking gel was used to increase separation and transfer of large proteins.

*2.8.3.3 Transfer*

Proteins were transferred from gels to polyvinylidene difluoride (PVDF) membranes using either semi-dry (usually) or wet (for co-immunoprecipitation experiments and huntingtin blots) transfer methods, in a Tris-glycine transfer buffer with 20% methanol.

*2.8.3.4 Detection*

PVDF membranes were blocked in Tris-buffered saline with 0.1% Tween 20 (TBS-T) and 5% milk powder for 30 minutes at room temperature, then incubated in TBS-T with 1% milk powder and appropriate dilutions of primary antibodies. Primary antibody

incubations (see Table 2.5) were performed at 4°C overnight except for anti-glyceraldehyde dehydrogenase (GAPDH), which was incubated for 1 hr at room temperature. Membranes were washed in TBS-T, then incubated in TBS-T with 1% milk and 1:10,000 dilution of secondary antibodies for 2 hrs at room temperature and washed again. Enhanced chemiluminescence reagent (ECL; ThermoFisher) was added and membranes were exposed to AGFA X-Ray film, which was then developed. Films were scanned and density analysis of bands was performed in ImageJ.

| Target | Supplier | Host species | Target species | Dilution |
|---|---|---|---|---|
| Primary antibodies: | | | | |
| ASM | Santa Cruz (sc-11352) | rabbit | human, mouse, rat, hamster | 1:1000 |
| EEA1 | BD Pharmingen (610456) | mouse | human, rat, hamster | 1:1000 |
| GAPDH | Novus Biologicals (NB300-221) | mouse | human, mouse, rat, hamster | 1:10,000 |
| huntingtin | Merck Millipore (MAB2166) | mouse | human | 1:1000 |
| NPC1 | Novus Biologicals (NB400-148) | rabbit | human, mouse, rat, hamster | 1:1000 |
| NPC1 | Merck Millipore (MABS739) | rabbit | human, mouse, rat | 1:1000 |
| NPC2 | Sigma Aldrich (HPA000835) | rabbit | human, mouse, rat | 1:1000 |
| Secondary antibodies: | | | | |
| HRP-linked anti-rabbit IgG | Cell Signalling Technology (7074) | goat | rabbit | 1:10,000 |
| HRP-linked anti-mouse IgG | Cell Signalling Technology (7076) | horse | mouse | 1:10,000 |

**Table 2.5 Antibodies used for western blotting**

## 2.9 Lipid biochemistry

### 2.9.1 Enzymatic cholesterol assay

Cholesterol content of samples was measured using an enzymatic assay (Gamble *et al.*, 1978). To measure cholesterol, cholesterol oxidase is added, which produces $H_2O_2$ in proportion to the amount of cholesterol present. $H_2O_2$ is detected using horseradish peroxidase (HRP) and Amplex Red, producing the pink, highly fluorescent product resorufin.

Samples and standards were diluted in reaction buffer (0.1 M potassium phosphate pH 7.4 with 0.05 M NaCl, 5 mM cholic acid and 0.1% Triton X-100) and added to a 96 well

plate (Greiner) at 50 µL per well, in duplicate. Reaction mixture (cholesterol oxidase, HRP and 150 µM Amplex Red in reaction buffer) was added to wells in the same volume, and the assay was incubated at 37°C until developed (appearance of pink colour). Fluorescence was measured at 530 nm excitation and 590 nm emission and cholesterol concentrations were calculated based on standards.

### 2.9.2 Thin layer chromatography

*2.9.2.1 Lipid extractions*

For thin layer chromatography (TLC) analysis of lipid levels, cell and tissue samples were homogenised, BCA assays were performed, and samples were diluted in MilliQ water to equal volumes. To extract lipids, chloroform : methanol (C:M; both from ThermoFisher) 1:2 equal to 5X the sample volume was added to samples and incubated on a roller at 4°C overnight. Samples were centrifuged and supernatants were collected. The sample pellet was re-suspended in the same volume of C:M 1:2 and incubated on a roller at room temperature for 3 hr, centrifuged again, and this supernatant was combined with the first. Samples were washed 1 - 5 times depending on salt or other contamination (consistent treatment within experiments), by addition of equal volumes of DPBS and C:M 1:2 and removal of the aqueous phase. Lipid extracts were dried and used or stored.

*2.9.2.2 Separation of species*

Samples were re-suspended in C:M 1:1 and sonicated for 10 minutes to produce a uniformly distributed suspension. Silica gel high-performance TLC (HPTLC) plates (Merck Millipore) were dried at 50°C, then samples were loaded and dried alongside a lipid standard (Avanti Polar Lipids). Lipid extracts were separated using a saturated solvent system consisting of either C:M:water 65:25:4, for separation of general lipid species, or C:M:CaCl 0.22% 60:35:8 for separation of gangliosides.

*2.9.2.3 Developing plates*

Plates were dried, then sprayed with dye solutions and developed by gradual heating to 90°C. For a general lipid TLC, anisaldehyde spray (0.5ml p-anisaldehyde in 50ml glacial acetic acid and 1 ml concentrated sulphuric acid (ThermoFisher)) was used, and for a ganglioside TLC orcinol spray (1% orcinol in 50% sulphuric acid) was used. Resolved plates were scanned and the density of lipid bands was analysed using ImageJ.

## 2.10 Fluorescence microscopy

Microscopy was performed using an inverted Zeiss Colibri LED widefield fluorescence microscope with a high speed MRm monochrome charge-coupled device (CCD) camera and Axiovision 4.7.1 software, with a 40x magnification oil immersion lens. $Ca^{2+}$ data was captured and analysed using the Physiology package of Axiovision 4.7.1.

## 2.11 Other equipment

Absorbance plate assays were performed using a Tecan Infinite F50 microplate reader. Fluorescence plate assays were performed using a BMG Labtech POLARstar plate reader and FLUOstar software.

## 2.12 Data Analysis

Images were false coloured using Photoshop CS3. Where brightness and contrast of images were altered this was performed consistently within experiments, except in cases where brightness was altered to reveal changes in localisation (these cases are identified in figure legends). This was also performed using Photoshop CS3.

Density analysis (of western blots and TLC plates) and cell counts were performed using ImageJ. Measurement of average fluorescence intensity per spot, average size per spot, and number of spots detected per cell were all performed using the standard spot detection algorithm in the Icy bioimage software (de Chaumont *et al.*, 2012). Statistical tests were performed using Prism, and unless specified in figure legends are unpaired 2-sample t-tests (Janusonis, 2009; De Winter, 2013).

Huntingtin alignments to identify lysosomal targeting motifs were performed using the NCBI Needleman-Wunsch tool (NCBI Resource Coordinators, 2018) for pairwise alignments and EMBL-EBI Clustal Omega (Sievers *et al.*, 2011; Goujon *et al.*, 2010) for multiple sequence alignments, and the diagram of huntingtin used to show motifs was drawn using the Cuckoo IBS Illustrator for Biological Sequences (Liu *et al.*, 2015).

# CHAPTER 3 LYSOSOMAL STORAGE PHENOTYPES IN HUNTINGTON'S DISEASE

## 3.1 Introduction

### 3.1.1 Outline

Huntington's disease has defects in lysosomal function and lipid metabolism, phenotypes similar to a class of diseases called lysosomal storage disorders, and in particular to an LSD called Niemann-Pick type C. Lysosomal lipid storage and other lysosomal disease phenotypes may be present in HD, a component of HD pathogenesis which has not previously been investigated.

Lipid levels and distribution were examined in multiple cell models of HD. Accumulation of LBPA and lysosomal storage of cholesterol, GM1 and sphingomyelin were observed. HD cell models also had defects in endocytic trafficking, including a block in glycolipid trafficking, and reduced lysosomal $Ca^{2+}$ signalling.

HD therefore has lysosomal storage and cellular trafficking defects similar to those seen in Niemann-Pick type C. These defects will contribute to HD pathology and may suggest common mechanisms between HD and LSDs, providing further useful avenues of research.

### 3.1.2 Lysosomal storage phenotypes in HD

Existing literature suggests that HD cells have expanded lysosomes, the key phenotype in lysosomal storage diseases (LSDs). HD cells have increased Lysotracker staining (Camnasio *et al.*, 2012; Castiglioni *et al.*, 2012), indicating expansion of the lysosomal compartment, and the lysosomal protein LAMP2 is increased in HD models (Koga *et al.*, 2011). There are over sixty LSDs and while lysosomal expansion is the common phenotype, the materials stored and the mechanisms involved vary widely (Platt, Boland & van der Spoel, 2012). With lysosomal expansion present in HD models, it would be interesting to look for other LSD phenotypes, and to consider whether there are similarities to specific disorders, which might provide us with useful information on pathogenesis, treatment or further lines of mechanistic investigation in HD. HD is not identical to any known LSD, which are generally severe and distinctive, and there is no evidence that any known LSD involves huntingtin dysfunction, but partial defects in the

pathways which fail catastrophically in LSDs could be a component of HD pathogenesis.

LSDs involve aberrant accumulation of materials in the lysosome. In HD, cholesterol accumulates in multiple models (Valenza *et al.*, 2010; 2007a) and is mislocalised to punctate structures within HD cells (Trushina *et al.*, 2006; Del Toro *et al.*, 2010; Marullo *et al.*, 2012), suggesting lysosomal storage. Several LSDs involve cholesterol storage or trafficking defects (Schultz *et al.*, 2011; Walkley & Vanier, 2009). Lysosomal cholesterol accumulation can lead to increased cellular cholesterol overall, or instead to redistribution of cholesterol without a change in levels (Lloyd-Evans & Platt, 2010). This can differ even within a single disease, across different tissues, model species, or culture conditions (Lloyd-Evans & Platt, 2010; Walkley & Vanier, 2009).

Cholesterol storage occurs as a primary phenotype in Tangier disease (loss of ABCA1), and esterified cholesterol is stored in lysosomal acid lipase (LAL) deficiency (Wolman disease), and in a subtype of this disease called cholesteryl ester storage disease (CESD). Lysosomal cholesterol storage is also seen to varying degrees as a secondary defect in the sphingolipidoses Niemann-Pick A and B, GM1 and GM2 gangliosidosis, and several mucopolysaccharidoses (MPS) (Walkley & Vanier, 2009). In these cases, primary storage of either sphingomyelin or glycosphingolipids leads to coordinate storage of cholesterol due to altered lysosomal function and cellular trafficking, or biophysical interactions (for example between sphingomyelin and cholesterol (Slotte, Pörn & Härmälä, 1994). In Niemann-Pick type C, the primary defect is not in a specific enzyme so multiple major lipid species are stored, including cholesterol (Vanier, 2010; Lloyd-Evans & Platt, 2010).

Of the LSDs listed above where cholesterol is stored, ganglioside storage is also present in NPC, the gangliosidoses, and some MPS subtypes (Walkley & Vanier, 2009). Ganglioside metabolism is altered (largely reduced) in HD (Maglione *et al.*, 2010) and gangliosides may accumulate in some models (Del Toro *et al.*, 2010). The primary storage materials in α-mannosidosis and the MPSs are glycoproteins and glycosaminoglycans (GAGs) respectively, and sphingomyelin is dramatically increased in NPA and B, more than in NPC. There are no reports of changes to these materials in HD (Tsang *et al.*, 2006; Handley *et al.*, 2016), which may allow us to rule the mechanisms behind these diseases out. Based on storage materials, HD is most similar

to NPC, though it also shares features with the other cholesterol storage diseases and gangliosidoses.

The clinical presentation of these diseases can help us narrow down potential links. Many LSDs present as a spectrum of cases, with both severe childhood forms and milder adult-onset cases, which is useful when comparing to HD. Of the diseases listed, Niemann-Pick A & C, the two gangliosidoses and the MPSs are neurodegenerative and so of most interest when comparing to HD. The other disorders are either primarily visceral (Wolman, CESD, Tangier and NPB), or present with muscular and skeletal abnormalities or intellectual disabilities (α-mannosidosis and the MPSs) which are not present in HD.

| Disorder | Gene defect | Pathology | Symptoms |
|---|---|---|---|
| Primary cholesterol storage: | | | |
| **Wolman & CESD** | LAL | cholesteryl ester storage | fatty deposits, digestive defects, liver disease |
| **Tangier** | ABCA1 | cholesterol and phospholipid storage, reduced HDL | cholesterol deposits, peripheral neuropathy, cardiovascular disease |
| Secondary cholesterol storage: | | | |
| **Niemann-Pick type A & B** | ASM | sphingomyelin storage | Neurodegeneration (type A), lung disease, hepatosplenomegaly |
| **GM1 gangliosidosis** | β-galacto-sidase | ganglioside storage | Neurodegeneration, motor defects, muscular and skeletal abnormalities, retinal degeneration |
| **GM2 gangliosidoses** | β-hexos-aminidase | ganglioside storage | Neurodegeneration, motor defects, retinal degeneration |
| **α-mannosidosis** | α-D-manno-sidase | glycoprotein storage | intellectual disability, muscular and skeletal abnormalities, hearing loss, hepatosplenomegaly |
| **MPS** | enzymes of GAG degra-dation | glycosaminoglycan (GAG) storage | intellectual disability, muscular and skeletal abnormalities |
| Multiple lipid storage: | | | |
| **Niemann-Pick type C** | NPC1 or NPC2 | multiple lipid storage, $Ca^{2+}$ and trafficking defects | neurodegeneration, cerebellar ataxia, hepatosplenomegaly |

**Table 3.1 LSDs and other disorders with lysosomal cholesterol storage**

While NPA is neurodegenerative, it is caused by almost total loss of ASM and is fatal within 2-3 years of birth. Total loss of ASM is therefore incompatible with the clinical course of HD, and less severe ASM defects lead to NPB, which generally does not have neurodegenerative involvement. NPC, on the other hand, can present as adult-onset neurodegenerative forms (not the case for all LSDs), and like HD is primarily a motor disease, although NPC defects are cerebellar and ataxic rather than choreic. Like NPC, the gangliosidoses are neurodegenerative diseases with motor defects, though they

also have characteristic retinal degeneration which is largely not present in HD. As with storage materials, clinical phenotypes suggest that NPC and perhaps the gangliosidoses bear some resemblance to HD.

One other disease, Smith-Lemli-Opitz syndrome (SLOS), may also have interesting mechanistic links to HD. This is not a lysosomal storage disorder, but instead is a disease of defective cholesterol metabolism, caused by loss of the final enzyme in the cholesterol biosynthetic pathway, *DHCR7* (DeBarber *et al.*, 2011). In SLOS, decreased cholesterol metabolism leads to altered levels of sterol intermediates that affect cholesterol trafficking and induce lipid accumulation in cells (Waller-Evans *et al.,* unpublished), mechanisms which may be of interest in trying to understand the complex cholesterol changes apparently present in HD.

HD has several similarities to LSDs, particularly both phenotypic and clinical similarities to NPC which suggest an NPC-like phenotype may be present in HD. NPC has a characteristic set of pathogenic changes which would be present in HD if common mechanisms are occurring in both diseases. In addition to the storage of lipids discussed above - cholesterol, gangliosides and sphingomyelin - LBPA and sphingosine also accumulate in the lysosome, endosomal trafficking is blocked at the late endosomal-lysosomal stage, and lysosomal $Ca^{2+}$ content and release are reduced (Lloyd-Evans *et al.*, 2008). These are phenotypes which we can investigate in HD to support or rule out a mechanistic link.

**3.1.3 Aims**

In this chapter, we aim to look for lysosomal phenotypes in HD, expanding the work done in an ST14A cell line model of HD and including new models, the STHdh cell line and HD patient fibroblasts. We aim to focus on known NPC phenotypes so that we can compare HD and NPC and determine whether common mechanisms could be involved.

## 3.2 Results

### 3.2.1 HD model cell lines have an altered lysosomal compartment

Existing reports and previous work in the lab using the ST14A cell line have shown that several HD models have an expanded lysosomal compartment, so our first step with the ST*Hdh* cells was to investigate lysosomal markers in this additional cell line. We
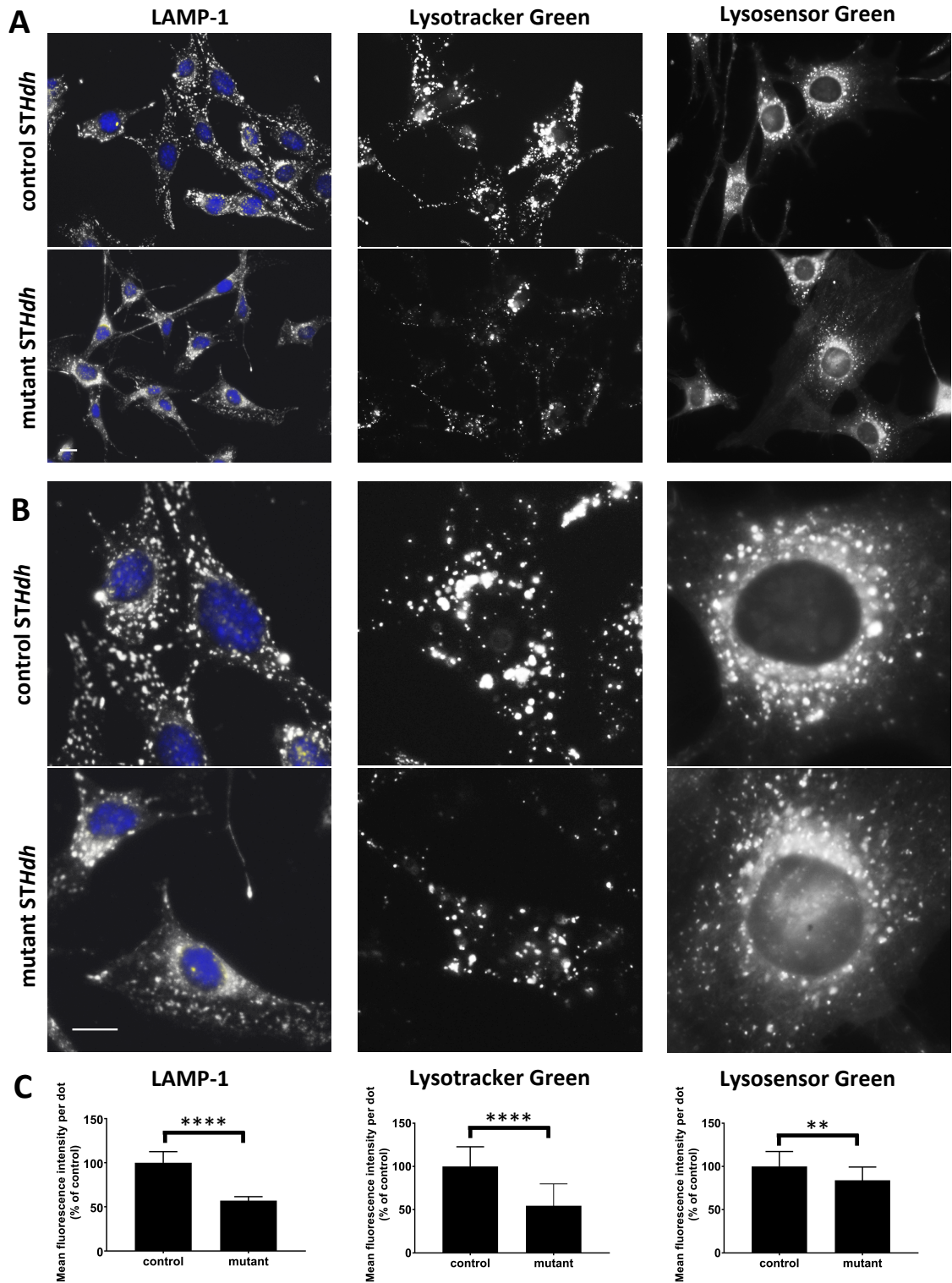
**Figure 3.1 HD model cell lines have an altered lysosomal compartment**
**A** ST*Hdh* control and HD cells stained with LAMP1 antibody, Lysotracker Green, or Lysosensor Green. Representative images; scale bar 5 μm. LAMP1 n = 2, Lysotracker n = 3, Lysosensor n = 1. **B** Expanded panels from images in A. Scale bar 5 μm. **C** Mean fluorescence intensity per dot of lysosomal markers, compared to control cells. Error bars indicate standard deviation. ** p < 0.01 **** p < 0.0001 by unpaired 2-sample t-test.

stained these cells with antibodies against LAMP1, one of the lysosomal outer membrane glycoproteins (Figure 3.1). In HD cells, LAMP1 staining is altered, with a dense perinuclear accumulation of punctae and staining and somewhat reduced punctae in the periphery of the cell. Mean fluorescence intensity per dot is significantly reduced in the experiments presented here. Lysotracker Green, a fluorescent dye which loads into lysosomes, is significantly reduced in HD ST*Hdh* cells (Figure 3.1), and is distributed differently, with fewer punctae in the perinuclear region than are seen in LAMP1 staining. These two stains should both label the same compartment, and so the discrepancy is curious. Another probe, Lysosensor, is related to Lysotracker but its fluorescence varies with lysosomal pH as well as lysosomal volume. In an initial test, Lysosensor staining is similar or slightly reduced in HD compared to control ST*Hdh* cells, with little apparent change in localisation (Figure 3.1).

**3.2.2 HD model cell lines have lysosomal lipid storage**

Next, we examined lipid levels and localisation in ST*Hdh* cells. We looked at lipids which have previously been seen to be altered in HD models and in the ST14A HD cell line, and at lipids which are stored or mistrafficked in NPC, including LBPA, cholesterol, GM1 and sphingolipids. In addition to the control (Q7) and mutant huntingtin (Q111) ST*Hdh* cells, we also included a drug-induced NPC model for comparison in a number of these experiments. This model was produced by treating control cells with the NPC1 inhibitor U18666A (Lu *et al.*, 2015), a widely used method (Cenedella, 2009).

LBPA (lysobisphosphatidic acid) is a lysophospholipid found only in the late endosome which can be used as a marker for the compartment, and which is increased in NPC disease (Kobayashi *et al.*, 1999). Staining with an anti-LBPA antibody showed increased labelling in HD ST*Hdh* and ST14A cells compared to their respective controls, an effect which is significant in the ST14A cells, and also showed an increase in perinuclear rather than distributed punctate labelling, similar to that seen in LAMP1 staining (Figure 3.2). The increased labelling in HD cells is similar to, though less severe than, that seen in the U18666A treated cells, and suggests expansion of the late endosome and lysosomal compartment and accumulation of LBPA.
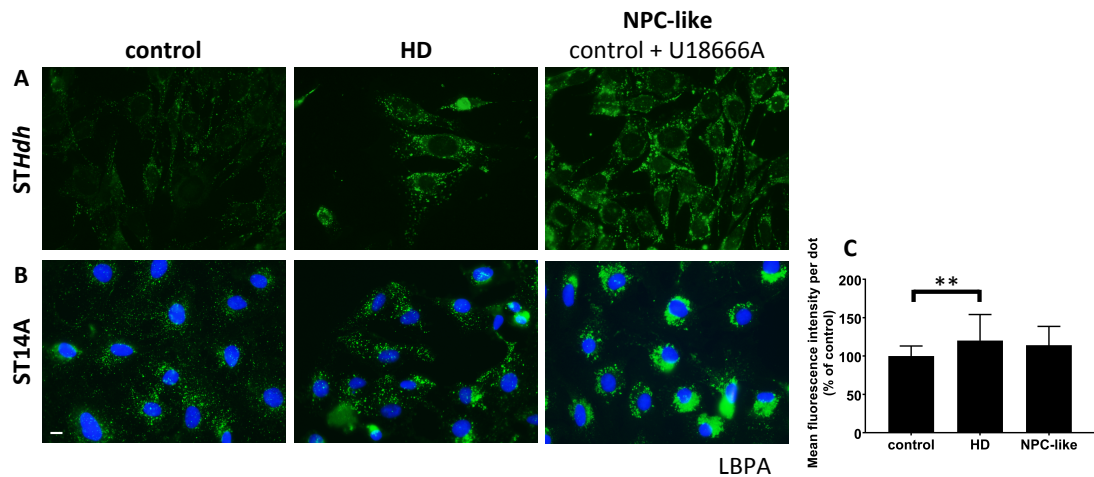
**Figure 3.2 HD model cells have increased LBPA**
ST*Hdh* (**A**) and ST14A (**B**) control and HD cells, and control cells treated with 2 µg/ml U18666A for 24 hours to induce a NPC-like phenotype, were stained with an antibody against LBPA. Representative images; scale bar 5 µm. ST*Hdh* n = 4, ST14A n = 3. **C** Mean fluorescence intensity per dot in ST14A cells, compared to control. Error bars represent standard deviation. ** $p < 0.01$ by one-way ANOVA and Tukey's multiple comparison post test.

Cholesterol storage in lysosomes is a key phenotype of NPC (Lloyd-Evans & Platt, 2010; Ioannou, 2005), and changes to cholesterol have been reported in HD (Del Toro *et al.*, 2009; Trushina *et al.*, 2006). We therefore labeled both cell lines with filipin, a fluorescent antibiotic which specifically binds cholesterol, to visualise cholesterol localisation (Vruchte, 2004). In both sets of cell lines, some of the HD cells display a change from diffuse to punctate localisation of staining (Figure 3.3). The pattern of distribution differs slightly between ST*Hdh* and ST14A HD cells, but is similar to the staining after U18666A treatment in the relevant cell line. All the U18666A treated cells displayed the characteristic bright, dense peri-nuclear punctate staining which indicates lysosomal storage of cholesterol in NPC. For ST*Hdh* cells, we scored the cells as either diffuse (low intracellular fluorescence with some plasma membrane and peri-nuclear endocytic recycling compartment staining) or punctate (larger punctae in the peri-nuclear region and throughout the cell, indicating mislocalisation). In the ST*Hdh* cell lines, 27.0% of the HD cells have punctate staining compared to only 4.6% of controls, a significant increase. In the ST14A cell lines, we measured the mean number of dots per cell using a spot detection algorithm. The mean number of dots per cell was slightly but significantly increased in HD ST14A cells compared to controls. While

the HD models are much less severe, the increased punctate distribution of filipin staining, with some elevation in the peri-nuclear region, is similar to the localisation of cholesterol in the U18666A treated cells.
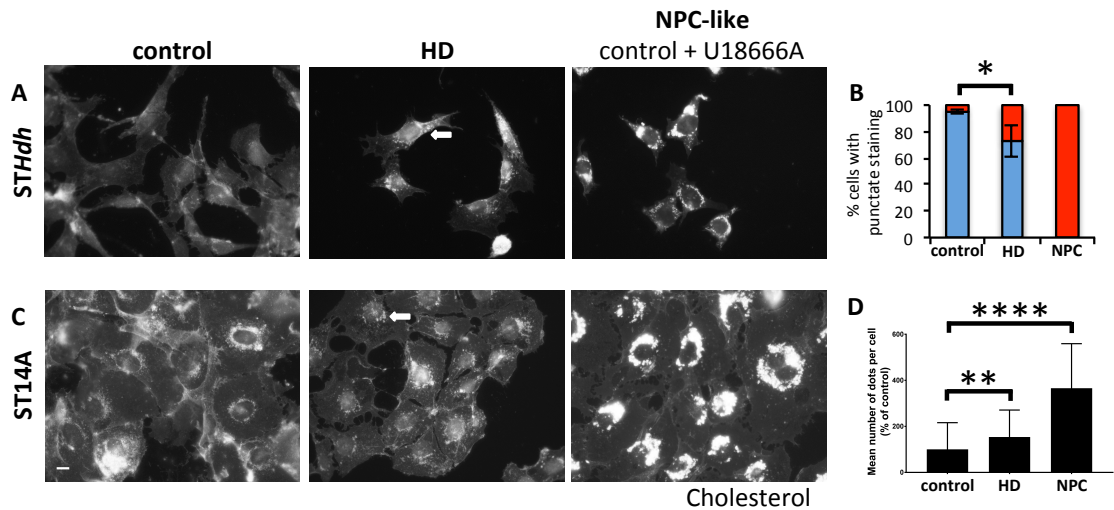


**Figure 3.3 HD model cells have punctate distribution of cholesterol**
*STHdh* (**A** & **B**) and ST14A (**C** & **D**) control and HD cells, and control cells treated with 2 µg/ml U18666A for 24 hours to induce a NPC-like phenotype, were stained with filipin. **A** & **C** Representative images; white arrows indicate example cells with filipin punctae; scale bar 5 µm. **B** Staining in ST*Hdh* cells was scored as either diffuse (blue) or punctate (red), and the mean percentage of cells with punctate staining across all experiments was calculated. Error bars are standard deviation; n = 4. * $p < 0.05$ by unpaired 2-sample t-test. **D** Mean number of dots per cell in ST14A cells. Error bars are standard deviation; n = 3. ** $p < 0.01$ **** $p < 0.0001$ by one-way ANOVA and Tukey multiple comparison test.
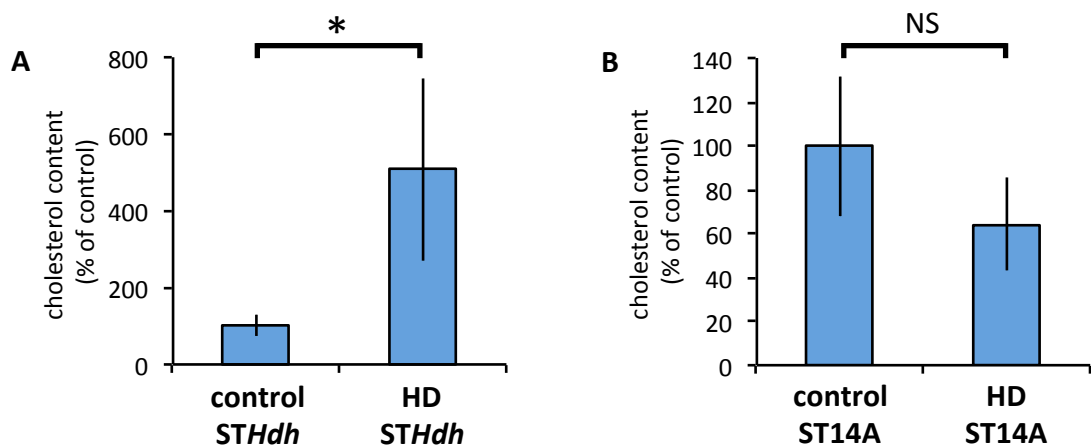


**Figure 3.4 HD model cells have altered cholesterol levels**
Cholesterol content of *STHdh* (**A**) and ST14A (**B**) control and HD cells was measured using an enzymatic assay. n = 3 for each cell line; duplicate measurements in each experiment; presented as mean percentage of control; error bars are standard deviation. * $p < 0.05$ by unpaired 2-sample t-test.

61

Filipin staining is useful for examining cellular distribution of cholesterol but is not representative of cholesterol levels as it does not bind in a 1:1 ratio (Marullo *et al.*, 2012). Instead, we used an enzymatic assay which measures free (non-esterified) cholesterol. In the ST*Hdh* cell lines, the HD model cells had a three- to five-fold increase in cholesterol content compared to controls, a significant effect, whereas in the ST14As levels of cholesterol are not significantly altered in the HD models though on average they are decreased compared to controls (Figure 3.4).

GM1, another lipid which accumulates in NPC, has also been observed to both increase and decrease in HD (Del Toro *et al.*, 2010; Maglione *et al.*, 2010). We therefore stained the two sets of cell lines with FITC-conjugated cholera toxin B subunit (FITC-CtxB), which binds GM1 (Hansson, Holmgren & Svennerholm, 1977), and again included a U18666A-treated positive control for comparison (Figure 3.5). While sufficient experiments for statistical analysis are not presented here, in both cell lines, staining of GM1 across the whole cell is considerably higher in HD than in control cells. Redistribution of GM1 staining is also visible. In the ST*Hdh* cell lines, the percentage of cells with punctate staining increased from 12.9% of controls to 63.4% in the HD line.
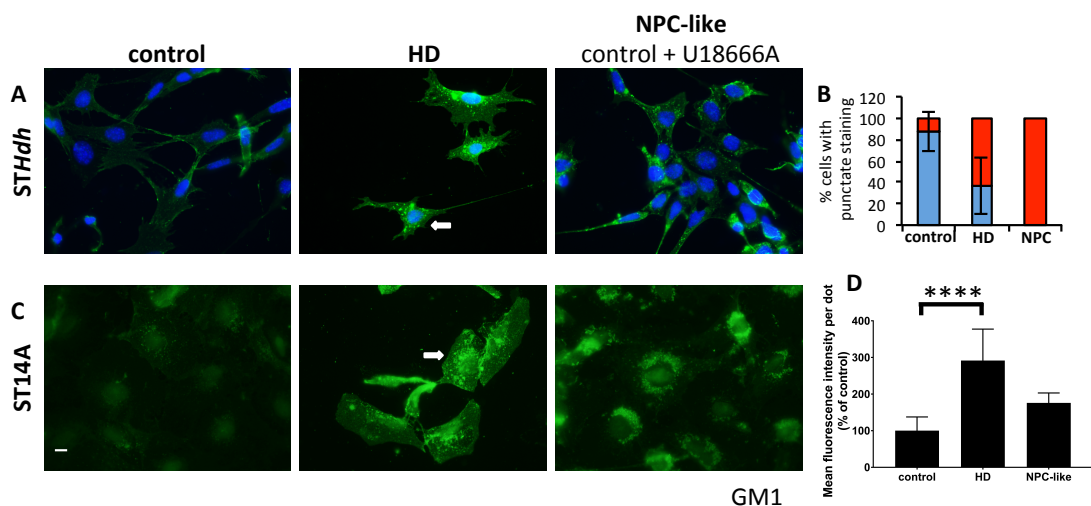


**Figure 3.5 HD model cells have punctate distribution of ganglioside GM1**
ST*Hdh* (**A** & **B**) and ST14A (**C** & **D**) control and HD cells, and control cells treated with 2 µg/ml U18666A for 24 hours to induce a NPC-like phenotype, were stained with FITC-CtxB. **A** & **C** Representative images; white arrows indicate example cells with FITC-CtxB puncta; scale bar 5 µm. **B** Staining in ST*Hdh* cells was scored as either diffuse (blue) or punctate (red), and the mean percentage of cells with punctate staining was calculated. Error bars are standard deviation. **D** Mean fluorescence intensity per dot in ST14A cells compared to control. Error bars are standard deviation. **** $p < 0.0001$ by one-way ANOVA and Dunnett multiple comparison test. ST*Hdh* n = 2, ST14A n = 1.

In the ST14A HD cells the proportion of punctate cells is similarly increased (not shown), and fluorescence intensity per dot, measured using a spot detection method, is dramatically increased compared to control, an effect which is significant in the single experiment presented here. The U18666A treated cells display an NPC-like phenotype, with high levels of punctate staining, which is also seen in the HD cells, but a reduction in GM1 at the cell periphery rather than the increase seen in these HD cell lines.

In preliminary experiments to visualise sphingomyelin, we labelled these cells with lysenin toxin (Figure 3.6). In ST*Hdh*, overall levels of fluorescence are unaltered or slightly reduced in HD cells, but punctate staining is increased. In ST14A cells, the HD cells display considerably higher labelling throughout the cell, but there is limited evidence of punctate staining.
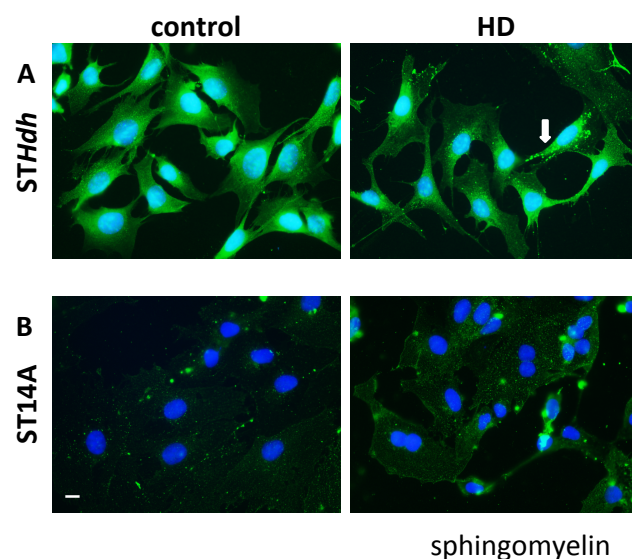


**Figure 3.6 ST*Hdh* cells may have altered cellular sphingomyelin**
*STHdh* (**A**) and ST14A (**B**) control and HD cells were stained with lysenin. Representative images; white arrows indicate example cells with lysenin puncta; scale bar 5 µm. ST*Hdh* n = 1, ST14A n = 1.

The punctate structures labelled with lipid stains in HD cells suggest these lipids are being stored in lysosomes. In a preliminary attempt to confirm that these punctate structures are lysosomal, we co-stained with the lysosomal marker LAMP1 (Figure 3.7). In ST*Hdh* HD cells which had punctate structures containing either cholesterol or GM1, these structures also labelled with LAMP1. Some lipid punctae do not overlap with

LAMP1 directly, but are close to LAMP1-labelled punctae, suggesting vesicles which are being trafficked to or from the lysosome, or one stain surrounds the other in ring-like structures, suggesting vesicles large enough and in the appropriate focal plane for detail to be visible. These co-labelled compartments suggest that punctate lipid structures in ST*Hdh* cells do indeed indicate lysosomal storage of these lipids.
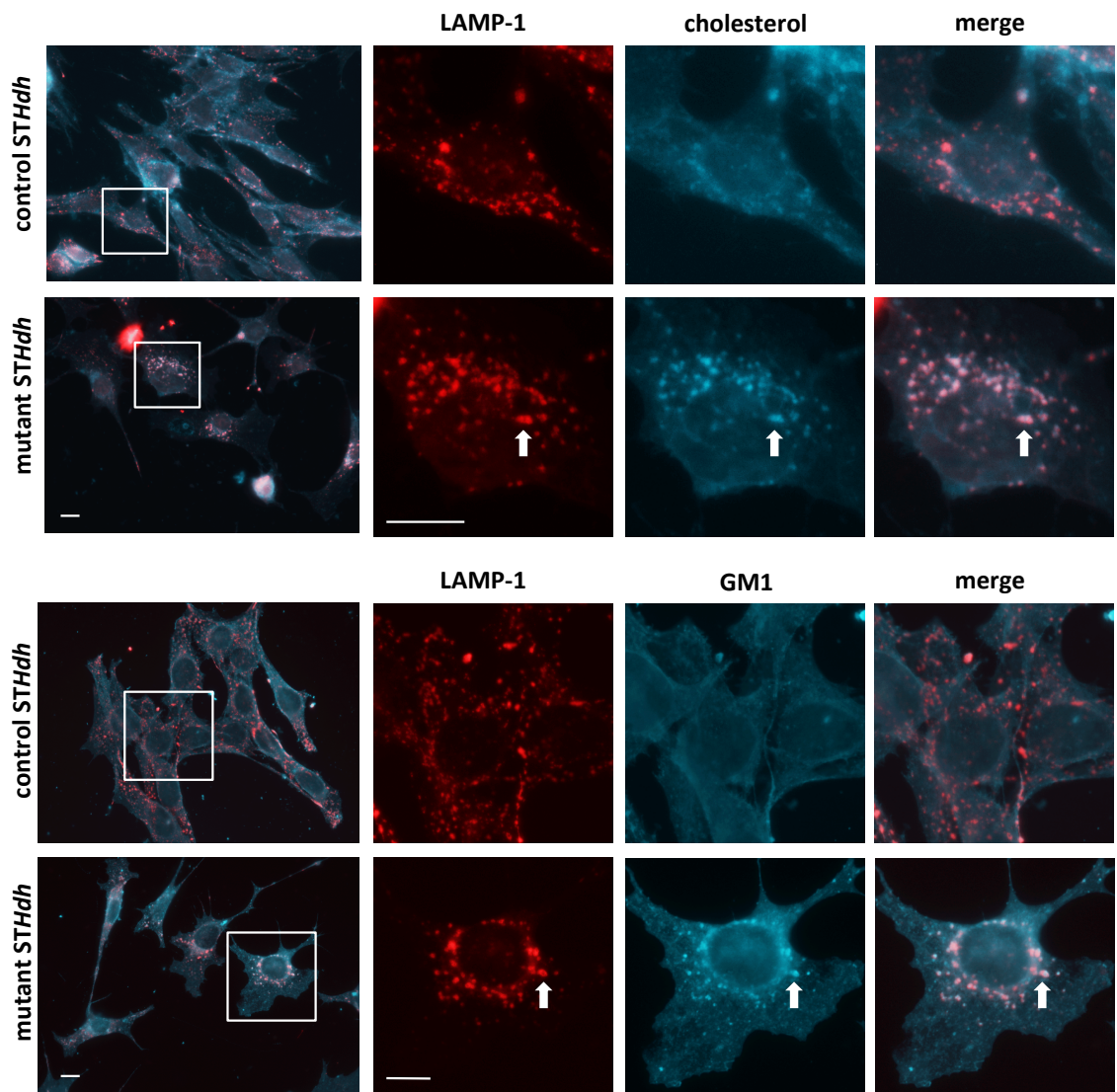


**Figure 3.7 Lipid storage bodies also contain the lysosomal marker LAMP1**
Control and HD ST*Hdh* cells were co-labelled with either filipin (cholesterol) or FITC-CtxB (GM1), and anti-LAMP1 antibody. Regions of images indicated by white boxes were expanded (centre) and merged (right). Arrows indicate examples of co-labelled compartments. Scale bar 5 μm. n = 1.
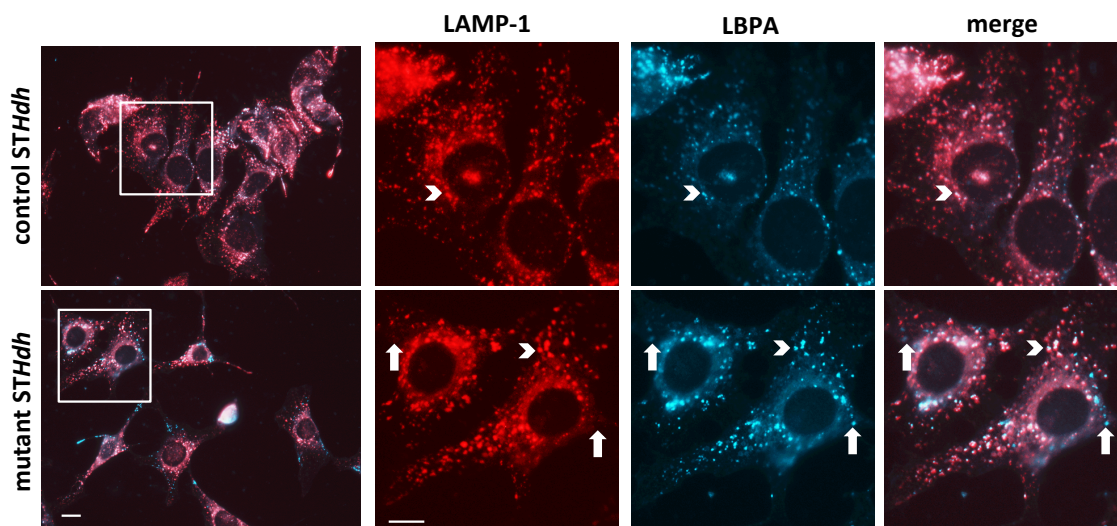
**Figure 3.8 LBPA does not fully colocalise with the lysosomal marker LAMP1 in HD**
Control and HD ST*Hdh* cells were co-labelled with antibodies against LBPA and LAMP1. Regions indicated by white boxes were expanded and merged (right). Arrowheads indicate costained compartments, and arrows indicate compartments with LBPA labelling but without LAMP1. Scale bar 5 μm. n = 1.

We also costained ST*Hdh* cells with LAMP1 and LBPA, which we would expect to label overlapping lysosomal and late endosomal compartments. While this is the case in the ST*Hdh* control cells, where the two stains almost entirely label the same structures, it is not fully the case in the HD cells (Figure 3.8). In HD ST*Hdh* cells, some structures label with both LAMP1 and LBPA, particularly in the perinuclear region. However, there are also a large number of LBPA-positive LAMP1 negative structures, particularly in more peripheral regions of the cell, and some LAMP1-positive LBPA-negative punctae, suggesting that different subpopulations of vesicles could be present.

### 3.2.3 HD model cell lines have endocytic trafficking defects

NPC cells have a severe block in cellular trafficking at the late endosome to lysosome stage. One method for measuring this is by monitoring trafficking of ganglioside GM1 (Sugimoto *et al.*, 2001). GM1 labelled with FITC-CtxB would normally traffic via endocytosis and through the lysosome to reach the Golgi. In NPC cells, this is blocked or dramatically slowed, and the labelled GM1 remains in punctate endocytic structures rather than reaching the Golgi. In control ST14A cells, FITC-CtxB labelled GM1 reaches the Golgi in almost 90% of cells, whereas in HD cells only approximately 50% of cells
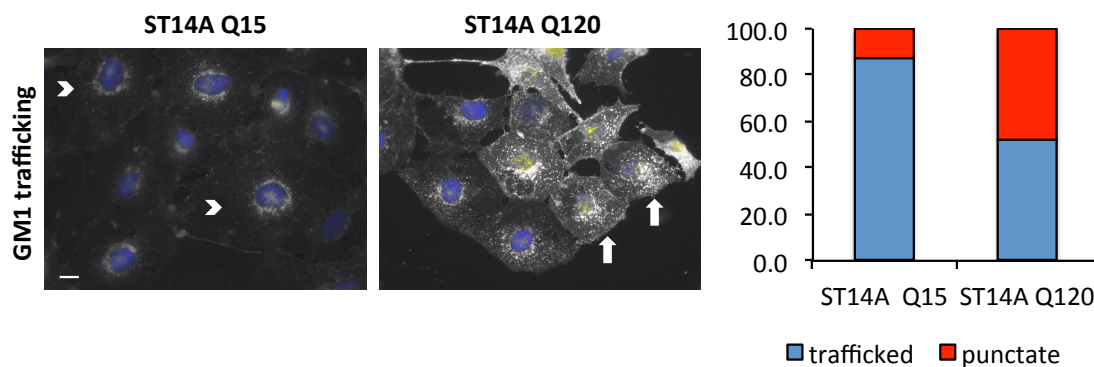
**Figure 3.9 Lipid trafficking is altered in HD cells**
Control and HD ST*Hdh* cells were labelled with FITC-CtxB and trafficking of GM1 was monitored. Cells were scored as having either Golgi staining (correct trafficking; arrowheads) or punctate staining (indicating a block in trafficking; arrows). Scale bar 5 µm. n = 1.
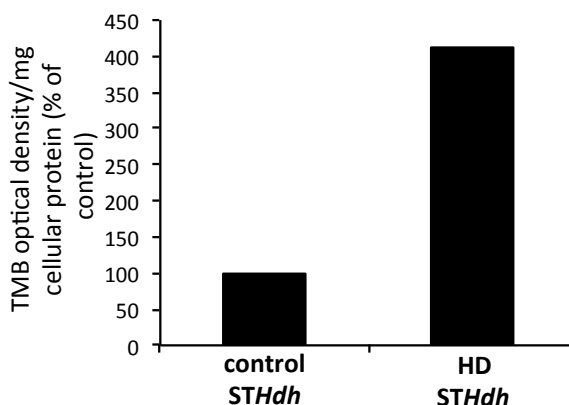


**Figure 3.10 Uptake of endocytic cargoes is increased in HD ST*Hdh* cells**
Uptake of HRP in Control and HD ST*Hdh* cells was measured using a colourimetric HRP substrate. Activity of HRP (measured in absorbance units of product produced) was corrected to mg of cellular protein and given as percentage of control. n = 2.

have Golgi labelling and the remainder are punctate (Figure 3.9), consistent with previous work in this cell line (Dr. Haslett, Mr. Badell-Grau). This indicates that ganglioside trafficking is blocked in HD cells, similar to the defect in NPC.

While NPC trafficking defects are at the late endocytic stage, HD cells have broad cellular trafficking defects, including at earlier endocytic stages. To compare these to known NPC phenotypes, we measured fluid phase endocytosis via uptake of HRP (horseradish peroxidase). Preliminary data suggests uptake was increased in ST*Hdh* HD cells, which contained four times more endocytosed HRP than controls (Figure 3.10).

This may indicate both increased uptake and a decrease in early endosomal recycling, which preliminary data suggests may be reduced in these cells (not shown), and which has previously been shown in HD (Li *et al.*, 2009; Akbergenova & Littleton, 2017).

### 3.2.4 HD model cell lines have altered cellular and lysosomal $Ca^{2+}$ signalling

Dysregulation of lysosomal $Ca^{2+}$ is a key feature of NPC (Lloyd-Evans *et al.*, 2008). HD cells are known to have defects in cellular $Ca^{2+}$ handling (Lim *et al.*, 2008; Giacomello *et al.*, 2013) (altered ER and mitochondrial signalling, dysregulation of cytoplasmic $Ca^{2+}$) but the status of lysosomal $Ca^{2+}$ signalling in HD has not been reported. We used live $Ca^{2+}$ imaging to characterise aspects of cellular $Ca^{2+}$ signalling in ST*Hdh* cells.

To measure lysosomal $Ca^{2+}$, we clamp other cellular stores by treating cells with ionomycin, and then release lysosomal $Ca^{2+}$ by addition of GPN (see Chapter 2.6). Treatment of ST*Hdh* cells with 300 μM GPN produced a lysosomal $Ca^{2+}$ response in HD cells which was a third of that seen in controls (Figure 3.11), a significant decrease. This reduction in lysosomal $Ca^{2+}$ is similar to the change seen in NPC, and will cause disruption of the $Ca^{2+}$ signalling needed for endocytic trafficking and lysosomal function.
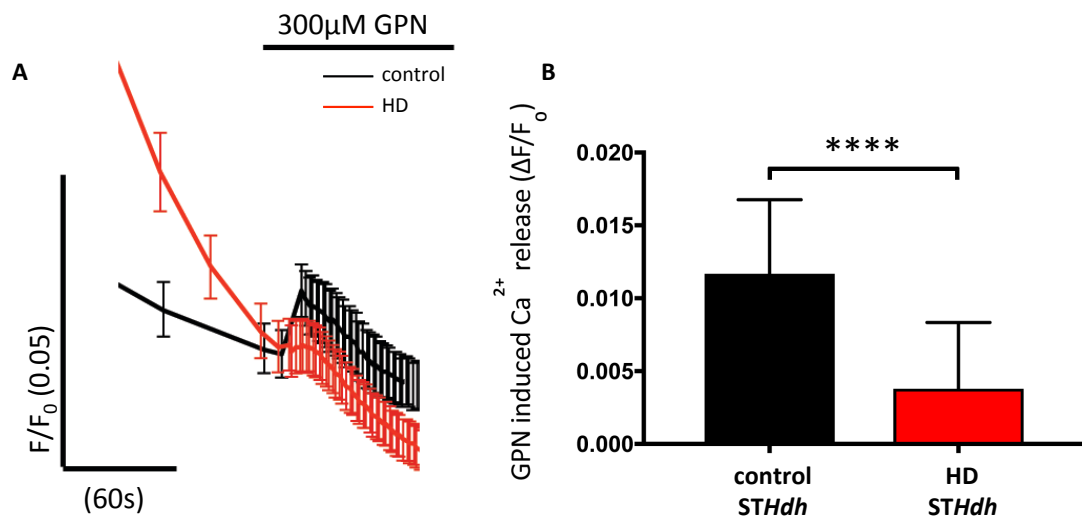


**Figure 3.11 GPN-induced release of lysosomal $Ca^{2+}$ is reduced in HD ST*Hdh* cells**
Fura-2-AM $Ca^{2+}$ measurements of response to 300 μM GPN in control and HD ST*Hdh* cells, after ionomycin stimulation to clamp other cellular stores. **A** example traces of $Ca^{2+}$ release after 300 μM GPN treatment. Black indicates control cells and red indicates HD cells. Average of cells from one experiment; n = 15 cells each. **B** $Ca^{2+}$ release ($\Delta F/F_0$) after 300 μM GPN treatment in control and HD cells. Error bars are SD. Average of 2 independent experiments; n > 20 cells. **** p < 0.0001 by unpaired 2-sample t-test.

We also examined other aspects of cellular $Ca^{2+}$ signalling in these cells to compare to known HD defects. Increases in resting cytosolic $Ca^{2+}$ have been reported in some models, but are not always present (Giacomello, Hudec & Lopreiato, 2011). We compared basal $Ca^{2+}$ measurements in HD and control ST*Hdh* cells and found no difference in Fura-2 fluorescence under the conditions we used (Figure 3.12). Changes to SERCA and ER $Ca^{2+}$ signalling have previously been reported in HD cells (Giacomello *et al.*, 2013). We tested this and found that treatment with 5 µM thapsigargin (a SERCA inhibitor) triggered a significantly larger increase in Fura-2 fluorescence in ST*Hdh* HD cells (0.21 $\Delta F/F_0$) than in controls (0.11 $\Delta F/F_0$), indicating a larger increase in cytosolic $Ca^{2+}$ in agreement with previous reports (Figure 3.13).
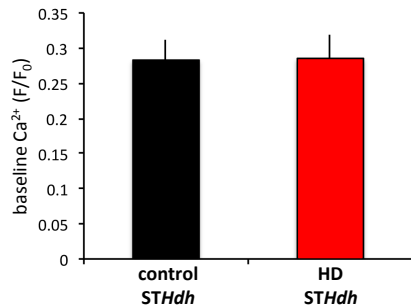


**Figure 3.12 Resting cytosolic $Ca^{2+}$ is unchanged in HD ST*Hdh* cells**
Baseline Fura-2-AM $Ca^{2+}$ measurements ($F/F_0$) in control and HD ST*Hdh* cells before drug treatments. Data is an average from at least 10 experiments for each cell line. Error bars represent standard deviation. p = 0.449 by unpaired 2-sample t-test.
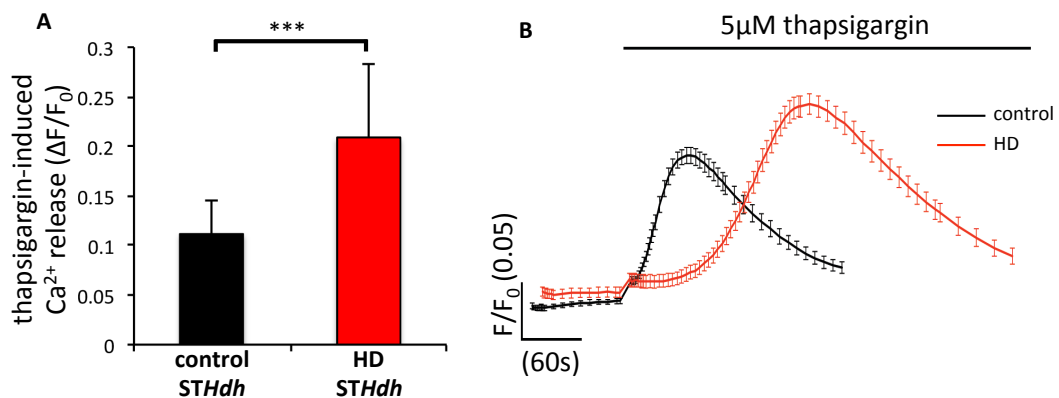


**Figure 3.13 HD ST*Hdh* cells have altered ER $Ca^{2+}$ release**
Fura-2-AM $Ca^{2+}$ measurements of responses to thapsigargin in ST*Hdh* cells in $Ca^{2+}$-free buffer. **A** $Ca^{2+}$ release ($\Delta F/F_0$) after 5 µM thapsigargin treatment in control and HD cells. Error bars are standard deviation. Average of 2 experiments each for control cells and 3 experiments each for controls. *** p < 0.001 by unpaired 2-sample t-test. **B** Example traces of $Ca^{2+}$ release after 5 µM thapsigargin treatment in control and HD cells. Red indicates HD cells and black indicates control cells. Average of cells from one experiment; n > 15 cells in each condition.
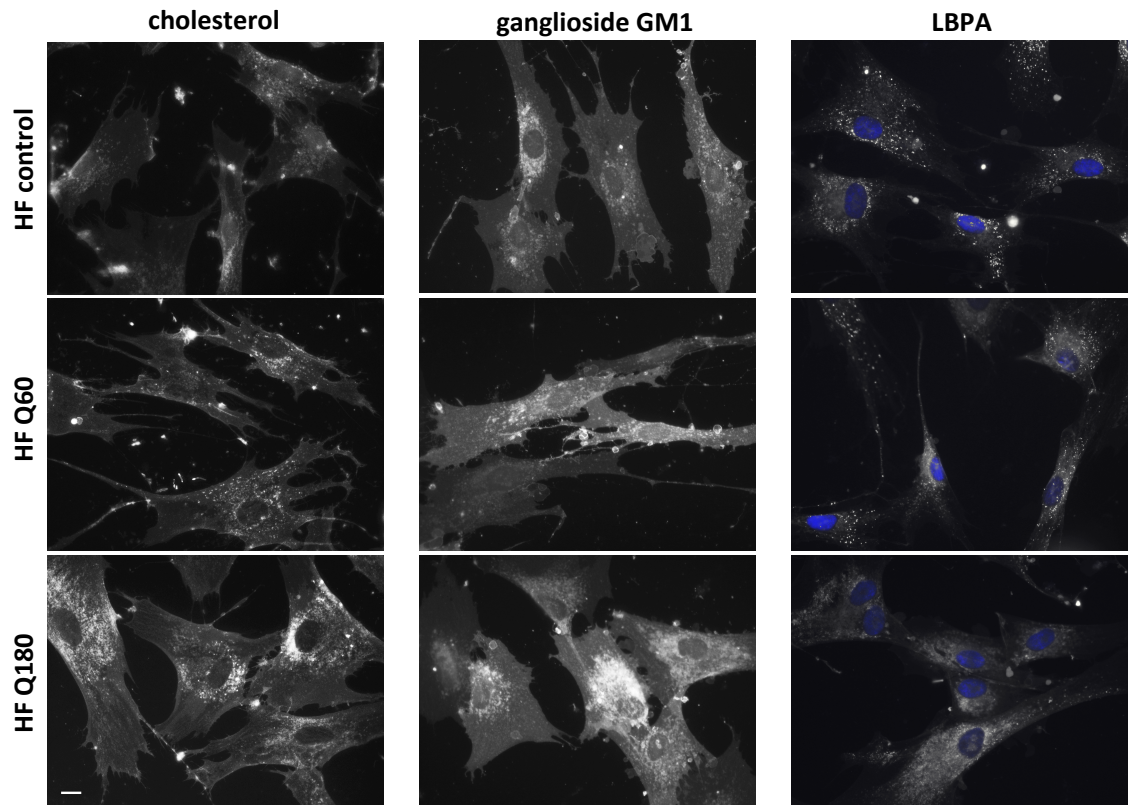
**Figure 3.14 Lipid storage in HD patient fibroblasts**
Human fibroblast cells were stained with probes for cholesterol (filipin), ganglioside GM1 (FITC-CtxB) and LBPA (anti-LBPA antibody). Representative images; scale bar 5 µm. n = 3.

### 3.2.5 HD patient fibroblasts have abnormal lipid storage

We also looked at lipid storage in HD patient fibroblasts. These cell lines are more relevant to the cellular defects present in actual disease cases, and fibroblasts have been used to model cellular defects in neurodegenerative disease research, including $Ca^{2+}$ (Kilpatrick *et al.*, 2016) defects and lipid storage (Ganley & Pfeffer, 2006). Both of the patient cell lines we used were cases of more severe disease, with one young adult (Q60) and one juvenile (approximately Q180) case, whereas classical adult-onset disease has an average polyglutamine repeat of 45-50. Both Q60 and Q180 fibroblast cells had punctate cholesterol staining, punctate GM1 labelling and increased levels of GM1 compared to control, and increased levels of LBPA staining compared to controls (Figure 3.14). The effects in Q60 cells are smaller, whereas the Q180 cells, a very severe childhood HD case, have very severe lipid storage phenotypes, comparable to the levels that could be expected in cells from an LSD patient (for example in (Walter,

Davies & Ioannou, 2003)). However, analysis of these images based on spot detection and measurement produced mixed results, indicating less clear results than the images suggest, and alternative analysis such as biochemical measurement of lipids may be needed to confirm the changes in these cells.

## 3.3 Discussion

### 3.3.1 Preliminary comments

Lysosomal expansion and lipid accumulation are present in existing studies of HD, and in preliminary work done by Dr. Lloyd-Evans and Dr. Haslett. They observed lipid storage, trafficking defects and reduced lysosomal $Ca^{2+}$ in an ST14A cell line model of HD, and initial tests suggested that lipid storage was also present in HD mouse tissues and iPSC-derived neuronal precursor cells. In addition to the ST*Hdh* cell line, I continued the work in ST14A cells alongside Dr. Haslett and Mr. Badell-Grau (described in Table 3.2), but have presented only my own, partial data here and will discuss individual and combined observations below, with data from additional cell models.

| Phenotype | Repeats in ST14A | Effect observed in HD compared to control |
|---|---|---|
| Lysotracker | 4 | Increased |
| LBPA | 3 | Increased |
| Cholesterol | 5 | Increased punctate staining instead of diffuse cellular staining |
| GM1 | 5 | Increase in intensity of staining, increased punctate staining |
| Sphingomyelin | 2 | Increase in intensity of staining in both repeats, increased punctate staining once |
| Lipid storage (TLC) | 2-3 | Significantly increased cholesterol, LBPA, and sphingoid bases, decreased phospholipid |
| Lipid trafficking (FITC-CtxB) | 6 | Significant inhibition of trafficking |
| Lysosomal $Ca^{2+}$ release | 5 | Significantly decreased lysosomal $Ca^{2+}$ |

**Table 3.2 NPC-like phenotypes in ST14A cells by Dr. Haslett and Mr. Badell-Grau**

### 3.3.2 HD cells have altered lysosomes

Lysosomal expansion has been seen in HD, both in existing literature (Castiglioni *et al.*, 2012; Camnasio *et al.*, 2012) and in the ST14A cell line we have previously used (Table 3.2). The lysosomal changes seen in ST*Hdh* are different, so it is possible they are particular to this cell line, but they are still of interest. LAMP1, Lysotracker and Lysosensor staining are decreased in HD cells compared to control (Figure 3.1). The

reduction in Lysotracker intensity per dot is significant, and the reduction in intensity of the other two stains is significant in the initial experiments presented here, though this data is still incomplete. The distribution of LAMP1 and Lysotracker is also different, as there is an increase in large peri-nuclear LAMP1 punctae in HD cells, whereas Lysotracker punctae are more peripheral. In a single experiment, the localisation and size of Lysosensor labelled structures is not altered between HD and control cells (Figure 3.1). Distribution of Lysosensor staining is more similar to LAMP1 than to Lysotracker, with denser staining in the peri-nuclear region (Figure 3.1).

These stains are all labels for the late endosome / lysosome, but LAMP1 is a structural component, whereas Lysotracker and Lysosensor are dependent on activity and function of lysosomes, and Lysosensor is affected by changes in pH. A reduction in lysosomal pH would explain the reduction in Lysotracker fluorescence (as Lysotracker will not accumulate and fluoresce in less acidic compartments), but Lysosensor is not altered and existing evidence suggests there are no pH defects in HD (Martinez-Vicente *et al.*, 2010; Erie *et al.*, 2015), which may suggest this is not the case. The difference in distribution of the three stains suggests there may be separate compartments which are labelling differently, although previous work on lysosomal subpopulations found that lysosomes further from the cell surface were more acidic (Johnson *et al.*, 2016), which would suggest Lysotracker staining should not be reduced.

LBPA is found in the late endosome (Kobayashi *et al.*, 1999) and under normal conditions co-localises with LAMP and can be used as a late endosomal / lysosomal marker (White *et al.*, 2006; Dunster, Toh & Sentry, 2002). In ST*Hdh* cells, increased LBPA staining (**Figure 3.2**) would therefore indicate an increased late endosomal / lysosomal compartment in HD. However, costaining LBPA and LAMP1 in these cells shows they do not completely overlap, at least not compared to the controls where almost all of the structures visible are labelled with both markers (Figure 3.8). In the HD cells, the presence of LBPA-positive vesicles without LAMP1 staining strongly suggests a block in trafficking, fusion or maturation in the late endosomal and lysosomal compartment.

Both the difference between LAMP1 and Lysotracker distribution and the altered overlap between LAMP1 and LBPA suggest that HD ST*Hdh* cells may have separate

subpopulations of organelles, rather than the normal closely interconnected late endosomal and lysosomal compartments, or that trafficking of LAMPs or other lysosomal components is altered in HD. This might produce or involve a pH defect, and so could be connected to the unexpected decrease in Lysotracker staining.

### 3.3.3 HD model cells have NPC-like defects

In addition to lysosomal dysfunction, there are changes to lipids in both HD model cell lines we have used. Both the ST14A and ST*Hdh* HD cells have increased LBPA, cholesterol, GM1 and sphingomyelin, and there is punctate (lysosomal) storage of cholesterol and GM1 in both cell lines, and potentially also of sphingomyelin. We have focused on these particular lipids, and on other known NPC defects, to be able to compare HD to NPC.

Lysosomal cholesterol storage, a key NPC phenotype, is present in HD cells. In both sets of cell lines, the HD cells have punctate staining of cholesterol (Figure 3.3 and Table 3.2), and in initial tests in ST*Hdh* cells these structures co-stain with LAMP1 (Figure 3.7), supporting our theory that the storage is lysosomal. Total levels of cholesterol are less conclusive, as ST*Hdh* cells have a significant increase whereas ST14A cells show a decrease (which is not significant) in this assay, but have increased cholesterol in the TLC performed by Dr. Luke Haslett (Table 3.2). The enzymatic assay used here may be able to measure other sterols in addition to cholesterol (Marullo *et al.*, 2012), and could therefore be measuring a combination of cholesterol and cholesterol precursors, which have beeen shown to be reduced in this and other models (Valenza *et al.*, 2005; Marullo *et al.*, 2012).

In addition, lysosomal storage of cholesterol does not always lead to changes in total level. In NPC, absolute cholesterol levels are increased in the liver and other peripheral organs, but in the brain there is no total change as cholesterol accumulates in lysosomes but is reduced in other parts of the cell (Karten *et al.*, 2002; Lloyd-Evans & Platt, 2010). The difference between these two cell lines also matches the variability seen in existing HD literature, where some models or methods show an increase in total cholesterol and others a decrease (Chapter 1.6.9).

The other NPC storage lipids are also altered in HD. GM1 is present in punctate storage bodies in both cell lines, which agrees with our other work in ST14A cells (Figure 3.5 and Table 3.2), and these punctate bodies co-localise with LAMP1 in initial tests (Figure

3.7), suggesting storage is lysosomal. There is also an overall increase in GM1 staining throughout the cell (though we have not quantified this using biochemical methods), a phenotype agrees with previous reports of increased surface GM1 in ST*Hdh* and primary HD mouse cells (Del Toro *et al.*, 2010).

Some punctate storage of sphingomyelin was observed in ST*Hdh* cells (**Figure 3.6**), and the combined data in ST14A cells (**Figure 3.6** and **Table 3.2**) suggests an overall increase in sphingomyelin and potentially an increase in punctate labelling in HD cells compared to controls. However, this data set is incomplete due to difficulties in obtaining the sphingomyelin stain, lysenin, which is no longer commercially available. LBPA is also increased in both HD cells compared to their controls (**Figure 3.2** and **Table 3.2**), although preliminary co-labelling with LAMP1 in the ST*Hdh* cells (Figure 3.8) suggests that other trafficking defects are present which would be worth confirming in a second cell type and would be interesting to investigate further.

We looked briefly at two aspects of cellular and endocytic trafficking in HD cells. Measuring ganglioside GM1 trafficking (or trafficking of other GSLs) in NPC reveals a late endosomal / lysosomal block in lipid trafficking which prevents GM1 from reaching the Golgi as normal (Lloyd-Evans *et al.*, 2008) (a defect which is also present in a number of other LSDs (Pagano, 2003)). This block is also present in HD cells (**Figure 3.9**), though to a lesser extent than the total block observed in NPC. Initial tests show that uptake of HRP by fluid phase endocytosis is increased in HD cells (**Figure 3.10**). While this is only preliminary data and needs to be completed, it matches existing reports of endocytic changes in HD cells, and may be due to a decrease in recycling from early endosomal compartments which has previously been seen in HD (Li *et al.*, 2009; Akbergenova & Littleton, 2017). This is different to NPC, where initial uptake is slightly reduced, but recycling out of the cell is increased, leading to reduced internalisation (Mayran, Parton & Gruenberg, 2003; Lloyd-Evans *et al.*, 2008). In addition to altered LBPA localisation (Figure 3.8), these changes to cellular trafficking suggest that an NPC-like late endosomal block in endosomal lipid trafficking is present in these cells as a component of broader cellular trafficking defects known in HD.

The co-staining experiments demonstrate that cholesterol and GM1 storage are in bodies which co-stain with LAMP1 (Figure 3.7), so lipid storage is likely to be in vesicles which are positive for both LAMP1 and LBPA rather than those which lack LAMP1. In

NPC, cholesterol co-localises with both LBPA and LAMP (Kobayashi *et al.*, 1999; Kwiatkowska *et al.*, 2014), suggesting the lipids are in a single compartment, potentially a different pattern. While this could be a defect specific to this cell line, like the potential pH defect which we have not seen elsewhere, it could also be due to the extensive cellular trafficking defects known to be present in HD, which could interact with an NPC-like phenotype to produce different effects.

### 3.3.4 HD patient cells have NPC-like defects

NPC-like lipid storage is also present in the HD patient fibroblasts we used here, although age-matched controls were not available for these experiments. Cholesterol and GM1 are stored in punctate structures in patient cells, and LBPA staining is increased (Figure 3.14). The patient cells we selected are both from more severe HD cases, which may mean that cellular defects are more extreme, but the presence of these phenotypes in patient-derived cell lines suggests they are relevant to real disease cases as well as to HD models. These cell lines also suggest that the NPC-like phenotypes vary with huntingtin CAG repeat length, a possible indication of relevance to HD, as storage was considerably more severe in the Q180 cells than the Q60 cells.

### 3.3.5 HD cells have altered $Ca^{2+}$ signalling

HD cells of both the ST*Hdh* (Figure 3.11) and the ST14A (previous work by Dr. Haslett and Mr. Badell-Grau) cell lines have decreased $Ca^{2+}$ release in response to GPN compared to controls, indicating decreased lysosomal $Ca^{2+}$ and dysfunction of lysosomal $Ca^{2+}$ signalling. This is a key feature of NPC pathology (Lloyd-Evans *et al.*, 2008; Lloyd-Evans & Platt, 2011), and its presence in HD cells will contribute to defects in late endosomal / lysosomal trafficking and fusion, affecting endocytosis, autophagy and phagocytosis, as $Ca^{2+}$ release from lysosomes is required for these events (Lloyd-Evans *et al.*, 2010; Li, Garrity & Xu, 2013; Medina *et al.*, 2015). It is therefore a factor in HD pathogenesis, potentially contributing to the endocytic defects seen here and in previous studies, and the defects in autophagy known in HD. These cells also have increased $Ca^{2+}$ release from the ER in response to thapsigargin treatment (Figure 3.13), a known HD defect (Giacomello *et al.*, 2013). Extensive $Ca^{2+}$ dyshomeostasis is present in HD (Chapter 1.6), involving increased release from the ER, increased entry into the cell, and decreased ability of the mitochondria to buffer changes in cytoplasmic $Ca^{2+}$ (Giacomello *et al.*, 2013). We potentially also saw some evidence of these defects, as

the HD cells were slower to return to baseline than controls after responding to thapsigargin (Figure 3.13).

### 3.3.6 Consistency and variability between HD cell models

There are differences in phenotypes between the two cell models we have used, and differences when compared to studies using other HD models. In particular, the reduced Lysotracker labelling in HD ST*Hdh* cells (Figure 3.1) is different to the ST14A cell line (Dr. Luke Haslett and Mr. Badell-Grau) and previous reports (Camnasio *et al.*, 2012; Castiglioni *et al.*, 2012), and changes in total cholesterol are different between cell lines (Figure 3.4). These are interesting as they match the known variability of lipid changes in HD (Chapter 1). It is difficult to say from this study why these different models produce different results, but there are a number of factors which could contribute.

Firstly, the mutant form of huntingtin used in each model is slightly different, as the ST*Hdh* mutant cells are a knock-in model homozygous for full-length huntingtin with a human first exon and either a Q7 or Q111 polyglutamine repeat (Trettel *et al.*, 2000), whereas the ST14As have a mutant human first exon fragment (1-548aa, Q120) expressed in addition to endogenous normal huntingtin. Protein interactions or aggregation could therefore be affected differently. While the ST*Hdh* and ST14A cell lines are both striatal-derived cell types, the patient cells are fibroblasts, and species differences between rat, mouse and human could contribute: high huntingtin CAG repeat lengths are required to produce disease models in rodents whereas they cause severe disease in humans, and pathways of lipid metabolism have a different balance between species (Quinn, Georgiou & Payne, 1985; Bergen & Mersmann, 2005; Yin *et al.*, 2012). Culture methods can also impact cell models: for example, lipid storage may not occur if the cell is not supplied with lipids, even though the storage and trafficking defects are still present (Pentchev *et al.*, 1985).

However, a number of observed defects are consistently present across the different models we have used. Cholesterol, GM1 and LBPA storage are seen in all three sets of cell lines, and trafficking and lysosomal $Ca^{2+}$ signalling defects have been seen in both ST14A and ST*Hdh*, based on this study and other work done in the lab. The consistency of these phenotypes is strong evidence that they are real effects, and are a relevant component of HD pathogenesis.

### 3.3.7 Conclusions

We have identified lysosomal and lipid defects in HD which have not been previously described. In general our observations here also agree with known defects in HD, with altered lipids, ER Ca$^{2+}$, and cellular trafficking, and variability in total cholesterol levels. Unlike other HD models, Lysotracker staining is decreased in ST*Hdh* cells, although other markers suggest lysosomal expansion may be present.

Between submission and finalisation of this thesis, a study was published detailing chromosomal abnormalities and altered cell size and proliferation in the ST*Hdh* cell model of HD, and suggesting that these abnormalities are likely to confound studies using these cell models (Singer *et al.*, 2017). It is likely that this explains the variability which we observed in this cell line, both within individual experiments and when compared to other models. While this paper brings into question some of the data included here, we can still be confident of phenotypes which we have also observed in other cell models.

We have focused on known LSD phenotypes as our interest was in comparing HD to NPC. Several similarities to NPC pathogenesis are present in HD cells, including lipid storage, altered lysosomal Ca$^{2+}$, and a block in ganglioside GM1 trafficking. There are also differences, including increases in GM1 and sphingomyelin throughout the cell, and more extensive disruption to endocytic and cellular trafficking. While they are different diseases with different causes, this data suggests that there are NPC-like components to HD pathology, contributing to or interacting with other HD mechanisms. These are previously uncharacterised components of HD pathogenesis, which highlight the importance of the lysosome in disease, but they also suggest mechanistic links which may account for these phenotypic similarities between the two diseases.

# CHAPTER 4 NPC1 FUNCTION IS DISRUPTED IN HUNTINGTON'S DISEASE

## 4.1 Introduction

### 4.1.1 Outline

Lysosomal storage disease phenotypes are present in HD models in this study and in existing literature, and studies have identified involvement of huntingtin in the endocytic and lysosomal system. The NPC-like phenotypes suggest that lysosomal dysfunction in HD specifically includes defects in the proteins involved in NPC disease, NPC1 and NPC2.

Distribution of NPC1 and levels of NPC2 are altered in HD ST*Hdh* cells compared to controls, and function of the two proteins may be reduced. NPC1 co-immunoprecipitates with huntingtin, indicating a direct interaction between these two proteins. NPC-like storage phenotypes are not present in two other polyglutamine expansion disorders, the spinocerebellar ataxias 1 and 3, suggesting a specific effect of mutant huntingtin rather than a general effect of polyglutamine expansion.

These experiments reveal a specific disruption of NPC1 via interaction with mutant huntingtin, providing a mechanism for the presence of lysosomal storage defects in HD. NPC-like phenotypes are not ubiquitous in polyglutamine expansion disorders, although different forms of lysosomal dysfunction may be present. In combination with other work in the lab, also this expands the evidence for a role of normal huntingtin in the lysosome, and suggests targets for further research and therapeutic intervention.

### 4.1.2 Screening predicts endocytic and lysosomal involvement in HD

In addition to a number of studies which show association of huntingtin with the lysosome in HD (summarised in Chapter 1.6.7), genetic and proteomic screening studies support the involvement of the endocytic and lysosomal system in this disease. Large-scale studies have identified, among other factors, a number of endocytic and lysosomal genes, which are altered in, or associated with, HD.

Neueder and Bates (Neueder & Bates, 2014) analysed gene expression in HD postmortem brain and identified networks of transcriptional dysregulation associated

with mutant huntingtin, and several lysosomal genes were among those altered. Increased expression of the NPC protein NPC2 was observed in the caudate, the region most affected in HD, and expression of transcription factor EB (TFEB), a core regulator of lysosomal biogenesis, function and signalling (Napolitano & Ballabio, 2016) was altered. There were also changes to expression of several subunits of the lysosomal V-ATPase, possibly mirroring increased lysosomal volume as there are no reports of altered lysosomal pH in HD (Erie *et al.*, 2015), and cathepsin processing, an indicator of lysosomal pH, is not altered (Martinez-Vicente *et al.*, 2010).

In a different genetics approach, HD genetics consortia led by Gusella, Jones and Tabrizi performed genome-wide association (GWA) analyses to identify polymorphisms which modify clinical onset and progression of HD (Genetic Modifiers of Huntington's Disease (GeM-HD) Consortium, 2015). Based on gene annotation, the major pathways identified are related to mitochondrial function, DNA repair, and immunity, but pathways related to vesicle trafficking and, interestingly, V-ATPase are also present, and a number of proteins annotated as having involvement in the major pathways are also known to be lysosomal proteins. Further analysis of this to identify lysosomal proteins would be interesting and might provide future lysosomal targets for investigation.

Studies using yeast-2-hybrid experiments to identify huntingtin interactors have also identified proteins involved in endocytosis and vesicle trafficking (Kaltenbach *et al.*, 2007; Tourette *et al.*, 2014). These include the adaptor protein AP-2A, subunits of the Golgi-to-ER vesicle coat complex COP-I, and components of dynein and dynamin transport complexes, the latter of which is involved in endo-lysosomal cholesterol transport and can lead to cholesterol storage if inhibited (Robinet *et al.*, 2006).

The identification of endocytic and lysosomal genes in these studies supports the theory that huntingtin has a role in endocytic trafficking, as discussed in Chapter 1, and may point towards mechanisms for the lysosomal defects identified in Chapter 3.

### 4.1.3 Huntingtin modulates endocytic and lysosomal function

Both normal and mutant huntingtin have been shown to be associated with the endocytic and lysosomal system, and to affect its structure and function. Huntingtin associates with or is in endosomal and lysosomal bodies (Kegel *et al.*, 2000; Martin *et al.*, 2015; Kang *et al.*, 2007), and mutant huntingtin leads to altered lysosomal

structure (Kegel *et al.*, 2000; Martin *et al.*, 2015; Camnasio *et al.*, 2012; Castiglioni *et al.*, 2012; Koga & Cuervo, 2011). Huntingtin and the mutant form of the protein also affect lysosomal distribution and movement within the cell (Erie *et al.*, 2015; Caviston *et al.*, 2011), important modulators of lysosomal function (Pu *et al.*, 2016; Johnson *et al.*, 2016; Korolchuk *et al.*, 2011; Korolchuk & Rubinsztein, 2011). Autophagy is also affected by mutant huntingtin, with defects in both cargo recognition (Martinez-Vicente *et al.*, 2010) and vesicle trafficking (Wong & Holzbaur, 2014) leading to poor clearance of cargo and accumulation of autophagic components and toxic materials (Wong & Holzbaur, 2014; Martin *et al.*, 2015). Known cellular defects in HD may provide the mechanisms by which LSD phenotypes appear in these models. Disrupted vesicle trafficking will affect delivery of both cargo and lysosomal proteins to appropriate endocytic and lysosomal compartments, and lipid metabolism and lysosomal function depend on endocytic trafficking.

**4.1.4 Lysosomal dysfunction contributes to HD pathogenesis**

Lysosomal dysfunction is known to be a major factor in neurodegenerative disease (Zhang, Sheng & Qin, 2009; Maxfield, 2014; García-Arencibia *et al.*, 2010; Colacurcio & Nixon, 2016), including HD (Cortes & La Spada, 2014; Erie *et al.*, 2015; Qin, 2003) (see Chapter 1.6.7). Lysosomal dysfunction increases huntingtin aggregation and alters proteolytic cleavage of huntingtin, contributing to an increase in abnormal huntingtin forms in HD (Qin, 2003).

Lysosomal dysfunction may contribute to other defects in cellular function seen in HD. Reduced lysosomal $Ca^{2+}$ signalling, a feature of NPC which we have observed in HD cells, disrupts endocytic and lysosomal trafficking (Lloyd-Evans *et al.*, 2010), and can contribute to cellular $Ca^{2+}$ dysfunction via lysosomal modulation of other stores and pathways (López Sanjurjo *et al.*, 2013; López Sanjurjo, Tovey & Taylor, 2014; Penny *et al.*, 2015; Patel & Cai, 2015). Failure of vesicle trafficking and lysosomal fusion can lead to defects in autophagy, known to be present in HD, which then contribute to failure to clear huntingtin aggregates or damaged mitochondria (Martin *et al.*, 2015). The presence of lysosomal storage phenotypes and mechanisms, and the associated lysosomal dysfunction, could therefore be an important component of HD pathogenesis.

### 4.1.5 Polyglutamine expansion diseases

Including HD, there are 14 known diseases caused by expansion of trinucleotide repeats in different genes (Orr & Zoghbi, 2007), 9 of which are polyglutamine disorders caused by CAG repeat expansion (Fan *et al.*, 2014). All of these are dominantly inherited (except for fragile X syndrome which is X-linked), and the majority are neurodegenerative diseases, but the genes involved and the clinical presentation of the diseases are diverse (Orr & Zoghbi, 2007).

Other than HD, the majority of polyglutamine disorders are spinocerebellar ataxias (SCAs). SCAs have diverse causes, including both polyglutamine disorders and other mutations, but are clinically and pathologically similar, involving loss of cerebellar Purkinje neurons and presenting with ataxia (Hekman & Gomez, 2014). SCAs have more clinical similarity to NPC than HD does, as cerebellar ataxia and loss of Purkinje neurons are also primary defects in NPC (Vanier, 2010). In this project, we used two of these polyglutamine-expansion SCAs to investigate lysosomal function: SCA1 and Machado-Joseph disease (MJD/SCA3). Both diseases are poorly understood, but SCA1 is caused by polyglutamine expansion in ataxin-1 (ATXN1), a DNA binding protein which forms nuclear aggregates in the mutant form, and MJD is caused by mutation of ataxin-3 (ATXN3), a deubiquitinase enzyme.

### 4.1.6 Aims

We aim to look for the mechanisms behind the lysosomal defects and lysosomal storage phenotypes which we have observed in HD, with particular focus on the NPC1 protein as we have seen an NPC-like phenotype in HD cells. To do so, we will investigate the presence and function of the NPC proteins in HD cells, and test for direct interactions between NPC1 and huntingtin.

## 4.2 Results

### 4.2.1 NPC proteins are altered in HD models

HD cell models have NPC-like lipid storage defects and cellular dysfunction, potentially due to NPC-mediated mechanisms in HD. There are two proteins involved in NPC disease: most cases are caused by loss of NPC1, but rarely NPC2 is defective instead (Wassif *et al.*, 2015). We investigated these two proteins, particularly NPC1, in HD models.

We used western blotting to measure protein levels in control and HD ST*Hdh* cells. Levels of NPC1 are unaltered in HD cells compared to control (Figure 4.1). NPC2 levels, on the other hand, are increased approximately 3 fold in the HD model cells compared to controls, though the extent of the NPC2 increase is variable between different cell samples (Figure 4.1).
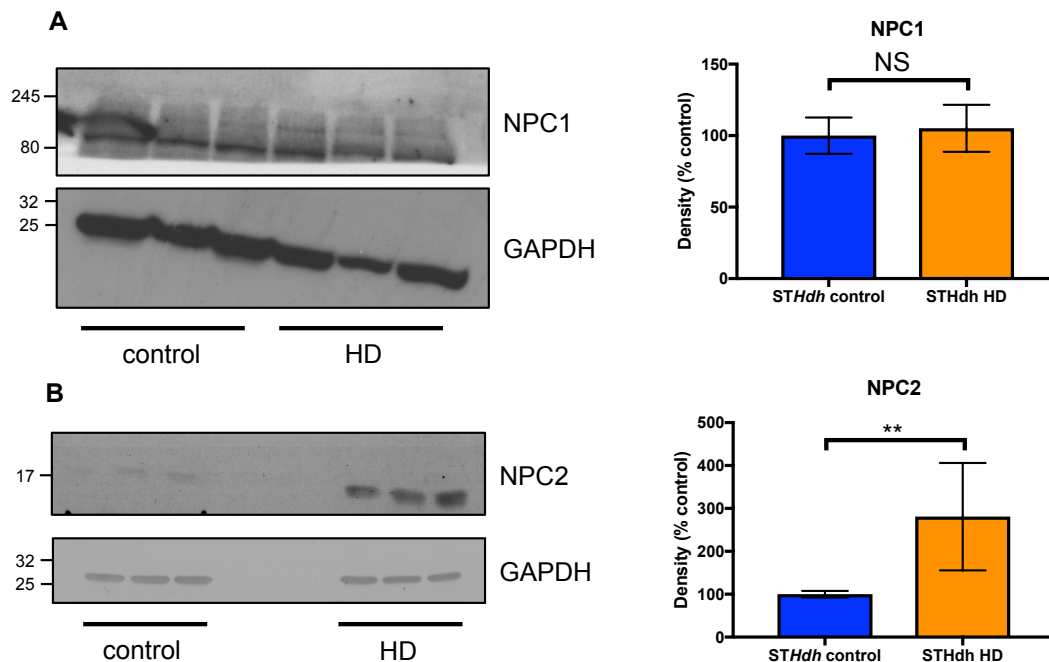


**Figure 4.1 NPC2 protein is dramatically increased in HD model cells**
**A** Levels of NPC1 protein were measured via western blot in control and HD ST*Hdh* cells (anti-NPC1 antibody Novus NB400-148). **B** Levels of NPC2 protein were measured via western blot in control and HD ST*Hdh* cells. n = 3. Error bars are standard deviation. ** p < 0.01 by unpaired 2-sample t-test.

To investigate cellular distribution of NPC1, we stained cells with an anti-NPC1 antibody. For these experiments we used a Novus polyclonal antibody (NB400-148) which was well established as a good anti-NPC1 antibody and has been used extensively (Deffieu & Pfeffer, 2011; Fu *et al.*, 2013; Blom *et al.*, 2012), but which unfortunately ceased to specifically label NPC1 after the batch changed partway through this project.

This antibody revealed an altered distribution of NPC1 in ST*Hdh* cells. The control cells show staining in fine puncta distributed throughout the cell, whereas staining in the HD cells has larger, brighter puncta and distinct voids in addition to the fine punctate staining (Figure 4.2). This could indicate that NPC1 is in enlarged lysosomal storage

bodies, or in another compartment. Appropriate localisation of NPC1 to the lysosome and late endosome is essential for it to work properly (Blom, 2003), so this altered staining may indicate an NPC1 defect in HD model cells.
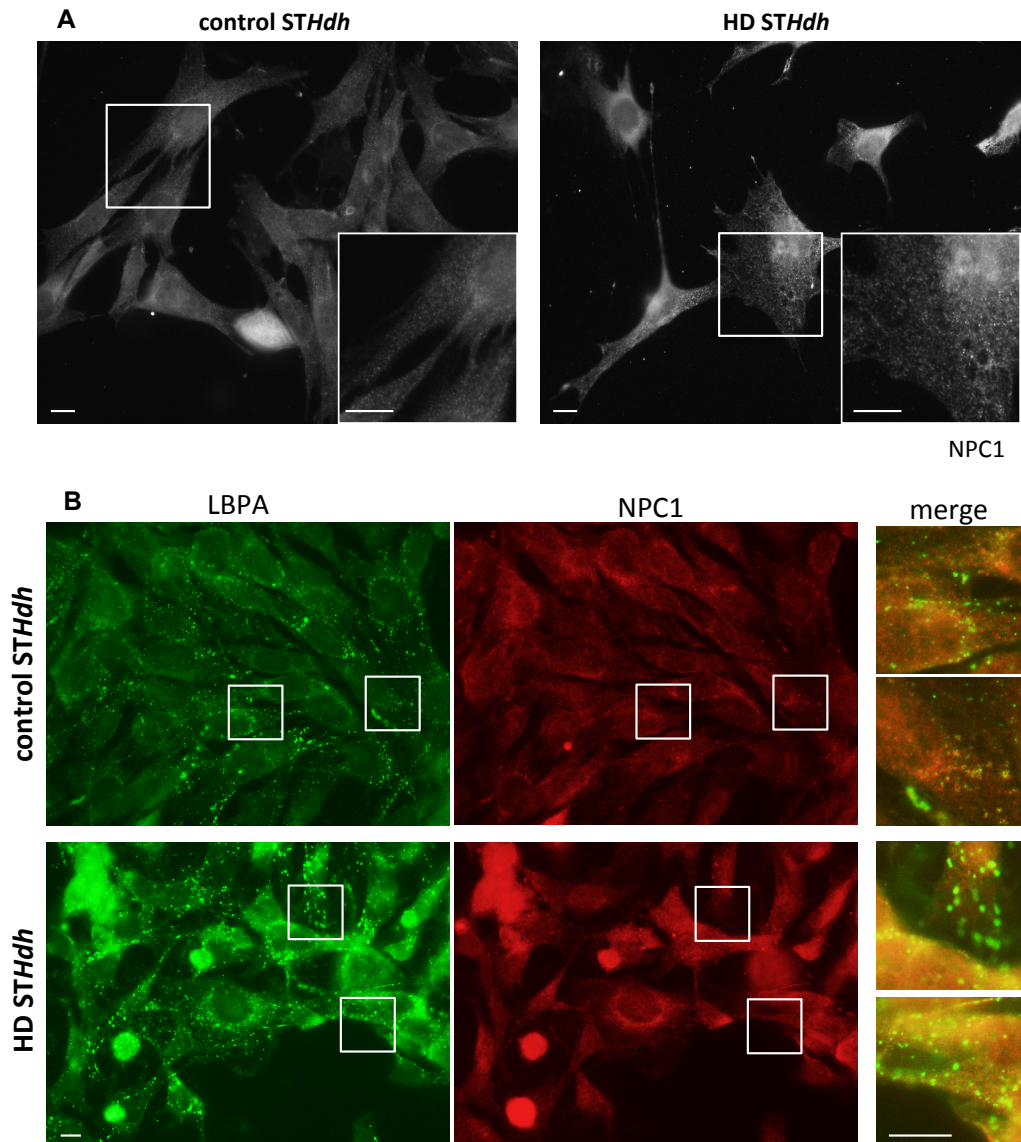


**Figure 4.2 Localisation of NPC1 is altered in HD model cells**
**A** Control and HD cells were stained with an anti-NPC1 antibody (Novus NB400-148). Inset shows an expanded area of the image (regions indicated by white boxes in main images). **B** Control and HD ST*Hdh* cells were stained with antibodies against LBPA (green) and NPC1 (red). Regions in white boxes were merged and expanded (right). n = 1 for both experiments. Scale bars 5 μm.

To look further at localisation of NPC1 in these cells, ST*Hdh* cells were labelled with both anti-LBPA and anti-NPC1 antibodies. Under normal conditions, LBPA is a marker for the late endosome and lysosome (Kobayashi *et al.*, 1999) and should costain with

NPC1, which also resides in these compartments. In ST*Hdh*, our experiments have shown that LBPA localisation is altered, suggesting LBPA is not a marker of the same compartments in these cells. In control ST*Hdh* cells labelled with both LBPA and NPC1, most punctae are labelled with both stains at least to some extent. However, in HD cells, there are large, bright LBPA punctae which do not have corresponding NPC1 staining (Figure 4.2), suggesting an altered distribution of NPC1 and accumulation of LBPA in different compartments.
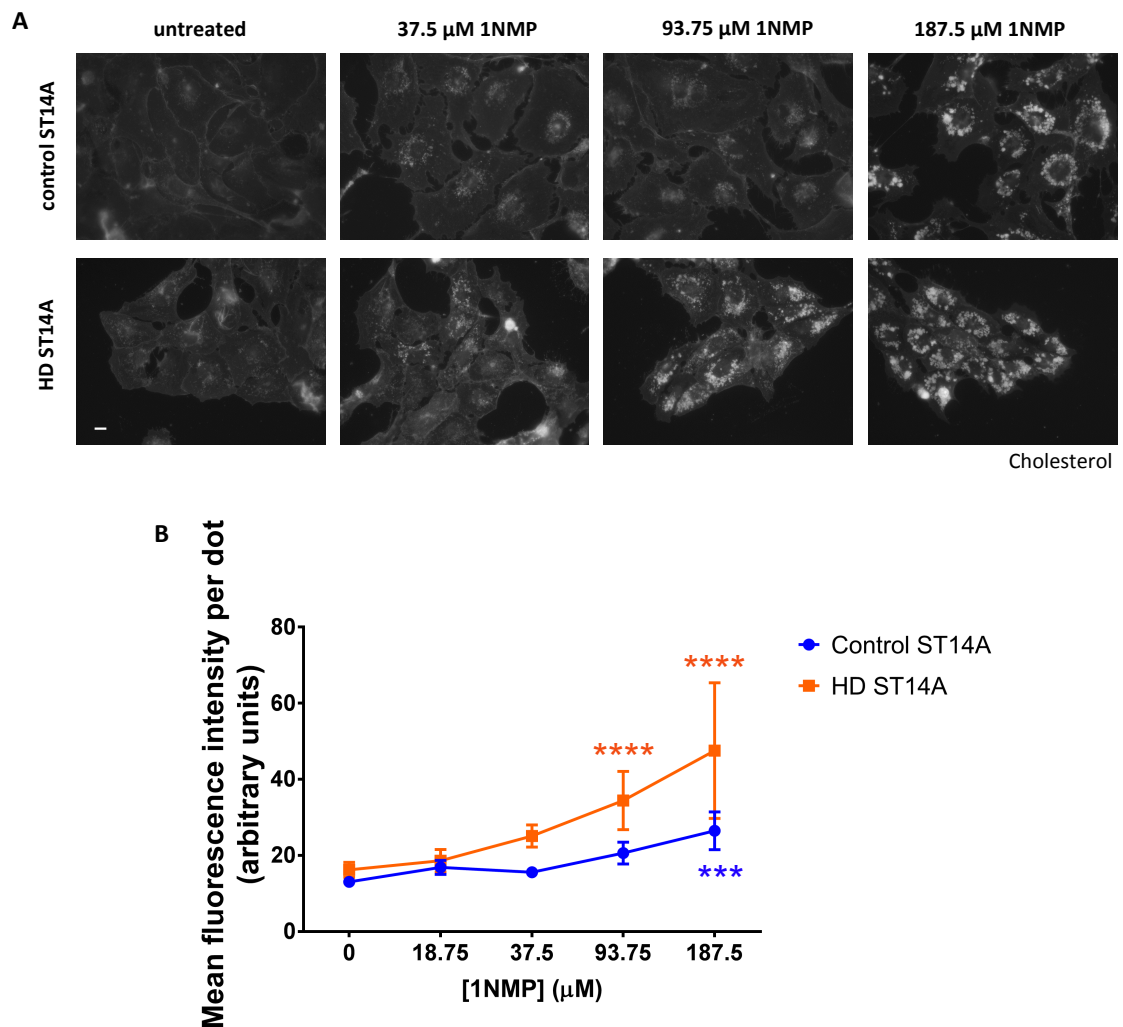


**Figure 4.3 HD model cells are more sensitive to NPC1 inhibitors**
Control and HD ST14A cells were treated with increasing concentrations of the NPC1 inhibitor 1NMP, then stained with filipin to visualise cholesterol. **A**, representative images of ST14A cells treated with 1NMP. Scale bar = 5 μm. **B** Mean fluorescence intensity per dot of filipin staining. Significance indicates groups where fluorescence is significantly increased compared to untreated cells of the same genotype in this single experiment. Blue lines represent control cells and orange lines represent HD cells in each group. n = 1. *** p < 0.001 **** p < 0.0001 by two-way ANOVA and Tukey's multiple comparison test.

### 4.2.2 Function of NPC proteins are altered in HD models

As NPC phenotypes are present in these cells and NPC proteins are altered, we attempted to determine if there was a deficit in functional NPC1 or NPC2, which could explain the presence of NPC phenotypes.

We treated cells with 1NMP, an NPC1 inhibitor which induces NPC phenotypes in normal cells (an analogue of a piperazine NPC1 inhibitor (Côté *et al.*, 2011); C. Gribben *et al.*, unpublished data), then stained the cells with filipin to visualise cholesterol storage (Figure 4.3). Lower concentrations of 1NMP were required to induce significant cholesterol storage (compared to untreated cells) in the HD cells than in control cells. A similar effect was also seen in ST*Hdh* cells (not shown) and with another NPC1 inhibitor (not shown), U18666A (Lu *et al.*, 2015), commonly used to model NPC (Cenedella, 2009). Although each of these treatments is only a single experiment and needs to be repeated, the presence of an effect with both NPC1 inhibitors suggests this is a phenotype which should be further tested and confirmed.

NPC2, the other protein which can cause cases of NPC, is a soluble, secreted protein which can be taken up by cells and transported to the lysosome when it is provided in medium. In NPC2 mutant cells, supplementation with NPC2 protein via this route reduces NPC defects (Naureckiene, 2000), a process called cross-correction. If NPC2 function is reduced in HD, we may be able to uncover this deficit by supplementing cells with NPC2 and testing for correction of phenotypes.

We took either control (NPC2$^{+/+}$) or NPC2 patient fibroblast cells and used them to produce conditioned culture medium. To test the conditioned medium, we treated control and NPC2 fibroblasts with either unconditioned, control-conditioned, or NPC2-conditioned medium, then stained with filipin (Figure 4.4). We measured cholesterol storage by counting the number of cells where intensity of filipin fluorescence was above an arbitrary threshold (selected based on control cells). Control-conditioned medium reduced the percentage of NPC2 fibroblasts with high cholesterol to 9.7%, compared to 23.6% of those grown in unconditioned medium, whereas NPC2-conditioned medium made no difference (storage in 24.2% of cells). control-conditioned medium did not produce complete correction of NPC2 patient cells, suggesting that NPC2 is present in conditioned medium at low concentration. Little or
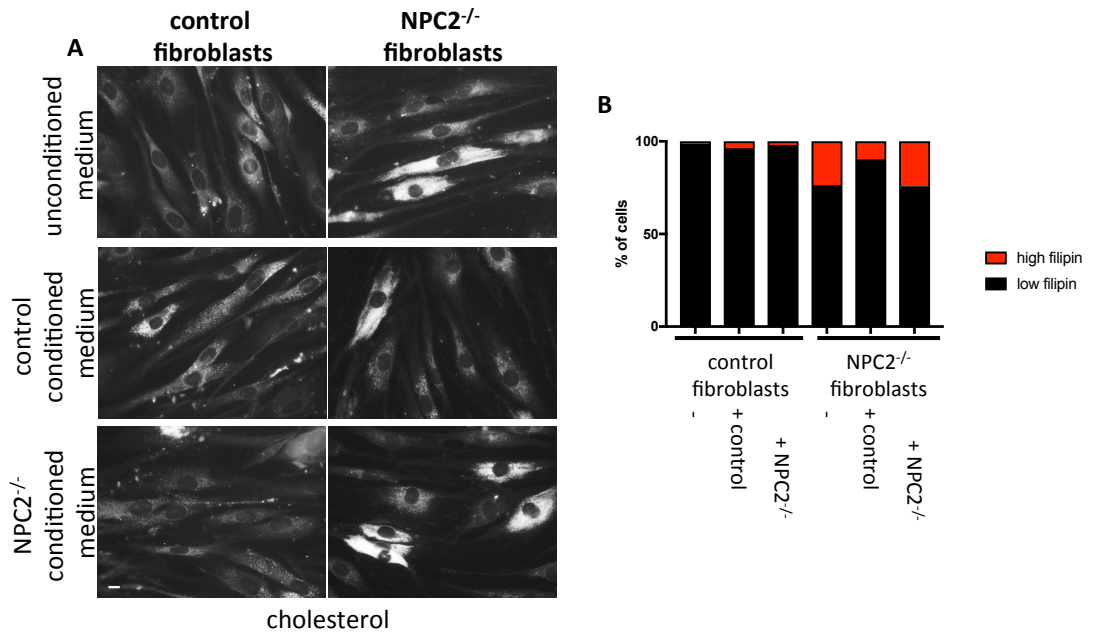
**Figure 4.4 Supplementation with NPC2 in NPC2$^{-/-}$ fibroblasts**

NPC2$^{+/+}$ and NPC2$^{-/-}$ fibroblasts were treated with conditioned medium for 24 hours, then fixed and cholesterol was stained using filipin (**A**, representative images). Cells were scored as having filipin fluorescence either above (red) or below (black) a threshold based on the staining seen in controls (**B**). n = 1; scale bars 5 μm.
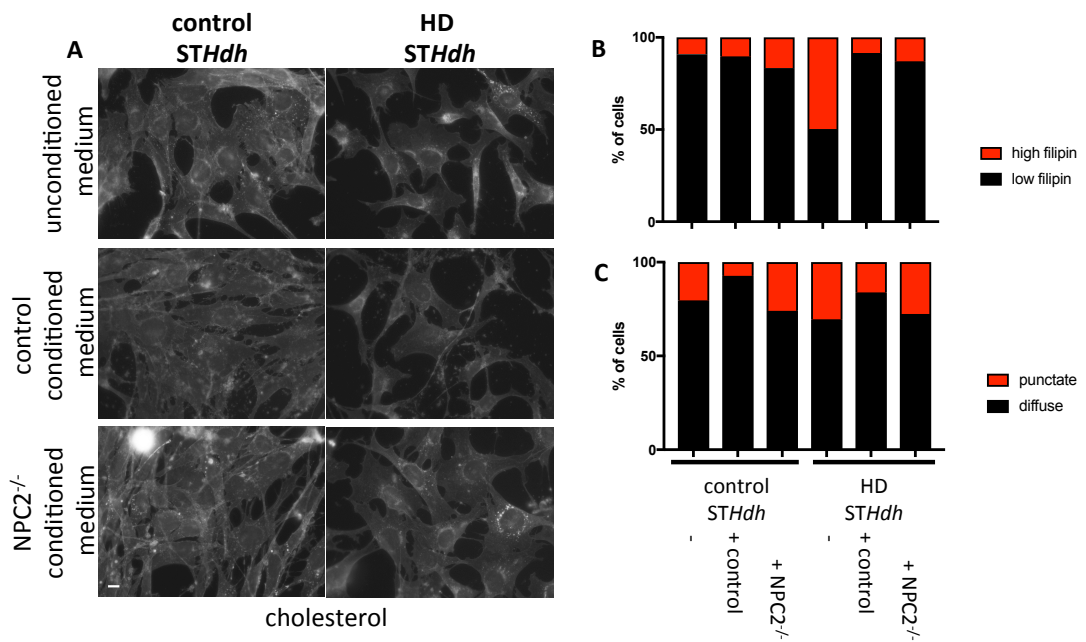


**Figure 4.5 Supplementation with fibroblast conditioned medium in ST*Hdh* cells**

Control and HD ST*Hdh* cells were treated with conditioned medium for 24 hours, then fixed and cholesterol was stained using filipin (**A**, representative images). Cells were scored as having filipin fluorescence either above (red) or below (black) a threshold based on the staining seen in controls (**B**), or by diffuse (black) or punctate (red) cholesterol staining (**C**). n = 1; scale bars 5 μm.

no change to cholesterol was seen in control fibroblasts between different treatments, suggesting that conditioned medium does not contain other factors that would confound the experiment in fibroblasts (for example high levels of cholesterol or LDL released by cells).

Conditioned medium produced by this method was then used to treat ST*Hdh* cells (Figure 4.5). In a single experiment, HD ST*Hdh* cells had higher cholesterol than control cells when analysed using the threshold method used for the NPC2 patient fibroblasts: 49.7% of cells above threshold, compared to 9.1% in controls. Medium conditioned using either control or NPC2 fibroblasts reduced the percentage of cells with filipin levels above the threshold to 8.5% and 13.0% respectively, suggesting an effect which is not specific to the presence of NPC2. In addition to the threshold method, treated ST*Hdh* cells were scored based on localisation of filipin fluorescence, as previously (Chapter 3). Control-conditioned medium reduced the percentage of cells with punctate cholesterol staining in both control and HD cells (20.4% to 7.3% in controls, which were unusually high in this experiment, and 30.5% to 16.1% in HD cells), while unconditioned medium had no effect in this preliminary experiment.

### 4.2.3 NPC1 directly interacts with huntingtin

We tested for direct interactions between NPC1 and huntingtin via co-immunoprecipitation experiments. Using PC12 cell lines which expressed huntingtin with either Q23 or Q73 polyglutamine repeats and a C-terminal RFP tag, and anti-RFP magnetic beads (RFP-Trap, Chromotek), we precipitated RFP-tagged huntingtin and analysed the precipitated samples for the presence of NPC1 (Figure 4.6).

In samples from PC12 cells which were not expressing an RFP-tagged huntingtin, neither huntingtin or NPC1 were present in anti-RFP bead preparations, indicating that neither huntingtin or NPC1 bound to the beads non-specifically. In all experiments, using either 2 or 4 mg/mL of cellular protein sample, NPC1 was co-immunoprecipitated in samples produced by precipitating mutant (Q73) huntingtin, indicating that the two proteins interact (Figure 4.6A). In two experiments where higher concentrations of cell protein samples (4 mg/mL) were used to perform the precipitation experiments, low levels of NPC1 were also detected after precipitation of control huntingtin (Figure 4.6B), indicating an interaction with both forms under appropriate conditions.
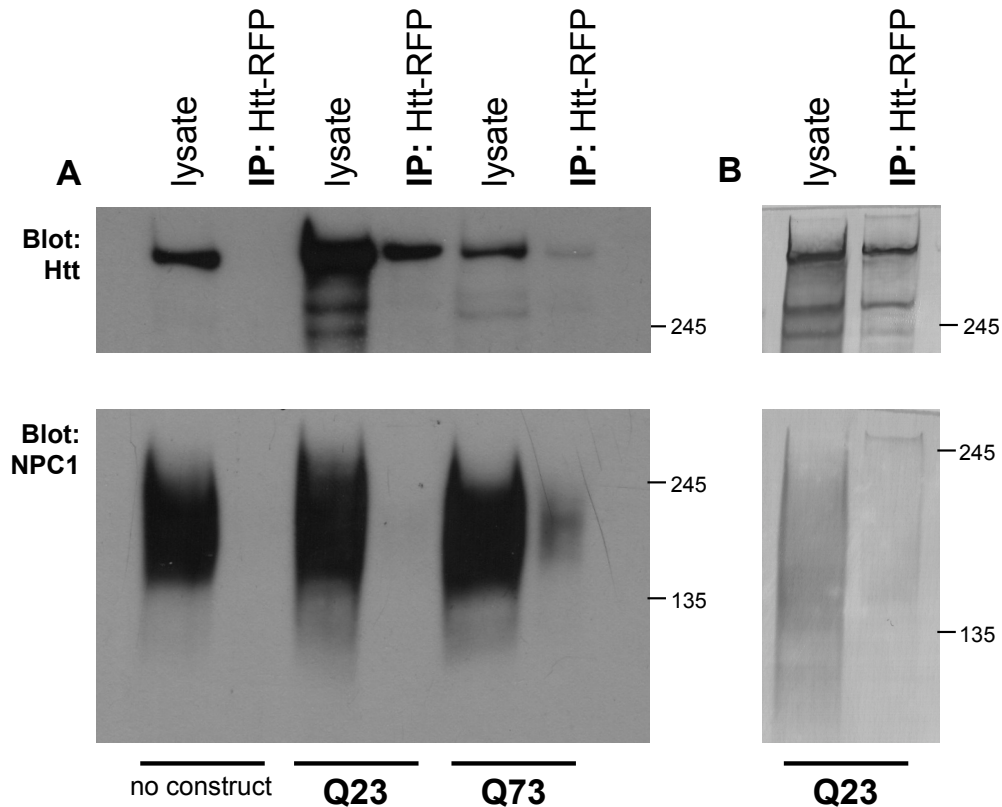
**Figure 4.6 Co-immunoprecipitation of NPC1 with huntingtin**
Anti-RFP magnetic agarose beads (RFP-Trap, Chromotek) were used to precipitate samples from PC12 cells expressing either RFP-tagged Q23 huntingtin, RFP-tagged Q73 huntingtin or no RFP-tagged construct, which were then blotted for huntingtin and NPC1. **A** Co-immunoprecipitation of NPC1 with mutant huntingtin, n = 3 using either 2 mg/mL or 4 mg/mL PC12 sample for precipitation. **B** Co-immunoprecipitation of NPC1 with Q23 huntingtin, n = 2 using 4 mg/mL PC12 sample for precipitation.

### 4.2.4 Huntingtin has highly conserved lysosomal targeting motifs

Huntingtin has been observed to associate with the lysosome (Kegel *et al.*, 2000; Kang *et al.*, 2007; Trajkovic, Jeong & Krainc, 2017). Most lysosomal membrane proteins reach the lysosome due to targeting motifs which interact with adaptor proteins in the endocytic system (Braulke & Bonifacino, 2009). There are two classical motifs: the acidic-dileucine motif (amino acid sequence D/EXXLL) and the tyrosine-hydrophobic residue motif (YXXØ). We identified versions of these motifs present in the human huntingtin sequence, then compared other sequences to test if the motifs were conserved, which could support an important or functional role for them.

There are at least 14 putative lysosomal targeting motifs in the human huntingtin sequence (NCBI ID NP_002102), listed in Table 4.1. Some of these are variants, but

several are very close to the classical motifs: in particular ELFLL (amino acid position 132), YTHF (1365), DSALL (2115), YPQF (3010) and YKVF (3019). Three motifs are close to the C-terminal end of the protein, where functional lysosomal targeting motifs are classically found (Braulke & Bonifacino, 2009; Akasaki *et al.*, 2010), and three others (132, 306 and 322) are near the C-terminal ends of fragments produced by calpain or caspase cleavage of huntingtin (Landles *et al.*, 2010).

First we compared human huntingtin with the huntingtin sequences from mouse, chicken and zebrafish. The huntingtin protein is very highly conserved among this group of sequences: the greatest difference is between human and zebrafish huntingtin, which are still approximately 70% identical. We performed a multiple sequence alignment of these four huntingtin sequences, using EMBL-EBI Clustal Omega (Sievers *et al.*, 2011; Goujon *et al.*, 2010), and compared the lysosomal targeting motifs (Table 4.1, Figure 4.7A). Three of the putative motifs (at 1365, 3010 and 3019) are identical in all four sequences, and a further five (132, 306, 846, 1994 and 3128) are slightly altered in one or more sequences, but retain the key features of functional motifs (a tyrosine plus a hydrophobic residue, or an acidic residue followed by two leucines). The remaining putative motifs are missing from at least one sequence, mostly the zebrafish huntingtin, and are therefore not as highly conserved.

| Human sequence | | Alignment (blue indicates putative lysosomal targeting motifs, white indicates sequences which are unlikely to act as lysosomal targeting motifs) | | |
|---|---|---|---|---|
| Putative motif | Position | Mouse | Chicken | Zebrafish |
| ELFLL | 132 | identical | identical | EMFLL |
| DEHSTLLI | 306 | EEHSTLLI | DDHPTLLI | EEHSSHLI |
| YLVPLL | 322 | CLVPLL | YLIPLL | YLMPLI |
| DCIPLL | 808 | identical | identical | NFVPLL |
| ELGLQLI | 846 | DLGLQLL | identical | ELGLQLL |
| YLKLL | 963 | identical | identical | HLQLL |
| YNLL | 989 | YSLL | YNML | FNLC |
| YTHF | 1365 | identical | identical | identical |
| EHLTWLI | 1916 | identical | identical | EHLTWLT |
| YVDRLL | 1994 | identical | YVDKLL | YVDKLL |
| DSALL | 2115 | identical | identical | EGALY |
| YPQF | 3010 | identical | identical | identical |
| YKVF | 3019 | identical | identical | identical |
| YHRLL | 3128 | identical | identical | YYQLL |

**Table 4.1 Conservation of putative lysosomal targeting motifs in human huntingtin**

**A**

```
human      301  LVPVEDEHSTLLILGVLLTLRYLVPLLQQQVKDTSLKGSFGVTRKEMEVSPSAEQLVQVY   360
mouse           LVPMEEEHSTLLILGVLLTLRCLVPLLQQQVKDTSLKGSFGVTRKEMEVSPSTEQLVQVY
chicken         LVPVEDDHPTLLILGVLLTLRYLIPLLQQQVKDTSLKGSFGVTRKETEISPSPEQLIQVY
zebrafish       VVPVDEEHSSHLILGVLLTLRYLMPLIQQQTPSTSLKGSFGLVRKEADVTPAPEQLIQVY
                :**::::* : *********  *:**:***. .********:.*** :::*: ***:***
```

```
          3006  NQQFYPQFMATVVYKVFQTLHSTGQSSMVRDWVMLSLSNFTQRAPVAMATWSLSCFFVSA  3065
                NQQFYPQFMATVVYKVFQTLHSAGQSSMVRDWVMLSLSNFTQRTPVAMAMWSLSCFLVSA
                NQQFYPQFMATVVYKVFQTLHTTGQSSMVRDWVMLSLSNFTQRTPVAMAMWSLSCFFVSA
                NQQFYPQFMATVVYKVFQTLHATGQSSMVRDWVLLSLSNFTQRTPVAMAMWSLSCFFVSA
                ***********:*********:***::*********:********:***** ******:***
```

```
          3126  SPYHRLLTCLRNVHKVTTC  3144
                SPYHRLLACLQNVHKVTTC
                TPYHRLLTCLQNVHKVTAC
                SPYYQLLCCLQSIHQDTSL
                :**::** **:.:*: *:
```

**B**

```
human            3009  PYPQFMATVVYKVFQTLHSTGQSSMVRDWVMLSLSNFTQRAPVAMATWSLSCFFVSASTS
D. melanogaster  3435  PHCDVIAMIVYQVFRSAIDSSYLQMLQDWLICTLPTFLD-QPEQQGVWGLSVIFLSASIN
C. intestinalis  2805  PFPASVAQILYEVFQSLLERDQSHLVQEWVMLSLGNAIQRTPLQTAVWCLTCLFSSASTN
                       *. * ::*:**: . .  ::::*::.:* . : *  ..* *::* *** .
```

```
                 PWVAAILPHVISRMG-----------------------K-LEQVDVNLFCLVATDFYR
                 LHLIKLFPLVLGIGASNSAAAATTATTATTEAEAAAPAMARKLGQHEIALFVTAAQDFHA
                 RWISSMVPLIISRVH-----------------------DPTLDVDWTCFCKAAVDFYT
                 : :.* ::.                              : :   *  .* **:
```

```
                 HQIEEELDRRAFQSVLEV---VAAPGSPYHRLLTCLRNVHKVTTC--     3144
                 KLSGEQ--RQRFREAFG----SFKRSQVYGRMLQCL-----------   3583
                 CQLSEELDRRSFHAIFSTSSSSREPGSPYKLLLDCISRINGEQGILQ   2946
                 *:  *: *: :           ..* :* *:
```

**C**



**Figure 4.7 Huntingtin has highly conserved lysosomal targeting motifs**

Alignment of huntingtin amino acid sequences from multiple species reveals conservation of putative lysosomal targeting motifs identified in human huntingtin. **A** Selected regions of CLUSTAL Omega multiple sequence alignment of human (NCBI ID NP_002102), mouse (P42859), chicken (E1BZK0) and zebrafish (B7ZDE9) huntingtin sequences. Potential lysosomal targeting sequences are coloured red; red boxes indicate motifs conserved across all species, and black boxes indicate that one or more species does not have a lysosomal targeting motif at this position (also see Table 4.1). **B** CLUSTAL Omega alignment of final 145 amino acids of human huntingtin (NCBI ID NP_002102) with corresponding regions of the *Drosophila melanogaster* (Q9V3N4) and *Ciona intestinalis* (A0A1W2VPZ3) huntingtin sequences. Annotation as in **A**. **C** Diagram of human huntingtin with putative lysosomal targeting motifs. The amino acid position of putative motifs in the human huntingtin sequence is given: black text indicates motifs which are only partially conserved, blue indicates motifs conserved between all four species in **A** (Table 4.1), and red indicates the two motifs which are additionally conserved in **C**. The polyglutamine (polyQ) region and a region with multiple functional protease target sites (Landles *et al.*, 2010) are indicated.

89

We then compared human huntingtin with the huntingtin sequences from *Drosophila melanogaster* and the sea squirt *Ciona intestinalis*, which are more distantly related. Each of these two proteins are 20-30% identical to the human sequence, and only segments of the protein are conserved (Li *et al.*, 1999). The proteins therefore do not align well overall, but we used pairwise NCBI Needleman-Wunsch global alignments (NCBI Resource Coordinators, 2018) to identify regions corresponding to the final 150 amino acids of human huntingtin and aligned these using EMBL-EBI Clustal Omega (Sievers *et al.*, 2011; Goujon *et al.*, 2010) multiple alignment (Figure 4.7B). While the putative motif at 3010 in the human sequence is not present in these two proteins, the final two C-terminal motifs are present and highly conserved in both *D. melanogaster* and *C. intestinalis* huntingtin.

### 4.2.5 Other polyglutamine diseases have a range of lysosomal defects

To investigate whether storage phenotypes are specific to HD or are a general feature of polyglutamine expansion diseases, we looked for NPC-like lipid storage in patient fibroblasts from two spinocerebellar ataxias (SCAs) caused by polyglutamine expansion, SCA1 and Machado-Joseph disease (MJD or SCA3). Two clinically normal lines were used as controls, one from a 1 year old child and one from a 54 year old, which is more similar in age to the MJD cell line.

Cells were first stained with Lysotracker (Figure 4.8). SCA1 fibroblasts have increased Lysotracker staining in some cells, but no overall change compared to controls, whereas Lysotracker in MJD cells is consistently and significantly decreased compared to control lines. LBPA staining (Figure 4.8) in SCA1 cells was similar to that in controls, and MJD cells again had significantly decreased labelling compared to controls. The aged control line has decreased Lysotracker and increased LBPA compared to the younger controls, and greater variability in staining.

We also stained cells for the main lipids stored in NPC (ganglioside GM1, cholesterol and sphingomyelin; Figure 4.8). Ganglioside GM1 was largely unchanged between the four cell lines, though some cells with punctate accumulation were present in the SCA1 cell line. When stained with filipin, all four cell lines have relatively high cholesterol but there is no endo-lysosomal punctate accumulation of cholesterol in either of the SCA cell lines compared to controls. Sphingomyelin staining is essentially unchanged
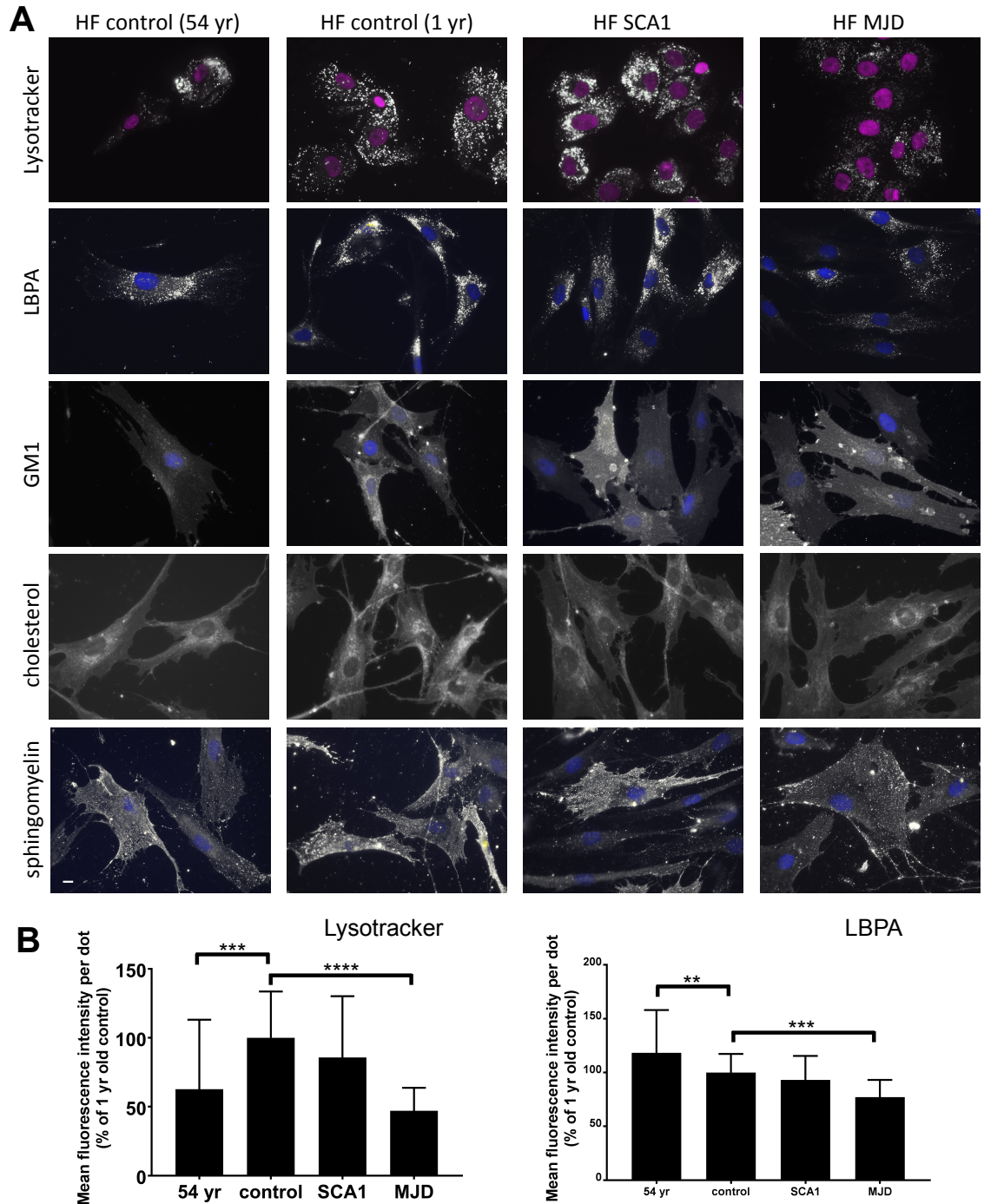
**Figure 4.8 Polyglutamine expansion disease cells have altered lysosomal phenotypes**
**A** SCA1 and MJD patient fibroblasts and two control fibroblast lines from clinically normal donors were stained for lysosomal markers and lipids. Lysotracker staining was performed in live cells, and all other stains were performed after fixation in 4% PFA. Representative images, scale bar 5 μm. n = 3. **B** Mean fluorescence intensity per dot in Lysotracker (left) and LBPA (right) stained fibroblasts, corrected to 1 year old control. Error bars represent standard deviation. ** $p < 0.01$ *** $p < 0.001$ **** $p < 0.0001$ by one-way ANOVA and Dunnett multiple comparison test.

between groups. Surface labelling is variable throughout but there is no evidence of intracellular or punctate sphingomyelin storage in any line. The two SCA cell lines are therefore quite different in terms of lysosomal phenotypes, and do not have NPC-like phenotypes, though SCA1 may have LSD-like lysosomal expansion.

## 4.3 Discussion

### 4.3.1 NPC-like defects suggest lysosomal mechanisms in HD pathogenesis

NPC-like defects in HD cell models suggest that lysosomal storage disease mechanisms, particularly NPC disease mechanisms, may be present in HD pathogenesis. We investigated the two NPC proteins, NPC1 and NPC2, to determine whether this was the case, and what mechanisms lay behind these similarities.

### 4.3.2 NPC proteins are affected in HD

The level of NPC1 protein is not altered in ST*Hdh* based on western blotting (Figure 4.1). Immunocytochemical staining of this cell line supports this (Figure 4.2), though altered levels have been seen in HD iPSC-derived neuronal cells (Dr. Haslett). This may therefore be a phenotype which varies between models, dependent on protein homeostasis, differentiation (in iPSC-derived cells) and other factors.

NPC2 is dramatically increased in HD ST*Hdh* cells compared to controls (Figure 4.1). This matches the increased NPC2 expression previously seen in HD caudate (Neueder & Bates, 2014). An increase in NPC2 would not lead to storage defects, but interestingly, NPC2 is increased in NPC1 mutant cells (Blom, 2003; Chen, Gordon & Ioannou, 2005) and under other conditions where NPC1 is lost or inhibited or where cholesterol accumulates in the lysosomes, possibly as a cellular response to altered lipid or lysosomal signalling.

While information on NPC1 localisation is limited due to antibody issues, we observed changes to NPC1 localisation to a less punctate, more reticular distribution in HD ST*Hdh* cells (Figure 4.2). This agrees with previous work by Dr. Haslett, who observed similar changes in localisation in HD patient iPSC-derived neuronal cells. We initially aimed to perform extensive colocalisation experiments between huntingtin, NPC1 and NPC2, and markers for the lysosome, late endosome and other compartments (particularly the ER) but were not able to do so due to problems with antibody availability. The experiment which is included here, costaining LBPA and NPC1 in

ST*Hdh* (Figure 4.2), is complicated by the earlier experiments (Figure 3.8) which showed that LBPA does not colocalise with LAMP1 in these HD cells. However, NPC1 should colocalise with LBPA (Piccoli *et al.*, 2011) under normal conditions, as it does in these control cells but not in the HD ST*Hdh* cells. NPC1 should also colocalise with LAMP1 (Blom, 2003; Poirier *et al.*, 2013), which needs to be confirmed in these cells. However, the separate LBPA- and NPC1-containing compartments suggest trafficking issues in these HD model cells, which may disrupt NPC1 transport and function and interfere with lysosomal function.

Our experiments to probe NPC1 and NPC2 function are limited but interesting. HD cells from both ST*Hdh* and ST14A are more responsive to NPC1 inhibitors in a single experiment with each treatment (Figure 4.3). While the HD cells start with a higher level of punctate cholesterol staining, they also respond to lower concentrations of inhibitor, supporting the idea that these cells have a deficit in NPC1 function. A deficit in function in cells where levels of normal NPC1 are unchanged (Figure 4.1) could potentially be caused by the NPC1 mislocalisation we have observed in preliminary experiments (Figure 4.2), or by changes in signalling such as altered levels of sterol precursors (Valenza *et al.*, 2005), some of which have been seen to inhibit NPC1 in SLOS (Dr. Waller-Evans *et al.*, unpublished).

We attempted an NPC2 supplementation experiment (Figure 4.5) to see whether these cells had a defect in NPC2 function which we could reveal, but this was not successful. We were able to produce conditioned medium which partially corrected NPC2 patient cells (Figure 4.4), indicating that there was secreted NPC2 in the medium though at a low concentration. Treating ST*Hdh* HD cells with this medium led to a slight reduction in percentage of cells with punctate staining, but both control- and NPC2 mutant-conditioned medium reduced levels of filipin staining (Figure 4.5). These preliminary results would suggest that another factor in the fibroblast-conditioned medium is beneficial, not NPC2 specifically, which would make sense considering that NPC2 is already elevated in these cells (Figure 4.1). This experiment was therefore inconclusive. Using purified NPC2 instead of conditioned medium, or using HD patient fibroblasts instead of ST*Hdh* cells so that the species and cell type remains consistent, may be better methods, though this experiment may not be useful to continue and

instead it may only be necessary to confirm that NPC2 is correctly localised to the lysosome in HD.

### 4.3.3 NPC1 interacts with huntingtin

We identified an interaction between NPC1 and huntingtin by co-immunoprecipitation experiments (Figure 4.6). The interaction between NPC1 and mutant huntingtin may be due to the increased ability of mutant huntingtin to bind to other proteins (Arrasate & Finkbeiner, 2012), and may indicate that NPC1 is being aberrantly bound or drawn into huntingtin aggregates, which would lead to reduced NPC1 function and NPC-like phenotypes. Interestingly however, we have also seen evidence of an interaction between NPC1 and normal huntingtin. This suggests that there could be a normal role for huntingtin relating to NPC1: as NPC1 is mislocalised in the HD cells we have examined, this could relate to trafficking of NPC1 to the lysosome or its dynamic transport within the endocytic system. Loss of this function could also be the cause of the NPC-like phenotypes in HD models. As other defects in HD pathogenesis appear to be due to both loss of normal huntingtin function and gain of mutant function (Cattaneo *et al.*, 2001; Saudou & Humbert, 2016), both routes could be involved.

NPC1 interaction with mutant (Q73) huntingtin is detectable at lower sample concentrations than the interaction with wildtype (Q23) huntingtin and more NPC1 is present in precipitates (Figure 4.6). While experimental conditions may not be optimal to identify this interaction and there are other potential confounding factors, this could indicate that NPC1 interacts differently with these two proteins: the interaction with huntingtin may be weaker or more transient in normal cellular conditions than with the mutant form. However, the immunoprecipitation results could also be affected by differences in the expression level, fragmentation and processing, or association with beads, of the two different constructs in these PC12 cell lines. Additionally, endogenous normal huntingtin could compete with the RFP-tagged normal huntingtin in binding to NPC1, although this still suggests that the interaction with mutant huntingtin is stronger as it is not outcompeted by endogenous protein. Performing the opposing experiment, precipitating NPC1 and measuring huntingtin in the precipitate, will help answer this question, but these experiments still need to be completed.

To further investigate whether huntingtin has a normal function which involves NPC1, we had hoped to look in huntingtin-null cells (Zhang *et al.*, 2008; Ritch *et al.*, 2012), but were not able to obtain these. Instead, Mr. Copner and Mr. Badell-Grau performed siRNA experiments. SH-SY5Y cells treated with anti-huntingtin siRNA had cholesterol storage and a distinct block in GM1 trafficking, measured using FITC-CtxB, strongly suggesting that loss of normal huntingtin function induces NPC-like phenotypes. However, the extent of huntingtin knockdown was difficult to confirm, and we would like in future to look at these phenotypes and at NPC1 localisation in huntingtin-null cells.

There are other experiments which would be useful to continue or complete this section of the project. Firstly, we would extend the colocalisation experiments to identify where NPC1 is in HD cells, and to investigate whether it colocalises with huntingtin under either normal or pathogenic circumstances. This may require expression of tagged NPC1, tagged huntingtin, or both, which would overcome our difficulties in finding reliable, specific antibodies for immunocytochemistry of these two proteins.

Another interesting approach, in addition to colocalisation, is to examine trafficking of NPC1 in normal and HD cells, which we may be able to do via analysis of glycosylation. NPC1 is delivered to the lysosome via the endocytic system (Saftig & Klumperman, 2009; Luzio *et al.*, 2014), possibly dependent on adaptor protein AP-3 (Berger *et al.*, 2007). Initial glycosylation of proteins occurs in the ER, but complex and specific glycoconjugates are not produced until proteins pass through the Golgi and to their target organelles (Lodish *et al.*, 2000; Spiro, 2002). Endoglycosidase H is able to cleave ER glycoconjugates but not those which have been altered elsewhere, and so it is possible to investigate trafficking of a protein based on deglycosylation by endoglycosidase H (Freeze & Kranz, 2010). This would allow us to investigate trafficking of NPC1 in HD cells, and confirm whether it reaches the lysosome when mutant huntingtin is present.

### 4.3.4 Huntingtin may have a lysosomal function

Lysosomal defects in HD do not necessarily indicate a normal huntingtin function in this compartment, as there is broad cellular dysfunction in HD. However, association of huntingtin with the lysosome (Kegel *et al.*, 2000; Kang *et al.*, 2007; Martin *et al.*, 2015;

Trajkovic, Jeong & Krainc, 2017) and the interaction between normal huntingtin and NPC1 support the possibility of a normal role in the lysosome.

In addition, we have identified multiple putative lysosomal targeting motifs in human huntingtin, several of which are highly conserved between species (Figure 4.7). Two common targeting motifs are present in lysosomal membrane proteins (Braulke & Bonifacino, 2009), the acidic-dileucine motif (DXXLL) and the tyrosine-hydrophobic residue motif (YXXØ), which associate with adaptor proteins (GGAs and AP1-4) in the Golgi and direct proteins into the endocytic system, from where they traffic to the lysosome. Both of these motifs are present several times in human huntingtin, including towards the C-terminus of the full length protein and the exon 1 fragment (Landles *et al.*, 2010), where they are commonly found (Braulke & Bonifacino, 2009; Akasaki *et al.*, 2010). In particular, the motifs at amino acid positions 132, 1365, 3010, 3019 and 3128 of the human huntingtin sequence are close to the classical consensus sequences, well conserved, and appropriately positioned, and would be worth further investigation. Those motifs that are not conserved when compared with zebrafish are less likely to be functional, but could also indicate features of the protein only present in certain species (similar to the expanded polyglutamine domain). Further analysis would be needed to confirm whether these motifs are functional, but their presence suggests that huntingtin is deliberately targeted for delivery to the lysosome.

We also investigated the potential lysosomal involvement of huntingtin via lysosomal purification experiments performed by Mr. Badell-Grau. Magnetic nanoparticles can be used to prepare a highly pure extract of lysosomes from cell samples (Walker & Lloyd-Evans, 2015), and when samples were prepared from ST14A cells both normal and mutant huntingtin was detected in the lysosomal fraction, indicating its presence in or association with the lysosome. This agrees with previous observations of huntingtin associating with (Kegel *et al.*, 2000; Martin *et al.*, 2015; Kang *et al.*, 2007) the lysosome. While this could be due to lysosomal degradation of huntingtin, it suggests that the observed lysosomal targeting motifs are functional and huntingtin is directed to the lysosome. The purpose of this is unknown, although one possible answer is the recent finding that huntingtin is secreted via a lysosomal exocytosis pathway (Trajkovic, Jeong & Krainc, 2017).

### 4.3.5 NPC-like defects are not ubiquitous in diseases of polyglutamine expansion

To test whether NPC1 dysfunction is specific to HD or is a general feature of polyglutamine expansion diseases (Fan *et al.*, 2014), we looked for NPC-like defects in two SCAs caused by polyglutamine expansion (Figure 4.8), which had similar polyglutamine repeat lengths to the Q60 huntingtin cells we used in Chapter 3 (52 in the SCA1 cells and 71 in MJD).

Age is an important factor to consider when comparing human fibroblast lines, as age at collection can affect diverse cellular factors including $Ca^{2+}$ signalling (Kilpatrick *et al.*, 2016) and lysosomal function. We used two control lines, from clinically normal 1 and 54 year olds. The older line is a reasonable control for the MJD cell line, and though neither are ideal for the SCA1 cells, these are a close match to the Q60 HD line which is useful in comparing the two. However, the older clinically normal cell line has significantly different Lysotracker and LBPA staining compared to the young control cells, which may be age-related changes, or may suggest an abnormality in these cells.

While we have not examined all known NPC phenotypes in these SCA cell lines, our screen suggests that SCA1 may have some LSD phenotypes but MJD does not (Figure 4.8). Both have altered lysosomes based on Lysotracker and LBPA staining, with SCA1 having increased lysosomal staining in some cells and MJD being reduced, but there is no evidence that the characteristic NPC lipids cholesterol, ganglioside GM1, and sphingomyelin, are being stored in either cell line. While the lysosomal changes present are beyond the scope of this study to investigate, the experiment does answer our initial question. LSD-like phenotypes and lysosomal dysfunction may be present in other polyglutamine expansion diseases, and NPC1 dysfunction cannot be ruled out in diseases we have not looked at, but NPC1 dysfunction is not ubiquitous in polyglutamine diseases. NPC1 involvement in HD pathogenesis may therefore be via specific mechanisms.

### 4.3.6 Conclusions

We have identified alterations to the two NPC proteins in HD cells, and a direct interaction between NPC1 and huntingtin, and can suggest possible mechanisms for the presence of NPC-like phenotypes as a component of HD pathogenesis. NPC2 levels are increased both in our experiments and in previous studies, and it is therefore less

likely that storage results from loss of NPC2 function. This may instead be a response to cellular dysfunction, rather than a cause of it.

NPC1 binds to huntingtin and its cellular distribution is altered in the models we have investigated. Interactions between NPC1 and mutant huntingtin would disrupt NPC1 distribution and movement in the late endocytic system and lysosome, preventing proper localisation to the lysosome and potentially segregating NPC1 in protein aggregates. Interestingly, NPC1 also associates with normal huntingtin, suggesting that huntingtin may be involved in normal trafficking of NPC1 to the lysosome or within the late endocytic system, and loss of this function could lead to protein becoming trapped in the ER, Golgi or elsewhere and not correctly reaching the lysosome. Both of these potential pathways would lead to reduced functional NPC1 and therefore to the defects in endocytic trafficking, lysosomal $Ca^{2+}$ signalling and lipid storage which we see in HD.

# CHAPTER 5 MIGLUSTAT IN HUNTINGTON'S DISEASE

## 5.1 Introduction

### 5.1.1 Outline

Our data and others suggest that Huntington's disease has lysosomal and lipid phenotypes similar to those in NPC, suggesting common mechanisms, and the NPC1 protein directly interacts with huntingtin. No disease-modifying therapy is available for HD, but one is available for NPC: miglustat, an inhibitor of glycosphingolipid synthesis. As similarities are present between the two diseases, miglustat could potentially be beneficial in HD.

Neural precursor cells derived from HD patient iPSCs were treated with miglustat. Ganglioside trafficking and lysosomal $Ca^{2+}$ signalling, which were defective in HD cells, were improved by miglustat treatment, though lipid storage was not altered. To perform initial tests of miglustat in a whole-organism model of HD, a *Drosophila melanogaster* model expressing mutant huntingtin was obtained and tested. Miglustat reduces glycosphingolipid levels in wildtype flies and does not have acute negative side effects, and treatment with miglustat leads to small improvements in climbing ability in HD flies.

Miglustat therefore has beneficial effects on function in two HD models. While these are simple models, both have previously been used to provide relevant data to develop mouse and human trials of potential HD therapies, and trials of miglustat in HD patients are now being planned.

### 5.1.2 The NPC therapy miglustat

Miglustat is the only approved disease-modifying therapy for NPC (though it is not approved in the USA). It inhibits glucosylceramide synthase, the glucosyltransferase which catalyses the first step in GSL synthesis, and thereby reduces production of all GSLs. Miglustat was developed as a substrate-reduction therapy in Gaucher disease, an LSD where glucocerebrosidase (GBA1) deficiency leads to lysosomal storage of glucosylceramide (Stirnemann *et al.*, 2017).

Due to the presence of GSL storage in NPC, miglustat was also tested and developed as an NPC therapy (Lachmann *et al.*, 2004; Patterson *et al.*, 2007). In NPC, miglustat reduces GSLs, sphingosine (Stein *et al.*, 2012) and overall lysosomal volume (Lachmann

*et al.*, 2004). The block in endocytic trafficking is alleviated (Lachmann *et al.*, 2004) and lysosomal calcium signalling is improved (Haslett and Lloyd-Evans, unpublished). In patients treated with miglustat, progression of symptoms can be slowed or even halted, particularly dysphagia and particularly in adult-onset patients (Patterson *et al.*, 2007; Wraith *et al.*, 2010).

### 5.1.3 Therapeutic screening in iPSC models

While we have used cell lines from rodent models for most of our initial phenotyping and mechanism work, we wanted to use a more relevant model for testing miglustat. Cell models derived from induced pluripotent stem cells (iPSCs) from patients are a powerful new tool (Yamanaka, 2012; Shi *et al.*, 2017). Fibroblasts from patient skin biopsies can be used to produce iPSCs, and these can then be differentiated to produce cell types which are otherwise impossible to obtain and study (Juopperi *et al.*, 2012; Reddington, Rosser & Dunnett, 2014). In the case of neurodegenerative diseases, this allows us to study human neurons and neuronal precursors with actual patient defects (Young & Goldstein, 2012; Zhang *et al.*, 2015b). These models are still developing, but have been used for both basic research and therapeutic screening and testing (Zhang *et al.*, 2015b). They make it possible to test potential therapies in a human model with relevant patient defects

### 5.1.4 *Drosophila melanogaster* models of human disease

The fruit fly *Drosophila melanogaster* is a simple model organism used widely in scientific research. It is easy to maintain and handle, and is particularly useful because it is easy to genetically manipulate. In the lab, they live 2-3 months, dependent on temperature, and develop from embryo to adult (through larval and pupal stages) over approximately 10 days at 25°C.

One of the major tools in *D. melanogaster* genetics, the GAL4-UAS system (which we use in this project), is derived from the galactose system in yeast. The transcriptional activator protein GAL4 is expressed under the control of different fly gene promotors, to induce expression in different tissues or at different times. Reporter genes or genes of interest are then placed under the control of the UAS (upstream activating sequence), the target of GAL4, and combination of a GAL4 and a UAS line allows controlled expression of proteins of interest in specific tissues (Duffy, 2002). Extensive

libraries of GAL4 and UAS flies are available, including flies with UAS-huntingtin constructs.

While *D. melanogaster* is a simple organism, it can provide useful tools or models for studying human disease, including neurodegeneration (Ugur, Chen & Bellen, 2016; Yamamoto *et al.*, 2014; Chintapalli, Wang & Dow, 2007). They have a complex nervous system, with multiple neuronal and glial subtypes and a blood-brain barrier, making it possible to study factors such as interactions between neurons and glia, and, in spite of obvious differences, there is considerable conservation to mammalian systems. One study in 2002 estimated that of approximately 900 human disease-related genes they identified from the OMIM database, at least two thirds had homologues in *D. melanogaster* (Chien *et al.*, 2002). Though functional tests should not be considered directly analogous to human clinical features, many useful measures have been developed (Ugur, Chen & Bellen, 2016), and disease models in flies can be useful for mechanistic studies, as well as for drug screening or initial tests of potential therapies.

There are *D. melanogaster* models of several LSDs. Knockout of the fly homologue of the Gaucher gene *GBA1* (Kinghorn *et al.*, 2016) recapitulates many features of human disease, including accumulation of glucosylceramide, lysosomal defects and a block in autophagy, and reduced lifespan and motor ability. Mutations in the fly prosaposin homologue lead to lysosomal expansion, neurodegeneration and reduced lifespan, modelling human saposin deficiencies (Hindle *et al.*, 2017), and these flies were used to investigate potential $Ca^{2+}$ defects associated with prosaposin mutation. There is also a *D. melanogaster* model of NPC, null for a homologue of NPC1, which has accumulation of cholesterol and multi-vesicular bodies followed by neurodegeneration. This fly arrests and dies at the first larval molt but can be rescued by providing the molting hormone ecdysone or steroid hormone precursors, indicating a block in cholesterol trafficking and metabolism (Phillips *et al.*, 2008). While this is a fly system not present in humans, it provides another approach to investigate NPC1 function, information which may still be informative even when translating from insects to mammals. For us, these two examples demonstrate LSD genes and mechanisms are conserved between flies and humans, despite differences in areas such as lipid metabolism.

HD models - or at least models of mutant huntingtin expression - have also been produced using *D. melanogaster* (Marsh, Pallos & Thompson, 2003; Lewis & Smith, 2016). Flies have a huntingtin gene (*dhtt*) which is similar to human huntingtin but does not have a polyglutamine repeat (Tartari *et al.*, 2008). As in mammals, fly huntingtin is involved in neuronal function (Zhang *et al.*, 2009), although loss of huntingtin is not embryonic lethal as it is in mice (Duyao *et al.*, 1995). Expressing human mutant huntingtin in flies leads to neurodegeneration, motor defects and reduced lifespan, whereas human huntingtin with normal CAG repeats is not harmful (Marsh, Pallos & Thompson, 2003; Lewis & Smith, 2016). While systems such as motor networks in the brain, lipid metabolism and immunity are different between flies and mammals, and huntingtin function may be different (Zhang *et al.*, 2009), features of human disease such as protein aggregation are present, and comparable defects in neurodegeneration and motor function, making flies a useful model for HD.

### 5.1.5 Lipid metabolism in *Drosophila melanogaster*

We intend to test miglustat, a glycosphingolipid-modulating drug, in *D. melanogaster* models of HD. Miglustat has not previously been used in *D. melanogaster*, and we therefore need to consider how lipid metabolism in the fly compares to mammalian lipid metabolism.

*D. melanogaster* produces GSLs which have many equivalent roles to mammalian lipids, though their structure and synthesis has both similarities and differences (Kraut, 2011). The initial step of GSL synthesis is catalysed by a fly homologue of glucosylceramide synthase (Kraut, 2011), which is approximately 50% identical to the human gene (Campbell *et al.*, 1998; Marks *et al.*, 2001), the target of miglustat. Further steps in the pathway diverge from the mammalian system, though a number of enzymes are homologous (Wandall *et al.*, 2005; Kraut, 2011; Acharya & Acharya, 2005). GSLs are involved in *D. melanogaster* development (Kraut, 2011; Wandall *et al.*, 2005), via Notch signalling (Haines & Irvine, 2003; Chen *et al.*, 2007) and other pathways (Pizette *et al.*, 2009), as well as motor function and behaviour (Haines & Stewart, 2007; Chen *et al.*, 2007).

GSLs produced by *D. melanogaster* are structurally different to mammalian lipids in several ways. Fly sphingolipids and GSLs have different chain lengths, with the most common species of sphingoid bases and fatty acids having 14 and 20 carbon chains

respectively instead of the 16-18 carbons common in mammals (Kraut, 2011). The core structure and extent of glycosylation varies (Kraut, 2011; Seppo *et al.*, 2000), with the fly GSLs containing mannose residues in the core instead of galactose in mammals (Seppo *et al.*, 2000; Wandall *et al.*, 2005; Chen *et al.*, 2007). The fly does not use sialic acids in lipid head groups; there is only one identified sialyltransferase in *D. melanogaster,* which works primarily on polysaccharides, is partially active on glycosylated proteins and has no activity on lipid substrates (Koles, 2003). However, the fly does produce other complex charged GSLs equivalent to gangliosides, by incorporating modified GlcNAc (N-acetylglucosamine) residues (Kraut, 2011).

The fly is a sterol auxotroph - it is not able to synthesise cholesterol (Liu & Huang, 2012; Niwa & Niwa, 2011). As in mammals, cholesterol is required for structure of cell membranes and for synthesis of steroid hormones, though in insects the primary steroid hormones are ecdysone and other ecdysteroids, primarily involved in larval development. *D. melanogaster* has multiple homologues of each of the NPC proteins - two NPC1 genes, and eight NPC2 genes (Niwa & Niwa, 2011). Knockout of *NPC1a* (Huang *et al.*, 2005; Fluegel, Parker & Pallanck, 2006) or double knockout of *NPC2a* and *NPC2b* (Huang *et al.*, 2007) leads to intracellular cholesterol storage and blocks production of ecdysteroid hormones, leading to arrest of larval development at the first moult which can be rescued by hormone addition. Interestingly, *D. melanogaster* has a SREBP gene which appears to be involved solely in fatty acid regulation (Kunte, Matthews & Rawson, 2006; Seegmiller *et al.*, 2002), whereas in mammals the SREBP family are regulators of both cholesterol and fatty acid homeostasis (Horton, Goldstein & Brown, 2002).

**5.1.6 Aims**

We aim to test the effect of miglustat on LSD phenotypes and on functional outcomes in HD models. Firstly, we tested miglustat in human iPSC-derived models, as a more relevant model than the cell lines we have used for basic phenotyping and mechanism studies.

Then, we obtained and established a *D. melanogaster* model of HD. We wished to confirm that the system we chose was an effective model in our hands, and select and test phenotypes to use for screening the effect of miglustat. We also aimed to confirm

that this model could be given miglustat without harmful side-effects, and that GSLs were altered. Finally, we aimed to test miglustat in the *D. melanogaster* HD model.

## 5.2 Results

### 5.2.1 Storage defects in HD iPSC-derived cells are not altered by miglustat treatment

We used HD patient iPSC derived neural precursor cells to test miglustat in HD, as these cell lines are more relevant to patient defects than the rodent model cell lines we have previously used. The control cells used have a polyglutamine repeat length of Q33, whereas the two HD lines have one normal allele and one of either Q60 or Q109, an early-onset and a juvenile form respectively. Cells were grown under appropriate culture conditions with or without 50 µM miglustat for 7 days before analysis was performed.

Firstly, we stained control and HD cells with Lysotracker, to look for lysosomal expansion (Figure 5.1). Both Q60 and Q109 cells have elevated lysotracker compared to control, which is slightly reduced by miglustat treatment. We also observed abnormal large, round, Lysotracker-labelled bodies in both the Q60 and Q109 cells.



**Figure 5.1 HD patient iPSC-derived neural precursor cells have increased Lysotracker**
Cells derived from either control or HD patient iPSCs were grown in appropriate conditions to produce neural precursor cells, with or without miglustat treatment, for one week, then stained with Lysotracker. n = 2. Lysotracker is printed in white and nuclei in red. Scale bar is 5µm.

We also stained these cells with filipin and scored those which had internal cholesterol labelling instead of cell surface labelling (Figure 5.2). We observed no increase in levels of filipin staining or in the percentage of cells with internalised cholesterol in HD cells compared to controls, and no alteration in response to miglustat treatment. In all lines, approximately 30% of cells had some internal cholesterol, indicating that cholesterol storage is not present in these cells under these conditions.
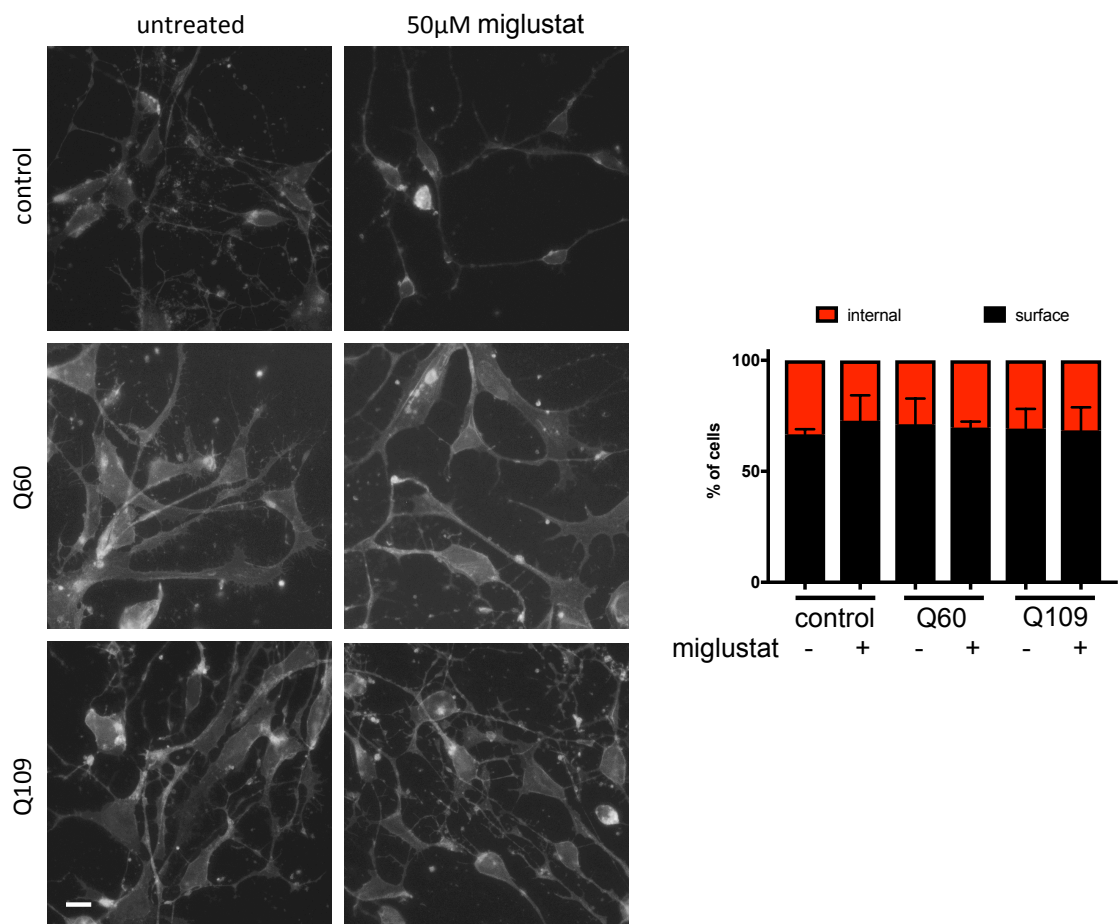


**Figure 5.2 Cholesterol is not mislocalised in HD patient iPSC-derived neural precursor cells**
Cells derived from either control or HD patient iPSCs were grown in appropriate conditions to produce neural precursor cells, with or without miglustat treatment, for one week, then stained with filipin. Cells were scored as having either surface cholesterol staining or the presence of internal cholesterol deposits. n = 3. Scale bar is 5µm. Error bars indicate standard deviation.
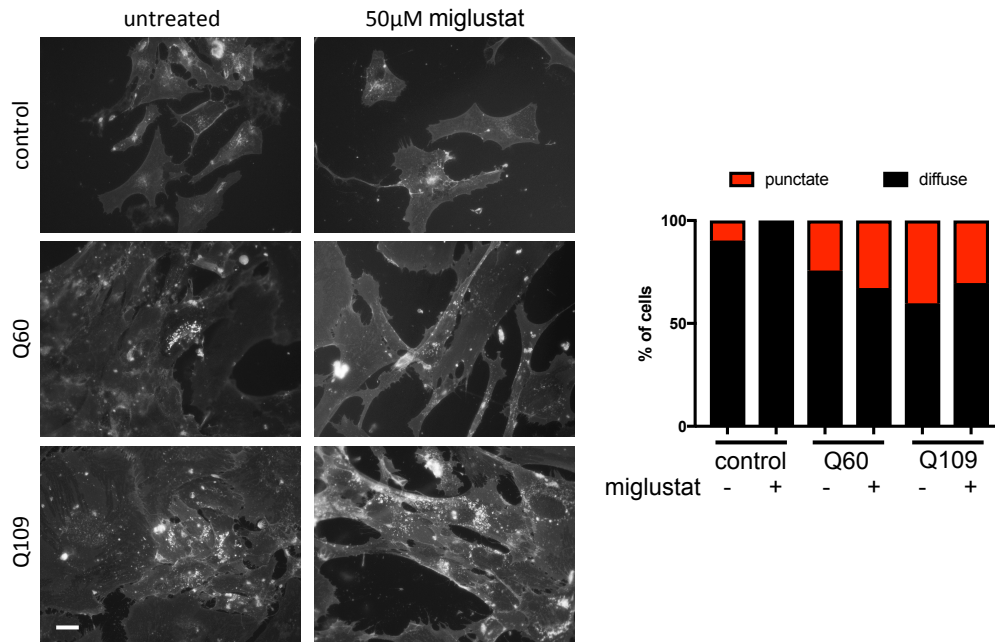
**Figure 5.3 HD patient iPSC-derived cells are sensitised to additional cholesterol and show lysosomal lipid storage**

Cells derived from either control or HD patient iPSCs were grown in medium with 10% FBS, with or without miglustat treatment, for one week, then stained with filipin. Cells were scored as having either diffuse or punctate cholesterol staining. n = 1. Scale bar 5µm
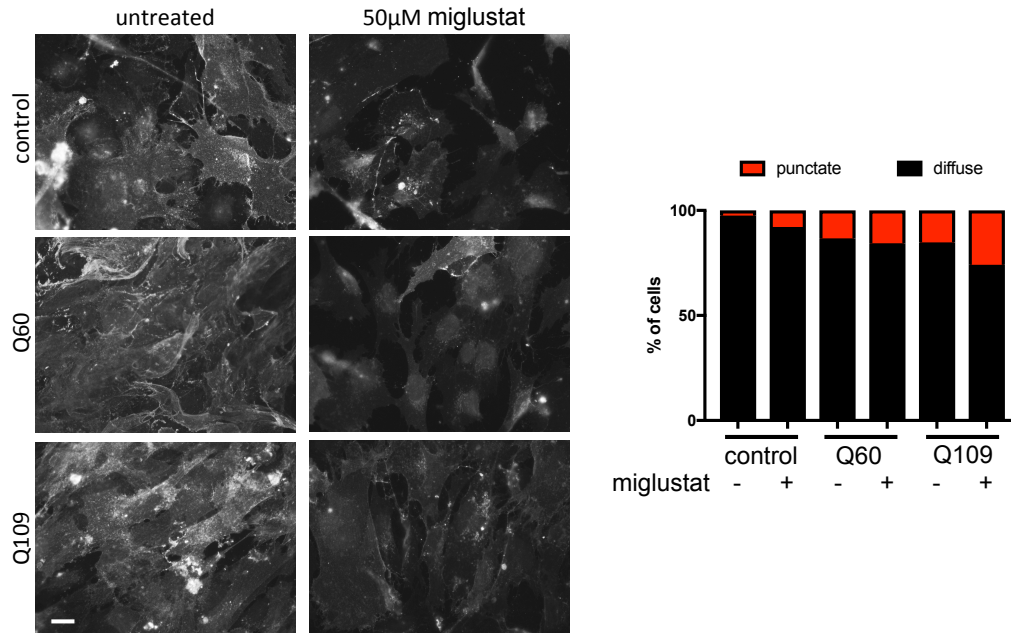


**Figure 5.4 HD patient iPSC-derived cells are sensitised to additional GM1 and show lysosomal lipid storage**

Cells derived from either control or HD patient iPSCs were grown in medium with 10% FBS, with or without miglustat treatment, for one week, then stained with FITC-CtxB. Cells were scored as having either diffuse or punctate FITC-CtxB staining. n = 1. Scale bar is 5µm

Cell culture conditions, in particular the availability of lipid in the medium, can affect the phenotypes present in cell models of LSDs (Pentchev *et al.*, 1985). We therefore grew these cells in FBS-containing medium instead of in appropriate conditions for maintaining neuronal precursor cells (Chapter 2), which produced larger, flatter (squamous) cells which we did not characterise, but also provided the cells with higher levels of lipid, including lipoproteins. In this single experiment, HD patient iPSC-derived cells grown in FBS-containing containing medium had punctate storage of both cholesterol (Figure 5.3) and ganglioside GM1 (Figure 5.4), whereas control cells have normal distribution. 24.3% of Q60 cells and 40.2% of Q109 cells have punctate cholesterol staining in this experiment, compared to only 9.7% of controls. Miglustat treatment has no clear effect on cholesterol storage, with the percentage slightly



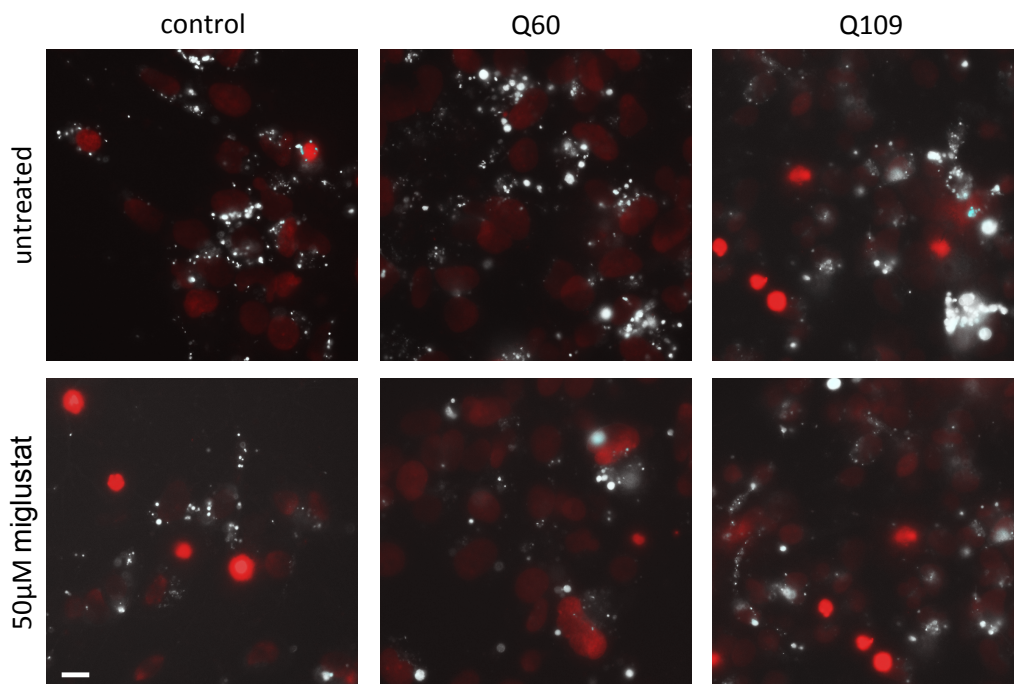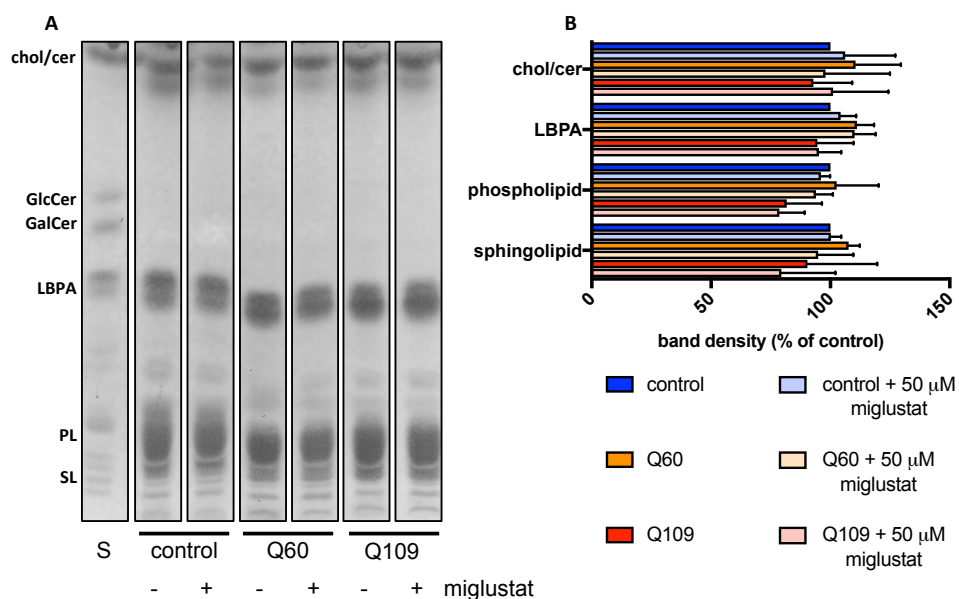**Figure 5.5 Lipids are not altered in HD patient iPSC-derived neural precursor cells**
Cells derived from either control or HD patient iPSCs were grown in appropriate conditions to produce neural precursor cells, with or without miglustat treatment, for one week, then lipids were analysed via thin layer chromatography (**A**). Lipid levels were quantified by measuring band density and correcting to levels in untreated control (**B**). Abbreviations: chol/cer = cholesterol / ceramide (which run together), GlcCer = glucosylceramide, GalCer = galactosylceramide, LBPA = lyso-bisphosphatidic acid, PL = phospholipids, SL = sphingolipids. n = 3. Error bars indicate standard deviation.

reduced in controls and Q109s, but slightly increased in Q60s after treatment. Control cells stained with FITC-CtxB had very little punctate storage of ganglioside GM1, present in only 2.5% of cells. Approximately 15% of cells in both the Q60 and Q109 HD lines had punctate GM1, an increase compared to controls though not correlated with increasing polyglutamine length. Miglustat reduced the overall level of GM1 staining, indicating it is reducing GSL synthesis as expected, but did not reduce the percentage of cells with punctate GM1 storage.
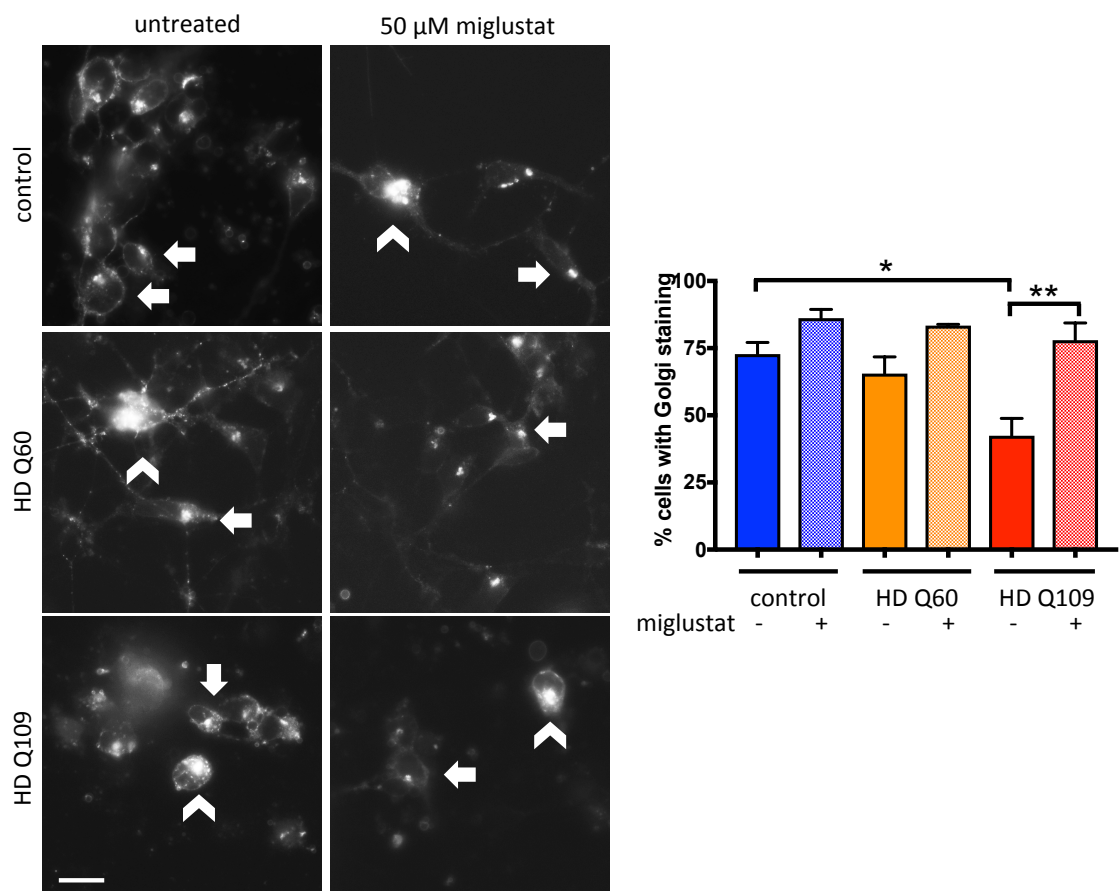


**Figure 5.6 HD patient iPSC-derived neural precursor cells have defects in ganglioside trafficking which are improved by miglustat treatment**
Cells derived from either control or HD patient iPSCs were treated with 50 μM miglustat for one week, then FITC-CtxB was used to measure trafficking of ganglioside GM1. Cells were scored as having either Golgi (normal trafficking) or punctate (blocked trafficking) staining. **A** Representative images. Images have been edited to show localisation more clearly, so levels have not been kept consistent. Scale bar 5 μm. **B** Quantification of trafficking. * $p < 0.05$ ** $p < 0.01$ by two-way ANOVA and Tukey multiple comparison post test. n = 3.

To look for lipid storage in these cells, we used thin layer chromatography to measure lipid levels in treated and untreated cells (Figure 5.5). We observed no change in cholesterol/ceramide (which do not separate well using this solvent phase), LBPA, phospholipids or sphingolipids between HD cells and control, and no changes in response to miglustat using this method.

## 5.2.2 Miglustat improves functional defects in HD iPSC-derived cells

In addition to storage phenotypes, we tested NPC-like functional defects in HD iPSC-derived cells after miglustat treatment. GM1 trafficking, measured using FITC-CtxB, is slightly reduced in HD Q60 cells and significantly reduced in Q109 cells, from 72.8% of cells with normal trafficking to 42.% (Figure 5.6). Miglustat treatment improves trafficking in both the control and Q60 cell lines, though the increase in cells with correct localisation is not significant in either. Miglustat also improves trafficking in the Q109s, where the percentage of cells with normal FITC-CtxB localisation returned to control levels after miglustat treatment, a significant effect.
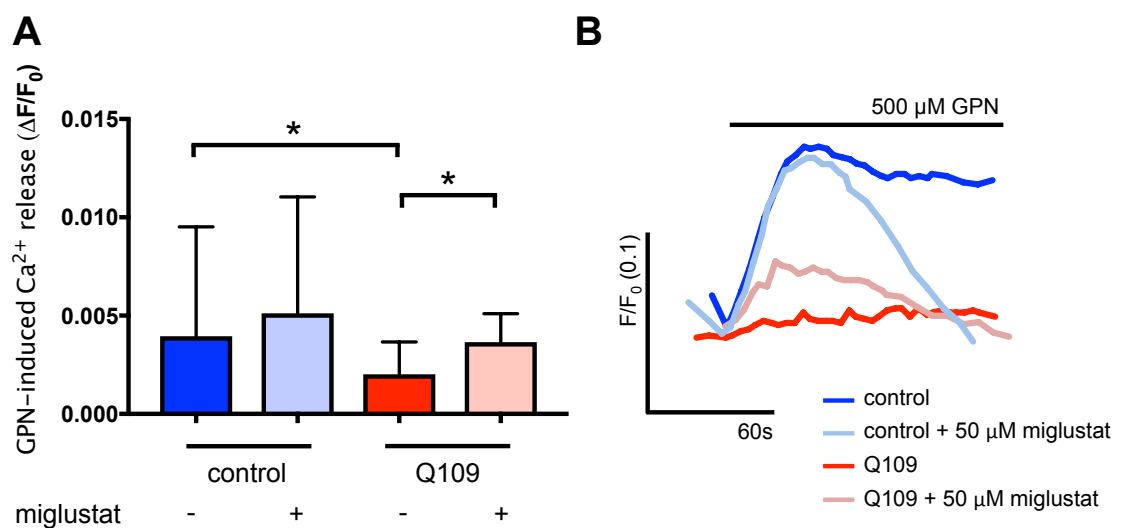


**Figure 5.7 HD patient iPSC-derived neural precursor cells have decreased lysosomal Ca$^{2+}$ release which is improved after miglustat treatment**

Cells derived from either control or HD patient iPSCs were grown in appropriate conditions to produce neuronal precursor cells, with or without miglustat treatment, for one week, then Fura-2 Ca$^{2+}$ imaging was used to measure lysosomal Ca$^{2+}$ release in response to 500 μM GPN. **A** Mean GPN-induced Ca$^{2+}$ release. Error bars indicate standard deviation. Data from two separate experiments (at least 55 cells per condition) except for miglustat-treated control where data is from one experiment (43 cells). * $p < 0.05$ by two-way ANOVA and Tukey multiple comparison post test. **B** Representative traces of GPN-induced Ca$^{2+}$ release in experiments from **A**.

Lysosomal Ca$^{2+}$ release in response to GPN is also reduced in Q109 neural precursor cells compared to controls. Fura-2,AM loaded cells were first stimulated with ionomycin, to clamp other stores, then with 500 µM GPN to induce lysosomal Ca$^{2+}$ release. Q109 cells have significantly reduced Ca$^{2+}$ release in response to GPN, approximately half that in controls, which is significantly improved after miglustat treatment, returning to approximately control levels (Figure 5.7).

**5.2.3 *Drosophila melanogaster* models of HD have defects in lifespan and climbing**

We chose *D. melanogaster* as a simple whole-organism model of HD to use for initial tests of miglustat. *D. melanogaster* models of HD have neurodegeneration, reduced lifespans, and motor defects (Marsh, Pallos & Thompson, 2003; Lewis & Smith, 2016). We obtained two sets of fly lines carrying UAS-huntingtin constructs with different polyglutamine repeat lengths, and crossed these with elav-GAL4 lines to produce flies expressing different huntingtins in the nervous system. To confirm these flies had measurable defects, we tested lifespan and climbing ability in flies maintained at both ambient temperature and 25°C.
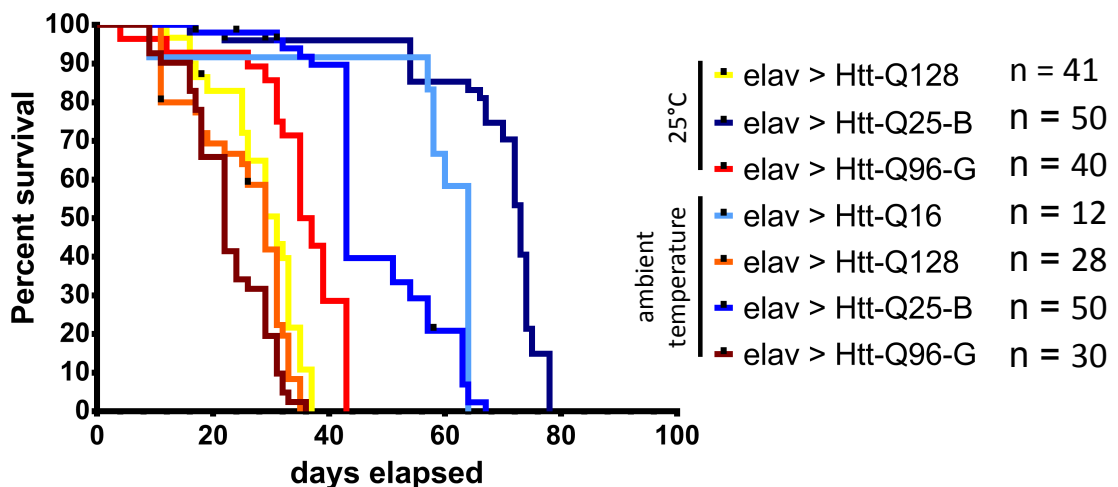


**Figure 5.8 *Drosophila melanogaster* models of HD have reduced lifespans**
Crosses were performed to produce flies expressing different UAS-huntingtin constructs under the control of elav-GAL4, producing expression throughout the nervous system. Flies were then maintained at either ambient temperature or in a 25°C incubator, and survival was measured. In each pair of lines (wtHtt vs mHtt, wtHtt-B vs mHtt-G), lifespan is significantly shorter for flies expressing mutant huntingtin instead of control; <0.0001 by Log-rank (Mantel-Cox) test. Fly numbers per group: Htt-Q25-B - 50 flies at each temperature, Htt-Q96-G - 30 at ambient temperature and 40 at 25°C, Htt-Q16 - 12 flies, Htt-Q128 - 28 at ambient temperature and 41 at 25°C.
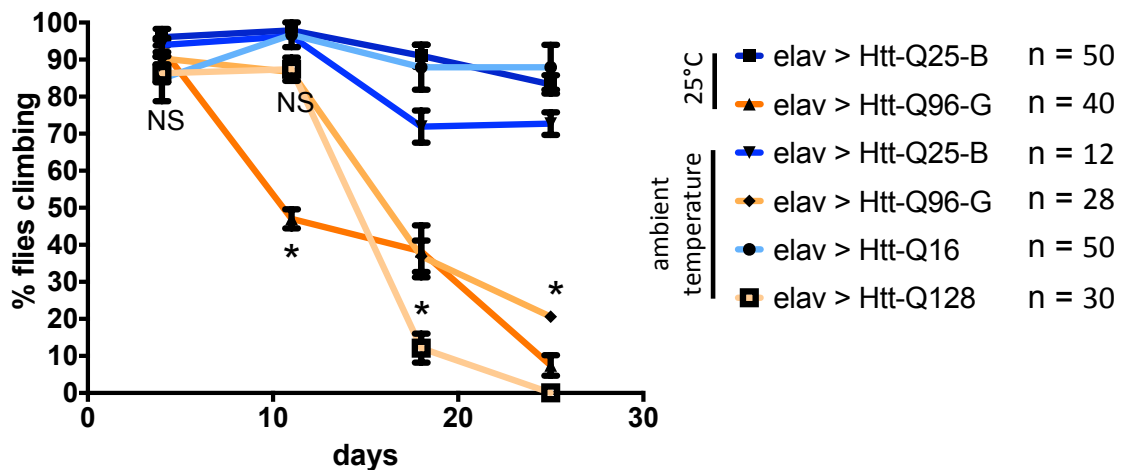
**Figure 5.9 *Drosophila melanogaster* models of HD have motor defects**
Crosses were performed to produce flies expressing different UAS-huntingtin constructs under the control of elav-GAL4, producing expression throughout the nervous system. Flies were then maintained at either ambient temperature or in a 25°C incubator, and climbing (negative geotaxis) assays were performed. Ability to climb was measured based on the percentage of flies per vial which climbed above a 5 cm mark within 10 seconds after being tapped to the base of the vial. NS indicates no significant difference, and * indicates a significant difference in climbing ability between mutant-huntingtin expressing flies and their paired controls (2 way ANOVA and Bonferroni multiple comparisons post test). Fly numbers per group: Htt-Q25-B - 50 flies at each temperature, Htt-Q96-G - 30 at ambient temperature and 40 at 25°C, Htt-Q16 - 12 flies, Htt-Q128 - 28.

We used Kaplan-Meier survival analysis to measure lifespan of the different HD model flies, which compares median lifespans and allows flies to be censored from the analysis if, for example, they escape. Each group of flies expressing mutant huntingtin (either Q96 or Q128) had significantly shorter lifespans than their paired control lines (expressing either Q25 or Q16 huntingtin respectively) (Figure 5.8). Flies expressing Q96-huntingtin had a median survival of 29 days at 25°C and 31 days at room temperature, whereas the Q25 controls had a median survival of 43 or 73 days at the two different temperatures.

*D. melanogaster* have a negative geotaxis response, so if they are tapped to the base of a fresh vial they will climb to the top of it. We measured this response by filming the flies and counting those which climbed above a 5 cm threshold within 10 seconds. Flies expressing mutant huntingtin in the nervous system have a progressive motor defect which interferes with climbing (Figure 5.9), reducing the proportion of flies which are

able to reach the 5 cm mark in a given time. At 4 days old, there were no differences in climbing ability by this test, although more stringent measures suggested that motor defects were already developing (not shown). At 11 days, the Q96-huntingtin flies maintained at 25°C had a significant defect in climbing compared to controls (Q25 flies at 25°C), and from the next experiment (18 days) onwards all the HD flies had significant deficits compared to their respective controls (Figure 5.9).

### 5.2.4 Miglustat can be given to *Drosophila melanogaster*

Miglustat has not previously been tested in *D. melanogaster*. We therefore needed to confirm that miglustat acted as an inhibitor of GSL synthesis in flies, that it was not acutely toxic, and that the flies did not refuse to eat it due to the potentially bitter taste (Priestman *et al.*, 2008).

While fly glycosphingolipids are different, the first step of GSL synthesis is the same in *D. melanogaster* as in mammals (Kraut, 2011), and flies have a glucosylceramide synthase which is similar to the human gene (Campbell *et al.*, 1998; Marks *et al.*, 2001). We initially tested miglustat in the *D. melanogaster* cell line S2R+. Cells were treated with 50 µM miglustat for 5 or 8 days, and samples were collected for thin layer chromatography. GSLs were reduced in S2R+ cells after miglustat treatment (Figure 5.10), with the decrease greater after 8 days than after the 5 day treatment which is optimal in mammalian cells (Vruchte, 2004) (not shown).

We then took 1 day old adult wildtype flies and moved them to food with either vehicle (PBS) or miglustat for 1 week at 25°C. We collected heads from female flies and extracted lipids for thin layer chromatography. Under these conditions, 300 µM miglustat reduced GSLs to approximately a quarter of control levels, but 100 µM or lower miglustat treatments did not produce a detectable decrease (Figure 5.10).

As miglustat has not previously been tested in flies, it could potentially have negative effects on survival, fertility or development, or could prompt the flies to refuse food containing the drug. We moved 1 day old flies to food containing miglustat at 25°C and measured survival for 11 days. None of the miglustat treatments significantly reduced survival of flies across this period (Figure 5.11). Miglustat also did not affect the average mass of female or male (which are smaller) flies collected after 7 days of miglustat treatment (Figure 5.11). This indicates that there was no acute toxicity from the drug, or starvation due to flies refusing to eat miglustat-containing food.
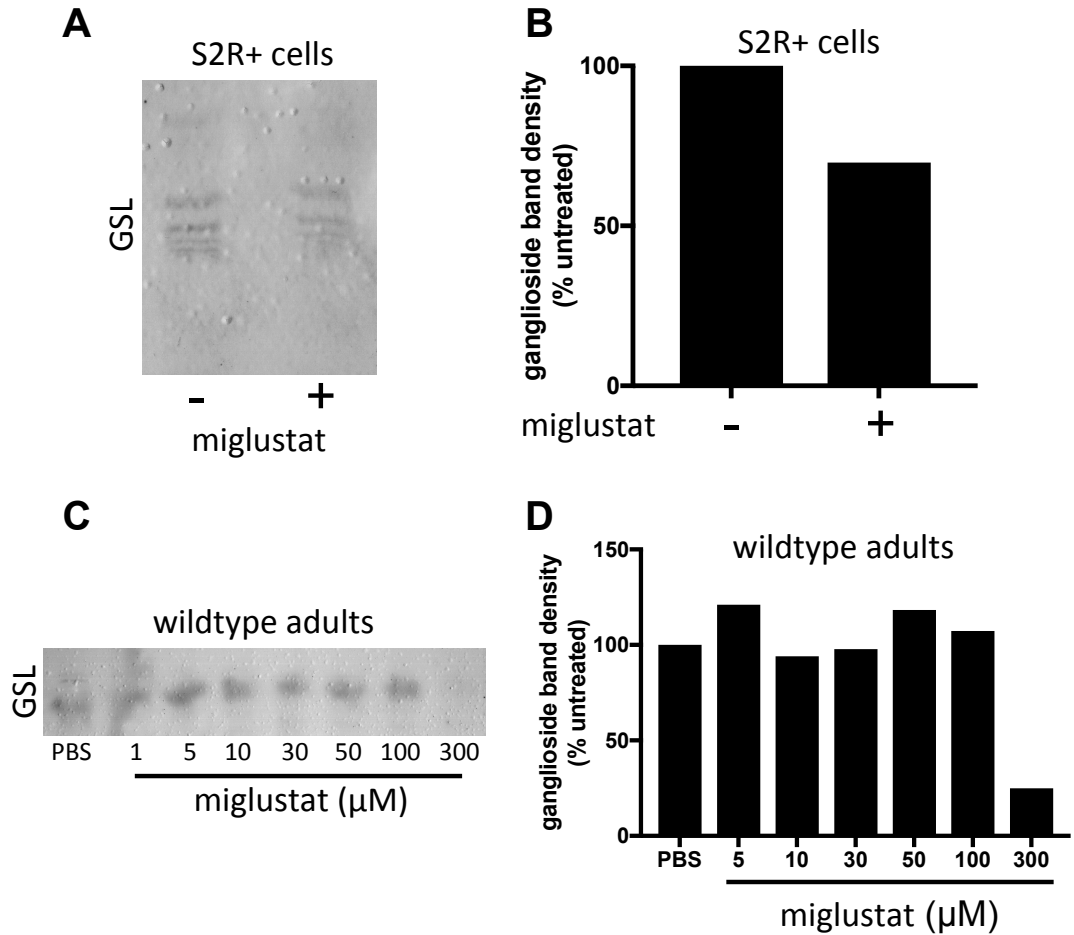
**Figure 5.10 Miglustat treatment reduces GSLs in *Drosophila melanogaster* cells and adult flies**
**A** S2R+ cells were treated with miglustat and levels of glycosphingolipids were measured via thin layer chromatography. n = 2. **B** Quantification of glycosphingolipid band density in miglustat-treated S2R+ cells. **C** *Drosophila melanogaster* were added to miglustat-containing food and collected after 7 days, and levels of glycosphingolipids in heads of female flies (30 flies) were measured via thin layer chromatography. **D** Quantification of glycosphingolipid band density in miglustat-treated *Drosophila melanogaster.*

We also used these flies to test for effects of miglustat on fertility and development. After adult flies had died or been removed, the vials of food were retained at 25°C. We first tracked the development of flies, and found no difference in timing of the fly lifecycle after miglustat treatments. The first pupae appeared within 24 hours of those in PBS-treated flies in all treatments, and adult flies also all appeared within one day across all treatments (Table 5.1). Based on visual assessment, there was no change in appearance or behaviour of larvae, pupae or adult flies grown on food containing miglustat.
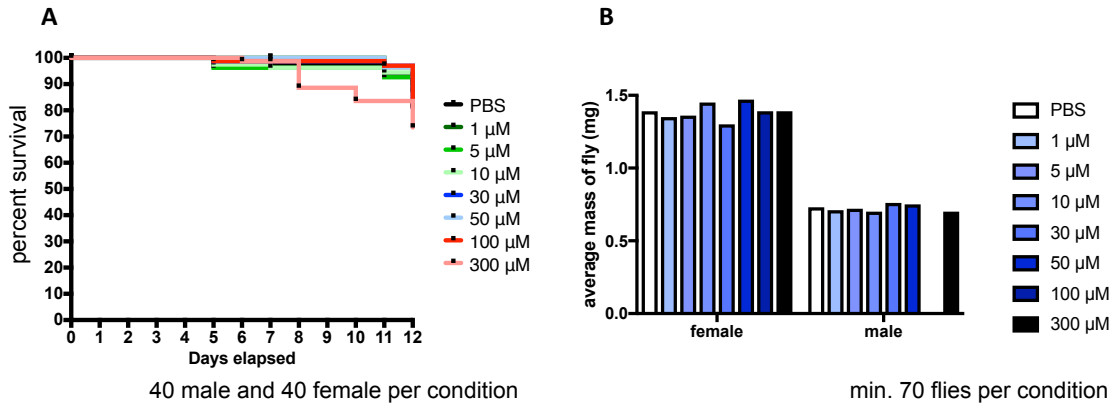
**Figure 5.11 Miglustat is not toxic to adult wildtype *Drosophila melanogaster***
Young adult wildtype flies were added to food containing either vehicle (PBS) or increasing concentrations of miglustat. **A** Survival of flies was measured for 12 days, long enough to ensure no short-term toxicity or starvation was observed (survival is expressed as a percentage). 40 males and 40 females per condition. No significant differences by Log-rank (Mantel-Cox) test. **B** Flies raised on miglustat-containing food were collected at 1 week old, killed by freezing, and weighed. Average mass (in mg) of flies is not altered across different concentrations of miglustat treatment. Minimum of 70 flies per condition.

In addition to the timing of development, we also counted the number of offspring produced in these conditions. There were no consistent changes to the number of offspring produced by miglustat-treated adult flies (Figure 5.12), and no difference in the proportion of male and female flies in any condition (Chi-square test, not shown). The highest miglustat treatment (300 µM) was not included, but based on visual assessment the numbers of offspring were not altered. We also retained adult flies from those grown entirely on miglustat food and confirmed that crosses between male and female wildtype flies grown on miglustat also produced offspring. Miglustat does not appear to cause a fertility defect in *D. melanogaster*.

## 5.2.5 Initial tests of miglustat treatment show small effects in *Drosophila melanogaster* HD models

As motor defects appeared early in HD fly models (Figure 5.9), and the effect of miglustat in S2R+ cells was potentially slower than it is in mammalian cells (Figure 5.10), we began treatment of flies as early as possible. Crosses of elav-GAL4 and UAS-huntingtin flies to produce experimental (huntingtin-expressing) flies were performed on food containing 300 µM miglustat or PBS at 25°C, so that flies were exposed to miglustat throughout. Flies were then collected and maintained on either treatment or

control food at 25°C. Survival of flies expressing mutant (Q96) huntingtin was again significantly reduced compared to control flies (Q25 huntingtin), and was not altered by treatment with 300 μM miglustat (Figure 5.13; median survival of 36 compared to 34 days). Control flies (Q25 huntingtin) treated with 300 μM miglustat actually have slightly but significantly reduced survival compared to untreated controls (Figure 5.13; 74 rather than 91 days), an unexpected effect which may confound our attempt to look for improvements in HD flies.

| [miglustat] | PBS | 1 μM | 5 μM | 10 μM | 30 μM | 50 μM | 100 μM | 300 μM |
|---|---|---|---|---|---|---|---|---|
| first pupae (day) | 8 | 7 | 7 | 7 | 7 | 7 | 8 | 8 |
| first adults (day) | 12 | 12 | 12 | 11 | 12 | 12 | 12 | 12 |

**Table 5.1 *Drosophila melanogaster* life-cycle after miglustat treatment**
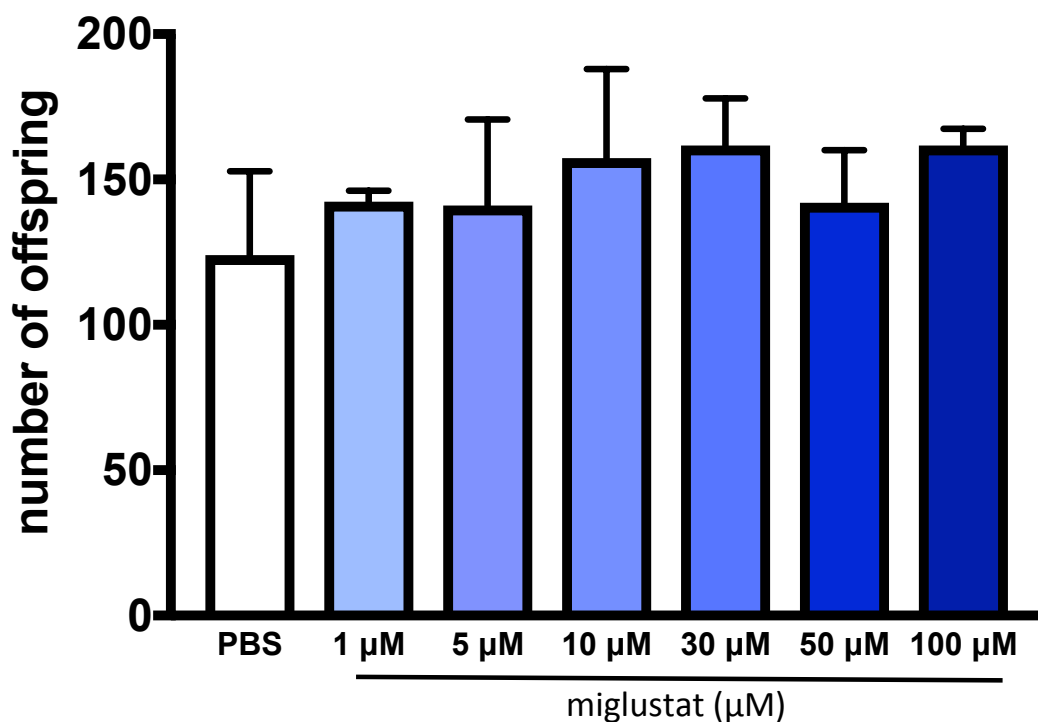


**Figure 5.12 Miglustat treatment does not affect fertility in *Drosophila melanogaster*** Young adult wildtype flies were added to food containing either vehicle (PBS) or increasing concentrations of miglustat. Adults were left in vials for several days, then discarded, and vials were kept at 25°C. Emerging offspring were collected and counted over several days.
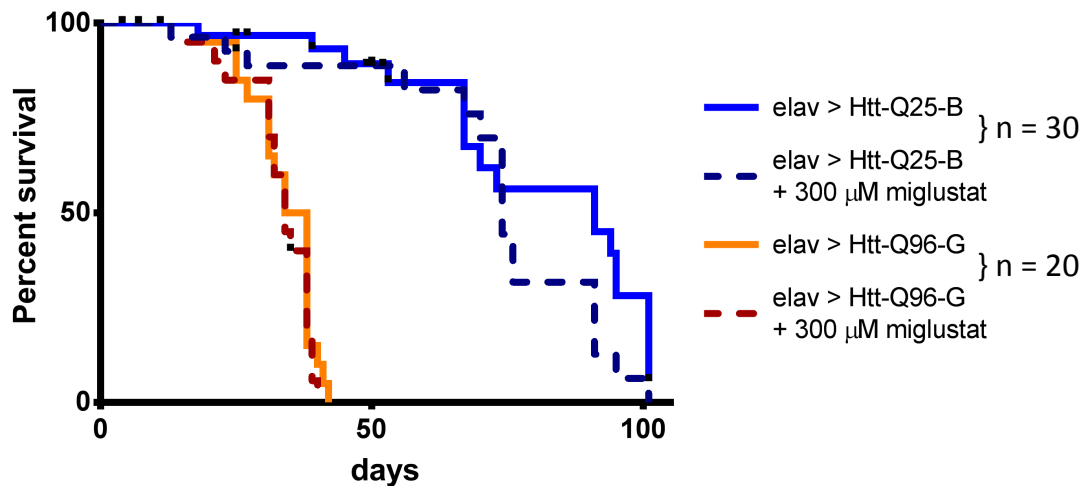
**Figure 5.13 Miglustat does not improve lifespan in *D. melanogaster* models of HD**
Flies expressing either control (Q25) or mutant (Q96) huntingtin were produced via crosses performed on food containing either 300 μM miglustat or vehicle control (PBS). Adult flies were then sorted and maintained on appropriate food at 25°C in an incubator with a 12 hour light-dark cycle, and survival was measured. No differences based on Kaplan-Meier survival analysis. 30 flies each condition for Htt-Q25-B, 20 flies each condition for Htt-Q96-G.
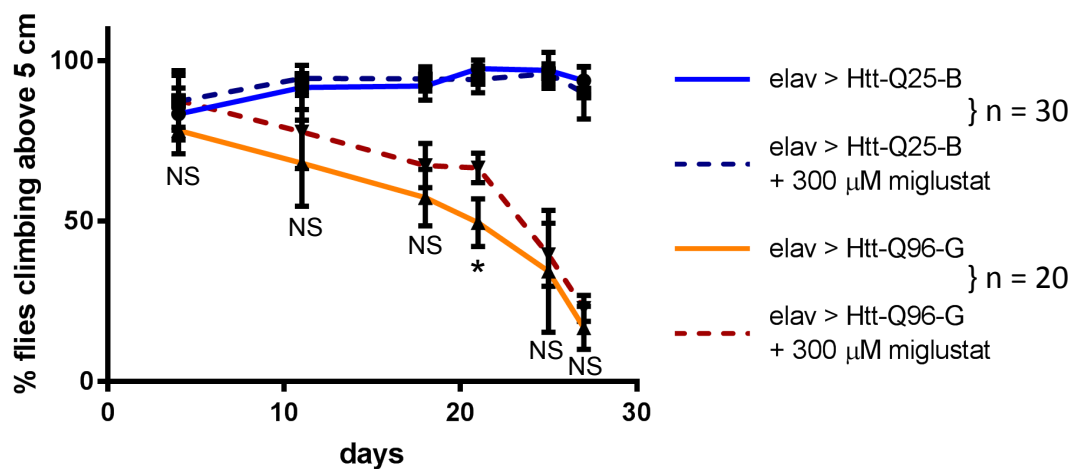


**Figure 5.14 Miglustat partially improves climbing in *D. melanogaster* models of HD**
Crosses were performed on vehicle or drug containing food to produce flies expressing UAS-huntingtin constructs under the control of elav-GAL4. Flies were then maintained on vehicle or drug containing food at either ambient temperature or in a 25°C incubator, and climbing (negative geotaxis) assays were performed. Ability to climb was measured based on the percentage of flies per vial which climbed above a 5 cm mark within 10 seconds after being tapped to the base of the vial. NS indicates no significant difference and * indicates a significant difference in climbing ability between untreated and miglustat-treated mutant huntingtin-expressing flies (2 way ANOVA and Bonferroni multiple comparisons post test). 30 flies each condition for Htt-Q25-B, 20 flies each condition for Htt-Q96-G.

We also tested climbing ability in this cohort of flies (Figure 5.14). We used the same measure of climbing as in our previous experiment, counting the percentage of flies able to climb past 5 cm within 10 seconds. Climbing assays were performed once a week for the first two weeks, and twice a week for the next two weeks to gain additional data as the flies became more severely affected. The controls remained consistently high across this time period, and the treated and untreated control flies remained very similar to each other throughout. The flies expressing mutant (Q96) huntingtin had a progressive decline in climbing ability. The miglustat-treated mutant flies had slightly better climbing ability throughout the first three weeks, with a significant difference at 21 days. Between 21 and 25 days, the miglustat-treated mutant flies decline suddenly and match the untreated mutant flies during the final week. While the difference is only significant at one time-point, there is a consistent small improvement in the climbing ability of HD flies after miglustat treatment.

## 5.3 Discussion

### 5.3.1 Miglustat is beneficial in HD cell models

Patient iPSCs and the cells which can be derived from them are a very useful new tool, allowing cell biology and, importantly, drug screening (Zhang *et al.*, 2015b), in cell types and gene defects which are relevant to human disease. The cells used here, like other HD cell models, have NPC-like defects, with some differences in phenotype between the Q60 HD cells and the more severe Q109 patient cells. The functional NPC-like defects present in these cells, though not the storage defects, are improved after treatment with the NPC therapy miglustat.

Lysotracker staining is increased in Q60 and Q109 cells compared to controls (Figure 5.1), and is slightly reduced by miglustat treatment. Miglustat does reduce Lysotracker staining (lysosomal volume) in NPC (Lachmann *et al.*, 2004), and in HD ST14A cells (Dr. Haslett, Mr. Badell-Grau) and might be expected to have a greater effect in these cells. In addition to normal cellular staining, the HD cells also have large round Lysotracker-stained bodies which are not present in the controls, and which are only slightly altered in response to miglustat. These bodies could represent very enlarged storage bodies, or fused lysosomes and autophagic vacuoles, or could possibly be extracellular. HD cells stained with cholesterol also showed unusual structures which may be related

to this Lysotracker staining, with similar large round bodies which largely clustered around points of contact between cells (Figure 5.2).

There is no evidence of cholesterol storage in these HD cells compared to controls, and no change in response to miglustat (Figure 5.2). While a small number of cells had distinct punctate storage, it was difficult to distinguish intracellular localisation as the cells were generally small and had a neuronal-like morphology, with a small cell body. Instead, cells were scored based on presence of internalised cholesterol, although the small cells and single focal plane meant that this was also difficult. Cholesterol storage has been seen (Dr. Luke Haslett) in some experiments in these cells and in neurons derived from them, but in this case there may be differences due to the stage of differentiation or the exact clonal lines used.

As cholesterol storage is a key feature of NPC (Vanier, 2010; Lloyd-Evans & Platt, 2010) and we expected to see it in these cells, we tested for lipid storage under different culture conditions, as the levels of lipid available to the cells can effect phenotypes in lysosomal storage disease models (Pentchev *et al.*, 1985). Instead of the medium used to maintain neuronal precursor cells, we used culture medium containing 10% FBS, to provide the cells with more lipid, including lipoproteins, which are taken up via endocytic pathways (Ikonen, 2008). These are not normal conditions for these cell lines and lead to differentiation into larger, more squamous cells, which were not characterised further. However, HD cells grown in these conditions had punctate storage of both cholesterol (Figure 5.3) and ganglioside GM1 (Figure 5.4), which although preliminary suggests that these cells do have lysosomal defects and the potential to store lipids. This suggests that the lack of cholesterol storage in the neural precursor cells from these iPSC lines (Figure 5.2) may be due to a difference in cell type or conditions, but that the NPC-like defects are present, an effect which has also been seen in iPSC models of NPC (Yu *et al.*, 2014b). Storage of cholesterol (Figure 5.3) and punctate localisation of GM1 (Figure 5.4) in these FBS-treated HD cells is not reduced after treatment with miglustat in this experiment. In NPC, miglustat partially corrects storage phenotypes (Lachmann *et al.*, 2004), and in HD ST14 cells cholesterol and sphingomyelin storage are partially reduced by miglustat treatment (Dr. Haslett, Mr. Badell-Grau).

Thin layer chromatography (TLC) of the neuronal-like cells revealed no detectable changes in lipids, either in HD cells when compared to controls or in miglustat-treated compared to untreated cells (Figure 5.5). It may be that the cell type and culture conditions have affected total lipid levels, as for cholesterol storage (Figure 5.2 and Figure 5.3). In NPC and other LSDs, phenotypes can differ between organs and cell types (Lloyd-Evans & Platt, 2010). GSLs in cell samples were not detectable via TLC, probably due to low levels in samples, but cell staining in both the FBS-treatment (Figure 5.4) and ganglioside trafficking (Figure 5.6) experiments is reduced, indicating miglustat is inhibiting GSL synthesis as expected.

Ganglioside trafficking, measured using FITC-CtxB, is slightly reduced in Q60 neural precursor cells and significantly reduced in Q109s compared to controls (Figure 5.6). Miglustat significantly improves trafficking in Q109 cells, returning them to approximately the same levels as controls. This is similar to HD ST14A cells (Dr. Haslett, Mr. Badell-Grau) and NPC (Lachmann $et$ $al.$, 2004), where miglustat treatment also leads to an improvement in trafficking. Curiously, correct localisation of ganglioside GM1 is increased after miglustat treatment in all three cell lines including the control, which is unexpected but may simply be due to reduced background staining and therefore clearer localisation after miglustat has reduced overall levels of GSLs.

Lysosomal $Ca^{2+}$ release is also reduced in HD neural precursor cells compared to controls, a key NPC phenotype (Lloyd-Evans $et$ $al.$, 2008) which we have also observed in other HD cell models. While tests of the Q60 line were not completed, the Q109s had a significant reduction in $Ca^{2+}$ release, which is significantly restored after miglustat treatment (Figure 5.7). This matches the results seen in both the HD ST14A cell line (Mr. Badell-Grau) and in NPC mutant cells (Lloyd-Evans $et$ $al.$, 2008).

In addition to the functional improvements seen here, Dr. Luke Haslett has also used these patient iPSC-derived neurons to look at excitotoxic defects in HD cells. Control neurons exposed to glutamate have elevated but consistent cytosolic $Ca^{2+}$ which returns to baseline when glutamate is removed, whereas HD neurons lose $Ca^{2+}$ homeostasis, leading to a gradual increase in cytosolic $Ca^{2+}$, failure to return to baseline, and poor survival. Miglustat significantly improves function in these cells, improving the ability of the HD cells to maintain $Ca^{2+}$ homeostasis and return to baseline.

Curiously, both increased (Del Toro *et al.*, 2010) and decreased (Desplats *et al.*, 2007; Maglione *et al.*, 2010) gangliosides have been seen in HD, and these groups have also shown that addition of GM1 is beneficial in HD models (Maglione *et al.*, 2010; Di Pardo *et al.*, 2012). Maglione *et al.* showed that addition of GM1 altered huntingtin phosphorylation and was protective against apoptosis in cell lines, and that inhibition of GSL synthesis with the glucosylceramide synthase inhibitor PPMP increased apoptosis in control cells (Maglione *et al.*, 2010), which may be due to an increase in ceramide. In mice, a month-long intra-ventricular infusion of GM1 in the YAC128 HD mouse model greatly improves motor function in mice for the duration of the infusion and up to 2 weeks afterwards (Di Pardo *et al.*, 2012). It is therefore curious that miglustat, which reduces GSLs, is also beneficial in HD models. Other GSLs rather than GM1 may be involved, or it could be a question of effects on lipid balance and localisation rather than on overall amounts, in which case restoring trafficking could have some similar effects to adding GM1, by increasing GM1 at the cell surface or in other compartments once it is not trapped in the endocytic system. Miglustat is only a partial inhibitor of glucosylceramide synthase, which may help avoid the negative effects seen previously (Maglione *et al.*, 2010), and addition of GM1 could alter regulation of ganglioside synthesis pathways. There may also be differences due to species and cell type, as for example different GSL changes seen in response to the glucosylceramide synthase inhibitor PPMP treatment in different cancer cell lines (Alam *et al.*, 2015).

In summary, NPC-like phenotypes are present in HD patient iPSC-derived cells, similar to (though not identical to) those seen in other HD models. Some of these differences are due to the cell type or culture conditions used, though other factors such as species differences may contribute. Most importantly, there are functional improvements in these cells after miglustat treatment, demonstrating that miglustat is beneficial in a patient-derived model of HD.

### 5.3.2 Establishing *Drosophila melanogaster* models

Our next aim was to test miglustat in a whole organism model of HD. While there are many mouse models of HD, which are extensively used, these models have limitations (Chapter 1.8), and we aimed to use a simple model for these initial tests. HD models are available in *D. melanogaster*, a simple model organism which nevertheless has a

complex nervous system and behaviour and can be used to model neurodegenerative disease (Ugur, Chen & Bellen, 2016; Chien *et al.*, 2002; Marsh, Pallos & Thompson, 2003).

We chose two simple functional measures to test in these models, lifespan and climbing. These were chosen as they were relatively easy to measure and we were interested in improvement in function of HD models. Ideally, we would also have looked at the extent of neurodegeneration, using the pseudopupil method to investigate neurons in the fly eye (Marsh, Pallos & Thompson, 2003), but we were not able to establish this method.

We were able to obtain these fly models and observe defects in HD flies compared to controls. The flies we used expressed UAS-huntingtin constructs throughout the nervous system, under the control of elav-GAL4. In each case, we used crosses between elav-GAL4 and UAS-huntingtin parental lines rather than establishing a stable line, partially due to time constraints and partially because we did not know whether a HD line would be stable or would have issues with fertility and development. From these crosses we selected mated females for use in experiments, as crosses to produce female huntingtin-expressing flies gave us a higher proportion of experimental flies, and ensuring they were all mated maintained consistency and avoided effects of altered germline signalling or other factors on lifespan (Lin *et al.*, 2001; Markow, 2011).

We tested two different sets of huntingtin-expressing flies, one with full length human huntingtin with either Q16 or Q128 and one expressing just the first exon of human huntingtin with either Q25 or Q96. Both HD lines had reduced survival and progressive climbing defects (Figure 5.8 and Figure 5.9), but the Q16-huntingtin parental line had some health problems and did not produce a reasonable number of offspring in crosses. We selected the Q25 and Q96 flies for further use.

For the climbing assay, we measured the percentage of flies which were able to climb past a 5 cm threshold within 10 seconds of being knocked to the base of a vial. This measure gave us a clear progressive defect across several weeks (Figure 5.9 and Figure 5.14). Using a more stringent test (a higher threshold or a shorter time) revealed the motor defect in the HD flies at younger age but later, as the HD flies became more severe, progression and differences could not be distinguished (not shown). We also

tried measuring the average height climbed by each fly, a method which treated each individual fly separately and so would have provided greater statistical power, but which was not ultimately useful as the variability within each cohort was high (not shown).

We have not included additional controls here but have looked at them in other experiments. We used a cohort of flies expressing a UAS-GFP construct under the control of elav-GAL4, as a control for the general effects of protein expression compared to the specific effects of expressing huntingtin in these flies. These elav > GFP flies were similar to the Q25-huntingtin-expressing control flies. Analysis of protein levels in these HD models would have been useful; firstly in the flies expressing Q25 and Q96 huntingtin constructs, to see if the level of expression was comparable, and secondly in treated flies where an improvement in climbing was seen, to confirm miglustat treatment was not protecting flies by altering levels of huntingtin expression compared to untreated flies.

These HD fly models are potentially interesting for future work on this project, as there are NPC proteins in flies, and an NPC model. There are several *D. melanogaster* NPC1 and NPC2 genes, which would allow a genetic approach to investigating the mechanisms of their involvement in HD - or at least, in fly models of HD, which have many differences but are still informative for studying human disease - by combining knockout or overexpression of the NPC proteins with the HD models. The defects present in the *Drosophila melanogaster* NPC model (Huang *et al.*, 2005; 2007; Fluegel, Parker & Pallanck, 2006) may also be useful for comparison with, or further analysis of the HD models and their response to miglustat.

### 5.3.3 Miglustat in *Drosophila melanogaster*

There are no existing reports of miglustat being used in *D. melanogaster.* We therefore needed to test whether miglustat was able to inhibit glycosphingolipid synthesis in the fly, as we cannot be certain it will (Hillig, Warnecke & Heinz, 2005), and whether there were any negative effects or refusal to eat the drugged food. The fly glucosylceramide synthase is similar to the mammalian enzyme (Campbell *et al.*, 1998; Marks *et al.*, 2001), but we did not have the facilities to produce purified enzyme or develop and test the enzyme assay (Gupta *et al.*, 2010) for the fly protein. Instead, we used GSL levels as an indicator of miglustat activity.

Miglustat reduces GSLs in wildtype *D. melanogaster* (Figure 5.10), though we have not optimised our TLC method for fly GSLs and cannot determine which species are involved. In S2R+ cells, 50 μM miglustat reduces GSLs, the same concentration which is effective in mammalian cells. We used both a 5 day treatment, as we normally use for mammalian cells, as well as an 8 day treatment. The longer treatment produced a greater reduction in fly cells, whereas miglustat does not tend to have an increasing effect over longer treatments in mammalian cells, suggesting slightly different kinetics of the drug in flies. We did not characterise this further. In adult flies, a week of treatment with 300 μM miglustat reduced GSLs in fly heads (Figure 5.10), but we did not test lipid levels over the whole course of the climbing and lifespan experiments. As this concentration of miglustat slightly reduced survival of the normal huntingtin flies (Figure 5.13), and we have some evidence from other experiments that 200 μM miglustat may not have this negative effect, it might have been useful to measure the levels of miglustat and the lipid levels across a longer time-course or the whole lifespan.

Our initial tests confirmed that miglustat was not acutely toxic to flies (Figure 5.11). Starvation or acute toxicity would have been apparent within the duration of this experiment, though long-term effects were not detectable until full lifespan experiments were conducted (Figure 5.13). Fertility and development of flies was also not affected by miglustat treatment. An effect on male fertility has previously been seen after miglustat treatment in a mouse model (Oko *et al.*, 2011), but not in other cases of its use, which led to our initial interest in this question. However, there were no effects of miglustat on timing (Table 5.1) or number (Figure 5.12) of offspring. Ms. Sophie Cook is continuing and extending this work, to confirm whether there are effects of long-term or high-concentration miglustat treatments.

We have therefore shown that it is possible to use miglustat in *D. melanogaster*, and so this is a suitable model for us to use to test miglustat in HD. This may also be useful for other LSD work in flies, as there are fly models of both NPC and Gaucher disease, the two diseases miglustat is licensed for. While we have not done enough characterisation to confirm this, if miglustat has side-effects in flies over the long term or at high concentrations it may also be an interesting tool for altering and investigating lipid metabolism and signalling in flies.

### 5.3.4 Miglustat has limited but beneficial effects in HD *Drosophila melanogaster*

In these experiments, treatment with 300 µM miglustat improves climbing ability but does not alter survival in flies expressing mutant huntingtin (Figure 5.14 and Figure 5.13). The fact that survival of the control flies is slightly reduced following miglustat treatment is curious, and may interfere with the tests in HD models. This could be due to too great a reduction in GSLs, or could be due to differences in *D. melanogaster* lipid biology. Data from a separate experiment using 200 µM miglustat suggests that this lower concentration was not harmful to flies, and while no significant improvements were seen, there was a slight improvement in survival of the HD flies which later dropped back down to the same level as the untreated flies, matching the pattern of the improvement we saw in climbing in the experiments presented here (Figure 5.14). Overall, this data is limited and requires further confirmation, but suggests that miglustat has beneficial effects in HD models, in agreement with the improvements we have seen in HD iPSCs.

There are a number of factors which could contribute to the limited effects of miglustat seen here. Most importantly, the numbers of flies involved were comparatively low, reducing the power and reliability of these experiments, though the data obtained is consistent and has produced observable effects. It is likely that we have not found an optimal concentration or treatment regimen for miglustat, and more work on long-term negative effects and on the kinetics of miglustat treatment in flies would have been useful. It is also possible that only relatively limited effects can be obtained using miglustat in *D. melanogaster* HD models, due to species differences in lipid metabolism or other factors, but the effects on climbing which we have observed suggest this is not the case.

### 5.3.5 Conclusion

In summary, miglustat has beneficial effects in both cell and fly models of HD. HD patient iPSC-derived cells have somewhat different phenotypes than the other model cell lines we have used, partially due to the effect of cell type and culture conditions. Miglustat improves functional defects in these cells, including aspects of altered $Ca^{2+}$ signalling, an important HD defect. In flies, at a miglustat dose which may not be optimal, survival was not altered but motor function was improved, an important

benefit, in a model system which has previously been used to develop therapies towards human trials.

# CHAPTER 6 VECTORS FOR NUCLEIC ACID DELIVERY AFFECT LYSOSOMAL FUNCTION

## 6.1 Introduction

### 6.1.1 Outline

Methods for genetic modification rely on the ability to deliver nucleic acids to cells, often achieved by the use of lipid vectors. These vectors are designed to transport large, hydrophilic nucleic acid molecules into cells via the endocytic system, and deliver them to the cytoplasm by disrupting endocytic vesicles. However, the mechanisms by which lipid vectors deliver their cargo may also affect lysosomal function, causing problems when used to study the lysosome.

A number of lipid and polymer based vectors, used according to manufacturer's protocols, were tested for effects on lysosomal function. Initial screening identified several vectors which induced abnormal lysosomal expansion and these were selected for further characterisation. These vectors had a range of different effects, including induction of phospholipidosis and accumulation of other lipids in lysosomes, altered endocytic trafficking, and modulation of endocytic protein expression.

This study demonstrates that some lipid vectors independently disrupt endocytic and lysosomal function, making them unsuitable for use in studies of lysosomal function or lysosomal disease. Some of these effects on lysosomal function could improve their efficiency, or potentially even benefit the cell. In particular, observed elevation of NPC1 levels could alter vector trafficking or even be therapeutically useful. Studying these effects will help to refine and improve the tools used to study lysosomal disease, will help direct development of more effective transfection vectors, and will contribute to the development of suitable methods for therapeutic use of RNAi, particularly for lysosomal diseases.

### 6.1.2 Genetic modification

*6.1.2.1 Manipulation of gene expression is a useful tool*

There are a number of methods for altering gene expression in cells and whole organisms, including RNA interference, addition of transgenes, and genetic editing techniques such as CRISPR. These methods are valuable, powerful research tools and

also have potential as therapies for genetic disease, so appropriate, efficient methods to deliver genetic material to cells are essential.

RNA interference (RNAi) is a mechanism for specific gene silencing at the post-transcriptional level. Small interfering RNAs (siRNAs), double-stranded RNAs around 22 nucleotides long, either endogenous or derived from viral RNA, bind to the RNA-induced silencing complex (RISC) and guide it to complementary target mRNA which is then degraded, suppressing gene expression (Hannon, 2002). Modulation of gene expression by endogenous small RNAs is seen throughout eukaryotes (Hannon, 2002) and has several roles in cells and organisms, including modifying gene expression (primarily miRNA) (Hannon, 2002; Wilson & Doudna, 2013), defence against viruses (siRNA) (Zambon, Vakharia & Wu, 2006; Jeang, 2012), and defence against transposons (piRNA) (Siomi *et al.*, 2011).

The RNAi pathway was first discovered by Fire, Mello, Kemphues and others (Hannon, 2002; Fire *et al.*, 1998) who were investigating suppression of gene expression in *C. elegans*. Anti-sense RNA had been used for several years (Nellen & Lichtenstein, 1993; Guo & Kemphues, 1995) before Fire *et al.* realised that double-stranded RNA (dsRNA) worked more effectively, and identified the dsRNA mechanism outlined above (Fire *et al.*, 1998). Since then, a great deal of work has gone into both investigating the endogenous pathways and developing RNAi as a research tool. Synthesised siRNAs, when provided to cells, will bind to RISC and suppress gene expression via the same mechanism as endogenous siRNA. Sequences can be designed to specifically target any gene, making RNAi a flexible and powerful research tool.

Gene expression can also be altered by adding exogenous DNA which the cell will then express. This can include plasmids and other forms of extrachromosomal DNA, or DNA which is integrated into the genome (by using viral vectors, for example), and can allow expression of tagged proteins, or expression of specific proteins in different backgrounds, among many other uses, and can be important in research, therapy and biotechnology (Glover, Lipps & Jans, 2005; Lewandoski, 2001; Khan, 2013).

### 6.1.2.2 Gene therapies

Gene therapy is theoretically an incredibly powerful treatment route for genetic diseases, and a possible component of therapies for other conditions, including cancer. In practice, safe and efficient delivery of therapies remains difficult, and there have

historically been severe adverse reactions to vectors, both immune reactions and cases of leukemia due to off-target gene insertions (Naldini, 2015; Hacein-Bey-Abina *et al.*, 2008). However, advances in genetics and vector design have led to continued improvement, and a number of trials have shown that safe, effective gene therapies are possible (Collins & Thrasher, 2015; Naldini, 2015). Two of the areas in which it is being used are the diseases discussed in this thesis - LSDs and Huntington's disease (Deng *et al.*, 2014; Biffi, 2016; Wyant, Ridder & Dayalu, 2017).

LSDs caused by loss of soluble lysosomal enzymes are amenable targets. In these diseases, partial restoration of enzyme can be sufficient to provide normal function (Amalfitano & Rastall, 2015), and cross-correction is possible if the enzyme is a secreted protein. Cross-correction involves release of proteins by one cell which can then traffic to the lysosome of another cell via capture and endocytosis and become functional (Fratantoni, Hall & Neufeld, 1968; Platt & Lachmann, 2009). Therefore, as long as gene therapies can reach some cells or cell types, enough correction can be produced to be clinically effective (Amalfitano & Rastall, 2015; Biffi, 2016). There is an ongoing trial of gene therapy in the LSD metachromatic leukodystrophy (MLD), a deficiency in arylsulphatase A (ARSA) which leads to demyelination and death in childhood. Bone marrow cells with corrected ARSA genes were re-infused into patients, and the treatment has halted progression and prevented onset in the children so far (Aiuti *et al.*, 2013; Sessa *et al.*, 2016). Gene therapy for NPC is a more distant target, but there has been recent success with an AAV9-delivered therapy producing benefits in a mouse model of NPC, demonstrating that the approach is viable (Chandler *et al.*, 2017).

Huntington's disease is different, as the aim here is to remove or suppress mutant huntingtin, rather than replacing a missing protein. Two approaches are being used (Wyant, Ridder & Dayalu, 2017): suppression of mutant huntingtin expression (Alterman *et al.*, 2015; Grondin *et al.*, 2015), including a trial of antisense oligonucleotides begun in 2016 by Ionis Pharmaceuticals, and gene editing, which is in earlier stages but has shown potential in cell and animal studies (Casaca-Carreira *et al.*, 2015; Kolli *et al.*, 2017).

### 6.1.3 Delivery of nucleic acids to cells

Any method involving adding nucleic acids to cells has the challenge of getting the nucleic acid molecules across the plasma membrane. Even siRNA molecules are relatively large, charged and hydrophilic, and constructs such as plasmids are even larger. These molecules are unable to diffuse across the plasma membrane, and while mammalian cells do take up DNA (Loyter, Scangos & Ruddle, 1982; Lehmann & Sczakiel, 2005), they are less competent at doing so than bacteria (Mell & Redfield, 2014; Chen & Dubnau, 2004). RNA molecules must reach the RNAi machinery which is localised in the cytoplasm (and interestingly, possibly in the endocytic system to some extent (Gibbings *et al.*, 2009; Gibbings & Voinnet, 2010; Zhang *et al.*, 2015a)), and DNA must reach the nucleus. Methods for delivery are therefore required, and the available solutions are similar to those for other delivery challenges, like delivery of certain small molecule or peptide therapies. There are three main groups: viral vectors, mechanical approaches, and molecular conjugates or vehicles.

Viral vectors are modified viruses, commonly lentiviruses or adeno-associated virus (AAV), which have been altered to carry the target nucleic acids rather than the viral genome. These are highly effective in whole organisms as they take advantage of the results of viral evolution to invade and infect cells, and can be used to integrate transgenes into the target genome. However, production of virus particles (nucleic acids properly packaged into viral protein coats) can be complex, and use of some virus types in whole organisms has been made more complicated - and clinically, potentially dangerous - by immune responses and vector-induced cancers (Collins & Thrasher, 2015).

Mechanical methods include both microinjection and electroporation (using an electric pulse which makes the cell membrane more permeable). Electroporation is effective in many cultured cell types, and microinjection is effective and specific and so is widely used for modifying model organisms, particularly in embryos or germline. However, these methods require specialist equipment and training, and can cause high rates of cell death (Kang, McNaughton & Espinosa, 2016).

Conjugation involves covalently linking groups (called adducts) which help the nucleic acid cross the plasma membrane (Lorenz *et al.*, 2004; Soutschek *et al.*, 2004), such as cholesterol (Alterman *et al.*, 2015; DiFiglia *et al.*, 2007) or cell-penetrating peptides (El-

Sayed *et al.*, 2008; Kloß *et al.*, 2009). This can help targeting to cells or tissues in whole organisms and avoids viral side effects, but requires conjugation reactions for every new construct and carries the risk that the adduct can alter the structure or function of the cargo or cause off-target or immune responses.

Using molecular vehicles involves coating or loading the cargo into something which will allow it to cross the plasma membrane. The major type of vehicle is lipid vectors (also called liposomes or lipid nanoparticles), which we are interested in here. These do not work well in whole organisms or in certain cell types such as neurons, but they are simple and adaptable to use in the lab, a range of different formulations are easily available, and they are generally effective, efficient and non-toxic in most cell types.

### 6.1.4 Lipid vectors for delivery of genetic material

*6.1.4.1 Structure and function*

Lipid vectors are lipid mixtures which form bilayers, micelles or particles with the nucleic acid cargo. The lipids used are selected based on their ability to condense and pack nucleic acids and interact with cells to promote efficient and successful delivery. The materials used are reviewed in greater technical detail by others (Zhang, Zhi & Huang, 2012; Zatsepin, Kotelevtsev & Koteliansky, 2016; Puri *et al.*, 2009; Tam, Chen & Cullis, 2013; Cheng & Lee, 2016), but a brief outline is useful here (see Figure 6.1).

Cationic lipids such as the first lipid vector, DOTMA (Felgner *et al.*, 1987), are the main component of most lipid vectors. These have dual roles - they associate with nucleic acids and promote packing, and they also interact with and destabilise cellular membranes to release nucleic acid to the cytoplasm (Wan, Allen & Cullis, 2014). Cholesterol is another multifunctional component, as it stabilises the vector nanoparticle and also helps the vector particles fuse with and disrupt cell membranes (Zatsepin, Kotelevtsev & Koteliansky, 2016; Dabkowska *et al.*, 2012a; 2012b). Other materials, sometimes called helper lipids, can be added which increase destabilisation of cell membranes (such as phospholipids (Zatsepin, Kotelevtsev & Koteliansky, 2016)) or which stabilise and mask the vector particle (PEG modifications (Zatsepin, Kotelevtsev & Koteliansky, 2016; Cheng & Lee, 2016; Kumar *et al.*, 2014)). In addition, new materials have been developed by modifying or adding to these lipids to promote their biological activity. This includes lipids which become destabilised or gain charge at low pH or in reducing environments, to improve release of nucleic acids in the late

endocytic system or cytoplasm respectively (Zhang, Zhi & Huang, 2012). Details of the composition of commercial vectors is generally proprietary or trademarked, but the available information on the vectors used in this study is given in Table 6.1.

Lipid vectors are generally considered to enter cells via the endocytic system (Nguyen & Szoka, 2012; Juliano, Ming & Nakagawa, 2012). Basha *et al*. compared the effectiveness of a number of cationic lipid formulations, and used fluorescently-labelled siRNA to observe endocytic uptake of lipid-siRNA complexes and their escape
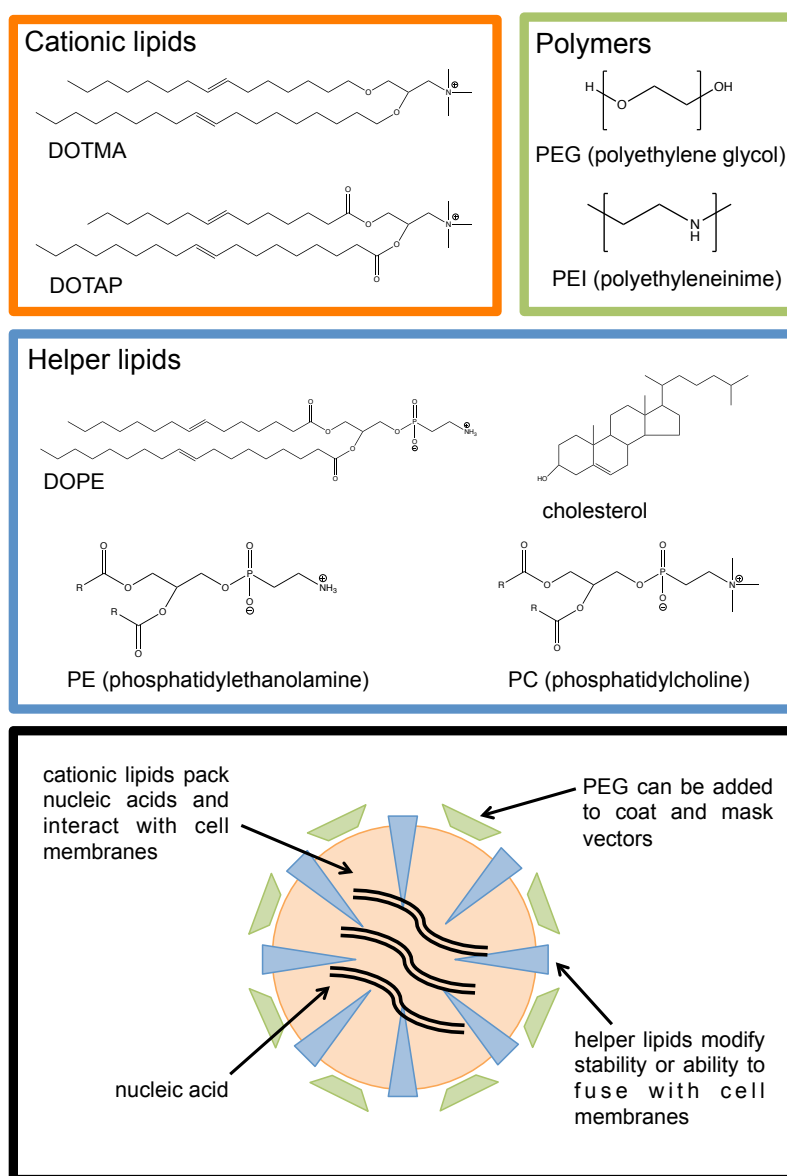


**Figure 6.1 Components of lipid and polymer vectors**
Examples of some components of lipid and polymer vectors. Structures show common cationic lipids, polymers and helper lipids used in producing nucleic acid vectors, alongside a representation of some of their functions in vectors.

to the cytoplasm in bone marrow macrophages and dendritic cells (Basha *et al.*, 2011). Initially, all of their lipid-siRNA formulations were taken up into endocytic vesicles, shown by colocalisation with EEA1, and over time they observed different degrees of retention in the endocytic system or escape to the cytoplasm, depending on the lipids used (Basha *et al.*, 2011). Both Sahay *et al.* and Zephati *et al.* used labelled lipid nanoparticles to observe colocalisation with endocytic and lysosomal markers, and showed that inhibiting the endocytic system altered vector trafficking and siRNA delivery (Zelphati & Szoka, 1996a; Sahay *et al.*, 2013). Labelled phosphatidylethyleneimine (PEI) : DNA complexes also colocalise with endocytic and lysosomal markers when tracked in cells (Godbey, Wu & Mikos, 1999; Suh *et al.*, 2012). Interestingly, a study using an older lipid vector formulation, DharmaFECT1, also showed that lipid-siRNA complexes were present in the endocytic system and that inhibiting clathrin-mediated endocytosis prevented their uptake, but in this case siRNA delivery was not affected (Lu, Langer & Chen, 2009). They propose that for this vector, siRNA can enter the cell via vector fusion with the plasma membrane, either primarily or as an additional route alongside endocytosis. This agrees with the first report of a cationic lipid vector for DNA (Felgner *et al.*, 1987), where a fluorescent version of their DOTMA:phosphatidylethanolamine lipid vector mixture was shown to bind to and distribute through cell membranes. An alternative mixture containing phosphatidylcholine, not tested for DNA delivery, instead produced punctate fluorescence in cells, suggesting loading into endocytic vesicles and demonstrating the effect of changing vector composition on activity (Felgner *et al.*, 1987). It is possible that some types of lipid vector enter cells via fusion with the plasma membrane, whereas those developed more recently make greater use of the endocytic system.

There are two models for how lipid vectors disrupt endocytic vesicles to deliver nucleic acids to the cytoplasm (Nguyen & Szoka, 2012; Juliano, Ming & Nakagawa, 2012). The first involves interactions between lipid vectors and cell membranes (particularly endosomal membranes) (Nguyen & Szoka, 2012; Juliano, Ming & Nakagawa, 2012; Basha *et al.*, 2011). The fusion, lipid mixing and membrane curvature events destabilise both the vector particles, promoting release of nucleic acid from the complex, and the endosomal membrane, allowing it to escape to the cytoplasm. This is largely based on studies of membrane biophysics and stability (Xu & Szoka, 1996;

Hafez, Maurer & Cullis, 2001; Zelphati & Szoka, 1996b; Dabkowska *et al.*, 2012b; Blumenthal *et al.*, 2003), though there is also evidence of the importance of these properties for vector function in cells (Zelphati & Szoka, 1996a). The second model is that materials in the vector act as buffers in the low pH of the late endocytic system, inducing osmotic swelling and lysis of the endocytic vesicle (Nguyen & Szoka, 2012; Juliano, Ming & Nakagawa, 2012; Sonawane, Szoka & Verkman, 2003). This has been demonstrated as an effect of polyamine polymers (including PEI) used as delivery vectors (Sonawane, Szoka & Verkman, 2003; Haensler & Szoka, 1993; Tang, Redemann & Szoka, 1996).

| Vector | Supplier | Composition |
|---|---|---|
| **Lipofectamine** | Invitrogen | cationic liposome (supplier description) |
| **Lipofectamine 3000** | Invitrogen | lipid nanoparticle (supplier description) |
| **INTERFERin** | Polyplus | no supplier description |
| **JetPEI** | Polyplus | polyethylenimine (PEI) polymer (supplier description) |
| **FuGENE HD** | Promega | non-liposomal mix of 'lipids and other components' (supplier description) |
| **ViaFect** | Promega | no supplier description |
| **TurboFect** | Thermo | cationic polymer mix (supplier description) |

**Table 6.1 Composition of vectors used in this chapter**

*6.1.4.2 Altered cellular function affects vector efficiency*

Altered endocytic function affects the efficiency of vectors, with different effects depending on vector formulation. Inhibition of endocytosis by reducing temperature or by inhibiting energy production, actin, or endosomal fusion blocked delivery of nucleic acids by DOTAP-based vectors (despite vectors still being able to bind to the plasma membrane), whereas preventing acidification or late endosomal trafficking did not (Zelphati & Szoka, 1996a). In contrast, Sahay *et al.* found that uptake and siRNA delivery by vectors composed of a different cationic lipid was reduced by inhibiting acidification (Sahay *et al.*, 2013), and a group using peptide-modified liposomes showed that uptake was reduced but not abolished by reducing temperature (Iwasa *et al.*, 2006). Association with apolipoprotein E (ApoE) and the low-density lipoprotein (LDL) receptor has been shown to improve uptake of formulations of ionisable but not cationic lipid vectors (Akinc *et al.*, 2010). Inhibiting NPC1, either by using small molecule inhibitors or NPC1-null cells, blocks endocytic trafficking, and this has also been shown to have differential effects on lipid vectors. Loss of NPC1 function

increases retention and effectiveness of the lipid vectors used by Sahay *et al.* (Sahay *et al.*, 2013) and Wang *et al.*, (Wang *et al.*, 2016) but inhibits uptake and delivery of the polyamine polymers used by Eltoukhy *et al.* and has little effect on JetPEI (a different polymer) and Lipofectamine 2000 (a proprietary lipid formulation) (Eltoukhy *et al.*, 2014).

This variability indicates that while the endocytic system is the main route of entry, there are a wide variety of strategies and mechanisms at use within this pathway. Different vectors are likely to escape the endocytic system at different stages, controlled by the changes in lipid composition and pH of endocytic vesicles as they mature. Vectors will also be affected differently by degradation if they reach the late endosome and lysosome, with some becoming inactive and others requiring destabilisation to release nucleic acid. Different materials will also be differently targeted for degradation, recycling or exocytosis, affecting their localisation and time spent within the cell, and the balance of these pathways will be altered by changes to cellular function such as those used above.

### 6.1.4.3 Lipid vectors may affect cellular function

As lipid vectors enter cells via the endocytic system and are affected by its function, it would be beneficial for them to be able to modulate endocytic function. It is likely that some vectors do include materials that have these effects (Sahay *et al.*, 2013; Zelphati & Szoka, 1996a; 1996b; Xu & Szoka, 1996; Nguyen & Szoka, 2012; Zhang, Zhi & Huang, 2012; Zatsepin, Kotelevtsev & Koteliansky, 2016). While this is useful for increasing their effectiveness, it is a concern when using these vectors for studying the endosomal-lysosomal system. As in other fields of cell biology, genetic modification and RNAi are useful tools for studying lysosomes, but lipid vectors could potentially produce side effects and artefacts, or alter the background behaviour of the system we aim to study. Pryor has shown that several lipid vectors, used to transfect GFP into cells, increase size and aggregation of lysosomes to different extents (Pryor, 2012). However, as these findings have not been investigated further and may be relevant to endosomal and lysosomal research, we aim to investigate further here.

## 6.1.5 Aims

We aim to investigate whether lipid vectors alone affect endocytic and lysosomal function, and identify any phenotypes they produce. We are particularly interested in

phospholipidosis, a common side effect of drugs which traffic to the lysosome, and in the lipid storage phenotypes we study in lysosomal disease research.

## 6.2 Results

### 6.2.1 Treatment with lipid vectors alone alters lysosomal function

To screen for vectors that affect lysosomal function, we used a Lysotracker plate assay (Chapter 2.2 and 2.4). Higher fluorescence values indicate an increase in the number or size of lysosomes, which is indicative of a problem with lysosomal function (Vruchte *et al.*, 2014). We treated CHO-H1 cells with a panel of lipid-based vectors, using the manufacturer's recommended protocols and concentrations (as described in Chapter 2.2). Cells were treated with these vectors alone for either 24 or 72 hours, with no genetic material included (Figure 6.2).

At 24 hours, INTERFERin treatment leads to a significant ($p < 0.01$) increase in Lysotracker fluorescence compared to untreated cells. No other vector had a significant effect on Lysotracker, although treatment with TurboFect and JetPEI had a trend towards lower Lysotracker fluorescence. Observation of the cells and preliminary cell death data (not shown) suggests that these two vectors cause some cell toxicity, which may account for the reduction in fluorescence in these treatments.

After 72 hour treatment, both FuGENE HD and Lipofectamine treated cells are significantly higher than control ($p < 0.01$ and $p < 0.001$ respectively). INTERFERin no longer causes a significant increase in average fluorescence, although there are a group of replicates within the data set that are considerably higher than control. The other vectors - JetPEI, TurboFect and ViaFect - do not alter average fluorescence after 72 hours (Figure 6.2).

Based on these data, we selected INTERFERin and FuGENE HD for further characterisation, and the Lipofectamine family of lipid-based vectors for some experiments. INTERFERin will be used at 24 hours and the others at 72 hours. We also selected JetPEI and ViaFect as controls which do not appear to alter lysosomal function, to be used at both time points.
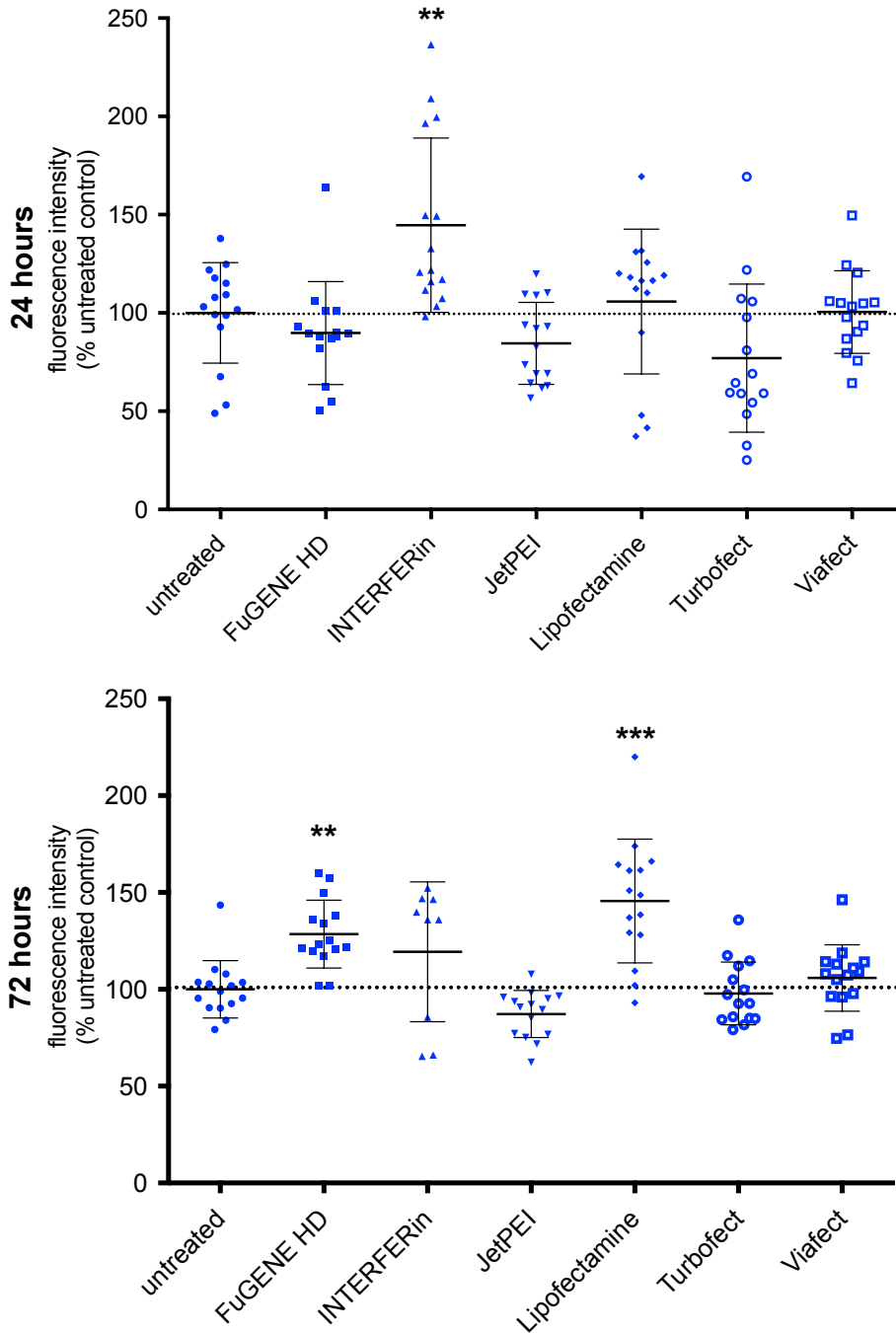
**Figure 6.2 Effect of vectors on lysosomes**

CHO-H1 cells were treated with lipid vectors according to manufacturer's protocols for either 24 or 72 hr, then stained with Lysotracker Green and fluorescence levels were measured. Lysotracker fluorescence is presented as percentage of the untreated control, which was set as 100%. Red symbols indicate individual replicates, horizontal black bars indicate the mean, error bars indicate standard error of the mean, and the horizontal red line marks the mean lysotracker intensity in untreated cells to aid comparison. n = 3 independent experiments with at least 3 replicate wells per condition in each. Significance was calculated using one-way ANOVA and Dunnett's multiple comparison test. * $p < 0.05$, ** $p < 0.01$, *** $p < 0.001$. Experiments performed and analysed by Mr. Ravin Shrestha.

To confirm the results obtained from the fluorescence assay, we also imaged Lysotracker-stained cells after 24 and 72 hour vector treatments (Figure 6.3 and Figure 6.4). 24 hour INTERFERin treatment produces significantly brighter puncta, and also in some cases larger puncta than are present in the control (Figure 6.3), though there is considerable variability. FuGENE HD treatment after 72 hours also produces a slight but significant increase in Lysotracker staining compared to untreated control cells (Figure 6.4). JetPEI and ViaFect at both time points do not produce obvious total changes from control, but there may be a greater variability in Lysotracker staining, or possibly clustering of lysosomes in some cells within these treated populations than there is in the untreated cells (Figure 6.4).
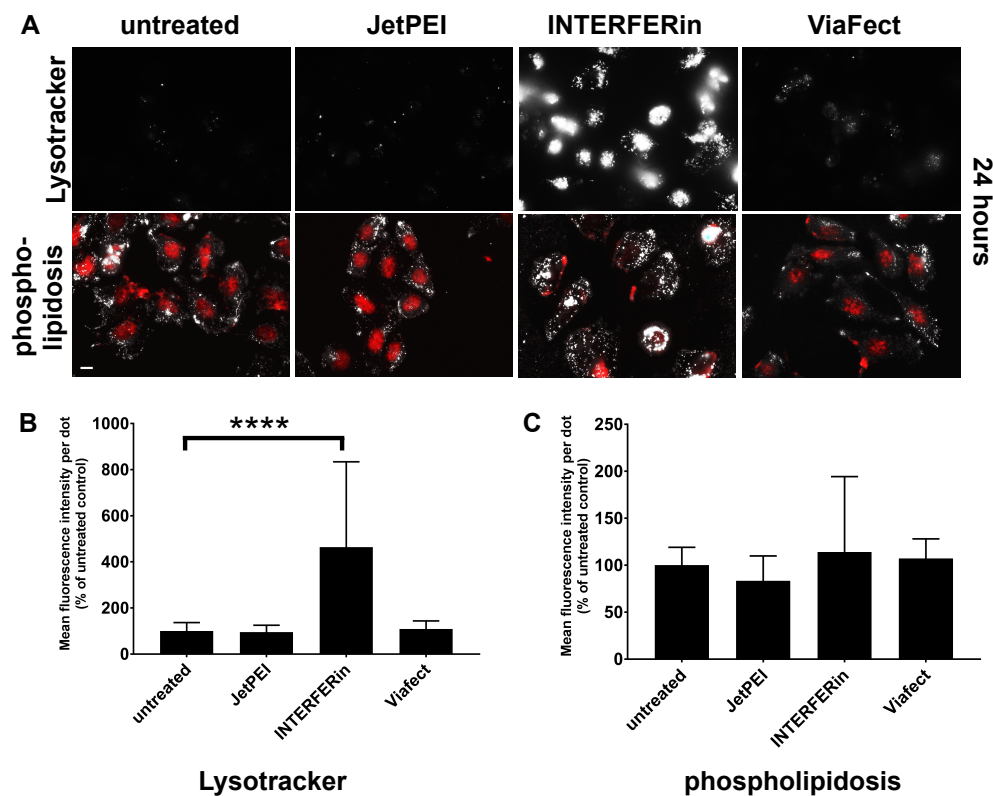


**Figure 6.3 INTERFERin affects lysosomal function after 24 hour treatment**
CHO-H1 cells were treated with lipid vectors according to manufacturer's protocols for 24 hr, then stained with either Lysotracker Green or LipidTox Red phospholipidosis detection reagent and imaged. n = 3 for both probes. **A** Representative images of treated CHO-H1 cells stained with either Lysotracker Green or LipidTox Red. Scale bar = 5 μm. **B** Mean fluorescence intensity of Lysotracker-stained dots in treated CHO-H1 cells, presented as percentage of untreated control. **C** Mean fluorescence intensity of LipidTox-stained dots in treated CHO-H1 cells, presented as percentage of untreated control. Error bars represent standard deviation. **** $p < 0.0001$ by one-way ANOVA and Dunnett's multiple comparison test. Experiments performed partially by Mr. Ravin Shrestha.

Phospholipidosis, the accumulation of phospholipid in the lysosome, is a form of lysosomal dysfunction which can be caused by loss of lysosomal phospholipase function (Hiraoka *et al.*, 2006) or as a side effect of various drugs (Halliwell, 1997). To test whether this is present in the cells treated with lipid-based vectors, we stained cells with LipidTox Red Phospholipid Detection Reagent and imaged them (Figure 6.3 and Figure 6.4). INTERFERin at 24 hours and FuGENE HD at 72 hours both cause an increase in LipidTox Red staining compared to control, an effect which is significant
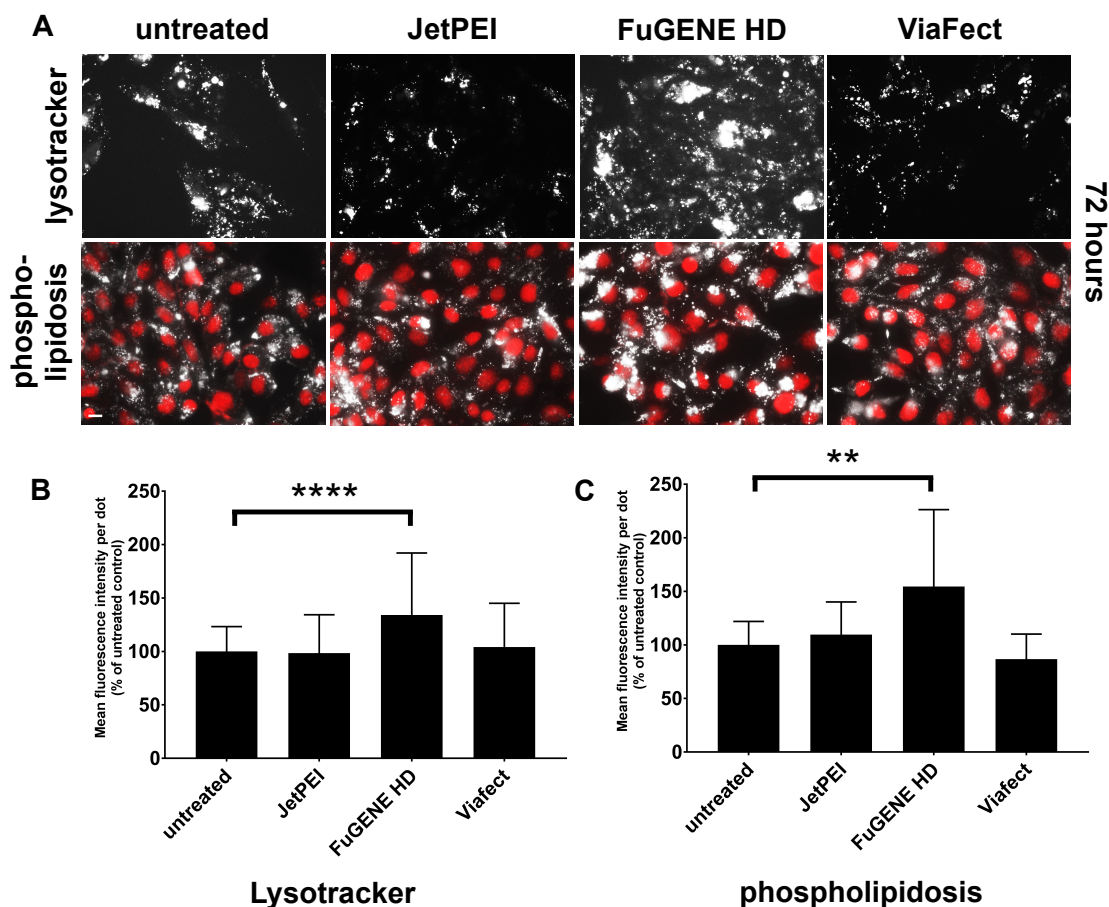


**Figure 6.4 FuGENE HD affects lysosomal function after 72 hour treatment**
CHO-H1 cells were treated with lipid vectors according to manufacturer's protocols for 72 hr, then stained with either Lysotracker Green or LipidTox Red phospholipidosis detection reagent. n = 3 for both probes. **A** Representative images of treated CHO-H1 cells stained with either Lysotracker Green or LipidTox Red. Scale bar = 5 µm. **B** Mean fluorescence intensity of Lysotracker-stained dots in treated CHO-H1 cells, presented as percentage of untreated control. **C** Mean fluorescence intensity of LipidTox-stained dots in treated CHO-H1 cells, presented as percentage of untreated control. Error bars represent standard deviation. ** $p < 0.01$ **** $p < 0.0001$ by one-way ANOVA and Dunnett's multiple comparison test . Experiments performed partially by Mr. Ravin Shrestha.

after FuGENE HD treatment but not significant and considerably variable after INTERFERin treatment. INTERFERin treated cells have larger, distinct bright peripheral punctae, and FuGENE HD treated cells have bright, dense clusters of staining, possibly the endocytic recycling compartment, and bright puncta in the periphery. JetPEI and ViaFect have no significant effect. Treatment with INTERFERin and FuGENE HD therefore seems to be inducing phospholipidosis, whereas JetPEI and ViaFect are not.

## 6.2.2 Some lipid vectors affect cellular lipid distribution

Due to the presence of phospholipidosis and the interaction with lipid storage seen by Sahay *et al.* (Sahay *et al.*, 2013; Eltoukhy *et al.*, 2014), we also wanted to look at what happens to other cellular lipids after treatment with lipid-based vectors. We chose LBPA, a lipid found only in the late endosome and lysosome, which is both a useful specific marker and functionally important in this compartment (Kobayashi *et al.*, 1999), and cholesterol, as storage of cholesterol is a phenotype we are interested in for our work on lysosomal diseases and Huntington's disease, and because it is a lipid that has a large effect on membrane properties and may be a component in lipid-based vectors (Zatsepin, Kotelevtsev & Koteliansky, 2016; Dabkowska *et al.*, 2012b). Specific, reliable probes are available for both these lipids (Bergy & Eble, 1968; Kobayashi *et al.*, 1999).

Cells treated with FuGENE HD for 72 hours have higher levels of LBPA staining and larger puncta than untreated cells (Figure 6.6). In initial tests, Lipofectamine 3000, the most recent version of the Lipofectamine family of vectors, also causes an overall increase in LBPA staining after 72 hours, and 24 hour treatment with INTERFERin increases LBPA staining in cells, producing bright, dense clusters of staining (Figure 6.5). The two control vectors, JetPEI and ViaFect, cause slight increases in LBPA staining at 72 hours and potentially at 24 hours, where there are a small proportion of cells with high LBPA staining after ViaFect treatment (Figure 6.5 and Figure 6.6).

We also stained treated cells for cholesterol. In a single test at 24 hours (Figure 6.5), INTERFERin induces an increase in cholesterol, and blebbing (membrane protrusion) is visible in a number of cells, possibly indicating toxicity (Charras, 2008). In the cells that are not affected by toxicity, there is still an increase in cholesterol compared to control, and punctate staining of cholesterol is present indicating lipid storage bodies.

ViaFect and, largely, JetPEI do not alter levels of cholesterol, although there may be cholesterol accumulation in a subset of cells after JetPEI treatment, an effect which requires further validation. At 72 hours (Figure 6.6), neither JetPEI, Viafect or FuGENE HD lead to increased cholesterol. Initial tests of Lipofectamine treatment indicate that it causes considerable accumulation of cholesterol compared to control, and an increased perinuclear localisation. There is some initial evidence (not shown) to suggest that Lipofectamine 3000 may induce punctate distribution of cholesterol, although it has less of an effect on overall cholesterol levels.
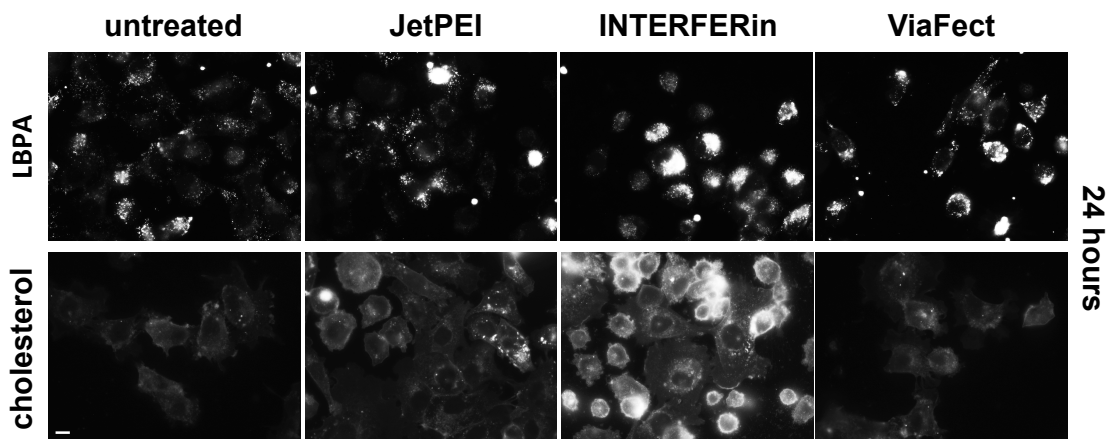


**Figure 6.5 24 hour treatment with INTERFERin increases cellular lipid levels**
CHO-H1 cells were treated with lipid-based vectors according to manufacturer's protocols for 24 hr, then stained for either LBPA (using a specific antibody) or cholesterol (using filipin). n = 1 for both probes. Scale bar = 5 μm.
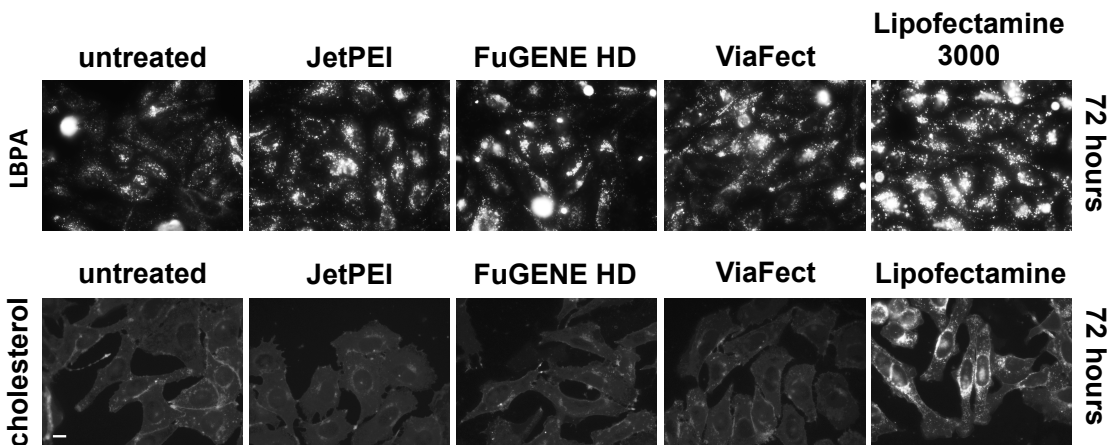


**Figure 6.6 The Lipofectamine family of lipid-based vectors alter cellular lipids**
CHO-H1 cells were treated with lipid-based vectors according to manufacturer's protocols for 72 hr, then stained for either LBPA (using a specific antibody) or cholesterol (using filipin). n = 3 for both probes, except for Lipofectamine and Lipofectamine 3000 treatments where n = 1. Scale bar = 5 μm. Experiments performed partially by Mr. Ravin Shrestha.

### 6.2.3 Lipid vectors alter levels of endocytic and lysosomal proteins

Due to our interest in NPC disease and the interactions observed by Sahay *et al.* (Sahay *et al.*, 2013; Eltoukhy *et al.*, 2014), we also looked at whether the vectors altered NPC1, a lysosomal transmembrane protein involved in endocytic trafficking and lipid recycling (Lloyd-Evans *et al.*, 2008). We used cells that had been treated with lipid-based vectors for 72 hours, to allow time for protein synthesis and turnover, and looked for NPC1 via immunocytochemistry (Figure 6.7), although we were only able to perform this experiment once as the NPC1 antibody became unavailable. There were considerable changes to NPC1 after treatment with most of the vectors. JetPEI, FuGENE HD and ViaFect all increase the level of NPC1 staining, though localisation remains finely punctate. Lipofectamine does not cause obvious changes to the level of staining, but the localisation changes to some extent - there is increased clustering around the nucleus and less fine punctate staining in the periphery, compared to the consistent fine punctate staining in the untreated controls.

We also looked at levels of other proteins by Western blot. We have looked at levels of acid sphingomyelinase (ASM), a soluble lysosomal enzyme whose loss of function leads to the LSDs Niemann-Pick A and B, and EEA1 (early endosome antigen 1), an early endosome specific tethering protein, to give us examples from different stages of the endocytic-lysosomal pathway (Figure 6.8). Unfortunately, our established NPC1 antibody became unavailable at this point, so NPC1 levels were not examined. ViaFect, FuGENE HD and Lipofectamine 3000 were used for 72 hour treatments. Both ViaFect and FuGENE HD (in two out of three experiments) reduced the levels of EEA1, though in a third repeat FuGENE HD and Lipofectamine 3000 instead dramatically increased EEA1. In a single experiment, all three vectors reduced the levels of ASM, with FuGENE HD having the greatest effect. Although this is variable and requires further validation, these vectors alone are able to alter levels of proteins across different stages of the endocytic-lysosomal pathway, which is a major change to cells.

### 6.2.4 Lipid vectors alter cellular function

As these vectors largely enter cells via the endocytic system (Sahay, Alakhova & Kabanov, 2010; Duncan & Richardson, 2012), and we have observed alterations in levels of endocytic proteins (see above), we performed an initial test of endocytic
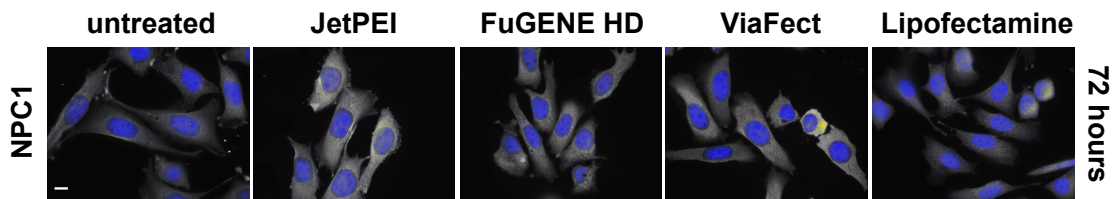
**Figure 6.7 Treatment with lipid-based vectors increases NPC1 in cells**
CHO-H1 cells were treated with lipid-based vectors according to manufacturer's protocols for 72 hr, then stained for NPC1. n = 1. Scale bar = 5 μm. Experiments performed by Mr. Ravin Shrestha.
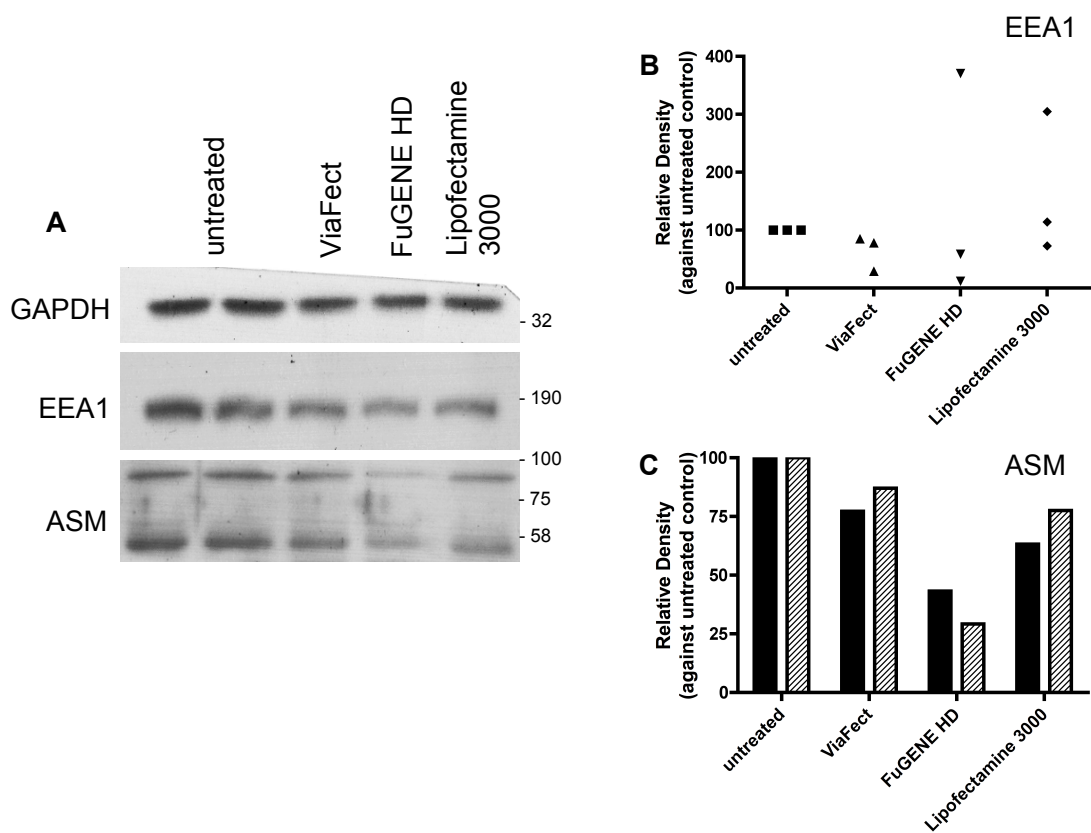


**Figure 6.8 Lipid vectors alter levels of endocytic and lysosomal proteins**
CHO-H1 cells were treated with lipid vectors according to manufacturer's protocols for 72 hr, then levels of lysosomal and endocytic proteins were analysed by Western blot. Density of bands was measured, corrected to GAPDH, then converted to relative density where the untreated control was set as 100%. **A**, representative blot. **B**, quantification of EEA1 levels, separate markers indicate independent repeats, n = 3. **C**, quantification of ASM levels. Black bars are density of the 80 kDa band, and striped bars are the 55 kDa band. n = 1.

function after lipid vector treatment by measuring uptake of HRP by cells (Gu *et al.*, 1997; Lloyd-Evans *et al.*, 2008). CHO-H1 cells treated with lipid vectors were incubated with HRP in fresh growth medium for two hours, then washed extensively to remove plasma membrane bound HRP and cell homogenates were assayed for HRP activity. In this single experiment, all four lipid vectors used increased endocytic uptake after a 72 hour treatment (Figure 6.9). Cells treated with FuGENE HD, INTERFERin and ViaFect contained twice as much HRP as untreated controls, and JetPEI treated cells had a 3.7-fold increase. This increase in internalised HRP suggests increased endocytic uptake of material, or both increased uptake and decreased recycling and removal of endocytosed material.
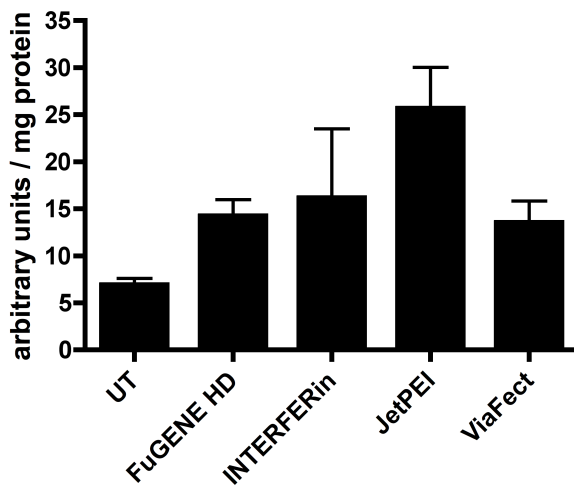


**Figure 6.9 Lipid vectors increase endocytic uptake**
CHO-H1 cells were treated with lipid vectors according to manufacturer's protocols for 72 hr, then endocytosis was assayed by measurement of HRP uptake. HRP activity was corrected against protein level. Bars represent mean HRP uptake and error bars represent standard deviation. Results from one experiment, analysed in triplicate. Experiment partially performed by Mr. Ravin Shrestha.

We also looked at cell survival after treatment with lipid vectors, as this is an important consideration when selecting vectors. We tested apoptotic cell death in cells treated with lipid vector for 72 hour by staining with fluorescent tagged annexin V. This probe binds phosphotidylserine, which only flips to the outer surface of the plasma membrane once the cell commits to apoptosis. Live cells therefore do not label with annexin V, whereas cells committed to apoptosis show surface labelling (Walton

*et al.*, 1997). In this single experiment, 6.8% of untreated CHO-H1 cells had some surface labelling with annexin V (Figure 6.10A). JetPEI treatment did not increase the percentage of apoptotic cells compared to control (4.8%), whereas FuGENE HD and ViaFect both slightly increased apoptotic cell death (13.8% and 16.8% of cells respectively, compared to 6.8%). For comparison, 2 hour treatment with nigericin was used as a positive control, an ionophore which induces cell death via interference with membrane potential, particularly in the mitochondria, and 65.6% of cells in this treatment were apoptotic.
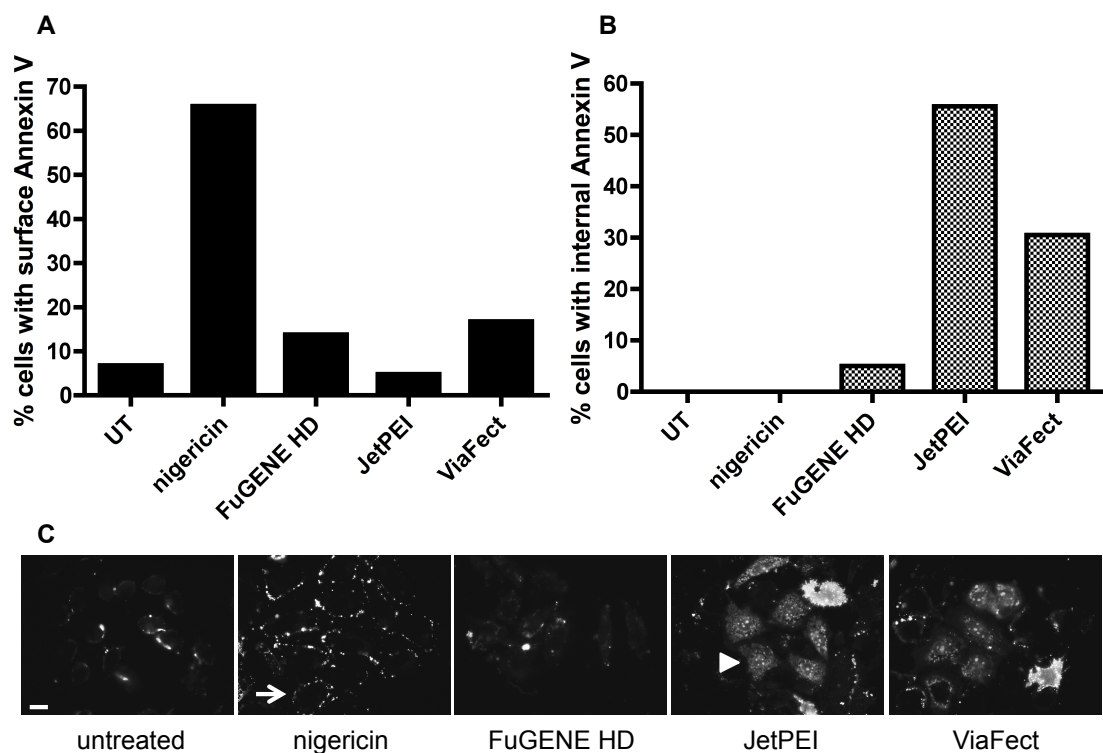


**Figure 6.10 Vectors alter apoptosis and lipid trafficking**
CHO-H1 cells were treated with lipid vectors according to manufacturer's protocols for 72 hr or with nigericin for 2 hr, then labelled with fluorescent-tagged annexin V. Cells were scored for annexin V plasma membrane staining, which indicates commitment to apoptosis. **A** Graph indicates percentage of cells positive for plasma membrane staining with annexin V. **B** Graph indicates percentage of cells positive for internalised annexin V. **C** Images of annexin V assay. Arrow indicates plasma membrane annexin V, arrowhead indicates internalised annexin V. Scale bar = 5 μm. Results from one experiment. Experiment partially performed by Mr. Ravin Shrestha.

This assay is performed below 16°C to suppress endocytosis and so prevent internalisation of the probe, so that it does not bind phosphotidylserine within the cell. However, unexpectedly, CHO-H1 cells treated with lipid vectors all showed some internalisation of annexin V, despite these conditions being sufficient to prevent untreated cells endocytosing the probe (Figure 6.10B). The effect of FuGENE HD treatment was small, but 55.6% of JetPEI treated cells and 30.5% of ViaFect treated cells contained some internalised annexin V, while none at all was observed in the untreated and nigericin (positive control for apoptosis) conditions. While this is a single experiment and requires further validation, this internalisation could suggest an increase in endocytosis in these cells after treatment with lipid vectors, which would agree with the HRP internalisation assay.

## 6.3 Discussion

### 6.3.1 Vectors alone affect lysosomes and cellular lipids

The preliminary work presented here demonstrates that vectors for nucleic acids independently affect endocytic and lysosomal function in cells. Several of the vectors we tested lead to storage of lipids, altered levels of endocytic and lysosomal proteins, and altered endocytic function. These effects are likely to be a direct result of vector design and structure, but are an issue for lysosomal research.

It is worth noting that, to some extent, these vectors form particles by assembling with or around the nucleic acid cargo (Wan, Allen & Cullis, 2014; Zatsepin, Kotelevtsev & Koteliansky, 2016). Using vectors alone, as we have done here, may produce atypical particle structures and sizes, but we feel that these experiments are still informative as initial work before replication in the presence of nucleic acid. The same vector components are being taken up into cells, and these partial or altered particles may well be present in normal use, either due to release of cargo, degradation of cargo-containing particles or a heterogeneous mix of particles forming when the vector and cargo are combined.

It is also important to state that we chose to test these vectors by using them as recommended in the protocols provided by suppliers. We decided not to attempt to standardise the vectors based on measures such as volume of stock solution, amount of material or proportion required for a specified amount of nucleic acid, as we felt

that this would produce an artificial situation which was less relevant to whether they had effects when used in practise in the lab, especially as many research groups will use the vectors as specified by the manufacturer.

The initial Lysotracker screen was used to select vectors which increased lysosomal volume for further characterisation. All three of the vectors which were selected - FuGENE HD, INTERFERin and Lipofectamine - had effects on cells, but these effects varied between vectors.

INTERFERin lives up to its name in our hands, as it increased labelling of lysosomes in the plate reader assay (Figure 6.2) While the cell imaging experiments for INTERFERin are only initial work, it significantly increases Lysotracker in cell imaging (Figure 6.3), may cause some phospholipidosis (lysosomal accumulation of phospholipids), and increases LBPA and cellular cholesterol (Figure 6.5), changes which most likely are the cause of the observed lysosomal expansion. It may also cause an increase in endocytic uptake (Figure 6.9). LBPA elevation has previously been seen in cases of drug-induced phospholipidosis (Mortuza *et al.*, 2003; Nonoyama & Fukuda, 2008), so these effects of INTERFERin may be connected. Interestingly, in the Lysotracker screen INTERFERin causes a significant increase at 24 hours but not after 72 hours, suggesting that either the cell quickly processes INTERFERin particles and recovers, or the change in cell density between the two conditions considerably modifies the effect.

FuGENE HD also significantly increases Lysotracker labelling in both the assay and the imaging experiments, in this case after 72 hours but not 24 (Figure 6.4). This agrees with the previous experiment on this topic by Pryor, which showed that an earlier version of this family, FuGENE 6, also caused an increase in lysosomal volume (Pryor, 2012), although we do not know how closely related the two reagents are. It causes phospholipidosis but has little effect on cholesterol or LBPA (Figure 6.4 and Figure 6.6). LBPA might have been expected to reflect the increased Lysotracker staining more closely, as both of these can be used as markers of the late-endocytic to lysosomal compartment (Kobayashi *et al.*, 1999; Lloyd-Evans *et al.*, 2008), but LBPA is a lipid product found predominantly in late endosomes whereas Lysotracker is a direct measure of lysosomal compartment volume, and these can therefore vary separately. FuGENE HD also induces changes (though these are not consistent) to EEA1, ASM and possibly also to NPC1 (Figure 6.7 and Figure 6.8), work which can now be confirmed

and completed as we have a new, validated, monoclonal NPC1 antibody. FuGENE HD treatment also appears to increase endocytic uptake as seen by uptake of HRP and Annexin V internalisation (Figure 6.9 and Figure 6.10). Though these observations are each from a single experiment, the same effect is seen with both measures, and to a similar extent in both, which suggests it may indeed be the case and certainly warrants further investigation.

We did not use Lipofectamine in all experiments, and we used two different members of the family - Lipofectamine and Lipofectamine 3000, the current formulation - to compare whether the modern version also affects cells. We therefore have obtained limited information on Lipofectamine compared to the other vectors, and only have a single cell imaging experiment for each phenotype. Like FuGENE HD, Lipofectamine increases Lysotracker staining at 72 hours but not at 24 hours (Figure 6.2) and alters EEA1 and possibly ASM levels (Figure 6.8), but unlike FuGENE HD, both Lipofectamine (data not shown) and Lipofectamine 3000 may increase cellular cholesterol (Figure 6.6). The Lipofectamine family are the most widely used vector formulation (or at least highly referenced, with over 2600 references in PubMed compared to 200 or less for FuGENE and JetPEI, and similar proportions in Google Scholar) as they are effective and well known, making these side effects a particular concern.

JetPEI and ViaFect were selected and used as controls for these experiments, as we commonly use JetPEI in the lab and neither caused changes in the initial Lysotracker screen (Figure 6.2). These two vectors do not cause phospholipidosis (Figure 6.3 and Figure 6.4) or increase cellular cholesterol (Figure 6.6) but may cause slight increases in LBPA (Figure 6.5 and Figure 6.6). Preliminary experiments suggest that they may alter the endocytic protein EEA1 and the lysosomal proteins ASM and NPC1 (Figure 6.7 and Figure 6.8), and may increase endocytic uptake. In both the HRP uptake and Annexin V internalisation experiments, JetPEI causes the greatest increase in internalisation (Figure 6.9 and Figure 6.10), and the consistency of the result between the two methods supports the effect even though these results still need validating.

In summary, all of the vectors we used in further testing appeared to affect endocytic proteins and trafficking to some extent, although only some altered lysosomal volume or lipid accumulation. Use of these vectors in research could potentially induce effects which are due to the vector rather than the gene modification performed, affecting

experimental outcomes and interpretation. Potentially - although the lack of information on formulations means this is speculative - the vectors composed of polyamine polymers may increase endocytosis but have fewer other effects on the endocytic and lysosomal system, whereas the lipid vectors may affect cellular lipid levels and localisation. Lipofectamine and FuGENE HD are lipid-based (Table 6.1) but no information is available about the formulation of INTERFERin, and JetPEI and TurboFect, which also did not alter Lysotracker in the initial screen (Figure 6.2), are polymer-based, though we do not know the composition of ViaFect. This may suggest that polymer-based vectors are more suitable for lysosomal research than lipid-based ones, though both still cause certain changes to endocytic function.

## 6.3.2 Vectors alone may affect cellular function

Endocytosis and cellular trafficking are important aspects of cellular function, particularly in lysosomal disease research. Our preliminary HRP uptake assay suggests that several of these vectors increase endocytic uptake, and the Annexin V experiment also supports this possibility. While we saw increases in apoptotic cell death using this method, it is already known that these vectors can affect cell viability to varying degrees. However, the internalisation of the probe despite cooling the cells to reduce endocytosis also suggests an alteration to endocytic and lipid trafficking pathways. While this data is from a single experiment so far the effect is interesting - and consistent between methods - and will need further study. It would also be interesting to investigate whether later stages of endocytic trafficking are altered.

This potential change to endocytosis may also have a bearing on the phospholipidosis data, as the LipidTox probe is a tagged phospholipid which enters the cell by endocytosis. Some of the accumulation seen may therefore be due to altered uptake of the probe rather than a phospholipidosis defect, although JetPEI appears to have the greatest effect on endocytosis in the experiments performed so far and does not have extensive phospholipidosis.

An important pathway which we did not look at here, but which would be interesting to investigate, is whether these vectors affect autophagy. This is another pathway which is altered based on changes to the lysosome and which relies on different but related trafficking routes in the cell, and it is also an important pathway in research into lysosomal function and neurodegenerative disease (Medina *et al.*, 2015; Nixon,

2013; García-Arencibia *et al.*, 2010). If vector treatments alter this pathway, this would be another area of concern where off-target effects and artefacts might be generated in research using these vectors.

### 6.3.3 Effects of vectors are variable

Our results from these experiments showed some variability in vector effects. This variability was present both within experiments (for example, the distribution of results in the initial Lysotracker screen, Figure 6.2), and between experiments (as in the case of the changes to EEA1 protein level, Figure 6.8). This may also have contributed to the different effects of vectors at different time points in the Lysotracker screen, although it is probably not the major component of those changes.

It is common that in siRNA or transfection experiments there is variable or mosaic effect within populations, often with neighbouring cells in the same experiment showing different levels of effect on gene and protein expression. This is why fluorescent labelling of transfected proteins or co-staining for siRNA targets is commonly used, to select cells where nucleic acids have successfully been delivered and protein expression is altered as required for the experiment (Ko *et al.*, 2001; Malathi *et al.*, 2004). There are a number of factors which may affect vector uptake and lead to delivery of nucleic acids to one cell but not another, and it is likely that these have all also contributed to variability in our experiments. Cells may be in different stages of the cell cycle, or have different degrees of expression of endocytic proteins or other relevant factors. Cell density also has an impact, affecting the dosage which each cell receives, and though we maintained the same cell density between treatments there were differences between the two time-points (Chapter 2.2.4).

The differences between time points may also be caused by several factors other than experimental variability. The ability of the cell to traffic and process each of the vectors will differ depending on formulation, and the vectors will also not be stable in cell growth medium for the same length of time. Changes to cell density could also contribute, as fewer cells were seeded for the 72 hour treatment to allow for cell growth during the treatment time. The manufacturer protocols all recommend scaling vector amounts based on cell growth area rather than volume when changing plate types, as the proportion of vector to cells is more important than the concentration of vector in growth medium (see manufacturers' recommendations).

### 6.3.4 Further work

Our main concern with this work is whether these vector-only experiments apply to a situation where vectors are used with cargo present. Vector particles which assemble with cargo present could potentially be quite different in size or structure compared to the particles which form from vector alone. In particular, when using JetPEI in experiments, we have sometimes observed that cell death is higher in the vector-alone control than in either the scramble or experimental siRNA conditions. As stated above, unformed particles and degradation products could mean the same components will be present regardless of whether cargo is included, but we could test this by including a nucleic acid cargo - either a scrambled siRNA control, or if we wished to track whether cells have taken up vector, a fluorescently-tagged siRNA (Basha *et al.*, 2011; Suh *et al.*, 2012) or an expression construct for a fluorescent protein (Malathi *et al.*, 2004). We could also combine this with an siRNA or correction experiment, for example expressing GFP-tagged NPC1 in NPC1 disease cells using different vectors, to compare the data obtained and determine whether effects of the vector alter experimental outcomes. There are also methods for measuring size and structure of nanoparticles (Mukherjee, Ray & Thakur, 2009) which could confirm whether the particles are altered.

The second question which remains is whether use of these vectors changes the background of a cell model enough to affect an experiment even if controls are included to allow obvious side effects to be discounted. As an example, the higher lipid load which has to be cleared as a result of treatment with a vector such as Lipofectamine could make a cell more susceptible to developing storage phenotypes if expression of a protein was suppressed, or enhanced endocytosis could alter trafficking or colocalisation of markers such as labelled dextrans. This question is difficult to test, and does not invalidate the use of these vectors for this type of research, but is a possible limitation which should be considered as it has the potential to affect the interpretation of data obtained when using these vectors.

### 6.3.5 Understanding the mechanisms of vectors is useful

What we have observed here as the negative (for our purposes) side effects of these type of vectors are likely to be a direct result of what they are designed to do. These effects are likely to be contributing factors in making them more effective at delivering

nucleic acids to the cell - increased endocytosis would increase vector uptake, and lipid storage and reduced recycling would increase the effectiveness of formulations which are better able to deliver nucleic acids if cell trafficking is blocked or slowed (Sahay *et al.*, 2013; Wang *et al.*, 2016). The Lipofectamine vectors we used are an interesting case in this respect. They are widely used as they have a reputation for being an efficient vector with comparatively low toxicity, but are one of the vectors which we observed causing considerable side effects.

On the other hand, some of these effects are likely to be purely incidental and not benefit vector function. The cationic lipids and polymers used in vector formulations will generally fall into a class of molecule known as cationic amphiphilic drugs (CADs), molecules with both a charged amine group and a hydrophobic component (Halliwell, 1997). These are known to end up in the lysosome in cells and interfere with phospholipid degradation, leading to phospholipidosis (Halliwell, 1997; Anderson & Borlak, 2006), which was seen in response to several of the vector treatments we used here. Lipid accumulation could also be a result of build-up of components from the vector once nucleic acid has been delivered. These side effects may be possible to avoid by careful vector selection, whereas effects which contribute to vector function would be more difficult to remove.

Our aim was to investigate the side effects of these vectors rather than the mechanisms by which they are acting, but it is interesting to consider how the delivery mechanisms involve and interact with endocytic and lysosomal function, and further research into this question remains valuable (Sahay *et al.*, 2013; Eltoukhy *et al.*, 2014; Duncan & Richardson, 2012). Lysosomal phenotypes and assays of endocytic function are potentially useful approaches for those who are trying to investigate or develop vector mechanisms, as they could provide additional tools or targets.

Effects that are a problem when these vectors are used as research tools could be either problematic or beneficial when developing delivery methods for therapies. This will vary depending on the specific application in question. For example, inducing further lipid storage in a storage disease would be a cause for concern, but would be a benefit in other cases if it helps the vector deliver the cargo. Increases in endocytic proteins or increased trafficking could in themselves be beneficial in some diseases in addition to the therapy being delivered, so combining vectors which have these effects

with relevant therapies could be very useful. Unfortunately, due to time constraints, we were unable to test this in HD or NPC cell models, but it would be interesting to see what effect a vector which increased NPC1 (Figure 6.7) had on cells with a partial NPC1 defect such as HD cells, NPC1 heterozygote cells, or NPC patient cells with trafficking rather than functional mutations, which benefit from NPC1 overexpression (Gelsthorpe *et al.*, 2008).

### 6.3.6 Conclusions

In conclusion, lipid and polymer vectors have wide-ranging effects on the endocytic and lysosomal system. While we still need to confirm whether these effects are altered when nucleic acids are also present in the mixture, and would be interested in looking at how the changes induced by vectors interact with cellular defects including lipid storage in HD, it is clear that these types of vectors could cause problems when used to study endocytic or lysosomal function or role in disease. They are still useful - and the polymer-based formulations may be more useful than the lipid-based ones - but are not ideal. Better understanding of these side effects can tell us what to avoid, and hopefully help develop better nucleic acid vectors for research and therapeutic use.

# CHAPTER 7 DISCUSSION AND CONCLUSIONS

In this thesis, we have investigated the lysosomal expansion and lipid defects seen in HD models, and identified NPC-like lysosomal storage disease defects which may contribute to HD pathogenesis. While some of the work presented here is only preliminary, we have characterised lysosomal defects which are consistent across several cell models of HD, and have tested an NPC therapy, miglustat, which we have found is beneficial in HD models.

## 7.1 NPC-like defects are part of HD pathogenesis

There is lipid storage and lysosomal dysfunction in HD cells which is likely to be a component of or a contributor to HD pathogenesis. In our work, we have observed lysosomal accumulation of cholesterol and ganglioside GM1, elevation of LBPA and lysosomal volume, and accumulation of sphingomyelin in some models, matching previous reports of lysosomal expansion (Castiglioni *et al.*, 2012; Camnasio *et al.*, 2012). Total levels of lipids increase in some models and by some methods while others are unchanged, leaving us with a less consistent answer to this question, though in general there is elevation of the lipids stored in NPC. It would be useful to test our lipids of interest further in animal models or patient samples, but existing reports of lipid levels in HD are also variable(Valenza *et al.*, 2010; Trushina *et al.*, 2006), and absolute increases in lipid are not seen in all cases in LSDs (Lloyd-Evans & Platt, 2010).

We also observed an NPC-like block in late endosomal-lysosomal lipid trafficking in HD cell models. While this characteristic NPC defect is present, other aspects of cellular trafficking such as endocytic uptake are affected differently in HD than in NPC (Li *et al.*, 2009; Akbergenova & Littleton, 2017; Mayran, Parton & Gruenberg, 2003), demonstrating that NPC-like dysfunction may contribute to cellular dysfunction in HD but will also interact with other components of HD pathogenesis. This is the clearest example in this thesis of the differences between loss of NPC1 in NPC and altered function when it is affected by huntingtin mutation instead. Reduced lysosomal $Ca^{2+}$ signalling, another NPC defect, is also present as one part of global $Ca^{2+}$ dysfunction in HD, where $Ca^{2+}$ signalling at the mitochondria, ER and cell surface are all also altered (Giacomello *et al.*, 2013). As lysosomal $Ca^{2+}$ signalling can modulate global $Ca^{2+}$ (López

Sanjurjo *et al.*, 2013; López Sanjurjo, Tovey & Taylor, 2014; Penny *et al.*, 2015), it is possible that this defect could contribute to or exacerbate other $Ca^{2+}$ signalling issues in HD.

There are two questions remaining for future work, which we have limited preliminary data on. First, we would like to confirm that lysosomal storage phenotypes are present in tissues from mouse models, or if possible, patient tissues. While there is existing data on cholesterol and gangliosides (Valenza *et al.*, 2010; Maglione *et al.*, 2010), we would like to confirm whether other NPC storage lipids are altered, and if possible investigate whether localisation is affected in the brains of these mouse models, which Dr. Haslett *et al.* have seen may be the case. We would also like to confirm whether sphingosine, a key lipid affected in NPC (Lloyd-Evans *et al.*, 2008), is altered in these tissues, as trafficking may be inhibited in the one cell model that has been tested (Dr. Haslett, Mr. Badell-Grau).

## 7.2 The lysosomal protein NPC1 interacts with huntingtin

The presence of NPC-like phenotypes, along with some preliminary evidence presented here (Chapter 4), suggests that NPC1 is dysfunctional in HD. The presence of NPC phenotypes could also suggest that NPC2 is involved, but our work and existing evidence (Neueder & Bates, 2014) indicate that NPC2 is elevated, making it less likely to be the origin of the phenotypes in HD. The changes to NPC2 may instead be a result of lysosomal expansion or NPC1 dysfunction, or a cellular response to altered cholesterol balance, and could be of interest as a potential biomarker in HD.

The direct interaction between NPC1 and huntingtin which we observed in co-immunoprecipitation experiments suggests that NPC1 function will be disrupted in the presence of mutant huntingtin, leading to the lipid storage and other lysosomal dysfunction observed in these cells. This interaction needs to be confirmed by both further validation of NPC1 binding to huntingtin, and completion of the colocalisation experiments. Investigating NPC1 localisation and function in huntingtin null cells, and comparing whether mutant and control huntingtin both co-immunoprecipitate if NPC1 is pulled down, may also give us some interesting insight into whether this disruption of NPC1 function occurs due to protein aggregation, the gain-of-function aspect of HD

pathogenesis, or due to loss of a normal huntingtin function relating to protein trafficking or other aspects of lysosomal activity.

## 7.3 Miglustat is beneficial in HD models

Identification of these defects has allowed us to test the NPC therapy miglustat in HD models, and we have found that this is beneficial in the models we have used so far. In HD patient iPSC-derived cell lines, a useful model for testing therapies due to their relevance to disease cases (Kaye & Finkbeiner, 2013; Zhang *et al.*, 2015b), miglustat produced improvements in trafficking and lysosomal $Ca^{2+}$ signalling, though further data on survival and cellular $Ca^{2+}$ dysfunction would be interesting to support our existing observations (here and by Dr. Luke Haslett).

Our tests of miglustat in the *Drosophila melanogaster* model of HD were partially successful, with slight but mostly non-significant improvements in climbing ability. This could have benefited from further work to identify optimal conditions and concentrations for miglustat treatment, and would be strengthened by repeats of the experiment to increase the numbers of flies used, but suggests this model can be used for these tests despite important differences in factors such as lipid metabolism between flies and mammals.

## 7.4 Nucleic acid vectors affect the lysosome

We and others commonly use siRNA delivery vectors in researching lysosomal disease, including work done by others in the lab on this HD project, and RNA interference and other related methods are potential therapies for these diseases. Liposomal and polymer-based vectors enter the cell via the endocytic system, and we wished to look at whether the activity of these vectors would cause side effects which would interfere with research outcomes. While this data is preliminary as we focused on the vectors alone rather than with nucleic acid cargos, the results were interesting. Several of the vectors we used caused lysosomal expansion or phospholipidosis, and altered endocytic function.

The effects we have observed suggest that lipid- and polymer-based vectors could indeed have negative effects on interpretation of research, although as other research has shown (Eltoukhy *et al.*, 2014), some of these effects will be beneficial for vector

efficiency in both research and therapeutic applications. To complete this work, several of the assays need repeating with nucleic acid included, to confirm whether this alters the vector structures and their effects, or whether the side effects we have observed are still present. This will also provide an opportunity to perform some further interesting experiments; potentially, labelled nucleic acids could be used to compare the localisation of the vectors with the observed side effects, or we could perform protein expression or knockdown studies with a range of vectors and determine whether artefacts are present when using those which cause side effects in the experiments presented here.

## 7.5 Limitations

While punctate mislocalisation of lipids is consistently present in these HD models, our data on lipid levels in HD, like the existing literature (Valenza *et al.*, 2010; Del Toro *et al.*, 2010; Maglione *et al.*, 2010), is varied. This may also be the case when biochemical analysis of tissues from mouse models is completed, or patient samples if these can be obtained, though brain sections from the mouse models will still be informative. However, unchanged or decreased absolute lipid levels do not preclude the presence of lysosomal storage, and absolute levels in some LSDs can vary between models and tissues (Lloyd-Evans & Platt, 2010). This discrepancy in HD, with punctate storage but mixed results regarding lipid levels, could be because the lysosomal storage phenotypes are only one component of HD pathogenesis, with effects on lipid metabolism occuring via other pathways. However, there could also be potential connections; signalling via NPC1, which contributes to regulation of mTORC1 by lipids (Castellano *et al.*, 2017), could be altered, or changes to sterol metabolism and levels of sterol precursors could affect NPC1 activity, as observed in SLOS (Waller-Evans *et al.,* unpublished).

The model systems available for HD research also have limitations, as is the case for any disease. HD mouse models are useful, but require extreme CAG repeat lengths to produce symptoms and do not fully recapitulate important features of the disease, such as choreic movements and neuronal death. Small organisms such as *Drosophila melanogaster*, used here, are useful for mechanism studies and have potential as drug

screening models, and the ongoing development of patient iPSC derived cells provides the ability to look at patient defects in relevant cell types.

In particular, the availability of patient cell lines makes it possible to investigate defects present when mutant huntingtin is in the human disease range of 40-50 CAG repeats, which are difficult to investigate otherwise as rodents and other models are not phenotypic in these ranges. We used more severe models in this project, with Q60, Q109 and Q180 CAG repeats, and observed defects in all of them to some degree, though the Q60 models often had only slight phenotypes or phenotypes which were not significant (Chapters 3 and 5). It would be interesting to see whether lysosomal storage defects are detectable in cells with lower CAG repeats, particularly if we were also able to compare this with data from patient tissues.

## 7.6 Huntingtin function

Some of the data obtained in this project supports the theory that huntingtin could have a role in the endocytic and lysosomal system, or be there for a specific purpose. The evidence of direct interaction between NPC1 and the control huntingtin protein indicates that the two proteins may meet and interact during normal cellular function, rather than just under pathogenic conditions with mutant huntingtin present. One possible huntingtin function is in vesicular or endocytic trafficking (Saudou & Humbert, 2016), and in this role it could potentially be involved in trafficking of NPC1 to the lysosome, although the adaptor complexes so far identified as being important for NPC1 transport (Berger *et al.*, 2007) are not known huntingtin interactors .

In agreement with other reports that huntingtin interacts with this compartment (Kegel *et al.*, 2000; Trajkovic, Jeong & Krainc, 2017), we have seen huntingtin (both normal and mutant) in the lysosomal fraction in a purification experiment. We also identified multiple conserved lysosomal targeting signals in huntingtin, matching the motifs which have so far been identified as being involved in trafficking lysosomal membrane proteins through the endocytic system to reach the lysosome (Braulke & Bonifacino, 2009). These signals are also found in the mannose-6-phosphate receptor, which delivers soluble lysosomal proteins to the lysosme via the same route (Braulke & Bonifacino, 2009). While we have not analysed whether these signals are functional in HD, the conservation of these motifs (particularly the C-terminal motifs) and the

multiple reports of huntingtin localisation to the lysosome suggests that they are, and this therefore suggests that huntingtin is in the lysosome for a specific purpose, not just as a stop along a protein degradation pathway. Part of this purpose may have been identified by a recent paper from the Krainc group, which showed that huntingtin is secreted from cells via lysosomal exocytosis (Trajkovic, Jeong & Krainc, 2017), but the possibility that huntingtin could have other roles or be involved in lysosomal protein trafficking is an intriguing one. Our next aim, to investigate this further, would be to look at the structure and composition of lysosomes in huntingtin null cells.

## 7.7 Future directions

The existence of these NPC-like defects in HD provides targets for future work, as there are other potential therapies for NPC, and a number of biomarkers indicative of lysosomal dysfunction. Biomarkers are essential for tracking disease progression, particularly in therapeutic trials. Currently the only markers available for HD are clinical outcome measures (Andre *et al.*, 2014), though brain imaging is being developed, as are a wide range of biochemical markers (Leoni *et al.*, 2008; Byrne & Wild, 2016; Andre *et al.*, 2014) There are many measures of lysosomal dysfunction and lysosomal storage in use or being developed in the lysosomal disease field which may also be useful for Huntington's disease (Vruchte *et al.*, 2014; Cluzeau *et al.*, 2012; Aerts *et al.*, 2008; Bobillo Lobato, Jiménez Hidalgo & Jiménez Jiménez, 2016). As one example, the enzyme chitotriosidase, a lysosomal disease marker (Hollak *et al.*, 1994; Sheth *et al.*, 2010), is also altered in cerebrospinal fluid in HD (Rodrigues *et al.*, 2016).

## 7.8 Lysosomes in disease

Lysosomal dysfunction is a component of a broad range of diseases including neurodegenerative diseases (Maxfield, 2014; Nixon, 2016) and cancer (Kirkegaard & Jäättelä, 2009), via altered lysosomal function, pH or autophagy (Colacurcio & Nixon, 2016; García-Arencibia *et al.*, 2010; Menzies, Fleming & Rubinsztein, 2015). Studying lysosomal storage disorders, which are rare, is important for patients and families who suffer from them, but is also incredibly informative about lysosomal function and dysfunction, and therefore provides knowledge and tools which can be applied in other fields. As is the case in this project, this can help us identify and understand

common mechanisms in other diseases, and suggests potential therapies which can be repurposed or developed for other diseases.

## 7.9 Conclusions

In conclusion, we have characterised lysosomal storage defects in HD pathogenesis, and an interaction between huntingtin and the lysosomal protein NPC1. While aspects of this study remain to be completed, we have shown that the NPC therapy miglustat is beneficial in HD models, and this is to be developed for human trials. This common mechanism may also provide targets for future work and biochemical biomarkers for use in developing therapies for HD.

# References

Abel, K., Anderson, R.A. & Shears, S.B. (2001) Phosphatidylinositol and inositol phosphate metabolism. *Journal of Cell Science*. 114 (Pt 12), pp. 2207–2208.

Acharya, U. & Acharya, J.K. (2005) Enzymes of Sphingolipid metabolism in *Drosophila melanogaster*. *Cellular and Molecular Life Sciences*. 62 (2), pp. 128–142.

Aerts, J.M., van Breemen, M.J., Bussink, A.P., Ghauharali, K., Sprenger, R., Boot, R.G., Groener, J.E., Hollak, C.E., Maas, M., Smit, S., Hoefsloot, H.C., Smilde, A.K., Vissers, J.P., de Jong, S., et al. (2008) Biomarkers for lysosomal storage disorders: identification and application as exemplified by chitotriosidase in Gaucher disease. *Acta paediatrica (Oslo, Norway : 1992)*. 97 (457), pp. 7–14.

Aiuti, A., Biasco, L., Scaramuzza, S., Ferrua, F., Cicalese, M.P., Baricordi, C., Dionisio, F., Calabria, A., Giannelli, S., Castiello, M.C., Bosticardo, M., Evangelio, C., Assanelli, A., Casiraghi, M., et al. (2013) Lentiviral Hematopoietic Stem Cell Gene Therapy in Patients with Wiskott-Aldrich Syndrome. *Science*. 341 (6148), pp. 1233151–1233151.

Akasaki, K., Suenobu, M., Mukaida, M., Michihara, A. & Wada, I. (2010) COOH-terminal isoleucine of lysosome-associated membrane protein-1 is optimal for its efficient targeting to dense secondary lysosomes. *Journal of Biochemistry*. 148 (6), pp. 669–679.

Akbergenova, Y. & Littleton, J.T. (2017) Pathogenic Huntington Alters BMP Signaling and Synaptic Growth through Local Disruptions of Endosomal Compartments. *Journal of Neuroscience*. 37 (12), pp. 3425–3439.

Akinc, A., Querbes, W., De, S., Qin, J., Frank-Kamenetsky, M., Jayaprakash, K.N., Jayaraman, M., Rajeev, K.G., Cantley, W.L., Dorkin, J.R., Butler, J.S., Qin, L., Racie, T., Sprague, A., et al. (2010) Targeted Delivery of RNAi Therapeutics With Endogenous and Exogenous Ligand-Based Mechanisms. *Molecular Therapy*. 18 (7), pp. 1357–1364.

Alam, S., Fedier, A., Kohler, R.S. & Jacob, F. (2015) Glucosylceramide synthase inhibitors differentially affect expression of glycosphingolipids. *Glycobiology*. 25 (4), pp. 351–356.

Alterman, J.F., Hall, L.M., Coles, A.H., Hassler, M.R., Didiot, M.-C., Chase, K., Abraham, J., Sottosanti, E., Johnson, E., Sapp, E., Osborn, M.F., DiFiglia, M., Aronin, N. & Khvorova, A. (2015) Hydrophobically Modifed siRNAs Silence Huntingtin mRNA in Primary Neurons and Mouse Brain. *Molecular Therapy—Nucleic Acids*. pp. 1–12.

Amalfitano, A. & Rastall, D. (2015) Recent advances in gene therapy for lysosomal storage disorders. *The Application of Clinical Genetics*. pp. 157.

Anderson, N. & Borlak, J. (2006) Drug-induced phospholipidosis. *FEBS Letters*. 580 (23), pp. 5533–5540.

Andrade, M.A. & Bork, P. (1995) HEAT repeats in the Huntington's disease protein. *Nature Genetics*. 11 (2), pp. 115–116.

Andre, R., Scahill, R.I., Haider, S. & Tabrizi, S.J. (2014) Biomarker development for Huntington's disease. *Drug Discovery Today*. pp. 1–8.

Arrasate, M. & Finkbeiner, S. (2012) Protein aggregates in Huntington's disease. *Experimental Neurology*. 238 (1), pp. 1–11.

Bano, D., Zanetti, F., Mende, Y. & Nicotera, P. (2011) Neurodegenerative processes in Huntington's disease. *Cell Death and Disease*. 2 (11), pp. e228–7.

Bartholomew, N.R., Burdett, J.M., VandenBrooks, J.M., Quinlan, M.C. & Call, G.B. (2015) Impaired climbing and flight behaviour in *Drosophila melanogaster* following carbon dioxide anaesthesia. *Scientific Reports*. 5pp. 15298.

Basha, G., Novobrantseva, T.I., Rosin, N., Tam, Y.Y.C., Hafez, I.M., Wong, M.K., Sugo, T., Ruda, V.M., Qin, J., Klebanov, B., Ciufolini, M., Akinc, A., Tam, Y.K., Hope, M.J., et al. (2011) Influence of cationic lipid composition on gene silencing properties of lipid nanoparticle formulations of siRNA in antigen-presenting cells. *Molecular Therapy*. 19 (12), pp. 2186–2200.

Baxa, M., Hruska-Plochan, M., Juhas, S., Vodicka, P., Pavlok, A., Juhasova, J., Miyanohara, A., Nejime, T., Klima, J., Macakova, M., Marsala, S., Weiss, A., Kubickova, S., Musilova, P., et al. (2013) A transgenic minipig model of Huntington's Disease. *Journal of Huntington's Disease*. 2 (1), pp. 47–68.

Berg, T.O., Strømhaug, E., Løvdal, T., Seglen, O. & Berg, T. (1994) Use of glycyl-L-phenylalanine 2-naphthylamide, a lysosome-disrupting cathepsin C substrate, to distinguish between lysosomes and prelysosomal endocytic vacuoles. *Biochemical Journal*. 300 ( Pt 1)pp. 229–236.

Bergen, W.G. & Mersmann, H.J. (2005) Comparative aspects of lipid metabolism: impact on contemporary research and use of animal models. *The Journal of Nutrition*. 135 (11), pp. 2499–2502.

Berger, A.C., Salazar, G., Styers, M.L., Newell-Litwa, K.A., Werner, E., Maue, R.A., Corbett, A.H. & Faundez, V. (2007) The subcellular localization of the Niemann-Pick Type C proteins depends on the adaptor complex AP-3. *Journal of Cell Science*. 120 (Pt 20), pp. 3640–3652.

Berggård, T., Linse, S. & James, P. (2007) Methods for the detection and analysis of protein–protein interactions. *PROTEOMICS*. 7 (16), pp. 2833–2842.

Bergy, M.E. & Eble, T.E. (1968) The filipin complex. *Biochemistry*. 7 (2), pp. 653–659.

Bezprozvanny, I. & Hayden, M.R. (2004) Deranged neuronal calcium signaling and Huntington disease. *Biochemical and Biophysical Research Communications*. 322 (4), pp. 1310–1317.

Biffi, A. (2016) Gene therapy for lysosomal storage disorders: a good start. *Human Molecular Genetics*. 25 (R1), pp. R65–R75.

Blom, T., Li, Z., Bittman, R., Somerharju, P. & Ikonen, E. (2012) Tracking Sphingosine Metabolism and Transport in Sphingolipidoses: NPC1 Deficiency as a Test Case. *Traffic*. 13 (9), pp. 1234–1243.

Blom, T.S. (2003) Defective endocytic trafficking of NPC1 and NPC2 underlying infantile Niemann-Pick type C disease. *Human Molecular Genetics*. 12 (3), pp. 257–272.

Blott, E.J. & Griffiths, G.M. (2002) Secretory lysosomes. *Nature Reviews Molecular Cell Biology*. 3 (2), pp. 122–131.

Blumenthal, R., Clague, M.J., Durell, S.R. & Epand, R.M. (2003) Membrane fusion. *Chemical Reviews*. 103 (1), pp. 53–69.

Boadu, E., Nelson, R.C. & Francis, G.A. (2012) ABCA1-dependent mobilization of lysosomal cholesterol requires functional Niemann–Pick C2 but not Niemann–Pick C1 protein. *BBA - Molecular and Cell Biology of Lipids*. 1821 (3), pp. 396–404.

Bobillo Lobato, J., Jiménez Hidalgo, M. & Jiménez Jiménez, L.M. (2016) Biomarkers in Lysosomal Storage Diseases. *Diseases (Basel, Switzerland)*. 4 (4).

Bonelli, R.M., Hödl, A.K., Hofmann, P. & Kapfhammer, H.-P. (2004) Neuroprotection in Huntington's disease: a 2-year study on minocycline. *International Clinical Psychopharmacology*. 19 (6), pp. 337–

342.

Braulke, T. & Bonifacino, J.S. (2009) Sorting of lysosomal proteins. *BBA - Molecular Cell Research*. 1793 (4), pp. 605–614.

Brooks, S.P., Jones, L. & Dunnett, S.B. (2012) Comparative analysis of pathology and behavioural phenotypes in mouse models of Huntington's disease. *Brain Research Bulletin*. 88 (2-3), pp. 81–93.

Brouillet, E. (2014) The 3-NP Model of Striatal Neurodegeneration. *Current Protocols in Neuroscience*. 67pp. 9.48.1–9.48.14.

Burke, K.A., Hensal, K.M., Umbaugh, C.S., Chaibva, M. & Legleiter, J. (2013) Huntingtin disrupts lipid bilayers in a polyQ-length dependent manner. *BBA - Biomembranes*. 1828 (8), pp. 1953–1961.

Byrne, L.M. & Wild, E.J. (2016) Cerebrospinal Fluid Biomarkers for Huntington's Disease. *Journal of Huntington's Disease*. 5 (1), pp. 1–13.

Cai, H., Reinisch, K. & Ferro-Novick, S. (2007) Coats, Tethers, Rabs, and SNAREs Work Together to Mediate the Intracellular Destination of a Transport Vesicle. *Developmental Cell*. 12 (5), pp. 671–682.

Calamini, B., Lo, D.C. & Kaltenbach, L.S. (2013) Experimental models for identifying modifiers of polyglutamine-induced aggregation and neurodegeneration. *Neurotherapeutics*. 10 (3), pp. 400–415.

Camnasio, S., Carri, A.D., Lombardo, A., Grad, I., Mariotti, C., Castucci, A., Rozell, B., Pietro Lo Riso, Castiglioni, V., Zuccato, C., Rochon, C., Takashima, Y., Diaferia, G., Biunno, I., et al. (2012) The first reported generation of several induced pluripotent stem cell lines from homozygous and heterozygous Huntington's disease patients demonstrates mutation related enhanced lysosomal activity. *Neurobiology of Disease*. 46 (1), pp. 41–51.

Campbell, J., Davies, G., Bulone, V. & Henrissat, B. (1998) A classification of nucleotide-diphospho-sugar glycosyltransferases based on amino acid sequence similarities. *Biochemical Journal*. 329 (Pt 3)pp. 719.

Carette, J.E., Raaben, M., Wong, A.C., Herbert, A.S., Obernosterer, G., Mulherkar, N., Kuehne, A.I., Kranzusch, P.J., Griffin, A.M., Ruthel, G., Cin, P.D., Dye, J.M., Whelan, S.P., Chandran, K., et al. (2011) Ebola virus entry requires the cholesterol transporter Niemann–Pick C1. *Nature*. 477 (7364), pp. 340–343.

Carmona-Gutierrez, D., Hughes, A.L., Madeo, F. & Ruckenstuhl, C. (2016) The crucial impact of lysosomes in aging and longevity. *Ageing Research Reviews*. 32pp. 2–12.

Carstea, E.D., Morris, J.A., Coleman, K.G., Loftus, S.K., Zhang, D., Cummings, C., Gu, J., Rosenfeld, M.A., Pavan, W.J., Krizman, D.B., Nagle, J., Polymeropoulos, M.H., Sturley, S.L., Ioannou, Y.A., et al. (1997) Niemann-Pick C1 disease gene: homology to mediators of cholesterol homeostasis. *Science*. 277 (5323), pp. 228–231.

Casaca-Carreira, J., Temel, Y., van Zelst, M. & Jahanshahi, A. (2015) Coexistence of Gait Disturbances and Chorea in Experimental Huntington's Disease. *Behavioural Neurology*. 2015pp. 970204.

Casaca-Carreira, J., Toonen, L.J.A., Evers, M.M., Jahanshahi, A., van-Roon-Mom, W.M.C. & Temel, Y. (2016) In vivo proof-of-concept of removal of the huntingtin caspase cleavage motif-encoding exon 12 approach in the YAC128 mouse model of Huntington. *Biomedicine et Pharmacotherapy*. 84pp. 93–96.

Castellano, B.M., Thelen, A.M., Moldavski, O., Feltes, M., van der Welle, R.E.N., Mydock-McGrane, L.,

Jiang, X., van Eijkeren, R.J., Davis, O.B., Louie, S.M., Perera, R.M., Covey, D.F., Nomura, D.K., Ory, D.S., et al. (2017) Lysosomal cholesterol activates mTORC1 via an SLC38A9-Niemann-Pick C1 signaling complex. *Science*. 355 (6331), pp. 1306–1311.

Castiglioni, V., Onorati, M., Rochon, C. & Cattaneo, E. (2012) Induced pluripotent stem cell lines from Huntington's disease mice undergo neuronal differentiation while showing alterations in the lysosomal pathway. *Neurobiology of Disease*. 46 (1), pp. 30–40.

Cattaneo, E. & Conti, L. (1998) Generation and characterization of embryonic striatal conditionally immortalized ST14A cells. *Journal of Neuroscience Research*. 53 (2), pp. 223–234.

Cattaneo, E., Rigamonti, D., Goffredo, D., Zuccato, C., Squitieri, F. & Sipione, S. (2001) Loss of normal huntingtin function: new developments in Huntington's disease research. *Trends in Neurosciences*. 24 (3), pp. 182–188.

Cattaneo, E., Zuccato, C. & Tartari, M. (2005) Normal huntingtin function: an alternative approach to Huntington's disease. *Nature Reviews Neuroscience*. 6 (12), pp. 919–930.

Caviston, J.P., Zajac, A.L., Tokito, M. & Holzbaur, E.L.F. (2011) Huntingtin coordinates the dynein-mediated dynamic positioning of endosomes and lysosomes. *Molecular Biology of the Cell*. 22 (4), pp. 478–492.

Cenedella, R.J. (2009) Cholesterol Synthesis Inhibitor U18666A and the Role of Sterol Metabolism and Trafficking in Numerous Pathophysiological Processes. *Lipids*. 44 (6), pp. 477–487.

Cesca, F., de Wittenau, G.D., Curcio, F. & Lonigro, R. (2014) Expression of plasma membrane (PMCA) and sarco/endoplasmic reticulum (SERCA) $Ca^{2+}$-ATPase pumps in cellular model of Huntington disease. *The FASEB Journal*.

Chan, A.W.S., Jiang, J., Chen, Y., Li, C., Prucha, M.S., Hu, Y., Chi, T., Moran, S., Rahim, T., Li, S., Li, X., Zola, S.M., Testa, C.M., Mao, H., et al. (2015) Progressive Cognitive Deficit, Motor Impairment and Striatal Pathology in a Transgenic Huntington Disease Monkey Model from Infancy to Adulthood. *PLoS ONE*. 10 (5), pp. e0122335.

Chandler, R.J., Williams, I.M., Gibson, A.L., Davidson, C.D., Incao, A.A., Hubbard, B.T., Porter, F.D., Pavan, W.J. & Venditti, C.P. (2017) Systemic AAV9 gene therapy improves the lifespan of mice with Niemann-Pick disease, type C1. *Human Molecular Genetics*. 26 (1), pp. 52–64.

Charman, M., Kennedy, B.E., Osborne, N. & Karten, B. (2010) MLN64 mediates egress of cholesterol from endosomes to mitochondria in the absence of functional Niemann-Pick Type C1 protein. *The Journal of Lipid Research*. 51 (5), pp. 1023–1034.

Charras, G.T. (2008) A short history of blebbing. *Journal of microscopy*. 231 (3), pp. 466–478.

Chen, F.W., Gordon, R.E. & Ioannou, Y.A. (2005) NPC1 late endosomes contain elevated levels of non-esterified ('free') fatty acids and an abnormally glycosylated form of the NPC2 protein. *Biochemical Journal*. 390 (2), pp. 549.

Chen, F.W., Li, C. & Ioannou, Y.A. (2010) Cyclodextrin induces calcium-dependent lysosomal exocytosis. *PLoS ONE*. 5 (11), pp. e15054.

Chen, I. & Dubnau, D. (2004) DNA uptake during bacterial transformation. *Nature Reviews Microbiology*. 2 (3), pp. 241–249.

Chen, Y.-W., Pedersen, J.W., Wandall, H.H., Levery, S.B., Pizette, S., Clausen, H. & Cohen, S.M. (2007) Glycosphingolipids with extended sugar chain have specialized functions in development and behavior of Drosophila. *Developmental Biology*. 306 (2), pp. 736–749.

Cheng, X. & Lee, R.J. (2016) The role of helper lipids in lipid nanoparticles (LNPs) designed for oligonucleotide delivery. *Advanced Drug Delivery Reviews*. 99 (Pt A), pp. 129–137.

Chien, S., Reiter, L.T., Bier, E. & Gribskov, M. (2002) Homophila: human disease gene cognates in Drosophila. *Nucleic Acids Research*. 30 (1), pp. 149–151.

Chintapalli, V.R., Wang, J. & Dow, J.A.T. (2007) Using FlyAtlas to identify better Drosophila melanogaster models of human disease. *Nature Genetics*. 39 (6), pp. 715–720.

Christian, A.E., Haynes, M.P., Phillips, M.C. & Rothblat, G.H. (1997) Use of cyclodextrins for manipulating cellular cholesterol content. *The Journal of Lipid Research*. 38 (11), pp. 2264–2272.

Chu, B.-B., Liao, Y.-C., Qi, W., Xie, C., Du, X., Wang, J., Yang, H., Miao, H.-H., Li, B.-L. & Song, B.-L. (2015) Cholesterol Transport through Lysosome-Peroxisome Membrane Contacts. *Cell*. 161 (2), pp. 291–306.

Cluzeau, C.V.M., Watkins-Chow, D.E., Fu, R., Borate, B., Yanjanin, N., Dail, M.K., Davidson, C.D., Walkley, S.U., Ory, D.S., Wassif, C.A., Pavan, W.J. & Porter, F.D. (2012) Microarray expression analysis and identification of serum biomarkers for Niemann-Pick disease, type C1. *Human Molecular Genetics*. 21 (16), pp. 3632–3646.

Colacurcio, D.J. & Nixon, R.A. (2016) Disorders of lysosomal acidification-The emerging role of v-ATPase in aging and neurodegenerative disease. *Ageing Research Reviews*. 32pp. 75–88.

Collins, M. & Thrasher, A. (2015) Gene therapy: progress and predictions. *Proceedings of the Royal Society B: Biological Sciences*. 282 (1821), pp. 20143003.

Conforti, P., Zuccato, C., Gaudenzi, G., Ieraci, A., Camnasio, S., Buckley, N.J., Mutti, C., Cotelli, F., Contini, A. & Cattaneo, E. (2013) Binding of the repressor complex REST-mSIN3b by small molecules restores neuronal gene transcription in Huntington's disease models. *Journal of Neurochemistry*. pp. n/a–n/a.

Cortes, C.J. & La Spada, A.R. (2014) The many faces of autophagy dysfunction in Huntington's disease: from mechanism to therapy. *Drug Discovery Today*. 19 (7), pp. 963–971.

Costa, V., Giacomello, M., Hudec, R., Lopreiato, R., Ermak, G., Lim, D., Malorni, W., Davies, K.J.A., Carafoli, E. & Scorrano, L. (2010) Mitochondrial fission and cristae disruption increase the response of cell models of Huntington's disease to apoptotic stimuli. *EMBO Molecular Medicine*. 2 (12), pp. 490–503.

Cox, T.M. & Cachón-González, M.B. (2012) The cellular pathology of lysosomal diseases. *The Journal of Pathology*. 226 (2), pp. 241–254.

Côté, M., Misasi, J., Ren, T., Bruchez, A., Lee, K., Filone, C.M., Hensley, L., Li, Q., Ory, D., Chandran, K. & Cunningham, J. (2011) Small molecule inhibitors reveal Niemann-Pick C1 is essential for Ebola virus infection. *Nature*. 477 (7364), pp. 344–348.

Criscitiello, M.F., Dickman, M.B., Samuel, J.E. & de Figueiredo, P. (2013) Tripping on acid: trans-kingdom perspectives on biological acids in immunity and pathogenesis. *PLoS Pathogens*. 9 (7), pp. e1003402.

Dabkowska, A.P., Barlow, D.J., Campbell, R.A., Hughes, A.V., Quinn, P.J. & Lawrence, M.J. (2012a) Effect of helper lipids on the interaction of DNA with cationic lipid monolayers studied by specular neutron reflection. *Biomacromolecules*. 13 (8), pp. 2391–2401.

Dabkowska, A.P., Barlow, D.J., Hughes, A.V., Campbell, R.A., Quinn, P.J. & Lawrence, M.J. (2012b) The effect of neutral helper lipids on the structure of cationic lipid monolayers. *Journal of the Royal*

*Society, Interface*. 9 (68), pp. 548–561.

Davidson, C.D., Ali, N.F., Micsenyi, M.C., Stephney, G., Renault, S., Dobrenis, K., Ory, D.S., Vanier, M.T. & Walkley, S.U. (2009) Chronic cyclodextrin treatment of murine Niemann-Pick C disease ameliorates neuronal cholesterol and glycosphingolipid storage and disease progression. *PLoS ONE*. 4 (9), pp. e6951.

Davies, J.P. (2000) Transmembrane Molecular Pump Activity of Niemann-Pick C1 Protein. *Science*. 290 (5500), pp. 2295–2298.

de Chaumont, F., Dallongeville, S., Chenouard, N., Hervé, N., Pop, S., Provoost, T., Meas-Yedid, V., Pankajakshan, P., Lecomte, T., Le Montagner, Y., Lagache, T., Dufour, A. & Olivo-Marin, J.-C. (2012) Icy: an open bioimage informatics platform for extended reproducible research. *Nature Methods*. 9 (7), pp. 690–696.

De Rooij, K.E., De Koning Gans, P.A., Roos, R.A., Van Ommen, G.J. & Dunnen, Den, J.T. (1995) Somatic expansion of the (CAG)n repeat in Huntington disease brains. *Human Genetics*. 95 (3), pp. 270–274.

De Rooij, K.E., Dorsman, J.C., Smoor, M.A., Dunnen, Den, J.T. & Van Ommen, G.J. (1996) Subcellular localization of the Huntington's disease gene product in cell lines by immunofluorescence and biochemical subcellular fractionation. *Human Molecular Genetics*. 5 (8), pp. 1093–1099.

De Winter, J. (2013) Using the Student's t-test with extremely small sample sizes. *Practical Assessment*.

DeBarber, A.E., Eroglu, Y., Merkens, L.S., Pappu, A.S. & Steiner, R.D. (2011) Smith-Lemli-Opitz syndrome. *Expert reviews in molecular medicine*. 13pp. e24.

Deffieu, M.S. & Pfeffer, S.R. (2011) Niemann-Pick type C 1 function requires lumenal domain residues that mediate cholesterol-dependent NPC2 binding. *Proceedings of the National Academy of Sciences*. 108 (47), pp. 18932–18936.

Del Toro, D., Alberch, J., Lázaro-Diéguez, F., Martín-Ibáñez, R., Xifró, X., Egea, G. & Canals, J.M. (2009) Mutant huntingtin impairs post-Golgi trafficking to lysosomes by delocalizing optineurin/Rab8 complex from the Golgi apparatus. *Molecular Biology of the Cell*. 20 (5), pp. 1478–1492.

Del Toro, D., Canals, J.M., Ginés, S., Kojima, M., Egea, G. & Alberch, J. (2006) Mutant huntingtin impairs the post-Golgi trafficking of brain-derived neurotrophic factor but not its Val66Met polymorphism. *Journal of Neuroscience*. 26 (49), pp. 12748–12757.

Del Toro, D., Xifró, X., Pol, A., Humbert, S., Saudou, F., Canals, J.M. & Alberch, J. (2010) Altered cholesterol homeostasis contributes to enhanced excitotoxicity in Huntington's disease. *Journal of Neurochemistry*. 115 (1), pp. 153–167.

Deng, Y., Wang, C.C., Choy, K.W., Du, Q., Chen, J., Wang, Q., Li, L., Chung, T.K.H. & Tang, T. (2014) Therapeutic potentials of gene silencing by RNA interference: Principles, challenges, and new strategies. *Gene*. 538 (2), pp. 217–227.

Denny, C.A., Desplats, P.A., Thomas, E.A. & Seyfried, T.N. (2010) Cerebellar lipid differences between R6/1 transgenic mice and humans with Huntington's disease. *Journal of Neurochemistry*. 115 (3), pp. 748–758.

Desnick, R.J., Thorpe, S.R. & Fiddler, M.B. (1976) Toward enzyme therapy for lysosomal storage diseases. *Physiological Reviews*. 56 (1), pp. 57–99.

Desplats, P.A., Denny, C.A., Kass, K.E., Gilmartin, T., Head, S.R., Sutcliffe, J.G., Seyfried, T.N. & Thomas, E.A. (2007) Glycolipid and ganglioside metabolism imbalances in Huntington's disease. *Neurobiology of Disease*. 27 (3), pp. 265–277.

Di Pardo, A., Amico, E., Favellato, M., Castrataro, R., Fucile, S., Squitieri, F. & Maglione, V. (2013) FTY720 (Fingolimod) is a neuroprotective and disease-modifying agent in cellular and mouse models of Huntington disease. *Human Molecular Genetics*.

Di Pardo, A., Maglione, V., Alpaugh, M., Horkey, M., Atwal, R.S., Sassone, J., Ciammola, A., Steffan, J.S., Fouad, K., Truant, R. & Sipione, S. (2012) Ganglioside GM1 induces phosphorylation of mutant huntingtin and restores normal motor behavior in Huntington disease mice. *Proceedings of the National Academy of Sciences*. 109 (9), pp. 3528–3533.

Diekmann, H., Anichtchik, O., Fleming, A., Futter, M., Goldsmith, P., Roach, A. & Rubinsztein, D.C. (2009) Decreased BDNF levels are a major contributor to the embryonic phenotype of huntingtin knockdown zebrafish. *Journal of Neuroscience*. 29 (5), pp. 1343–1349.

DiFiglia, M., Sapp, E., Chase, K.O., Davies, S.W., Bates, G.P., Vonsattel, J.P. & Aronin, N. (1997) Aggregation of huntingtin in neuronal intranuclear inclusions and dystrophic neurites in brain. *Science*. 277 (5334), pp. 1990–1993.

DiFiglia, M., Sena-Esteves, M., Chase, K., Sapp, E., Pfister, E., Sass, M., Yoder, J., Reeves, P., Pandey, R.K., Rajeev, K.G., Manoharan, M., Sah, D.W.Y., Zamore, P.D. & Aronin, N. (2007) Therapeutic silencing of mutant huntingtin with siRNA attenuates striatal and cortical neuropathology and behavioral deficits. *Proceedings of the National Academy of Sciences of the United States of America*. 104 (43), pp. 17204–17209.

Dragatsis, I., Levine, M.S. & Zeitlin, S. (2000) Inactivation of Hdh in the brain and testis results in progressive neurodegeneration and sterility in mice. *Nature Genetics*. 26 (3), pp. 300–306.

Duffy, J.B. (2002) GAL4 system in Drosophila: a fly geneticist's Swiss army knife. *Genesis (New York, N.Y. : 2000)*. 34 (1-2), pp. 1–15.

Duncan, R. & Richardson, S.C.W. (2012) Endocytosis and Intracellular Trafficking as Gateways for Nanomedicine Delivery: Opportunities and Challenges. *Molecular Pharmaceutics*. 9 (9), pp. 2380–2402.

Dunnett, S.B. & Rosser, A.E. (2007) Cell transplantation for Huntington's disease. *Brain Research Bulletin*. 72 (2-3), pp. 132–147.

Dunster, K., Toh, B.H. & Sentry, J.W. (2002) Early endosomes, late endosomes, and lysosomes display distinct partitioning strategies of inheritance with similarities to Golgi-derived membranes. *European Journal of Cell Biology*. 81 (3), pp. 117–124.

Duyao, M.P., Auerbach, A.B., Ryan, A., Persichetti, F., Barnes, G.T., McNeil, S.M., Ge, P., Vonsattel, J.P., Gusella, J.F. & Joyner, A.L. (1995) Inactivation of the mouse Huntington's disease gene homolog Hdh. *Science*. 269 (5222), pp. 407–410.

El-Sayed, A., Khalil, I.A., Kogure, K., Futaki, S. & Harashima, H. (2008) Octaarginine- and octalysine-modified nanoparticles have different modes of endosomal escape. *The Journal of Biological Chemistry*. 283 (34), pp. 23450–23461.

Eltoukhy, A.A., Sahay, G., Cunningham, J.M. & Anderson, D.G. (2014) Niemann-Pick C1 Affects the Gene Delivery Efficacy of Degradable Polymeric Nanoparticles. *ACS Nano*. 8 (8), pp. 7905–7913.

Erickson, R.P., Garver, W.S., Camargo, F., Hossain, G.S. & Heidenreich, R.A. (2000) Pharmacological and genetic modifications of somatic cholesterol do not substantially alter the course of CNS disease in Niemann-Pick C mice. *Journal of Inherited Metabolic Disease*. 23 (1), pp. 54–62.

Erie, C., Sacino, M., Houle, L., Lu, M. & Wei, J. (2015) Altered lysosomal positioning affects lysosomal functions in a cellular model of Huntington's disease. *European Journal of Neuroscience*. pp. n/a–

n/a.

Evans, S.J.W., Douglas, I., Rawlins, M.D., Wexler, N.S., Tabrizi, S.J. & Smeeth, L. (2013) Prevalence of adult Huntington's disease in the UK based on diagnoses recorded in general practice records. *Journal of Neurology, Neurosurgery & Psychiatry*. 84 (10), pp. 1156–1160.

Fan, H.-C., Ho, L.-I., Chi, C.-S., Chen, S.-J., Peng, G.-S., Chan, T.-M., Lin, S.-Z. & Harn, H.-J. (2014) Polyglutamine (PolyQ) diseases: genetics to treatments. *Cell Transplantation*. 23 (4-5), pp. 441–458.

Farge, E. (1995) Increased vesicle endocytosis due to an increase in the plasma membrane phosphatidylserine concentration. *Biophysical Journal*. 69 (6), pp. 2501–2506.

Fecarotta, S., Romano, A., Casa, Della, R., Del Giudice, E., Bruschini, D., Mansi, G., Bembi, B., Dardis, A., Fiumara, A., Di Rocco, M., Uziel, G., Ardissone, A., Roccatello, D., Alpa, M., et al. (2015) Long term follow-up to evaluate the efficacy of miglustat treatment in Italian patients with Niemann-Pick disease type C. *Orphanet Journal of Rare Diseases*. 10 (1), pp. 22.

Felgner, P.L., Gadek, T.R., Holm, M., Roman, R., Chan, H.W., Wenz, M., Northrop, J.P., Ringold, G.M. & Danielsen, M. (1987) Lipofection: a highly efficient, lipid-mediated DNA-transfection procedure. *Proceedings of the National Academy of Sciences of the United States of America*. 84 (21), pp. 7413–7417.

Finbow, M.E. & Harrison, M.A. (1997) The vacuolar H+-ATPase: a universal proton pump of eukaryotes. *Biochemical Journal*. 324 ( Pt 3)pp. 697–712.

Fire, A., Xu, S., Montgomery, M.K., Kostas, S.A., Driver, S.E. & Mello, C.C. (1998) Potent and specific genetic interference by double-stranded RNA in Caenorhabditis elegans. *Nature*. 391 (6669), pp. 806–811.

Fluegel, M.L., Parker, T.J. & Pallanck, L.J. (2006) Mutations of a Drosophila NPC1 gene confer sterol and ecdysone metabolic defects. *Genetics*. 172 (1), pp. 185–196.

Fratantoni, J.C., Hall, C.W. & Neufeld, E.F. (1968) Hurler and Hunter syndromes: mutual correction of the defect in cultured fibroblasts. *Science*. 162 (3853), pp. 570–572.

Freeze, H.H. & Kranz, C. (2010) Endoglycosidase and glycoamidase release of N-linked glycans. *Current protocols in molecular biology*. Chapter 17pp. Unit17.13A.

Friedland, N., Liou, H.-L., Lobel, P. & Stock, A.M. (2003) Structure of a cholesterol-binding protein deficient in Niemann-Pick type C2 disease. *Proceedings of the National Academy of Sciences of the United States of America*. 100 (5), pp. 2512–2517.

Friedrich, B., Euler, P., Ziegler, R., Kuhn, A., Landwehrmeyer, B.G., Luthi-Carter, R., Weiller, C., Hellwig, S. & Zucker, B. (2012) Comparative analyses of Purkinje cell gene expression profiles reveal shared molecular abnormalities in models of different polyglutamine diseases. *Brain Research*. 1481 (C), pp. 37–48.

Fu, R., Wassif, C.A., Yanjanin, N.M., Watkins-Chow, D.E., Baxter, L.L., Incao, A., Liscum, L., Sidhu, R., Firnkes, S., Graham, M., Ory, D.S., Porter, F.D. & Pavan, W.J. (2013) Efficacy of N-acetylcysteine in phenotypic suppression of mouse models of Niemann-Pick disease, type C1. *Human Molecular Genetics*. 22 (17), pp. 3508–3523.

Gamble, W., Vaughan, M., Kruth, H.S. & Avigan, J. (1978) Procedure for determination of free and total cholesterol in micro- or nanogram amounts suitable for studies with cultured cells. *Journal of Lipid Research*. 19 (8), pp. 1068–1070.

Ganley, I.G. & Pfeffer, S.R. (2006) Cholesterol Accumulation Sequesters Rab9 and Disrupts Late

Endosome Function in NPC1-deficient Cells. *Journal of Biological Chemistry*. 281 (26), pp. 17890–17899.

García-Arencibia, M., Hochfeld, W.E., Toh, P.P.C. & Rubinsztein, D.C. (2010) Autophagy, a guardian against neurodegeneration. *Seminars in Cell & Developmental Biology*. 21 (7), pp. 691–698.

Gaspar, M.L., Hofbauer, H.F., Kohlwein, S.D. & Henry, S.A. (2011) Coordination of storage lipid synthesis and membrane biogenesis: evidence for cross-talk between triacylglycerol metabolism and phosphatidylinositol synthesis. *Journal of Biological Chemistry*. 286 (3), pp. 1696–1708.

Gautschi, F. & Bloch, K. (1958) Synthesis of isomeric 4,4-dimethylcholestenols and identification of a lanosterol metabolite. *The Journal of Biological Chemistry*. 233 (6), pp. 1343–1347.

Gelsthorpe, M.E., Baumann, N., Millard, E., Gale, S.E., Langmade, S.J., Schaffer, J.E. & Ory, D.S. (2008) Niemann-Pick Type C1 I1061T Mutant Encodes a Functional Protein That Is Selected for Endoplasmic Reticulum-associated Degradation Due to Protein Misfolding. *Journal of Biological Chemistry*. 283 (13), pp. 8229–8236.

Genetic Modifiers of Huntington's Disease (GeM-HD) Consortium (2015) Identification of Genetic Factors that Modify Clinical Onset of Huntington's Disease. *Cell*. 162 (3), pp. 516–526.

Giacomello, M., Hudec, R. & Lopreiato, R. (2011) Huntington's disease, calcium, and mitochondria. *BioFactors*. 37 (3), pp. 206–218.

Giacomello, M., Oliveros, J.C., Naranjo, J.R. & Carafoli, E. (2013) Neuronal Ca(2+) dyshomeostasis in Huntington disease. *Prion*. 7 (1), pp. 76–84.

Gibbings, D. & Voinnet, O. (2010) Control of RNA silencing and localization by endolysosomes. *Trends in Cell Biology*. 20 (8), pp. 491–501.

Gibbings, D.J., Ciaudo, C., Erhardt, M. & Voinnet, O. (2009) Multivesicular bodies associate with components of miRNA effector complexes and modulate miRNA activity. *Nature Cell Biology*. 11 (9), pp. 1143–1149.

Gidalevitz, T., Wang, N., Deravaj, T., Alexander-Floyd, J. & Morimoto, R.I. (2013) Natural genetic variation determines susceptibility to aggregation or toxicity in a C. elegans model for polyglutamine disease. *BMC Biology*. 11 (1), pp. 100.

Glover, D.J., Lipps, H.J. & Jans, D.A. (2005) Towards safe, non-viral therapeutic gene expression in humans. *Nature Reviews Genetics*. 6 (4), pp. 299–310.

Godbey, W.T., Wu, K.K. & Mikos, A.G. (1999) Tracking the intracellular path of poly(ethylenimine)/DNA complexes for gene delivery. *Proceedings of the National Academy of Sciences of the United States of America*. 96 (9), pp. 5177–5181.

Godinho, B.M.D.C., Ogier, J.R., Darcy, R., O'Driscoll, C.M. & Cryan, J.F. (2013) Self-assembling Modified β-Cyclodextrin Nanoparticles as Neuronal siRNA Delivery Vectors: Focus on Huntington's Disease. *Molecular Pharmaceutics*. 10 (2), pp. 640–649.

Gong, X., Qian, H., Zhou, X., Wu, J., Wan, T., Cao, P., Huang, W., Zhao, X., Wang, X., Wang, P., Shi, Y., Gao, G.F., Zhou, Q. & Yan, N. (2016) Structural Insights into the Niemann-Pick C1 (NPC1)-Mediated Cholesterol Transfer and Ebola Infection. *Cell*. 165 (6), pp. 1467–1478.

Goujon, M., McWilliam, H., Li, W., Valentin, F., Squizzato, S., Paern, J. & Lopez, R. (2010) A new bioinformatics analysis tools framework at EMBL-EBI. *Nucleic Acids Research*. 38 (Web Server issue), pp. W695–W699.

Grant, B.D. & Donaldson, J.G. (2009) Pathways and mechanisms of endocytic recycling. *Nature Reviews Molecular Cell Biology*. 10 (9), pp. 597–608.

Green, E.W. & Giorgini, F. (2012) Choosing and using Drosophila models to characterize modifiers of Huntington's disease. *Biochemical Society Transactions*. 40 (4), pp. 739–745.

Grienberger, C. & Konnerth, A. (2012) Imaging Calcium in Neurons. *Neuron*. 73 (5), pp. 862–885.

Grondin, R., Ge, P., Chen, Q., Sutherland, J.E., Zhang, Z., Gash, D.M., Stiles, D.K., Stewart, G.R., Sah, D.W.Y. & Kaemmerer, W.F. (2015) Onset Time and Durability of Huntingtin Suppression in Rhesus Putamen After Direct Infusion of Antihuntingtin siRNA. *Molecular Therapy—Nucleic Acids*. pp. 1–13.

Group, T.H.D.C.R. (1993) A novel gene containing a trinucleotide repeat that is expanded and unstable on Huntington's disease chromosomes. *Cell*. 72 (6), pp. 971–983.

Grynkiewicz, G., Poenie, M. & Tsien, R.Y. (1985) A new generation of Ca2+ indicators with greatly improved fluorescence properties. *The Journal of Biological Chemistry*. 260 (6), pp. 3440–3450.

Gu, F., Aniento, F., Parton, R.G. & Gruenberg, J. (1997) Functional dissection of COP-I subunits in the biogenesis of multivesicular endosomes. *The Journal of Cell Biology*. 139 (5), pp. 1183–1195.

Guo, S. & Kemphues, K.J. (1995) par-1, a gene required for establishing polarity in C. elegans embryos, encodes a putative Ser/Thr kinase that is asymmetrically distributed. *Cell*. 81 (4), pp. 611–620.

Gupta, V., Patwardhan, G.A., Zhang, Q.-J., Cabot, M.C., Jazwinski, S.M. & Liu, Y.-Y. (2010) Direct quantitative determination of ceramide glycosylation in vivo: a new approach to evaluate cellular enzyme activity of glucosylceramide synthase. *Journal of Lipid Research*. 51 (4), pp. 866–874.

Gusella, J.F., Wexler, N.S., Conneally, P.M., Naylor, S.L., Anderson, M.A., Tanzi, R.E., Watkins, P.C., Ottina, K., Wallace, M.R. & Sakaguchi, A.Y. (1983) A polymorphic DNA marker genetically linked to Huntington's disease. *Nature*. 306 (5940), pp. 234–238.

Hacein-Bey-Abina, S., Garrigue, A., Wang, G.P., Soulier, J., Lim, A., Morillon, E., Clappier, E., Caccavelli, L., Delabesse, E., Beldjord, K., Asnafi, V., MacIntyre, E., Dal Cortivo, L., Radford, I., et al. (2008) Insertional oncogenesis in 4 patients after retrovirus-mediated gene therapy of SCID-X1. *Journal of Clinical Investigation*. 118 (9), pp. 3132–3142.

Haensler, J. & Szoka, F.C. (1993) Polyamidoamine cascade polymers mediate efficient transfection of cells in culture. *Bioconjugate Chemistry*. 4 (5), pp. 372–379.

Hafez, I.M., Maurer, N. & Cullis, P.R. (2001) On the mechanism whereby cationic lipids promote intracellular delivery of polynucleic acids. *Gene Therapy*. 8 (15), pp. 1188–1196.

Haines, N. & Irvine, K.D. (2003) Glycosylation regulates Notch signalling. *Nature Reviews Molecular Cell Biology*. 4 (10), pp. 786–797.

Haines, N. & Stewart, B.A. (2007) Functional roles for beta1,4-N-acetlygalactosaminyltransferase-A in Drosophila larval neurons and muscles. *Genetics*. 175 (2), pp. 671–679.

Halliwell, W.H. (1997) Cationic Amphiphilic Drug-Induced Phospholipidosis. *Toxicologic Pathology*. 25 (1), pp. 53–60.

Handley, R.R., Reid, S.J., Patassini, S., Rudiger, S.R., Obolonkin, V., McLaughlan, C.J., Jacobsen, J.C., Gusella, J.F., MacDonald, M.E., Waldvogel, H.J., Bawden, C.S., Faull, R.L.M. & Snell, R.G. (2016) Metabolic disruption identifed in the Huntington's disease transgenic sheep model. *Scientific Reports*. pp. 1–11.

Hannon, G.J. (2002) RNA interference. *Nature*. 418 (6894), pp. 244–251.

Hannun, Y.A. & Bell, R.M. (1989) Regulation of protein kinase C by sphingosine and lysosphingolipids. *Clinica chimica acta*. 185 (3), pp. 333–345.

Hansson, H.A., Holmgren, J. & Svennerholm, L. (1977) Ultrastructural localization of cell membrane GM1 ganglioside by cholera toxin. *Proceedings of the National Academy of Sciences of the United States of America*. 74 (9), pp. 3782–3786.

Harjes, P. & Wanker, E.E. (2003) The hunt for huntingtin function: interaction partners tell many different stories. *Trends in Biochemical Sciences*. 28 (8), pp. 425–433.

Hekman, K.E. & Gomez, C.M. (2014) The autosomal dominant spinocerebellar ataxias: emerging mechanistic themes suggest pervasive Purkinje cell vulnerability. *J Neurol Neurosurg Psychiatry*. pp. 1–9.

Helquist, P., Maxfield, F.R., Wiech, N.L. & Wiest, O. (2013) Treatment of Niemann--pick type C disease by histone deacetylase inhibitors. *Neurotherapeutics*. 10 (4), pp. 688–697.

Henderson, L.P., Lin, L., Prasad, A., Paul, C.A., Chang, T.Y. & Maue, R.A. (2000) Embryonic striatal neurons from Niemann-Pick type C mice exhibit defects in cholesterol metabolism and neurotrophin responsiveness. *The Journal of Biological Chemistry*. 275 (26), pp. 20179–20187.

Henshall, T.L., Tucker, B., Lumsden, A.L., Nornes, S., Lardelli, M.T. & Richards, R.I. (2009) Selective neuronal requirement for huntingtin in the developing zebrafish. *Human Molecular Genetics*. 18 (24), pp. 4830–4842.

Hillig, I., Warnecke, D. & Heinz, E. (2005) An inhibitor of glucosylceramide synthase inhibits the human enzyme, but not enzymes from other organisms. *Bioscience, biotechnology, and biochemistry*. 69 (9), pp. 1782–1785.

Hindle, S.J., Hebbar, S., Schwudke, D., Elliott, C.J.H. & Sweeney, S.T. (2017) A saposin deficiency model in Drosophila: Lysosomal storage, progressive neurodegeneration and sensory physiological decline. *Neurobiology of Disease*. 98pp. 77–87.

Hiraoka, M., Abe, A., Lu, Y., Yang, K., Han, X., Gross, R.W. & Shayman, J.A. (2006) Lysosomal phospholipase A2 and phospholipidosis. *Molecular and Cellular Biology*. 26 (16), pp. 6139–6148.

Hollak, C.E., Van Weely, S., van Oers, M.H. & Aerts, J.M. (1994) Marked elevation of plasma chitotriosidase activity. A novel hallmark of Gaucher disease. *Journal of Clinical Investigation*. 93 (3), pp. 1288–1292.

Hong, W. (2005) SNAREs and traffic. *Biochimica et biophysica acta*. 1744 (3), pp. 493–517.

Horton, J.D., Goldstein, J.L. & Brown, M.S. (2002) SREBPs: activators of the complete program of cholesterol and fatty acid synthesis in the liver. *Journal of Clinical Investigation*. 109 (9), pp. 1125–1131.

Howes, M.T., Mayor, S. & Parton, R.G. (2010) Molecules, mechanisms, and cellular roles of clathrin-independent endocytosis. *Current Opinion in Cell Biology*. 22 (4), pp. 519–527.

Hölttä Vuori, M., Tanhuanpää, K., Möbius, W., Somerharju, P. & Ikonen, E. (2002) Modulation of cellular cholesterol transport and homeostasis by Rab11. *Molecular Biology of the Cell*. 13 (9), pp. 3107–3122.

Huang, K., Yanai, A., Kang, R., Arstikaitis, P., Singaraja, R.R., Metzler, M., Mullard, A., Haigh, B., Gauthier-Campbell, C., Gutekunst, C.-A., Hayden, M.R. & El-Husseini, A. (2004) Huntingtin-Interacting Protein

HIP14 Is a Palmitoyl Transferase Involved in Palmitoylation and Trafficking of Multiple Neuronal Proteins. *Neuron*. 44 (6), pp. 977–986.

Huang, X., Suyama, K., Buchanan, J., Zhu, A.J. & Scott, M.P. (2005) A Drosophila model of the Niemann-Pick type C lysosome storage disease: dnpc1a is required for molting and sterol homeostasis. *Development*. 132 (22), pp. 5115–5124.

Huang, X., Warren, J.T., Buchanan, J., Gilbert, L.I. & Scott, M.P. (2007) Drosophila Niemann-Pick type C-2 genes control sterol homeostasis and steroid biosynthesis: a model of human neurodegenerative disease. *Development*. 134 (20), pp. 3733–3742.

Hughes, A. & Jones, L. (2011) Huntingtin localisation studies - a technical review. *PLoS Currents*. 3pp. RRN1211.

Hughes, A.C., Mort, M., Elliston, L., Thomas, R.M., Brooks, S.P., Dunnett, S.B. & Jones, L. (2014) Identification of novel alternative splicing events in the huntingtin gene and assessment of the functional consequences using structural protein homology modelling. *Journal of Molecular Biology*. 426 (7), pp. 1428–1438.

Hughes, A.R. & Putney, J.W. (1990) Inositol phosphate formation and its relationship to calcium signaling. *Environmental Health Perspectives*. 84pp. 141–147.

Humbert, S., Bryson, E.A., Cordelières, F.P., Connors, N.C., Datta, S.R., Finkbeiner, S., Greenberg, M.E. & Saudou, F. (2002) The IGF-1/Akt pathway is neuroprotective in Huntington's disease and involves Huntingtin phosphorylation by Akt. *Developmental Cell*. 2 (6), pp. 831–837.

Huwiler, A., Kolter, T., Pfeilschifter, J. & Sandhoff, K. (2000) Physiology and pathophysiology of sphingolipid metabolism and signaling. *Biochimica et biophysica acta*. 1485 (2-3), pp. 63–99.

Ikonen, E. (2008) Cellular cholesterol trafficking and compartmentalization. *Nature Reviews Molecular Cell Biology*. 9 (2), pp. 125–138.

Imarisio, S., Carmichael, J., Korolchuk, V., Chen, C.-W., Saiki, S., Rose, C., Krishna, G., Davies, J.E., Ttofi, E., Underwood, B.R. & Rubinsztein, D.C. (2008) Huntington's disease: from pathology and genetics to potential therapies. *Biochemical Journal*. 412 (2), pp. 191–209.

Infante, R.E., Wang, M.L., Radhakrishnan, A., Kwon, H.J., Brown, M.S. & Goldstein, J.L. (2008) NPC2 facilitates bidirectional transfer of cholesterol between NPC1 and lipid bilayers, a step in cholesterol egress from lysosomes. *Proceedings of the National Academy of Sciences*. 105 (40), pp. 15287–15292.

Ioannou, Y.A. (2005) Guilty until proven innocent: the case of NPC1 and cholesterol. *Trends in Biochemical Sciences*. 30 (9), pp. 498–505.

Irvine, R.F., Moor, R.M., Pollock, W.K., Smith, P.M. & Wreggett, K.A. (1988) Inositol phosphates: proliferation, metabolism and function. *Philosophical Transactions of the Royal Society B: Biological Sciences*. 320 (1199), pp. 281–298.

Ishida, Y., Tsuchiya, W., Fujii, T., Fujimoto, Z., Miyazawa, M., Ishibashi, J., Matsuyama, S., Ishikawa, Y. & Yamazaki, T. (2014) Niemann-Pick type C2 protein mediating chemical communication in the worker ant. *Proceedings of the National Academy of Sciences*. 111 (10), pp. 3847–3852.

Ismailoglu, I., Chen, Q., Popowski, M., Yang, L., Gross, S.S. & Brivanlou, A.H. (2014) Huntingtin protein is essential for mitochondrial metabolism, bioenergetics and structure in murine embryonic stem cells. *Developmental Biology*. pp. 1–11.

Iwasa, A., Akita, H., Khalil, I., Kogure, K., Futaki, S. & Harashima, H. (2006) Cellular uptake and

subsequent intracellular trafficking of R8-liposomes introduced at low temperature. *Biochimica et biophysica acta*. 1758 (6), pp. 713–720.

Jacobsen, J.C., Bawden, C.S., Rudiger, S.R., McLaughlan, C.J., Reid, S.J., Waldvogel, H.J., MacDonald, M.E., Gusella, J.F., Walker, S.K., Kelly, J.M., Webb, G.C., Faull, R.L.M., Rees, M.I. & Snell, R.G. (2010) An ovine transgenic Huntington's disease model. *Human Molecular Genetics*. 19 (10), pp. 1873–1882.

Janusonis, S. (2009) Comparing two small samples with an unstable, treatment-independent baseline. *Journal of Neuroscience Methods*. 179 (2), pp. 173–178.

Jeang, K.-T. (2012) RNAi in the regulation of mammalian viral infections. *BMC Biology*. 10pp. 58.

Johansen, J., Ramanathan, V. & Beh, C.T. (2012) Vesicle trafficking from a lipid perspective: Lipid regulation of exocytosis in Saccharomyces cerevisiae. *Cellular Logistics*. 2 (3), pp. 151–160.

Johnson, D.E., Ostrowski, P., Jaumouillé, V. & Grinstein, S. (2016) The position of lysosomes within the cell determines their luminal pH. *The Journal of Cell Biology*. 212 (6), pp. 677–692.

Juliano, R.L., Ming, X. & Nakagawa, O. (2012) Cellular uptake and intracellular trafficking of antisense and siRNA oligonucleotides. *Bioconjugate Chemistry*. 23 (2), pp. 147–157.

Juopperi, T.A., Kim, W.R., Chiang, C.-H., Yu, H., Margolis, R.L., Ross, C.A., Ming, G.-L. & Song, H. (2012) Astrocytes generated from patient induced pluripotent stem cells recapitulate features of Huntington's disease patient cells. *Molecular Brain*. 5 (1), pp. 1–1.

Kalatzis, V., Cherqui, S., Antignac, C. & Gasnier, B. (2001) Cystinosin, the protein defective in cystinosis, is a H(+)-driven lysosomal cystine transporter. *The EMBO Journal*. 20 (21), pp. 5940–5949.

Kalchman, M.A., Graham, R.K., Xia, G., Koide, H.B., Hodgson, J.G., Graham, K.C., Goldberg, Y.P., Gietz, R.D., Pickart, C.M. & Hayden, M.R. (1996) Huntingtin is ubiquitinated and interacts with a specific ubiquitin-conjugating enzyme. *The Journal of Biological Chemistry*. 271 (32), pp. 19385–19394.

Kaltenbach, L.S., Romero, E., Becklin, R.R., Chettier, R., Bell, R., Phansalkar, A., Strand, A., Torcassi, C., Savage, J., Hurlburt, A., Cha, G.-H., Ukani, L., Chepanoske, C.L., Zhen, Y., et al. (2007) Huntingtin Interacting Proteins Are Genetic Modifiers of Neurodegeneration. *PLoS Genetics*. 3 (5), pp. e82.

Kandutsch, A.A. & Russell, A.E. (1960) Preputial gland tumor sterols. 3. A metabolic pathway from lanosterol to cholesterol. *The Journal of Biological Chemistry*. 235pp. 2256–2261.

Kang, B.S., Ahn, J.-Y., Kim, M.K., Kim, H.-J., Kang, L., Lim, H.-C., Park, K.-S., Lee, J.-S., Seo, J.-S., Cha, C.I., Kim, S.U., Park, Y.J. & Kim, M. (2007) Heat shock protein 70 alters the endosome-lysosomal localization of huntingtin. *Experimental and Molecular Medicine*. 39 (1), pp. 38–46.

Kang, W., McNaughton, R.L. & Espinosa, H.D. (2016) Micro- and Nanoscale Technologies for Delivery into Adherent Cells. *Trends in Biotechnology*. 34 (8), pp. 665–678.

Kaplan, E.L. & Meier, P. (1958) Nonparametric Estimation from Incomplete Observations. *Journal of the American statistical association*.

Karten, B., Vance, D.E., Campenot, R.B. & Vance, J.E. (2002) Cholesterol accumulates in cell bodies, but is decreased in distal axons, of Niemann-Pick C1-deficient neurons. *Journal of Neurochemistry*. 83 (5), pp. 1154–1163.

Kaushik, S. & Cuervo, A.M. (2012) Chaperone-mediated autophagy: a unique way to enter the lysosome world. *Trends in Cell Biology*. 22 (8), pp. 407–417.

Kaye, J.A. & Finkbeiner, S. (2013) Modeling Huntington's disease with induced pluripotent stem cells. *Molecular and Cellular Neuroscience*. 56pp. 50–64.

Kegel, K.B., Kim, M., Sapp, E., McIntyre, C., Castaño, J.G., Aronin, N. & DiFiglia, M. (2000) Huntingtin expression stimulates endosomal-lysosomal activity, endosome tubulation, and autophagy. *Journal of Neuroscience*. 20 (19), pp. 7268–7278.

Khan, K.H. (2013) Gene expression in Mammalian cells and its applications. *Advanced pharmaceutical bulletin*. 3 (2), pp. 257–263.

Kilpatrick, B.S., Magalhaes, J., Beavan, M.S., McNeill, A., Gegg, M.E., Cleeter, M.W.J., Bloor-Young, D., Churchill, G.C., Duchen, M.R., Schapira, A.H. & Patel, S. (2016) Endoplasmic reticulum and lysosomal Ca²⁺ stores are remodelled in GBA1-linked Parkinson disease patient fibroblasts. *Cell Calcium*. 59 (1), pp. 12–20.

Kim, Y.J., Yi, Y., Sapp, E., Wang, Y., Cuiffo, B., Kegel, K.B., Qin, Z.H., Aronin, N. & DiFiglia, M. (2001) Caspase 3-cleaved N-terminal fragments of wild-type and mutant huntingtin are present in normal and Huntington's disease brains, associate with membranes, and undergo calpain-dependent proteolysis. *Proceedings of the National Academy of Sciences of the United States of America*. 98 (22), pp. 12784–12789.

Kinghorn, K.J., Gronke, S., Castillo-Quan, J.I., Woodling, N.S., Li, L., Sirka, E., Gegg, M., Mills, K., Hardy, J., Bjedov, I. & Partridge, L. (2016) A Drosophila Model of Neuronopathic Gaucher Disease Demonstrates Lysosomal-Autophagic Defects and Altered mTOR Signalling and Is Functionally Rescued by Rapamycin. *Journal of Neuroscience*. 36 (46), pp. 11654–11670.

Kirkegaard, T. & Jäättelä, M. (2009) Lysosomal involvement in cell death and cancer. *Biochimica et biophysica acta*. 1793 (4), pp. 746–754.

Kirkegaard, T., Roth, A.G., Petersen, N.H.T., Mahalka, A.K., Olsen, O.D., Moilanen, I., Zylicz, A., Knudsen, J., Sandhoff, K., Arenz, C., Kinnunen, P.K.J., Nylandsted, J. & Jäättelä, M. (2010) Hsp70 stabilizes lysosomes and reverts Niemann–Pick disease-associated lysosomal pathology. *Nature*. 463 (7280), pp. 549–553.

Kitatani, K., Idkowiak-Baldys, J. & Hannun, Y.A. (2008) The sphingolipid salvage pathway in ceramide metabolism and signaling. *Cellular Signalling*. 20 (6), pp. 1010–1018.

Klein, A., Amigo, L., Retamal, M.J., Morales, M.G., Miquel, J.F., Rigotti, A. & Zanlungo, S. (2006) NPC2 is expressed in human and murine liver and secreted into bile: Potential implications for body cholesterol homeostasis. *Hepatology*. 43 (1), pp. 126–133.

Kloß, A., Henklein, P., Siele, D., Schmolke, M., Apcher, S., Kuehn, L., Sheppard, P.W. & Dahlmann, B. (2009) The cell-penetrating peptide octa-arginine is a potent inhibitor of proteasome activities. *European Journal of Pharmaceutics and Biopharmaceutics*. 72 (1), pp. 219–225.

Kluenemann, H.H., Nutt, J.G., Davis, M.Y. & Bird, T.D. (2013) Parkinsonism syndrome in heterozygotes for Niemann-Pick C1. *Journal of the Neurological Sciences*. 335 (1-2), pp. 219–220.

Ko, D.C., Gordon, M.D., Jin, J.Y. & Scott, M.P. (2001) Dynamic movements of organelles containing Niemann-Pick C1 protein: NPC1 involvement in late endocytic events. *Molecular Biology of the Cell*. 12 (3), pp. 601–614.

Kobayashi, T., Beuchat, M.H., Lindsay, M., Frias, S., Palmiter, R.D., Sakuraba, H., Parton, R.G. & Gruenberg, J. (1999) Late endosomal membranes rich in lysobisphosphatidic acid regulate cholesterol transport. *Nature Cell Biology*. 1 (2), pp. 113–118.

Koga, H. & Cuervo, A.M. (2011) Chaperone-mediated autophagy dysfunction in the pathogenesis of

neurodegeneration. *Neurobiology of Disease*. 43 (1), pp. 29–37.

Koga, H., Martinez-Vicente, M., Arias, E., Kaushik, S., Sulzer, D. & Cuervo, A.M. (2011) Constitutive Upregulation of Chaperone-Mediated Autophagy in Huntington's disease. *Journal of Neuroscience*. 31 (50), pp. 18492–18505.

Koles, K. (2003) Functional Characterization of Drosophila Sialyltransferase. *Journal of Biological Chemistry*. 279 (6), pp. 4346–4357.

Kolli, N., Lu, M., Maiti, P., Rossignol, J. & Dunbar, G.L. (2017) CRISPR-Cas9 Mediated Gene-Silencing of the Mutant Huntingtin Gene in an In Vitro Model of Huntington's Disease. *International Journal of Molecular Sciences*. 18 (4).

Korolchuk, V.I. & Rubinsztein, D.C. (2011) Regulation of autophagy by lysosomal positioning. *Autophagy*. 7 (8), pp. 927–928.

Korolchuk, V.I., Saiki, S., Lichtenberg, M., Siddiqi, F.H., Roberts, E.A., Imarisio, S., Jahreiss, L., Sarkar, S., Futter, M., Menzies, F.M., O'Kane, C.J., Deretic, V. & Rubinsztein, D.C. (2011) Lysosomal positioning coordinates cellular nutrient responses. *Nature Cell Biology*. 13 (4), pp. 453–460.

Kraut, R. (2011) Roles of sphingolipids in Drosophila development and disease. *Journal of Neurochemistry*. 116 (5), pp. 764–778.

Kumar, V., Qin, J., Jiang, Y., Duncan, R.G., Brigham, B., Fishman, S., Nair, J.K., Akinc, A., Barros, S.A. & Kasperkovitz, P.V. (2014) Shielding of Lipid Nanoparticles for siRNA Delivery: Impact on Physicochemical Properties, Cytokine Induction, and Efficacy. *Molecular Therapy—Nucleic Acids*. 3pp. e210.

Kunte, A.S., Matthews, K.A. & Rawson, R.B. (2006) Fatty acid auxotrophy in Drosophila larvae lacking SREBP. *Cell Metabolism*. 3 (6), pp. 439–448.

Kwiatkowska, K., Marszałek-Sadowska, E., Traczyk, G., Koprowski, P., Musielak, M., Lugowska, A., Kulma, M., Grzelczyk, A. & Sobota, A. (2014) Visualization of cholesterol deposits in lysosomes of Niemann-Pick type C fibroblasts using recombinant perfringolysin O. *Orphanet Journal of Rare Diseases*. 9pp. 64.

Lachmann, R.H., Vruchte, te, D., Lloyd-Evans, E., Reinkensmeier, G., Sillence, D.J., Fernandez-Guillen, L., Dwek, R.A., Butters, T.D., Cox, T.M. & Platt, F.M. (2004) Treatment with miglustat reverses the lipid-trafficking defect in Niemann–Pick disease type C. *Neurobiology of Disease*. 16 (3), pp. 654–658.

Landles, C. & Bates, G.P. (2004) Huntingtin and the molecular pathogenesis of Huntington's disease. *EMBO reports*. 5 (10), pp. 958–963.

Landles, C., Sathasivam, K., Weiss, A., Woodman, B., Moffitt, H., Finkbeiner, S., Sun, B., Gafni, J., Ellerby, L.M., Trottier, Y., Richards, W.G., Osmand, A., Paganetti, P. & Bates, G.P. (2010) Proteolysis of Mutant Huntingtin Produces an Exon 1 Fragment That Accumulates as an Aggregated Protein in Neuronal Nuclei in Huntington Disease. *Journal of Biological Chemistry*. 285 (12), pp. 8808–8823.

Lehmann, M.J. & Sczakiel, G. (2005) Spontaneous uptake of biologically active recombinant DNA by mammalian cells via a selected DNA segment. *Gene Therapy*. 12 (5), pp. 446–451.

Lejeune, F.-X., Mesrob, L., Parmentier, F., Bicep, C., Vazquez-Manrique, R.P., Parker, J.A., Vert, J.-P., Tourette, C. & Neri, C. (2012) Large-scale functional RNAi screen in C. elegans identifies genes that regulate the dysfunction of mutant polyglutamine neurons. *BMC Genomics*. 13pp. 91.

Leoni, V., Mariotti, C., Nanetti, L., Salvatore, E., Squitieri, F., Bentivoglio, A.R., Bandettini di Poggio, M., Bandettini Del Poggio, M., Piacentini, S., Monza, D., Valenza, M., Cattaneo, E. & Di Donato, S.

(2011) Whole body cholesterol metabolism is impaired in Huntington's disease. *Neuroscience Letters*. 494 (3), pp. 245–249.

Leoni, V., Mariotti, C., Tabrizi, S.J., Valenza, M., Wild, E.J., Henley, S.M.D., Hobbs, N.Z., Mandelli, M.L., Grisoli, M., Björkhem, I., Cattaneo, E. & Di Donato, S. (2008) Plasma 24S-hydroxycholesterol and caudate MRI in pre-manifest and early Huntington's disease. *Brain*. 131 (Pt 11), pp. 2851–2859.

Lewandoski, M. (2001) Conditional control of gene expression in the mouse. *Nature Reviews Genetics*. 2 (10), pp. 743–755.

Lewis, E.A. & Smith, G.A. (2016) Using Drosophila models of Huntington's disease as a translatable tool. *Journal of Neuroscience Methods*. 265pp. 89–98.

Li, J. & Pfeffer, S.R. (2016) Lysosomal membrane glycoproteins bind cholesterol and contribute to lysosomal cholesterol export. *eLife*.

Li, X., Garrity, A.G. & Xu, H. (2013) Regulation of membrane trafficking by signalling on endosomal and lysosomal membranes. *The Journal of Physiology*. 591 (18), pp. 4389–4401.

Li, X., Standley, C., Sapp, E., Valencia, A., Qin, Z.H., Kegel, K.B., Yoder, J., Comer-Tierney, L.A., Esteves, M., Chase, K., Alexander, J., Masso, N., Sobin, L., Bellve, K., et al. (2009) Mutant Huntingtin Impairs Vesicle Formation from Recycling Endosomes by Interfering with Rab11 Activity. *Molecular and Cellular Biology*. 29 (22), pp. 6106–6116.

Li, X., Valencia, A., Sapp, E., Masso, N., Alexander, J., Reeves, P., Kegel, K.B., Aronin, N. & DiFiglia, M. (2010) Aberrant Rab11-dependent trafficking of the neuronal glutamate transporter EAAC1 causes oxidative stress and cell death in Huntington's disease. *Journal of Neuroscience*. 30 (13), pp. 4552–4561.

Li, X., Wang, J., Coutavas, E., Shi, H., Hao, Q. & Blobel, G. (2016) Structure of human Niemann–Pick C1 protein. *Proceedings of the National Academy of Sciences*. 113 (29), pp. 8212–8217.

Li, X.-J., Orr, A.L. & Li, S. (2010) Impaired mitochondrial trafficking in Huntington's disease. *Biochimica et biophysica acta*. 1802 (1), pp. 62–65.

Li, Z., Karlovich, C.A., Fish, M.P., Scott, M.P. & Myers, R.M. (1999) A putative *Drosophila* homolog of the Huntington's disease gene. *Human Molecular Genetics*.

Lim, D., Fedrizzi, L., Tartari, M., Zuccato, C., Cattaneo, E., Brini, M. & Carafoli, E. (2008) Calcium homeostasis and mitochondrial dysfunction in striatal neurons of Huntington disease. *The Journal of Biological Chemistry*. 283 (9), pp. 5780–5789.

Lin, K., Hsin, H., Libina, N. & Kenyon, C. (2001) Regulation of the *Caenorhabditis elegans* longevity protein DAF-16 by insulin/IGF-1 and germline signaling. *Nature Genetics*. 28 (2), pp. 139–145.

Liot, G., Zala, D., Pla, P., Mottet, G., Piel, M. & Saudou, F. (2013) Mutant Huntingtin alters retrograde transport of TrkB receptors in striatal dendrites. *Journal of Neuroscience*. 33 (15), pp. 6298–6309.

Liu, C. & Hermann, T.E. (1978) Characterization of ionomycin as a calcium ionophore. *The Journal of Biological Chemistry*. 253 (17), pp. 5892–5894.

Liu, W., Xie, Y., Ma, J., Luo, X., Nie, P., Zuo, Z., Lahrmann, U., Zhao, Q., Zheng, Y., Zhao, Y., Xue, Y. & Ren, J. (2015) IBS: an illustrator for the presentation and visualization of biological sequences. *Bioinformatics (Oxford, England)*. 31 (20), pp. 3359–3361.

Liu, X., Zhang, Q.-H. & Yi, G.-H. (2012) Regulation of metabolism and transport of sphingosine-1-phosphate in mammalian cells. *Molecular and Cellular Biochemistry*. 363 (1-2), pp. 21–33.

Liu, Z. & Huang, X. (2012) Lipid metabolism in Drosophila: development and disease. *Acta Biochimica et Biophysica Sinica*. 45 (1), pp. 44–50.

Lloyd-Evans, E. & Platt, F.M. (2010) Lipids on Trial: The Search for the Offending Metabolite in Niemann-Pick type C Disease. *Traffic*. 11 (4), pp. 419–428.

Lloyd-Evans, E. & Platt, F.M. (2011) Lysosomal Ca2+ homeostasis: Role in pathogenesis of lysosomal storage diseases. *Cell Calcium*. 50 (2), pp. 200–205.

Lloyd-Evans, E., Morgan, A.J., He, X., Smith, D.A., Elliot-Smith, E., Sillence, D.J., Churchill, G.C., Schuchman, E.H., Galione, A. & Platt, F.M. (2008) Niemann-Pick disease type C1 is a sphingosine storage disease that causes deregulation of lysosomal calcium. *Nature Medicine*. 14 (11), pp. 1247–1255.

Lloyd-Evans, E., Waller-Evans, H., Peterneva, K. & Platt, F.M. (2010) Endolysosomal calcium regulation and disease. *Biochemical Society Transactions*. 38 (6), pp. 1458.

Lodish, H., Berk, A., Zipursky, S.L., Matsudaira, P., Baltimore, D. & Darnell, J. (2000) Protein Glycosylation in the ER and Golgi Complex. *Molecular Cell Biology*.

Lombardi, G., Zanoni, R. & Moroni, F. (1989) Systemic treatments with GM1 ganglioside reduce quinolinic acid-induced striatal lesions in the rat. *European Journal of Pharmacology*. 174 (1), pp. 123–125.

Lorenz, C., Hadwiger, P., John, M., Vornlocher, H.-P. & Unverzagt, C. (2004) Steroid and lipid conjugates of siRNAs to enhance cellular uptake and gene silencing in liver cells. *Bioorganic & Medicinal Chemistry Letters*. 14 (19), pp. 4975–4977.

Louis, E.D., Anderson, K.E., Moskowitz, C., Thorne, D.Z. & Marder, K. (2000) Dystonia-predominant adult-onset Huntington disease: association between motor phenotype and age of onset in adults. *Archives of Neurology*. 57 (9), pp. 1326–1330.

Loyter, A., Scangos, G.A. & Ruddle, F.H. (1982) Mechanisms of DNA uptake by mammalian cells: fate of exogenously added DNA monitored by the use of fluorescent dyes. *Proceedings of the National Academy of Sciences of the United States of America*. 79 (2), pp. 422–426.

López Sanjurjo, C.I., Tovey, S.C. & Taylor, C.W. (2014) Rapid recycling of Ca2+ between IP3-sensitive stores and lysosomes. *PLoS ONE*. 9 (10), pp. e111275.

López Sanjurjo, C.I., Tovey, S.C., Prole, D.L. & Taylor, C.W. (2013) Lysosomes shape Ins(1,4,5)P3-evoked Ca2+ signals by selectively sequestering Ca2+ released from the endoplasmic reticulum. *Journal of Cell Science*. 126 (Pt 1), pp. 289–300.

Lu, F., Liang, Q., Abi-Mosleh, L., Das, A., De Brabander, J.K., Goldstein, J.L. & Brown, M.S. (2015) Identification of NPC1 as the target of U18666A, an inhibitor of lysosomal cholesterol export and Ebola infection. *eLife*. 4.

Lu, J.J., Langer, R. & Chen, J. (2009) A novel mechanism is involved in cationic lipid-mediated functional siRNA delivery. *Molecular Pharmaceutics*. 6 (3), pp. 763–771.

Lunkes, A., Lindenberg, K.S., Ben-Haïem, L., Weber, C., Devys, D., Landwehrmeyer, G.B., Mandel, J.-L. & Trottier, Y. (2002) Proteases acting on mutant huntingtin generate cleaved products that differentially build up cytoplasmic and nuclear inclusions. *Molecular Cell*. 10 (2), pp. 259–269.

Luo, S., Vacher, C., Davies, J.E. & Rubinsztein, D.C. (2005) Cdk5 phosphorylation of huntingtin reduces its cleavage by caspases: implications for mutant huntingtin toxicity. *The Journal of Cell Biology*. 169 (4), pp. 647–656.

Luthi-Carter, R., Taylor, D.M., Pallos, J., Lambert, E., Amore, A., Parker, A., Moffitt, H., Smith, D.L., Runne, H., Gokce, O., Kuhn, A., Xiang, Z., Maxwell, M.M., Reeves, S.A., et al. (2010) SIRT2 inhibition achieves neuroprotection by decreasing sterol biosynthesis. *Proceedings of the National Academy of Sciences*. 107 (17), pp. 7927–7932.

Luzio, J.P., Hackmann, Y., Dieckmann, N.M.G. & Griffiths, G.M. (2014) The biogenesis of lysosomes and lysosome-related organelles. *Cold Spring Harbor Perspectives in Biology*. 6 (9), pp. a016840.

Luzio, J.P., Parkinson, M.D.J., Gray, S.R. & Bright, N.A. (2009) The delivery of endocytosed cargo to lysosomes. *Biochemical Society Transactions*. 37 (5), pp. 1019.

Lytton, J., Westlin, M. & Hanley, M.R. (1991) Thapsigargin inhibits the sarcoplasmic or endoplasmic reticulum Ca-ATPase family of calcium pumps. *The Journal of Biological Chemistry*. 266 (26), pp. 17067–17071.

Maceyka, M., Harikumar, K.B., Milstien, S. & Spiegel, S. (2012) Sphingosine-1-phosphate signaling and its role in disease. *Trends in Cell Biology*. 22 (1), pp. 50–60.

Maceyka, M., Sankala, H., Hait, N.C., Le Stunff, H., Liu, H., Toman, R., Collier, C., Zhang, M., Satin, L.S., Merrill, A.H., Milstien, S. & Spiegel, S. (2005) SphK1 and SphK2, sphingosine kinase isoenzymes with opposing functions in sphingolipid metabolism. *The Journal of Biological Chemistry*. 280 (44), pp. 37118–37129.

Mackenzie, K.D., Lim, Y., Duffield, M.D., Chataway, T., Zhou, X.-F. & Keating, D.J. (2017) Accepted Manuscript. *Cellular Signalling*. pp. 1–37.

Maglione, V., Marchi, P., Di Pardo, A., Lingrell, S., Horkey, M., Tidmarsh, E. & Sipione, S. (2010) Impaired ganglioside metabolism in Huntington's disease and neuroprotective role of GM1. *Journal of Neuroscience*. 30 (11), pp. 4072–4080.

Malathi, K., Higaki, K., Tinkelenberg, A.H., Balderes, D.A., Almanzar-Paramio, D., Wilcox, L.J., Erdeniz, N., Redican, F., Padamsee, M., Liu, Y., Khan, S., Alcantara, F., Carstea, E.D., Morris, J.A., et al. (2004) Mutagenesis of the putative sterol-sensing domain of yeast Niemann Pick C-related protein reveals a primordial role in subcellular sphingolipid distribution. *The Journal of Cell Biology*. 164 (4), pp. 547–556.

Marchina, E., Misasi, S., Bozzato, A., Ferraboli, S., Agosti, C., Rozzini, L., Borsani, G., Barlati, S. & Padovani, A. (2014) Gene expression profile in fibroblasts of Huntington's disease patients and controls. *Journal of the Neurological Sciences*. 337 (1-2), pp. 42–46.

Markow, T.A. (2011) 'Cost' of virginity in wild *Drosophila melanogaster* females. *Ecology and Evolution*. 1 (4), pp. 596–600.

Marks, D.L., Dominguez, M., Wu, K. & Pagano, R.E. (2001) Identification of active site residues in glucosylceramide synthase. A nucleotide-binding catalytic motif conserved with processive beta-glycosyltransferases. *The Journal of Biological Chemistry*. 276 (28), pp. 26492–26498.

Marques Sousa, C. & Humbert, S. (2013) Huntingtin: here, there, everywhere! *Journal of Huntington's Disease*. 2 (4), pp. 395–403.

Marsh, J.L., Pallos, J. & Thompson, L.M. (2003) Fly models of Huntington's disease. *Human Molecular Genetics*. 12 (suppl 2), pp. R187–R193.

Martin, D.D.O., Heit, R.J., Yap, M.C., Davidson, M.W., Hayden, M.R. & Berthiaume, L.G. (2014) Identification of a post-translationally myristoylated autophagy-inducing domain released by caspase cleavage of Huntingtin. *Human Molecular Genetics*.

Martin, D.D.O., Ladha, S., Ehrnhoefer, D.E. & Hayden, M.R. (2015) Autophagy in Huntington disease and huntingtin in autophagy. *Trends in Neurosciences*. 38 (1), pp. 26–35.

Martinez-Vicente, M., Talloczy, Z., Wong, E., Tang, G., Koga, H., Kaushik, S., de Vries, R., Arias, E., Harris, S., Sulzer, D. & Cuervo, A.M. (2010) Cargo recognition failure is responsible for inefficient autophagy in Huntington's disease. *Nature Neuroscience*. 13 (5), pp. 567–576.

Marullo, M., Valenza, M., Leoni, V., Caccia, C., Scarlatti, C., De Mario, A., Zuccato, C., Di Donato, S., Carafoli, E. & Cattaneo, E. (2012) Pitfalls in the detection of cholesterol in Huntington's disease models. *PLoS Currents*.

Maxfield, F.R. (2014) Role of endosomes and lysosomes in human disease. *Cold Spring Harbor Perspectives in Biology*. 6 (5), pp. a016931.

Maxson, M.E. & Grinstein, S. (2014) The vacuolar-type $H^+$-ATPase at a glance - more than a proton pump. *Journal of Cell Science*. 127 (Pt 23), pp. 4987–4993.

Mayor, S., Parton, R.G. & Donaldson, J.G. (2014) Clathrin-independent pathways of endocytosis. *Cold Spring Harbor Perspectives in Biology*. 6 (6).

Mayran, N., Parton, R.G. & Gruenberg, J. (2003) Annexin II regulates multivesicular endosome biogenesis in the degradation pathway of animal cells. *The EMBO Journal*. 22 (13), pp. 3242–3253.

Mazzon, M. & Mercer, J. (2014) Lipid interactions during virus entry and infection. *Cellular Microbiology*. 16 (10), pp. 1493–1502.

McBride, S.D., Perentos, N. & Morton, A.J. (2016) A mobile, high-throughput semi-automated system for testing cognition in large non-primate animal models of Huntington disease. *Journal of Neuroscience Methods*. 265pp. 25–33.

Medina, D.L., Di Paola, S., Peluso, I., Armani, A., De Stefani, D., Venditti, R., Montefusco, S., Scotto-Rosato, A., Prezioso, C., Forrester, A., Settembre, C., Wang, W., Gao, Q., Xu, H., et al. (2015) Lysosomal calcium signalling regulates autophagy through calcineurin and TFEB. *Nature Cell Biology*. 17 (3), pp. 288–299.

Meikle, P.J., Hopwood, J.J., Clague, A.E. & Carey, W.F. (1999) Prevalence of lysosomal storage disorders. *JAMA*. 281 (3), pp. 249–254.

Mell, J.C. & Redfield, R.J. (2014) Natural Competence and the Evolution of DNA Uptake Specificity. *Journal of Bacteriology*. 196 (8), pp. 1471–1483.

Menzies, F.M., Fleming, A. & Rubinsztein, D.C. (2015) Compromised autophagy and neurodegenerative diseases. *Nature Reviews Neuroscience*. 16 (6), pp. 345–357.

Miller, W.L. & Bose, H.S. (2011) Early steps in steroidogenesis: intracellular cholesterol trafficking: Thematic Review Series: Genetics of Human Lipid Diseases. *The Journal of Lipid Research*. 52 (12), pp. 2111–2135.

Mitsche, M.A., McDonald, J.G., Hobbs, H.H. & Cohen, J.C. (2015) Flux analysis of cholesterol biosynthesis in vivo reveals multiple tissue and cell-type specific pathways. *eLife*. 4pp. e07999.

Morgan, A.J., Davis, L.C. & Galione, A. (2015) Imaging approaches to measuring lysosomal calcium. *Methods in Cell Biology*. 126pp. 159–195.

Mort, M., Carlisle, F.A., Waite, A.J., Elliston, L., Allen, N.D., Jones, L. & Hughes, A.C. (2015) Huntingtin Exists as Multiple Splice Forms in Human Brain. *Journal of Huntington's Disease*. 4 (2), pp. 161–171.

Mortuza, G.B., Neville, W.A., Delaney, J., Waterfield, C.J. & Camilleri, P. (2003) Characterisation of a potential biomarker of phospholipidosis from amiodarone-treated rats. *Biochimica et Biophysica Acta (BBA) - Molecular and Cell Biology of Lipids*. 1631 (2), pp. 136–146.

Mukherjee, S., Ray, S. & Thakur, R.S. (2009) Solid lipid nanoparticles: a modern formulation approach in drug delivery system. *Indian Journal of Pharmaceutical Sciences*. 71 (4), pp. 349–358.

Mutka, A.L., Lusa, S., Linder, M.D., Jokitalo, E., Kopra, O., Jauhiainen, M. & Ikonen, E. (2004) Secretion of Sterols and the NPC2 Protein from Primary Astrocytes. *Journal of Biological Chemistry*. 279 (47), pp. 48654–48662.

Naldini, L. (2015) Gene therapy returns to centre stage. *Nature*. 526 (7573), pp. 351–360.

Napolitano, G. & Ballabio, A. (2016) TFEB at a glance. *Journal of Cell Science*. 129 (13), pp. 2475–2481.

Nasir, J., Floresco, S.B., O'Kusky, J.R., Diewert, V.M., Richman, J.M., Zeisler, J., Borowski, A., Marth, J.D., Phillips, A.G. & Hayden, M.R. (1995) Targeted disruption of the Huntington's disease gene results in embryonic lethality and behavioral and morphological changes in heterozygotes. *Cell*. 81 (5), pp. 811–823.

Naureckiene, S. (2000) Identification of HE1 as the Second Gene of Niemann-Pick C Disease. *Science*. 290 (5500), pp. 2298–2301.

NCBI Resource Coordinators (2018) Database resources of the National Center for Biotechnology Information. *Nucleic Acids Research*. 46 (D1), pp. D8–D13.

Neculai, D., Schwake, M., Ravichandran, M., Zunke, F., Collins, R.F., Peters, J., Neculai, M., Plumb, J., Loppnau, P., Pizarro, J.C., Seitova, A., Trimble, W.S., Saftig, P., Grinstein, S., et al. (2013) Structure of LIMP-2 provides functional insights with implications for SR-BI and CD36. *Nature*. 504 (7478), pp. 172–176.

Nellen, W. & Lichtenstein, C. (1993) What makes an mRNA anti-sense-itive? *Trends in Biochemical Sciences*. 18 (11), pp. 419–423.

Neueder, A. & Bates, G.P. (2014) A common gene expression signature in Huntington's disease patient brain regions. *BMC Medical Genomics*. 7pp. 60.

Neufeld, E.F. (2006) Enzyme replacement therapy – a brief history. In: *Fabry Disease: Perspectives from 5 Years of FOS*. Oxford: Oxford PharmaGenesis.

Newman, T., Sinadinos, C., Johnston, A., Sealey, M. & Mudher, A. (2011) Using Drosophila models of neurodegenerative diseases for drug discovery. *Expert opinion on drug discovery*. 6 (2), pp. 129–140.

Nguyen, J. & Szoka, F.C. (2012) Nucleic acid delivery: the missing pieces of the puzzle? *Accounts of Chemical Research*. 45 (7), pp. 1153–1162.

Niwa, R. & Niwa, Y.S. (2011) The Fruit Fly *Drosophila melanogaster* as a Model System to Study Cholesterol Metabolism and Homeostasis. *Cholesterol*. 2011 (3), pp. 1–6.

Nixon, R.A. (2016) New perspectives on lysosomes in ageing and neurodegenerative disease. *Ageing Research Reviews*. 32pp. 1.

Nixon, R.A. (2013) The role of autophagy in neurodegenerative disease. *Nature Medicine*. 19 (8), pp. 983–997.

Nonoyama, T. & Fukuda, R. (2008) Drug-induced phospholipidosis - pathological aspects and its

prediction. *Journal of toxicologic pathology*.

Novak, M.J.U. & Tabrizi, S.J. (2010) Huntington's disease. *BMJ*. 340 (jun30 4), pp. c3109–c3109.

Oko, R., Donald, A., Xu, W. & van der Spoel, A.C. (2011) Fusion failure of dense-cored proacrosomal vesicles in an inducible mouse model of male infertility. *Cell and tissue research*. 346 (1), pp. 119–134.

Olson, J.A., Lindberg, M. & Bloch, K. (1957) On the demethylation of lanosterol to cholesterol. *The Journal of Biological Chemistry*. 226 (2), pp. 941–956.

Orr, H.T. & Zoghbi, H.Y. (2007) Trinucleotide repeat disorders. *Annual review of neuroscience*. 30pp. 575–621.

Pagano, R.E. (2003) Endocytic trafficking of glycosphingolipids in sphingolipid storage diseases. *Philosophical Transactions of the Royal Society B: Biological Sciences*. 358 (1433), pp. 885–891.

Pal, A., Severin, F., Lommer, B., Shevchenko, A. & Zerial, M. (2006) Huntingtin-HAP40 complex is a novel Rab5 effector that regulates early endosome motility and is up-regulated in Huntington's disease. *The Journal of Cell Biology*. 172 (4), pp. 605–618.

Panov, A.V., Gutekunst, C.-A., Leavitt, B.R., Hayden, M.R., Burke, J.R., Strittmatter, W.J. & Greenamyre, J.T. (2002) Early mitochondrial calcium defects in Huntington's disease are a direct effect of polyglutamines. *Nature Neuroscience*. 5 (8), pp. 731–736.

Park, W.D., O'Brien, J.F., Lundquist, P.A., Kraft, D.L., Vockley, C.W., Karnes, P.S., Patterson, M.C. & Snow, K. (2003) Identification of 58 novel mutations in Niemann-Pick disease type C: correlation with biochemical phenotype and importance of PTC1-like domains in NPC1. *Human Mutation*. 22 (4), pp. 313–325.

Patel, S. & Cai, X. (2015) Evolution of acidic $Ca^{2+}$ stores and their resident $Ca^{2+}$-permeable channels. *Cell Calcium*. 57 (3), pp. 222–230.

Patterson, M.C., Vecchio, D., Prady, H., Abel, L. & Wraith, J.E. (2007) Miglustat for treatment of Niemann-Pick C disease: a randomised controlled study. *The Lancet Neurology*. 6 (9), pp. 765–772.

Paulsen, J.S., Nehl, C., Hoth, K.F., Kanz, J.E., Benjamin, M., Conybeare, R., McDowell, B. & Turner, B. (2005) Depression and stages of Huntington's disease. *The Journal of Neuropsychiatry and Clinical Neurosciences*. 17 (4), pp. 496–502.

Pecho-Vrieseling, E., Rieker, C., Fuchs, S., Bleckmann, D., Esposito, M.S., Botta, P., Goldstein, C., Bernhard, M., Galimberti, I., Müller, M., Lüthi, A., Arber, S., Bouwmeester, T., van der Putten, H., et al. (2014) Transneuronal propagation of mutant huntingtin contributes to non-cell autonomous pathology in neurons. *Nature Neuroscience*. 17 (8), pp. 1064–1072.

Penny, C.J., Kilpatrick, B.S., Eden, E.R. & Patel, S. (2015) Coupling acidic organelles with the ER through Ca2+ microdomains at membrane contact sites. *Cell Calcium*. 58 (4), pp. 387–396.

Pentchev, P.G., Comly, M.E., Kruth, H.S., Vanier, M.T., Wenger, D.A., Patel, S. & Brady, R.O. (1985) A defect in cholesterol esterification in Niemann-Pick disease (type C) patients. *Proceedings of the National Academy of Sciences of the United States of America*. 82 (23), pp. 8247–8251.

Perentos, N., Martins, A.Q., Watson, T.C., Bartsch, U., Mitchell, N.L., Palmer, D.N., Jones, M.W. & Morton, A.J. (2015) Translational neurophysiology in sheep: measuring sleep and neurological dysfunction in CLN5 Batten disease affected sheep. *Brain*. 138 (Pt 4), pp. 862–874.

Petrov, A.M., Kasimov, M.R. & Zefirov, A.L. (2016) Brain Cholesterol Metabolism and Its Defects: Linkage

to Neurodegenerative Diseases and Synaptic Dysfunction. *Acta Naturae*. 8 (1), pp. 58–73.

Phillips, S.E., Woodruff, E.A., Liang, P., Patten, M. & Broadie, K. (2008) Neuronal Loss of Drosophila NPC1a Causes Cholesterol Aggregation and Age-Progressive Neurodegeneration. *Journal of Neuroscience*. 28 (26), pp. 6569–6582.

Piccoli, E., Nadai, M., Caretta, C.M., Bergonzini, V., Del Vecchio, C., Ha, H.R., Bigler, L., Dal Zoppo, D., Faggin, E., Pettenazzo, A., Orlando, R., Salata, C., Calistri, A., Palù, G., et al. (2011) Amiodarone impairs trafficking through late endosomes inducing a Niemann-Pick C-like phenotype. *Biochemical Pharmacology*. 82 (9), pp. 1234–1249.

Pizette, S., Rabouille, C., Cohen, S.M. & Therond, P. (2009) Glycosphingolipids control the extracellular gradient of the Drosophila EGFR ligand Gurken. *Development*. 136 (4), pp. 551–561.

Platt, F.M. & Lachmann, R.H. (2009) Treating lysosomal storage disorders: current practice and future prospects. *Biochimica et biophysica acta*. 1793 (4), pp. 737–745.

Platt, F.M., Boland, B. & van der Spoel, A.C. (2012) The cell biology of disease: lysosomal storage disorders: the cellular impact of lysosomal dysfunction. *The Journal of Cell Biology*. 199 (5), pp. 723–734.

Platt, F.M., Jeyakumar, M., Andersson, U., Priestman, D.A., Dwek, R.A., Butters, T.D., Cox, T.M., Lachmann, R.H., Hollak, C., Aerts, J.M., Van Weely, S., Hrebícek, M., Moyses, C., Gow, I., et al. (2001) Inhibition of substrate synthesis as a strategy for glycolipid lysosomal storage disease therapy. *Journal of Inherited Metabolic Disease*. 24 (2), pp. 275–290.

Poirier, S., Mayer, G., Murphy, S.R., Garver, W.S., Chang, T.Y., Schu, P. & Seidah, N.G. (2013) The Cytosolic Adaptor AP-1A Is Essential for the Trafficking and Function of Niemann-Pick Type C Proteins. *Traffic*. 14 (4), pp. 458–469.

Pontier, S.M. & Schweisguth, F. (2011) Glycosphingolipids in signaling and development: From liposomes to model organisms Amit Singh & Kenneth D Irvine (eds.). *Developmental Dynamics*. 241 (1), pp. 92–106.

Pontikis, C.C., Davidson, C.D., Walkley, S.U., Platt, F.M. & Begley, D.J. (2013) Cyclodextrin alleviates neuronal storage of cholesterol in Niemann-Pick C disease without evidence of detectable blood-brain barrier permeability. *Journal of Inherited Metabolic Disease*. 36 (3), pp. 491–498.

Poupetová, H., Ledvinová, J., Berná, L., Dvoráková, L., Kozich, V. & Elleder, M. (2010) The birth prevalence of lysosomal storage disorders in the Czech Republic: comparison with data in different populations. *Journal of Inherited Metabolic Disease*. 33 (4), pp. 387–396.

Priestman, D.A., van der Spoel, A.C., Butters, T.D., Dwek, R.A. & Platt, F.M. (2008) N-butyldeoxynojirimycin causes weight loss as a result of appetite suppression in lean and obese mice. *Diabetes, obesity & metabolism*. 10 (2), pp. 159–166.

Pringsheim, T., Wiltshire, K., Day, L., Dykeman, J., Steeves, T. & Jette, N. (2012) The incidence and prevalence of Huntington's disease: a systematic review and meta-analysis. *Movement Disorders*. 27 (9), pp. 1083–1091.

Pryor, P.R. (2012) Analyzing lysosomes in live cells. *Methods in Enzymology*. 505pp. 145–157.

Pu, J., Guardia, C.M., Keren-Kaplan, T. & Bonifacino, J.S. (2016) Mechanisms and functions of lysosome positioning. *Journal of Cell Science*. 129 (23), pp. 4329–4339.

Punnonen, E.L., Ryhänen, K. & Marjomäki, V.S. (1998) At reduced temperature, endocytic membrane traffic is blocked in multivesicular carrier endosomes in rat cardiac myocytes. *European Journal of*

*Cell Biology*. 75 (4), pp. 344–352.

Puri, A., Loomis, K., Smith, B., Lee, J.-H., Yavlovich, A., Heldman, E. & Blumenthal, R. (2009) Lipid-based nanoparticles as pharmaceutical drug carriers: from concepts to clinic. *Critical Reviews in Therapeutic Drug Carrier Systems*. 26 (6), pp. 523–580.

Qin, Z.H. (2003) Autophagy regulates the processing of amino terminal huntingtin fragments. *Human Molecular Genetics*. 12 (24), pp. 3231–3244.

Quarrell, O., O'Donovan, K.L., Bandmann, O. & Strong, M. (2012) The Prevalence of Juvenile Huntington's Disease: A Review of the Literature and Meta-Analysis. *PLoS Currents*. 4pp. e4f8606b742ef3.

Quinn, P.G., Georgiou, M. & Payne, A.H. (1985) Differences in the control of sterol metabolism between mouse and rat Leydig cells. *Endocrinology*. 116 (6), pp. 2300–2305.

Radhakrishnan, A., Ikeda, Y., Kwon, H.J., Brown, M.S. & Goldstein, J.L. (2007) Sterol-regulated transport of SREBPs from endoplasmic reticulum to Golgi: oxysterols block transport by binding to Insig. *Proceedings of the National Academy of Sciences of the United States of America*. 104 (16), pp. 6511–6518.

Raposo, G. & Stoorvogel, W. (2013) Extracellular vesicles: exosomes, microvesicles, and friends. *The Journal of Cell Biology*. 200 (4), pp. 373–383.

Ravikumar, B., Vacher, C., Berger, Z., Davies, J.E., Luo, S., Oroz, L.G., Scaravilli, F., Easton, D.F., Duden, R., O'Kane, C.J. & Rubinsztein, D.C. (2004) Inhibition of mTOR induces autophagy and reduces toxicity of polyglutamine expansions in fly and mouse models of Huntington disease. *Nature Genetics*. 36 (6), pp. 585–595.

Reddington, A.E., Rosser, A.E. & Dunnett, S.B. (2014) Differentiation of pluripotent stem cells into striatal projection neurons: a pure MSN fate may not be sufficient. *Frontiers in Cellular Neuroscience*. 8pp. 398.

Reddy, A., Caler, E.V. & Andrews, N.W. (2001) Plasma membrane repair is mediated by Ca(2+)-regulated exocytosis of lysosomes. *Cell*. 106 (2), pp. 157–169.

Reddy, P.H. & Shirendeb, U.P. (2012) Mutant huntingtin, abnormal mitochondrial dynamics, defective axonal transport of mitochondria, and selective synaptic degeneration in Huntington's disease. *Biochimica et biophysica acta*. 1822 (2), pp. 101–110.

Rich, J.T., Neely, J.G., Paniello, R.C., Voelker, C.C.J., Nussenbaum, B. & Wang, E.W. (2010) A practical guide to understanding Kaplan-Meier curves. *Otolaryngology - Head and Neck Surgery*. 143 (3), pp. 331–336.

Ridgway, N.D., Byers, D.M., Cook, H.W. & Storey, M.K. (1999) Integration of phospholipid and sterol metabolism in mammalian cells. *Progress in Lipid Research*. 38 (4), pp. 337–360.

Ritch, J.J., Valencia, A., Alexander, J., Sapp, E., Gatune, L., Sangrey, G.R., Sinha, S., Scherber, C.M., Zeitlin, S., Sadri-Vakili, G., Irimia, D., DiFiglia, M. & Kegel, K.B. (2012) Multiple phenotypes in Huntington disease mouse neural stem cells. *Molecular and Cellular Neuroscience*. 50 (1), pp. 70–81.

Robinet, P., Fradagrada, A., Monier, M.-N., Marchetti, M., Cogny, A., Moatti, N., Paul, J.-L., Vedie, B. & Lamaze, C. (2006) Dynamin is involved in endolysosomal cholesterol delivery to the endoplasmic reticulum: role in cholesterol homeostasis. *Traffic*. 7 (7), pp. 811–823.

Robinson, J.M. & Karnovsky, M.J. (1980) Evaluation of the Polyene Antibiotic Filipin as a Cytochemical Probe for Membrane Cholesterol. *Journal of Histochemistry & Cytochemistry*. 28 (2), pp. 161–168.

Rodrigues, F.B., Byrne, L.M., McColgan, P., Robertson, N., Tabrizi, S.J., Zetterberg, H. & Wild, E.J. (2016) Cerebrospinal Fluid Inflammatory Biomarkers Reflect Clinical Severity in Huntington's Disease. *PLoS ONE*. 11 (9), pp. e0163479.

Roos, R.A. (2010) Huntington's disease: a clinical review. *Orphanet Journal of Rare Diseases*. 5 (1), pp. 40.

Rosenbaum, A.I. & Maxfield, F.R. (2011) Niemann-Pick type C disease: molecular mechanisms and potential therapeutic approaches. *Journal of Neurochemistry*. 116 (5), pp. 789–795.

Ross, C.A. & Tabrizi, S.J. (2011) Huntington's disease: from molecular pathogenesis to clinical treatment. *Lancet Neurology*. 10 (1), pp. 83–98.

Ruas, M., Rietdorf, K., Arredouani, A., Davis, L.C., Lloyd-Evans, E., Koegel, H., Funnell, T.M., Morgan, A.J., Ward, J.A., Watanabe, K., Cheng, X., Churchill, G.C., Zhu, M.X., Platt, F.M., et al. (2010) Purified TPC isoforms form NAADP receptors with distinct roles for Ca(2+) signaling and endolysosomal trafficking. *Current Biology*. 20 (8), pp. 703–709.

Rubinsztein, D.C., Shpilka, T. & Elazar, Z. (2012) Mechanisms of autophagosome biogenesis. *Current Biology*. 22 (1), pp. R29–R34.

Saftig, P. & Klumperman, J. (2009) Lysosome biogenesis and lysosomal membrane proteins: trafficking meets function. *Nature Reviews Molecular Cell Biology*. 10 (9), pp. 623–635.

Sahay, G., Alakhova, D.Y. & Kabanov, A.V. (2010) Endocytosis of nanomedicines. *Journal of Controlled Release*. 145 (3), pp. 182–195.

Sahay, G., Querbes, W., Alabi, C., Eltoukhy, A., Sarkar, S., Zurenko, C., Karagiannis, E., Love, K., Chen, D., Zoncu, R., Buganim, Y., Schroeder, A., Langer, R. & Anderson, D.G. (2013) Efficiency of siRNA delivery by lipid nanoparticles is limited by endocytic recycling. *Nature Biotechnology*. 31 (7), pp. 653–658.

Salsano, E., Umeh, C., Rufa, A., Pareyson, D. & Zee, D.S. (2012) Vertical supranuclear gaze palsy in Niemann-Pick type C disease. *Neurological Sciences*. 33 (6), pp. 1225–1232.

Sands, M. & Davidson, B. (2006) Gene therapy for lysosomal storage diseases. *Molecular Therapy*. 13 (5), pp. 839–849.

Sathasivam, K., Amaechi, I., Mangiarini, L. & Bates, G. (1997) Identification of an HD patient with a (CAG)180 repeat expansion and the propagation of highly expanded CAG repeats in lambda phage. *Human Genetics*. 99 (5), pp. 692–695.

Sathasivam, K., Neueder, A., Gipson, T.A., Landles, C., Benjamin, A.C., Bondulich, M.K., Smith, D.L., Faull, R.L.M., Roos, R.A.C., Howland, D., Detloff, P.J., Housman, D.E. & Bates, G.P. (2013) Aberrant splicing of HTT generates the pathogenic exon 1 protein in Huntington disease. *Proceedings of the National Academy of Sciences*. 110 (6), pp. 2366–2370.

Saudou, F. & Humbert, S. (2016) The Biology of Huntingtin. *Neuron*. 89 (5), pp. 910–926.

Sánchez, I., Xu, C.J., Juo, P., Kakizaka, A., Blenis, J. & Yuan, J. (1999) Caspase-8 is required for cell death induced by expanded polyglutamine repeats. *Neuron*. 22 (3), pp. 623–633.

Schiefer, J., Landwehrmeyer, G.B., Lüesse, H.-G., Sprünken, A., Puls, C., Milkereit, A., Milkereit, E. & Kosinski, C.M. (2002) Riluzole prolongs survival time and alters nuclear inclusion formation in a transgenic mouse model of Huntington's disease. *Movement Disorders*. 17 (4), pp. 748–757.

Schmidt, O. & Teis, D. (2012) The ESCRT machinery. *Current Biology*. 22 (4), pp. R116–R120.

Schneider, I. (1972) Cell lines derived from late embryonic stages of Drosophila melanogaster. *Journal of Embryology and Experimental Morphology*. 27 (2), pp. 353–365.

Schultz, M.L., Tecedor, L., Chang, M. & Davidson, B.L. (2011) Clarifying lysosomal storage diseases. *Trends in Neurosciences*. 34 (8), pp. 401–410.

Seegmiller, A.C., Dobrosotskaya, I., Goldstein, J.L., Ho, Y.K., Brown, M.S. & Rawson, R.B. (2002) The SREBP pathway in Drosophila: regulation by palmitate, not sterols. *Developmental Cell*. 2 (2), pp. 229–238.

Segawa, K. & Nagata, S. (2015) An Apoptotic 'Eat Me' Signal: Phosphatidylserine Exposure. *Trends in Cell Biology*. 25 (11), pp. 639–650.

Sepers, M.D. & Raymond, L.A. (2014) Mechanisms of synaptic dysfunction and excitotoxicity in Huntington's disease. *Drug Discovery Today*.

Seppo, A., Moreland, M., Schweingruber, H. & Tiemeyer, M. (2000) Zwitterionic and acidic glycosphingolipids of the *Drosophila melanogaster* embryo. *European Journal of Biochemistry*. 267 (12), pp. 3549–3558.

Sessa, M., Lorioli, L., Fumagalli, F., Acquati, S., Redaelli, D., Baldoli, C., Canale, S., Lopez, I.D., Morena, F., Calabria, A., Fiori, R., Silvani, P., Rancoita, P.M.V., Gabaldo, M., et al. (2016) Lentiviral haemopoietic stem-cell gene therapy in early-onset metachromatic leukodystrophy: an ad-hoc analysis of a non-randomised, open-label, phase 1/2 trial. *Lancet*. 388 (10043), pp. 476–487.

Settembre, C. & Medina, D.L. (2015) TFEB and the CLEAR network. *Methods in Cell Biology*. 126pp. 45–62.

Sévin, M., Lesca, G., Baumann, N., Millat, G., Lyon-Caen, O., Vanier, M.T. & Sedel, F. (2007) The adult form of Niemann-Pick disease type C. *Brain*. 130 (Pt 1), pp. 120–133.

Sheth, J.J., Sheth, F.J., Oza, N.J., Gambhir, P.S., Dave, U.P. & Shah, R.C. (2010) Plasma chitotriosidase activity in children with lysosomal storage disorders. *Indian journal of pediatrics*. 77 (2), pp. 203–205.

Shi, X.-Z., Zhong, X. & Yu, X.-Q. (2012) Drosophila melanogaster NPC2 proteins bind bacterial cell wall components and may function in immune signal pathways. *Insect Biochemistry and Molecular Biology*. 42 (8), pp. 545–556.

Shi, Y., Inoue, H., Wu, J.C. & Yamanaka, S. (2017) Induced pluripotent stem cell technology: a decade of progress. *Nature Reviews Drug Discovery*. 16 (2), pp. 115–130.

Sievers, F., Wilm, A., Dineen, D., Gibson, T.J., Karplus, K., Li, W., Lopez, R., McWilliam, H., Remmert, M., Söding, J., Thompson, J.D. & Higgins, D.G. (2011) Fast, scalable generation of high-quality protein multiple sequence alignments using Clustal Omega. *Molecular systems biology*. 7pp. 539.

Singer, E., Walter, C., Weber, J.J., Krahl, A.-C., Mau-Holzmann, U.A., Rischert, N., Riess, O., Clemensson, L.E. & Nguyen, H.P. (2017) Reduced cell size, chromosomal aberration and altered proliferation rates are characteristics and confounding factors in the STHdh cell model of Huntington disease. *Scientific Reports*. 7 (1), pp. 16880.

Siomi, M.C., Sato, K., Pezic, D. & Aravin, A.A. (2011) PIWI-interacting small RNAs: the vanguard of genome defence. *Nature Reviews Molecular Cell Biology*. 12 (4), pp. 246–258.

Sittler, A., Lurz, R., Lueder, G., Priller, J., Lehrach, H., Hayer-Hartl, M.K., Hartl, F.U. & Wanker, E.E. (2001) Geldanamycin activates a heat shock response and inhibits huntingtin aggregation in a cell culture model of Huntington's disease. *Human Molecular Genetics*. 10 (12), pp. 1307–1315.

Sleat, D.E., Wiseman, J.A., El-Banna, M., Price, S.M., Verot, L., Shen, M.M., Tint, G.S., Vanier, M.T., Walkley, S.U. & Lobel, P. (2004) Genetic evidence for nonredundant functional cooperativity between NPC1 and NPC2 in lipid transport. *Proceedings of the National Academy of Sciences of the United States of America*. 101 (16), pp. 5886–5891.

Slotte, J.P., Pörn, M.I. & Härmälä, A.S. (1994) *Flow and distribution of cholesterol-effects of phospholipids*.

Smith, D., Wallom, K.-L., Williams, I.M., Jeyakumar, M. & Platt, F.M. (2009a) Beneficial effects of anti-inflammatory therapy in a mouse model of Niemann-Pick disease type C1. *Neurobiology of Disease*. 36 (2), pp. 242–251.

Smith, R., Bacos, K., Fedele, V., Soulet, D., Walz, H.A., Obermüller, S., Lindqvist, A., Björkqvist, M., Klein, P., Onnerfjord, P., Brundin, P., Mulder, H. & Li, J.-Y. (2009b) Mutant huntingtin interacts with beta-tubulin and disrupts vesicular transport and insulin secretion. *Human Molecular Genetics*. 18 (20), pp. 3942–3954.

Sokol, J., Blanchette-Mackie, J., Kruth, H.S., Dwyer, N.K., Amende, L.M., Butler, J.D., Robinson, E., Patel, S., Brady, R.O., Comly, M.E., Vanier, M.T. & Pentchev, P.G. (1988) Type C Niemann-Pick disease. Lysosomal accumulation and defective intracellular mobilization of low density lipoprotein cholesterol. *The Journal of Biological Chemistry*. 263 (7), pp. 3411–3417.

Sonawane, N.D., Szoka, F.C. & Verkman, A.S. (2003) Chloride accumulation and swelling in endosomes enhances DNA transfer by polyamine-DNA polyplexes. *The Journal of Biological Chemistry*. 278 (45), pp. 44826–44831.

Soutschek, J., Akinc, A., Bramlage, B., Charisse, K., Constien, R., Donoghue, M., Elbashir, S., Geick, A., Hadwiger, P., Harborth, J., John, M., Kesavan, V., Lavine, G., Pandey, R.K., et al. (2004) Therapeutic silencing of an endogenous gene by systemic administration of modified siRNAs. *Nature*. 432 (7014), pp. 173–178.

Spiegel, S. & Milstien, S. (2003) Sphingosine-1-phosphate: an enigmatic signalling lipid. *Nature Reviews Molecular Cell Biology*. 4 (5), pp. 397–407.

Spiro, R.G. (2002) Protein glycosylation: nature, distribution, enzymatic formation, and disease implications of glycopeptide bonds. *Glycobiology*. 12 (4), pp. 43R–56R.

Squitieri, F., Gellera, C., Cannella, M., Mariotti, C., Cislaghi, G., Rubinsztein, D.C., Almqvist, E.W., Turner, D., Bachoud-Levi, A.-C., Simpson, S.A., Delatycki, M., Maglione, V., Hayden, M.R. & Donato, S.D. (2003) Homozygosity for CAG mutation in Huntington disease is associated with a more severe clinical course. *Brain*. 126 (Pt 4), pp. 946–955.

Steffan, J.S., Agrawal, N., Pallos, J., Rockabrand, E., Trotman, L.C., Slepko, N., Illes, K., Lukacsovich, T., Zhu, Y.-Z., Cattaneo, E., Pandolfi, P.P., Thompson, L.M. & Marsh, J.L. (2004) SUMO modification of Huntingtin and Huntington's disease pathology. *Science*. 304 (5667), pp. 100–104.

Stein, V.M., Crooks, A., Ding, W., Prociuk, M., O'Donnell, P., Bryan, C., Sikora, T., Dingemanse, J., Vanier, M.T., Walkley, S.U. & Vite, C.H. (2012) Miglustat improves purkinje cell survival and alters microglial phenotype in feline Niemann-Pick disease type C. *Journal of neuropathology and experimental neurology*. 71 (5), pp. 434–448.

Stirnemann, J., Belmatoug, N., Camou, F., Serratrice, C., Froissart, R., Caillaud, C., Levade, T., Astudillo, L., Serratrice, J., Brassier, A., Rose, C., Billette de Villemeur, T. & Berger, M.G. (2017) A Review of Gaucher Disease Pathophysiology, Clinical Presentation and Treatments. *International Journal of Molecular Sciences*. 18 (2).

Sturley, S.L., Patterson, M.C., Balch, W. & Liscum, L. (2004) The pathophysiology and mechanisms of NP-

C disease. *Biochimica et Biophysica Acta (BBA) - Molecular and Cell Biology of Lipids*. 1685 (1-3), pp. 83–87.

Sugimoto, Y., Ninomiya, H., Ohsaki, Y., Higaki, K., Davies, J.P., Ioannou, Y.A. & Ohno, K. (2001) Accumulation of cholera toxin and GM1 ganglioside in the early endosome of Niemann-Pick C1-deficient cells. *Proceedings of the National Academy of Sciences of the United States of America*. 98 (22), pp. 12391–12396.

Suh, J., An, Y., Tang, B.C., Dempsey, C., Huang, F. & Hanes, J. (2012) Real-time gene delivery vector tracking in the endo-lysosomal pathway of live cells. *Microscopy Research and Technique*. 75 (5), pp. 691–697.

Sørensen, S.A. & Fenger, K. (1992) Causes of death in patients with Huntington's disease and in unaffected first degree relatives. *Journal of Medical Genetics*. 29 (12), pp. 911–914.

Tam, Y.Y.C., Chen, S. & Cullis, P.R. (2013) Advances in Lipid Nanoparticles for siRNA Delivery. *Pharmaceutics*. 5 (3), pp. 498–507.

Tang, M.X., Redemann, C.T. & Szoka, F.C. (1996) In vitro gene delivery by degraded polyamidoamine dendrimers. *Bioconjugate Chemistry*. 7 (6), pp. 703–714.

Tao, T. & Tartakoff, A.M. (2001) Nuclear relocation of normal huntingtin. *Traffic*. 2 (6), pp. 385–394.

Tartari, M., Gissi, C., Sardo, Lo, V., Zuccato, C., Picardi, E., Pesole, G. & Cattaneo, E. (2008) Phylogenetic Comparison of Huntingtin Homologues Reveals the Appearance of a Primitive polyQ in Sea Urchin. *Molecular Biology and Evolution*. 25 (2), pp. 330–338.

Terman, A., Kurz, T., Gustafsson, B. & Brunk, U.T. (2008) The involvement of lysosomes in myocardial aging and disease. *Current Cardiology Reviews*. 4 (2), pp. 107–115.

Tettamanti, G., Bassi, R., Viani, P. & Riboni, L. (2003) Salvage pathways in glycosphingolipid metabolism. *Biochimie*. 85 (3-4), pp. 423–437.

Teuling, E., Bourgonje, A., Veenje, S., Thijssen, K., de Boer, J., van der Velde, J., Swertz, M. & Nollen, E. (2011) Modifiers of mutant huntingtin aggregation: functional conservation of C. elegans-modifiers of polyglutamine aggregation. *PLoS Currents*. 3pp. RRN1255.

The HD iPSC Consortium (2012) Induced Pluripotent Stem Cells from Patients with Huntington's Disease Show CAG-Repeat-Expansion-Associated Phenotypes. *Stem Cell*. 11 (2), pp. 264–278.

Théry, C., Zitvogel, L. & Amigorena, S. (2002) Exosomes: composition, biogenesis and function. *Nature Reviews Immunology*. 2 (8), pp. 569–579.

Tomoda, H., Kishimoto, Y. & Lee, Y.C. (1989) Temperature effect on endocytosis and exocytosis by rabbit alveolar macrophages. *The Journal of Biological Chemistry*. 264 (26), pp. 15445–15450.

Tourette, C., Li, B., Bell, R., O'Hare, S., Kaltenbach, L.S., Mooney, S.D. & Hughes, R.E. (2014) A Large-scale Huntingtin Protein Interaction Network Implicates Rho GTPase Signaling Pathways in Huntington's Disease. *Journal of Biological Chemistry*.

Trajkovic, K., Jeong, H. & Krainc, D. (2017) Mutant huntingtin is secreted via a late endosomal/lysosomal unconventional secretory pathway. *Journal of Neuroscience*.

Trettel, F., Rigamonti, D., Hilditch-Maguire, P., Wheeler, V.C., Sharp, A.H., Persichetti, F., Cattaneo, E. & MacDonald, M.E. (2000) Dominant phenotypes produced by the HD mutation in STHdh(Q111) striatal cells. *Human Molecular Genetics*. 9 (19), pp. 2799–2809.

Trottier, Y., Biancalana, V. & Mandel, J.L. (1994) Instability of CAG repeats in Huntington's disease: relation to parental transmission and age of onset. *Journal of Medical Genetics*. 31 (5), pp. 377–382.

Trushina, E., Canaria, C.A., Lee, D.Y. & McMurray, C.T. (2013) Loss of caveolin-1 expression in knock-in mouse model of Huntington's disease suppresses pathophysiology in vivo. *Human Molecular Genetics*.

Trushina, E., Dyer, R.B., Badger, J.D., Ure, D., Eide, L., Tran, D.D., Vrieze, B.T., Legendre-Guillemin, V., McPherson, P.S., Mandavilli, B.S., Van Houten, B., Zeitlin, S., McNiven, M., Aebersold, R., et al. (2004) Mutant huntingtin impairs axonal trafficking in mammalian neurons in vivo and in vitro. *Molecular and Cellular Biology*. 24 (18), pp. 8195–8209.

Trushina, E., Singh, R.D., Dyer, R.B., Cao, S., Shah, V.H., Parton, R.G., Pagano, R.E. & McMurray, C.T. (2006) Mutant huntingtin inhibits clathrin-independent endocytosis and causes accumulation of cholesterol in vitro and in vivo. *Human Molecular Genetics*. 15 (24), pp. 3578–3591.

Tsang, T.M., Woodman, B., McLoughlin, G.A., Griffin, J.L., Tabrizi, S.J., Bates, G.P. & Holmes, E. (2006) Metabolic characterization of the R6/2 transgenic mouse model of Huntington's disease by high-resolution MAS 1H NMR spectroscopy. *Journal of Proteome Research*. 5 (3), pp. 483–492.

Ugur, B., Chen, K. & Bellen, H.J. (2016) Drosophila tools and assays for the study of human diseases. *Disease Models and Mechanisms*. 9 (3), pp. 235–244.

Valenza, M. & Cattaneo, E. (2011) Emerging roles for cholesterol in Huntington's disease. *Trends in Neurosciences*. 34 (9), pp. 474–486.

Valenza, M., Carroll, J.B., Leoni, V., Bertram, L.N., Björkhem, I., Singaraja, R.R., Di Donato, S., Lutjohann, D., Hayden, M.R. & Cattaneo, E. (2007a) Cholesterol biosynthesis pathway is disturbed in YAC128 mice and is modulated by huntingtin mutation. *Human Molecular Genetics*. 16 (18), pp. 2187–2198.

Valenza, M., Leoni, V., Karasinska, J.M., Petricca, L., Fan, J., Carroll, J., Pouladi, M.A., Fossale, E., Nguyen, H.P., Riess, O., MacDonald, M., Wellington, C., DiDonato, S., Hayden, M., et al. (2010) Cholesterol defect is marked across multiple rodent models of Huntington's disease and is manifest in astrocytes. *Journal of Neuroscience*. 30 (32), pp. 10844–10850.

Valenza, M., Leoni, V., Tarditi, A., Mariotti, C., Björkhem, I., Di Donato, S. & Cattaneo, E. (2007b) Progressive dysfunction of the cholesterol biosynthesis pathway in the R6/2 mouse model of Huntington's disease. *Neurobiology of Disease*. 28 (1), pp. 133–142.

Valenza, M., Rigamonti, D., Goffredo, D., Zuccato, C., Fenu, S., Jamot, L., Strand, A., Tarditi, A., Woodman, B., Racchi, M., Mariotti, C., Di Donato, S., Corsini, A., Bates, G., et al. (2005) Dysfunction of the cholesterol biosynthetic pathway in Huntington's disease. *Journal of Neuroscience*. 25 (43), pp. 9932–9939.

van Meer, G. & de Kroon, A.I.P.M. (2010) Lipid map of the mammalian cell. *Journal of Cell Science*. 124 (1), pp. 5–8.

Vanier, M.T. (2010) Niemann-Pick disease type C. *Orphanet Journal of Rare Diseases*. 5 (1), pp. 16.

Varma, H., Cheng, R., Voisine, C., Hart, A.C. & Stockwell, B.R. (2007) Inhibitors of metabolism rescue cell death in Huntington's disease models. *Proceedings of the National Academy of Sciences of the United States of America*. 104 (36), pp. 14525–14530.

Velier, J., Kim, M., Schwarz, C., Kim, T.W., Sapp, E., Chase, K., Aronin, N. & DiFiglia, M. (1998) Wild-type and mutant huntingtins function in vesicle trafficking in the secretory and endocytic pathways. *Experimental Neurology*. 152 (1), pp. 34–40.

Vellodi, A. (2005) Lysosomal storage disorders. *British Journal of Haematology*. 128 (4), pp. 413–431.

Vienken, H., Mabrouki, N., Grabau, K., Claas, R.F., Rudowski, A., Schömel, N., Pfeilschifter, J., Lutjohann, D., van Echten-Deckert, G. & Heringdorf, D.M.Z. (2017) Characterization of cholesterol homeostasis in sphingosine-1-phosphate lyase-deficient fibroblasts reveals a Niemann-Pick disease type C-like phenotype with enhanced lysosomal Ca. *Scientific Reports*. pp. 1–16.

Vruchte, te, D. (2004) Accumulation of Glycosphingolipids in Niemann-Pick C Disease Disrupts Endosomal Transport. *Journal of Biological Chemistry*. 279 (25), pp. 26167–26175.

Vruchte, te, D., Speak, A.O., Wallom, K.L., Eisa, Al, N., Smith, D.A., Hendriksz, C.J., Simmons, L., Lachmann, R.H., Cousins, A., Hartung, R., Mengel, E., Runz, H., Beck, M., Amraoui, Y., et al. (2014) Relative acidic compartment volume as a lysosomal storage disorder-associated biomarker. *Journal of Clinical Investigation*. 124 (3), pp. 1320–1328.

Vural, A. & Kehrl, J.H. (2014) Autophagy in Macrophages: Impacting Inflammation and Bacterial Infection. *Scientifica*. 2014pp. 825463.

Walker, M.W. & Lloyd-Evans, E. (2015) A rapid method for the preparation of ultrapure, functional lysosomes using functionalized superparamagnetic iron oxide nanoparticles. *Methods in Cell Biology*. 126pp. 21–43.

Walkley, S.U. & Vanier, M.T. (2009) Secondary lipid accumulation in lysosomal disease. *Biochimica et biophysica acta*. 1793 (4), pp. 726–736.

Walter, M., Davies, J.P. & Ioannou, Y.A. (2003) Telomerase immortalization upregulates Rab9 expression and restores LDL cholesterol egress from Niemann-Pick C1 late endosomes. *The Journal of Lipid Research*. 44 (2), pp. 243–253.

Walton, M., Sirimanne, E., Reutelingsperger, C., Williams, C., Gluckman, P. & Dragunow, M. (1997) Annexin V labels apoptotic neurons following hypoxia-ischemia. *Neuroreport*. 8 (18), pp. 3871–3875.

Wan, C., Allen, T.M. & Cullis, P.R. (2014) Lipid nanoparticle delivery systems for siRNA-based therapeutics. *Drug Delivery and Translational Research*. 4 (1), pp. 74–83.

Wandall, H.H., Pizette, S., Pedersen, J.W., Eichert, H., Levery, S.B., Mandel, U., Cohen, S.M. & Clausen, H. (2005) Egghead and Brainiac Are Essential for Glycosphingolipid Biosynthesis in Vivo. *Journal of Biological Chemistry*. 280 (6), pp. 4858–4863.

Wang, H., Tam, Y.Y.C., Chen, S., Zaifman, J., van der Meel, R., Ciufolini, M.A. & Cullis, P.R. (2016) The Niemann-Pick C1 Inhibitor NP3.47 Enhances Gene Silencing Potency of Lipid Nanoparticles Containing siRNA. *Molecular Therapy*. 24 (12), pp. 2100–2108.

Wang, M.L., Motamed, M., Infante, R.E., Abi-Mosleh, L., Kwon, H.J., Brown, M.S. & Goldstein, J.L. (2010) Identification of surface residues on Niemann-Pick C2 essential for hydrophobic handoff of cholesterol to NPC1 in lysosomes. *Cell Metabolism*. 12 (2), pp. 166–173.

Warby, S.C., Chan, E.Y., Metzler, M., Gan, L., Singaraja, R.R., Crocker, S.F., Robertson, H.A. & Hayden, M.R. (2005) Huntingtin phosphorylation on serine 421 is significantly reduced in the striatum and by polyglutamine expansion in vivo. *Human Molecular Genetics*. 14 (11), pp. 1569–1577.

Warby, S.C., Doty, C.N., Graham, R.K., Carroll, J.B., Yang, Y.Z., Singaraja, R.R., Overall, C.M. & Hayden, M.R. (2008) Activated caspase-6 and caspase-6-cleaved fragments of huntingtin specifically colocalize in the nucleus. *Human Molecular Genetics*. 17 (15), pp. 2390–2404.

Wassif, C.A., Cross, J.L., Iben, J., Sanchez-Pulido, L., Cougnoux, A., Platt, F.M., Ory, D.S., Ponting, C.P.,

Bailey-Wilson, J.E., Biesecker, L.G. & Porter, F.D. (2015) High incidence of unrecognized visceral/neurological late-onset Niemann-Pick disease, type C1, predicted by analysis of massively parallel sequencing data sets. *Genetics in Medicine*.

Wassif, C.A., Vied, D., Tsokos, M., Connor, W.E., Steiner, R.D. & Porter, F.D. (2002) Cholesterol storage defect in RSH/Smith-Lemli-Opitz syndrome fibroblasts. *Molecular Genetics and Metabolism*. 75 (4), pp. 325–334.

Weiss, K.R. & Littleton, J.T. (2016) Characterization of axonal transport defects in Drosophila Huntingtin mutants. *Journal of Neurogenetics*. 30 (3-4), pp. 212–221.

Wheeler, V.C., White, J.K., Gutekunst, C.-A., Vrbanac, V., Weaver, M., Li, X.-J., Li, S.-H., Yi, H., Vonsattel, J.-P. & Gusella, J.F. (2000) Long glutamine tracts cause nuclear localization of a novel form of huntingtin in medium spiny striatal neurons in HdhQ92 and HdhQ111 knock-in mice. *Human Molecular Genetics*. 9 (4), pp. 503–513.

White, I.J., Bailey, L.M., Aghakhani, M.R., Moss, S.E. & Futter, C.E. (2006) EGF stimulates annexin 1-dependent inward vesiculation in a multivesicular endosome subpopulation. *The EMBO Journal*. 25 (1), pp. 1–12.

White, J.K., Auerbach, W., Duyao, M.P., Vonsattel, J.P., Gusella, J.F., Joyner, A.L. & MacDonald, M.E. (1997) Huntingtin is required for neurogenesis and is not impaired by the Huntington's disease CAG expansion. *Nature Genetics*. 17 (4), pp. 404–410.

Williams, A., Sarkar, S., Cuddon, P., Ttofi, E.K., Saiki, S., Siddiqi, F.H., Jahreiss, L., Fleming, A., Pask, D., Goldsmith, P., O'Kane, C.J., Floto, R.A. & Rubinsztein, D.C. (2008) Novel targets for Huntington's disease in an mTOR-independent autophagy pathway. *Nature Chemical Biology*. 4 (5), pp. 295–305.

Wilson, R.C. & Doudna, J.A. (2013) Molecular Mechanisms of RNA Interference. *Annual Review of Biophysics*. 42 (1), pp. 217–239.

Wong, Y.C. & Holzbaur, E.L.F. (2014) The regulation of autophagosome dynamics by huntingtin and HAP1 is disrupted by expression of mutant huntingtin, leading to defective cargo degradation. *Journal of Neuroscience*. 34 (4), pp. 1293–1305.

Wraith, J.E., Vecchio, D., Jacklin, E., Abel, L., Chadha-Boreham, H., Luzy, C., Giorgino, R. & Patterson, M.C. (2010) Miglustat in adult and juvenile patients with Niemann-Pick disease type C: long-term data from a clinical trial. *Molecular Genetics and Metabolism*. 99 (4), pp. 351–357.

Wyant, K.J., Ridder, A.J. & Dayalu, P. (2017) Huntington's Disease - Update on Treatments. *Current Neurology and Neuroscience Reports*. pp. 1–11.

Xia, J., Lee, D.H., Taylor, J., Vandelft, M. & Truant, R. (2003) Huntingtin contains a highly conserved nuclear export signal. *Human Molecular Genetics*. 12 (12), pp. 1393–1403.

Xu, S., Benoff, B., Liou, H.-L., Lobel, P. & Stock, A.M. (2007) Structural basis of sterol binding by NPC2, a lysosomal protein deficient in Niemann-Pick type C2 disease. *The Journal of Biological Chemistry*. 282 (32), pp. 23525–23531.

Xu, Y. & Szoka, F.C. (1996) Mechanism of DNA release from cationic liposome/DNA complexes used in cell transfection. *Biochemistry*. 35 (18), pp. 5616–5623.

Yamaji, A., Sekizawa, Y., Emoto, K., Sakuraba, H., Inoue, K., Kobayashi, H. & Umeda, M. (1998) Lysenin, a novel sphingomyelin-specific binding protein. *The Journal of Biological Chemistry*. 273 (9), pp. 5300–5306.

Yamamoto, S., Jaiswal, M., Charng, W.-L., Gambin, T., Karaca, E., Mirzaa, G., Wiszniewski, W., Sandoval,

H., Haelterman, N.A., Xiong, B., Zhang, K., Bayat, V., David, G., Li, T., et al. (2014) A *Drosophila* genetic resource of mutants to study mechanisms underlying human genetic diseases. *Cell*. 159 (1), pp. 200–214.

Yamanaka, S. (2012) Induced pluripotent stem cells: past, present, and future. *Cell Stem Cell*. 10 (6), pp. 678–684.

Yanagawa, S., Lee, J.S. & Ishimoto, A. (1998) Identification and characterization of a novel line of Drosophila Schneider S2 cells that respond to wingless signaling. *The Journal of Biological Chemistry*. 273 (48), pp. 32353–32359.

Yang, H. & Hu, H.-Y. (2016) Sequestration of cellular interacting partners by protein aggregates: implication in a loss-of-function pathology. *FEBS Journal*. 283 (20), pp. 3705–3717.

Yang, H., Liu, C., Zhong, Y., Luo, S., Monteiro, M.J. & Fang, S. (2010) Huntingtin interacts with the cue domain of gp78 and inhibits gp78 binding to ubiquitin and p97/VCP. *PLoS ONE*. 5 (1), pp. e8905.

Yano, H., Baranov, S.V., Baranova, O.V., Kim, J., Pan, Y., Yablonska, S., Carlisle, D.L., Ferrante, R.J., Kim, A.H. & Friedlander, R.M. (2014) Inhibition of mitochondrial protein import by mutant huntingtin. *Nature Neuroscience*. 17 (6), pp. 822–831.

Yin, W., Carballo-Jane, E., McLaren, D.G., Mendoza, V.H., Gagen, K., Geoghagen, N.S., McNamara, L.A., Gorski, J.N., Eiermann, G.J., Petrov, A., Wolff, M., Tong, X., Wilsie, L.C., Akiyama, T.E., et al. (2012) Plasma lipid profiling across species for the identification of optimal animal models of human dyslipidemia. *Journal of Lipid Research*. 53 (1), pp. 51–65.

Young, J.E. & Goldstein, L.S.B. (2012) Alzheimer's disease in a dish: promises and challenges of human stem cell models. *Human Molecular Genetics*. 21 (R1), pp. R82–R89.

Yu, A., Shibata, Y., Shah, B., Calamini, B., Lo, D.C. & Morimoto, R.I. (2014a) Protein aggregation can inhibit clathrin-mediated endocytosis by chaperone competition. *Proceedings of the National Academy of Sciences*. 111 (15), pp. E1481–E1490.

Yu, D., Swaroop, M., Wang, M., Baxa, U., Yang, R., Yan, Y., Coksaygan, T., DeTolla, L., Marugan, J.J., Austin, C.P., McKew, J.C., Gong, D.-W. & Zheng, W. (2014b) Niemann-Pick Disease Type C: Induced Pluripotent Stem Cell-Derived Neuronal Cells for Modeling Neural Disease and Evaluating Drug Efficacy. *Journal of Biomolecular Screening*. 19 (8), pp. 1164–1173.

Yu, R.K., Tsai, Y.-T., Ariga, T. & Yanagisawa, M. (2011) Structures, biosynthesis, and functions of gangliosides--an overview. *Journal of oleo science*. 60 (10), pp. 537–544.

Yu, W., Ko, M., Yanagisawa, K. & Michikawa, M. (2005) Neurodegeneration in heterozygous Niemann-Pick type C1 (NPC1) mouse: implication of heterozygous NPC1 mutations being a risk for tauopathy. *The Journal of Biological Chemistry*. 280 (29), pp. 27296–27302.

Zambon, R.A., Vakharia, V.N. & Wu, L.P. (2006) RNAi is an antiviral immune response against a dsRNA virus in *Drosophila melanogaster*. *Cellular Microbiology*. 8 (5), pp. 880–889.

Zatsepin, T.S., Kotelevtsev, Y.V. & Koteliansky, V. (2016) Lipid nanoparticles for targeted siRNA delivery - going from bench to bedside. *International Journal of Nanomedicine*. 11pp. 3077–3086.

Zelphati, O. & Szoka, F.C. (1996a) Intracellular distribution and mechanism of delivery of oligonucleotides mediated by cationic lipids. *Pharmaceutical Research*. 13 (9), pp. 1367–1372.

Zelphati, O. & Szoka, F.C. (1996b) Mechanism of oligonucleotide release from cationic liposomes. *Proceedings of the National Academy of Sciences of the United States of America*. 93 (21), pp. 11493–11498.

Zhang, H., Das, S., Li, Q.-Z., Dragatsis, I., Repa, J., Zeitlin, S., Hajnóczky, G. & Bezprozvanny, I. (2008) Elucidating a normal function of huntingtin by functional and microarray analysis of huntingtin-null mouse embryonic fibroblasts. *BMC Neuroscience*. 9 (1), pp. 38.

Zhang, J., Li, S., Li, L., Li, M., Guo, C., Yao, J. & Mi, S. (2015a) Exosome and Exosomal MicroRNA: Trafficking, Sorting, and Function. *Genomics, Proteomics & Bioinformatics*. 13 (1), pp. 17–24.

Zhang, L., Sheng, R. & Qin, Z. (2009) The lysosome and neurodegenerative diseases. *Acta Biochimica et Biophysica Sinica*. 41 (6), pp. 437–445.

Zhang, M., Dwyer, N.K., Love, D.C., Cooney, A., Comly, M., Neufeld, E., Pentchev, P.G., Blanchette-Mackie, E.J. & Hanover, J.A. (2001) Cessation of rapid late endosomal tubulovesicular trafficking in Niemann-Pick type C1 disease. *Proceedings of the National Academy of Sciences of the United States of America*. 98 (8), pp. 4466–4471.

Zhang, M., Liu, P., Dwyer, N.K., Christenson, L.K., Fujimoto, T., Martinez, F., Comly, M., Hanover, J.A., Blanchette-Mackie, E.J. & Strauss, J.F. (2002) MLN64 mediates mobilization of lysosomal cholesterol to steroidogenic mitochondria. *The Journal of Biological Chemistry*. 277 (36), pp. 33300–33310.

Zhang, N., Bailus, B.J., Ring, K.L. & Ellerby, L.M. (2015b) iPSC-based drug screening for Huntington's disease. *Brain Research*. pp. 1–15.

Zhang, S., Feany, M.B., Saraswati, S., Littleton, J.T. & Perrimon, N. (2009) Inactivation of Drosophila Huntingtin affects long-term adult functioning and the pathogenesis of a Huntington's disease model. *Disease Models and Mechanisms*. 2 (5-6), pp. 247–266.

Zhang, S., Zhi, D. & Huang, L. (2012) Lipid-based vectors for siRNA delivery. *Journal of Drug Targeting*. 20 (9), pp. 724–735.

Zhao, C. & Dahlman-Wright, K. (2010) Liver X receptor in cholesterol metabolism. *The Journal of Endocrinology*. 204 (3), pp. 233–240.

Zhao, Y., Ren, J., Harlos, K. & Stuart, D.I. (2016) Structure of glycosylated NPC1 luminal domain C reveals insights into NPC2 and Ebola virus interactions. *FEBS Letters*. 590 (5), pp. 605–612.

Zuccato, C., Tartari, M., Crotti, A., Goffredo, D., Valenza, M., Conti, L., Cataudella, T., Leavitt, B.R., Hayden, M.R., Timmusk, T., Rigamonti, D. & Cattaneo, E. (2003) Huntingtin interacts with REST/NRSF to modulate the transcription of NRSE-controlled neuronal genes. *Nature Genetics*. 35 (1), pp. 76–83.